Estimation non paramétrique et problèmes inverses

Thomas Willer

HAL Id: tel-00121197

https://theses.hal.science/tel-00121197

Submitted on 19 Dec 2006

Université Paris VII - Denis Diderot
UFR de Mathématiques
Année 2006

Thèse

pour obtenir le titre de

Docteur de l'Université Paris 7

Spécialité : Mathématiques Appliquées

présentée par

Thomas WILLER

Estimation Non Paramétrique Et Problèmes Inverses

Directrice de thèse
Pr. Dominique PICARD

Soutenue publiquement le 8 Décembre 2006, devant le jury composé de :

M. Anestis ANTONIADIS, Université Joseph Fourier
M. Stéphane BOUCHERON, Université Paris 7
M. Yuri GOLUBEV, Université de Provence
M. Marc HOFFMANN, Université de Marne la Vallée
Mme Dominique PICARD, Université Paris 7
M. Markus REISS, Université de Heidelberg

au vu des rapports de :

M. Anestis ANTONIADIS, Université Joseph Fourier
M. Markus REISS, Université de Heidelberg

A mes parents

TABLE DES MATIÈRES

SOMMAIRE

Cette thèse traite principalement des problèmes inverses, mais s'inscrit dans une optique plus large que l'on peut décrire de la façon suivante. Dans le cadre de l'estimation non paramétrique, une technique particulièrement intéressante consiste à utiliser des bases d'ondelettes. Dans les modèles "simples", comme le bruit blanc ou la régression standard, celles ci fournissent des procédures d'estimation très efficaces, reposant sur une méthode simple d'estimation des coefficients dans la base d'ondelettes, et de débruitage par un algorithme de seuillage.

Face à des modèles plus complexes, la réaction la plus naturelle est d'adapter la procédure standard par une complexification de la méthode d'estimation des coefficients d'ondelettes ou du seuillage, laissant la base inchangée de peur de perdre les propriétés intéressantes des ondelettes. On reporte ainsi toutes les difficultés nouvelles sur des problèmes stochastiques, et l'on se heurte à des contraintes théoriques sur les paramètres du modèle. Dans de telles circonstances, serait il possible de reporter les difficultés plutôt sur la base, en sacrifiant éventuellement quelques unes des propriétés de type ondelette ? Ceci permettrait d'une part de gagner en simplicité au niveau de l'estimation séquentielle, et d'autre part d'offrir de nouveaux champs d'application, différents de ceux traités par les méthodes d'ondelettes. Les résultats établis dans cette thèse permettent d'apporter quelques éléments de réponse à cette vaste question.

Dans cette optique, nous donnons, au chapitre 3, une méthode d'estimation pour les problèmes inverses fondée sur l'utilisation d'une base localisée (ou même, dans certains cas, seulement d'un "frame" localisé) adaptée à l'opérateur du problème. Puis nous montrons dans le chapitre 4 que cette procédure est optimale sur le plan minimax. Dans le chapitre 5, nous mettons en parallèle le principe général de la procédure avec celui de plusieurs méthodes d'estimation pour les problèmes inverses, au moyen d'un schéma de classification commun. Puis nous nous intéressons à ses performances, tant théoriques que pratiques, en l'appliquant à un exemple concret de problème inverse, à savoir le problème de Wicksell. La procédure fournit des vitesses de convergence nouvelles ainsi que de bonnes performances pratiques. Dans le chapitre 6, nous proposons d'élargir le cadre à un modèle d'opérateur "aléatoire" (dans un sens original que nous détaillerons), et nous examinons quelles adaptations on peut alors apporter à la procédure dans un cas simple de déconvolution. Enfin, dans le chapitre 7, nous nous proposons de sortir du cadre des problèmes inverses et d'illustrer la problématique dans le cas de la régression en design aléatoire : une procédure fondée sur l'utilisation de bases atypiques a déjà été développée dans ce cas, et l'objet du chapitre est d'en étudier les performances numériques.

Chacun de ces chapitres peut être lu indépendamment des autres. Nous donnons un résumé des principaux résultats au chapitre 2. Mais avant cela, dans le chapitre 1, nous faisons une brève introduction sur les problèmes inverses ainsi que des rappels sur quelques notions de statistique non paramétrique.

Chapitre 1

INTRODUCTION

Dans ce premier chapitre, nous consacrons une première section 1.1 à la présentation des problèmes inverses, à leur modélisation statistique et à la description de quelques méthodes d'estimation bien connues pour ce type de problèmes. Puis dans la section 1.2, nous donnons quelques notions préliminaires liées à la théorie minimax, aux ondelettes et aux espaces fonctionnels de Besov.

1.1 Modèles inverses

1.1.1 Principe et exemples

Les problèmes inverses consistent essentiellement à déterminer des causes, connaissant des effets. Ils apparaissent ainsi comme l'inverse des problèmes directs, plus habituels, où l'on cherche à déduire les effets qu'auront certaines causes connues. Par exemple, un problème inverse peut consister à reconstituer l'état passé d'un système physique, connaissant son état actuel, contrairement au problème direct qui reviendrait à prédire l'état futur du système connaissant son état actuel. Ou, sous un angle plus représentatif des problèmes traités dans cette thèse, le problème inverse peut consister à identifier des paramètres du système, connaissant son évolution.

Le cadre mathématique générique pour modéliser de tels problèmes est le suivant. Soient $\mathbb{H}$ et $\mathbb{K}$ deux espaces de Hilbert et soit $K : \mathbb{H} \mapsto \mathbb{K}$ un opérateur. Un problème inverse consiste à déterminer une bonne approximation f_ε de la solution f de

$$g = Kf, \tag{1.1}$$

lorsque l'on ne dispose que d'une perturbation Y_ε de g.

Par exemple, dans un cadre de tomographie par rayons X, qui est la technique utilisée par les scanners, on peut schématiser le problème comme dans la figure 1.1 : des rayons sont émis vers un détecteur avec une intensité initiale I_e, et passent par un domaine au travers duquel ils sont atténués suivant une fonction d'atténuation f. En sortie, les rayons possèdent une intensité I_d au niveau du détecteur. Le problème inverse consiste alors à déterminer la fonction f, sachant que l'on ne dispose que d'observations I_e^ε et I_d^ε bruitées par des erreurs de mesure.
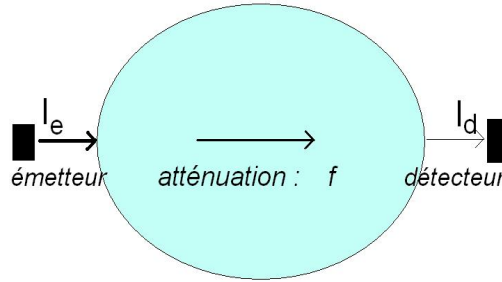
FIG. 1.1 – Tomographie par rayons X

Par rapport aux problèmes directs, la résolution de problèmes inverses peut s'avérer particulièrement difficile, voire impossible, suivant les propriétés de l'opérateur K. C'est le cas notamment dans tous les problèmes dits "mal posés", qui regroupent par exemple les cas où la solution n'existe pas (K n'est pas surjectif), ou n'est pas unique (K n'est pas injectif) ou elle ne dépend pas continûment des données (K^{-1} n'est pas continu). Nous nous intéresserons surtout à ce troisième type de problème par la suite.

De plus, on se placera généralement dans un cas particulier de problèmes linéaires mal posés, à savoir les problèmes à opérateur compact. Ceci signifie que pour chaque partie bornée $B \subset \mathbb{H}$, $K(B)$ est une partie relativement compacte de $\mathbb{K}$. Cette hypothèse usuelle pour les problèmes inverses est vérifiée pour de nombreux opérateurs, dont par exemple tous les opérateurs à noyaux $Kf(t) = \int_a^b k(t,s)f(s)ds$, $t \in]c,d[$ avec un noyau $k \in L^2(]c,d[,]a,b[)$. Elle permet d'établir un résultat important détaillé plus loin concernant la décomposition en valeurs singulières (SVD). Par ailleurs nous supposerons que K est injectif. Sous ces conditions, K^{-1} (s'il existe) n'est pas continu.

En pratique, les problèmes mal posés interviennent dans une multitude de domaines. Citons, par exemple, l'imagerie médicale (comme illustré plus haut pour la tomographie), le radar (détermination de la forme d'un obstacle) la mécanique quantique, ou encore le traitement d'image (restauration d'images floues). Parmi les opérateurs intervenant dans ces problèmes, détaillons en particulier ceux de deux modèles qui nous serviront souvent dans la suite, afin d'appliquer les procédures que nous avons développées à des problématiques concrètes.

Donnons premièrement le problème de déconvolution que nous considérons sous la forme suivante :
- $\mathbb{H} = \mathbb{K}$ est l'ensemble des fonctions $1-$ périodiques de carré intégrable pour la norme $\mathbb{L}^2([0,1], dx)$,
- K est donné par :

$$\forall f \in \mathbb{H},\ Kf(u) = \int_0^1 \gamma(u-t)f(t)dt \in \mathbb{H}$$

où γ est une fonction connue de $\mathbb{H}$.

Il s'agit de l'un des problèmes inverses les plus connus, et possède de nombreuses applications pratiques notamment en traitement du signal (voir par exemple Bertero et Boccacci [10], Harsdorf et Reuter [50] ou Johnstone et al [53]).

Deuxièmement, nous serons amenés à travailler sur le problème de Wicksell, que nous considérerons sous la forme donnée par Johnstone et Silverman [54] :
- $\mathbb{H} = \mathbb{L}^2([0,1], d\mu)$, $d\mu(x) = (4x)^{-1}dx$, $\mathbb{K} = \mathbb{L}^2([0,1], d\lambda)$, $d\lambda(x) = 4\pi^{-1}(1 - y^2)^{1/2}dy$,
- K est donné par :

$$Kf(y) = \frac{\pi}{4}y(1-y^2)^{-1/2}\int_y^1 (x^2 - y^2)^{-1/2}f(x)d\mu.$$

Dans un cadre statistique, ce modèle correspond au problème d'estimation de la loi suivie par des rayons de sphères réparties uniformément dans un milieu, lorsque l'on ne dispose que d'observations sur les rayons des disques obtenus par une coupe plane à travers le milieu (des précisions seront données plus loin). Il a des applications en biologie et en stéréologie, voir par exemple Nychka et al. [76] ou Antoniadis et al. [6].

Nous nous sommes intéressés tout particulièrement à ces deux modèles parce qu'ils correspondent à des comportements très différents du point de la SVD, et constituent donc des modèles tests intéressants, car complémentaires, pour les procédures d'estimation développées.

Notons enfin que par la suite nous nous concentrerons uniquement sur les problèmes inverses où K est un opérateur linéaire. Mais bien entendu de nombreux problèmes non linéaires existent aussi, comme certains problèmes d'estimation de paramètres dans des équations différentielles ou aux dérivées partielles. Toutefois, en statistique, les travaux sur l'approche non linéaire sont assez rares.

1.1.2 Modélisation statistique

Dans cette thèse, nous nous plaçons dans un cadre statistique, dans lequel la perturbation qui affecte g est représentée à l'aide d'un modèle aléatoire. On se donne donc un espace de probabilité $(\Omega, \mathcal{A}, P)$. De plus nous considérons que $\mathbb{H}$ et $\mathbb{K}$ sont deux espaces de Hilbert de dimension infinie, et nous aurons donc recours aux notions et aux outils de la statistique non paramétrique.

Dans ce cadre, il y a principalement deux modèles pour les problèmes inverses. Donnons d'abord la modélisation par un bruit blanc additif, qui sert de cadre d'étude à de nombreuses procédures d'estimation (dont la majeure partie de celles développées dans cette thèse) :

Définition 1.1.1. *Soient $\mathbb{H}$ et $\mathbb{K}$ deux espaces de Hilbert, $K : \mathbb{H} \mapsto \mathbb{K}$ un opérateur linéaire et $\varepsilon > 0$. Les paramètres K et ε sont déterministes et connus. On suppose que l'on observe Y_ε défini par :*

$$Y_\varepsilon = Kf + \varepsilon\dot{W}, \tag{1.2}$$

où $\dot{W}$ est un bruit blanc sur $\mathbb{K}$: pour tout couple $g, h \in \mathbb{K}$, $\xi(g) := (\dot{W}, g)_{\mathbb{K}}$, $\xi(h) := (\dot{W}, h)_{\mathbb{K}}$ est un vecteur gaussien centré de variance marginale $\|g\|_{\mathbb{K}}^2$, $\|h\|_{\mathbb{K}}^2$, et de covariance $(g, h)_{\mathbb{K}}$ (et on a une loi analogue dans le cas de k fonctions au lieu de 2).

Ici ε représente l'amplitude du bruit. Les performances des techniques d'estimation sont évaluées en fonction de ce paramètre d'un point de vue asymptotique, ce qui signifie que $f_\varepsilon - f$ doit tendre le plus vite possible vers 0 quand ε tend vers 0. Par la suite, nous serons parfois amenés à enlever l'indice ε pour Y (ou certaines quantités relatives à Y) pour alléger les notations. Pour être plus précis, le modèle 1.2 signifie que l'on observe une réalisation de l'application $Y^* : \Omega \mapsto \mathbb{K}^*$ (où $\mathbb{K}^*$ désigne l'espace dual de $\mathbb{K}$) définie par $Y_g^* := (Y_\varepsilon, g)_{\mathbb{K}}$, et dont la loi est décrite par :

$$\forall g \in \mathbb{K}, \quad Y_g^* = (Kf, g)_{\mathbb{K}} + \varepsilon \xi(g),$$

où $\xi(g) \sim N(0, \|g\|^2)$, et Y_g^*, Y_h^* sont des variables aléatoires indépendantes quand g et h sont deux fonctions orthogonales.

En pratique, de nombreux problèmes inverses sont aussi décrits par un modèle d'estimation de densité, défini comme suit :

Définition 1.1.2. *Soient $\mathbb{H}$ et $\mathbb{K}$ deux espaces de Hilbert, $K : \mathbb{H} \mapsto \mathbb{K}$ un opérateur linéaire et $n \in \mathbb{N}^*$. Les paramètres K et n sont déterministes et connus.*
Soit un échantillon (non observable) de variables aléatoires indépendantes identiquement distribuées $X_1, \ldots, X_n$, dont la loi de probabilité admet une densité f par rapport à la mesure sur $\mathbb{H}$, et supposons que l'on observe un échantillon de variables indépendantes identiquement distribuées $Y_1, \ldots, Y_n$, dont la loi de probabilité admet une densité f_2 par rapport à la mesure sur $\mathbb{K}$, et qui est liée à la fonction f par la relation :

$$f_2 = Kf. \tag{1.3}$$

Ici, le nombre d'observations n remplace le paramètre ε du modèle précédent, et l'asymptotique correspond à $n \to \infty$. Ce modèle de densité est souvent équivalent au modèle de bruit blanc, c'est à dire que l'on a des vitesses minimax du même ordre en posant $\varepsilon = \frac{1}{\sqrt{n}}$. Plus loin, nous aurons recours à ce modèle pour un opérateur bien précis, mais pour la suite de cette section 1.1 et dans l'essentiel du chapitre 2 nous nous plaçons dans le cadre du modèle 1.2.

En pratique, le caractère mal posé du problème signifie que l'opérateur lisse les fonctions sources, si bien que le problème d'estimation est plus difficile qu'un simple problème de débruitage. En effet, le bruit présent dans les observations Y_ε a tendance à être amplifié quand on cherche à lui appliquer K^{-1}. Si l'on quantifie le degré de lissage par un paramètre $\nu > 0$ (appelé degré d'"ill posedness" en anglais), cette difficulté se traduit sur le plan théorique par des vitesses minimax plus lentes que dans les cas d'observation directe. Ainsi, les procédures optimales d'estimation pour les problèmes inverses ont des vitesses de convergence plus lentes que les procédures classiques en régression et en estimation de densité, par exemple.

1.1.3 Principales méthodes d'estimation

La résolution d'un problème inverse mal posé passe par une régularisation, qui consiste à le transformer en une famille de problèmes bien posés dont les solutions servent d'approximation à la solution du modèle initial. Puis, on choisit l'une de ces solutions en ajustant des paramètres de régularisation, de façon à gagner au maximum en stabilité tout en contrôlant l'erreur d'approximation commise en modifiant le problème.

Dans cette optique, de nombreuses méthodes d'estimation pour les problèmes inverses linéaires ont été développées depuis plusieurs décennies, et les résumer toutes en quelques pages serait impossible. Néanmoins, introduisons la description suivante qui, bien que très schématique, convient à plusieurs procédures bien connues, ainsi (à quelques différences près) qu'aux méthodes proposées dans cette thèse. Nous proposons une classification plus précise dans le chapitre 5, qui permet une étude plus détaillée des principales procédures.

PRINCIPE GENERAL D'ESTIMATION :

- (i) On se ramène à un modèle séquentiel en choisissant une base $(u_l)_{l \in L}$ de $\mathbb{H}$ et une base $(v'_l)_{l' \in L'}$ de $\mathbb{K}$, où L et L' sont deux ensembles dénombrables d'indices. On décompose f sur la première ($f = \sum_{l \in L} c_l u_l$) et Y sur la seconde, ce qui donne, en notant $y_{l'} = (Y, v_{l'})_{\mathbb{K}}$:
$$y_{l'} = \sum_{l \in I_\varepsilon} (Ku_l, v_{l'}) c_l + \varepsilon \xi_{l'}.$$

- (ii) On calcule la solution $\widetilde{c}$ du problème correspondant à un bruit nul :
$$y_{l'} = \sum_{l \in I_\varepsilon} (Ku_l, v_{l'}) \widetilde{c}_l, \quad \forall l' \in L'_\varepsilon.$$
où $L_\varepsilon \subset L$ et $L'_\varepsilon \subset L'$ sont généralement des ensembles finis d'indices.

- (iii) On obtient des coefficients débruités $\hat{c}$ en appliquant un filtre λ_ε aux coefficients $\widetilde{c}$: $\hat{c} = \lambda_\varepsilon(\widetilde{c})$, et on obtient un estimateur $\hat{f}$ de f :
$$\hat{f} = \sum_{l \in L_\varepsilon} \hat{c}_l u_l.$$

Dans ce schéma, la régularisation du problème consiste d'une part en une troncature éventuelle du modèle séquentiel à l'étape (ii) où l'on ne considère qu'une partie des indices, et d'autre part en un lissage des données à l'étape (iii). En effet nous verrons que le filtrage λ_ε revient à multiplier les données $Y(v_{l'})$ (ou plus généralement une famille de combinaisons linéaires de celles ci) par une suite de poids pénalisant les données les plus bruitées. Ainsi, on s'est ramené à un problème bijectif et stable, c'est à dire, bien posé.

Le problème du choix des deux bases est crucial, puisque de lui dépend le coût et l'efficacité de la méthode lors des deux étapes suivantes. En effet, le choix de bases inadaptées

à l'opérateur conduit à des difficultés dans l'étape (ii), nécessitant d'inverser des matrices non creuses de grandes dimensions. D'autre part le choix d'une base (u_l) inadaptée à la fonction cible conduit à un problème de débruitage compliqué, car alors on obtient après (ii) une multitude de coefficients bruités, dont on mesure mal l'importance, et donc difficiles à filtrer. Ces deux problèmes seront illustrés plus loin.

Etant donné ce cadre général, on peut distinguer trois approches correspondant essentiellement à trois choix différents de bases.

Décomposition en valeurs singulières (SVD)

Commençons par énoncer le résultat suivant, qui joue un rôle primordial dans l'étude des problèmes inverses depuis quelques dizaines d'années :

Théorème 1.1.1. *Si K est un opérateur compact, alors il existe deux bases orthonormées $(e_l)_{l \in \mathbb{N}}$ de $\mathbb{H}$ et $(g_l)_{l \in \mathbb{N}}$ de $\mathbb{K}$, et une suite $(b_l)_{l \in \mathbb{N}}$, $b_l \to 0$ quand $l \to \infty$, telles que*

$$Ke_l = b_l g_l, \quad K^* g_l = b_l e_l,$$

où K^* désigne l'opérateur adjoint de K.

Ces deux bases seront appelées par la suite bases SVD. Notons aussi que $b_l > 0$ pour tout l sous l'hypothèse d'injectivité de K.

En adoptant le cadre introduit précédemment, la procédure consiste à choisir dans l'étape (i) les bases $(u_l) = (e_l)$ et $(v_l) = (g_l)$, ce qui donne un modèle séquentiel équivalent au modèle hétéroscédastique bien connu :

$$y_{l'} = (K \sum_l c_l e_l, g_{l'}) + \varepsilon \xi(g_{l'}) = b_{l'} c_{l'} + \varepsilon \xi_{l'}.$$

Le problème est diagonal donc l'étape (ii) est très simple :

$$\widetilde{c}_l = \frac{y_l}{b_l}.$$

Enfin, pour débruiter on applique un filtre formé par une suite $\lambda_k \in [0, 1]$ aux coefficients $\widetilde{c}$:

$$\forall l \in \mathbb{N}, \hat{c}_l = \lambda_l \widetilde{c}_l.$$

De nombreuses méthodes de filtrage ont été proposées, en voici quelques exemples :
  – La troncature spectrale :
$$\begin{cases} \lambda_l & = 1 \quad \text{si } l \leq N, \\ \lambda_l & = 0 \quad \text{si } l > N, \end{cases}$$

  – La régularisation de Tikhonov :
$$\lambda_l = \frac{b_l^2}{b_l^2 + \alpha^2},$$

– Les filtres de Tikhonov-Phillips :

$$\lambda_l = \frac{1}{1 + (l/\alpha)^\beta},$$

– Les filtres de Pinsker :

$$\lambda_l = (1 - (l/\alpha)^\beta)_+,$$

avec la notation $x_+ = \max(0, x)$.

Toutes ces méthodes nécessitent d'ajuster un ou plusieurs paramètres (N, α, β), ce qui se fait souvent de manière non adaptative par minimisation d'un majorant du risque de l'estimateur. Une méthode adaptative, c'est à dire permettant d'effectuer automatiquement cet ajustement sans information a priori sur la fonction cible, a été développée dans Cavalier et Tsybakov [16]. On y considère des filtres à valeurs constantes sur des blocs d'indices $I_j = [\kappa_{j-1}, \kappa_j - 1]$ avec $\kappa_0 = 1$ et $\kappa_J = N + 1$ déterminés par :

$$\begin{cases} \lambda_l = \left(1 - \frac{\sigma_j^2(1 + \Delta_j^\gamma)}{\|\bar{Y}\|_{(j)}^2}\right)_+ & \text{si } l \in I_j, \ j = 1, \dots J, \\ \lambda_l = 0 & \text{si } l > N, \end{cases}$$

avec :

$$\bar{Y}_l = \frac{Y_l}{b_l}, \quad \|\bar{Y}\|_{(j)}^2 = \sum_{l \in I_j} \bar{Y}_l^2, \quad \sigma_j^2 = \varepsilon^2 \sum_{l \in I_j} b_l^{-2}, \quad \Delta_j = \frac{\max_{l \in I_j} b_l^{-2}}{\sum_{l \in I_j} b_l^{-2}}, \quad 0 < \gamma < 1/2.$$

Et étant donné $\nu_\varepsilon \sim \max(5, \log\log(1/\varepsilon))$ et $\rho_\varepsilon = \frac{1}{\log(\nu_\varepsilon)}$, les blocs sont donnés par :

$$\begin{cases} \kappa_j = 1 & \text{si } j = 0, \\ \kappa_j = \nu_\varepsilon & \text{si } j = 1, \\ \kappa_j = \kappa_{j-1} + \lfloor \nu_\varepsilon \rho_\varepsilon (1 + \rho_\varepsilon)^{j-1} \rfloor & \text{si } j = 2, \dots, J, \end{cases}$$

pour un J suffisamment grand satisfaisant : $\kappa_J > \max\{m : \sum_{l=1}^m b_l^{-2} \leq \varepsilon^{-2} \rho_\varepsilon^{-3}\}$.

D'un point de vue numérique, le principal point fort de toutes ces méthodes est la rapidité et la stabilité de l'inversion de l'opérateur. Sur le plan théorique, l'optimalité asymptotique des estimateurs SVD a été établie dans de nombreuses situations. Citons par exemple Mathé et Pereverzev [65], Cavalier et al. [17], Tsybakov [88], Goldenshluger et Pereverzev [43], qui font l'hypothèse de décroissance polynomiale des valeurs propres : $b_k \asymp k^{-\nu}$ (où ν est le degré d'ill posedness). Des travaux ont aussi été faits dans le cas des problèmes sévèrement mal posés, c'est à dire avec une décroissance exponentielle des valeurs propres b_k (voir par exemple Golubev [44], Cavalier et al. [18] ou Butucea [13]). Par ailleurs il est à noter que l'hypothèse usuelle de compacité n'est en fait pas indispensable, pour implémenter la SVD. Certains opérateurs peuvent avoir des décompositions spectrales sans être compacts, et des méthodes SVD dans ce cas ont été développées par Cavalier [15].

L'approche SVD présente néanmoins quelques inconvénients. Premièrement, il existe des cas où les bases e et g sont difficiles à déterminer ou à manipuler numériquement, et l'estimateur est donc compliqué à implémenter. Deuxièmement, la base e servant à décomposer

la fonction cible est entièrement déterminée par l'opérateur et n'est donc pas forcément adaptée pour décrire f. Prenons l'exemple de l'opérateur de déconvolution, pour lequel $e_k(t) = g_k(t) = exp(2i\pi kt)$, et d'une fonction cible présentant de fortes variations locales (comme c'est souvent le cas en pratique) représentée sur la figure 1.2. Dans ce cas la décomposition de Fourier est peu lisible (voir la figure 1.3) : on obtient une multitude de grands coefficients dont on mesure mal l'importance quant aux caractéristiques locales de f. Ainsi il sera difficile de filtrer un spectre de ce type s'il est contaminé par du bruit.
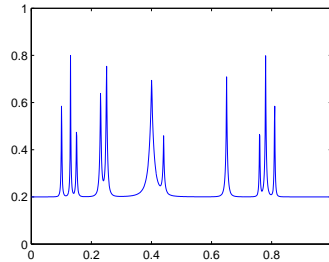
FIG. 1.2 –   La fonction 'Bumps'
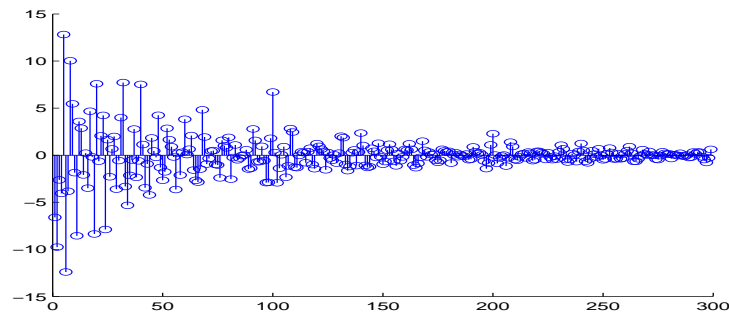
FIG. 1.3 –   Coefficients de Fourier de la fonction 'Bumps'

Cette observation se traduit aussi par des limites sur le plan théorique : on est restreint à étudier le risque de l'estimateur mesuré uniquement en norme hilbertienne et sur des espaces du type $\mathcal{F} = \{f = \sum c_k e_k, \ \sum a_k c_k^2 \leq M\}$, pour une suite a donnée décrivant la régularité des fonctions cibles. Ainsi, on ne peut mesurer les performances minimax de telles procédures que sur des espaces fonctionnels dépendant de l'opérateur, par le biais de la base e_k. Pourtant en pratique il n'y a souvent aucune raison de supposer qu'il y ait un lien entre la cible et l'opérateur.

Ondelettes et Vaguelettes

Une solution idéale serait évidemment d'avoir à la fois un problème d'inversion simple et un débruitage efficace, c'est à dire d'avoir des bases qui "diagonalisent à la fois l'opérateur K et l'information a priori sur f" pour reprendre les termes de Donoho (dans Donoho [35]). Trouver de telles bases est malheureusement impossible dans l'absolu, mais Donoho

propose une méthode valable pour une classe assez large d'opérateurs : la décomposition "Wavelet-Vaguelette" (WVD).

L'outil principal est l'analyse multirésolution des fonctions cibles à l'aide d'une base d'ondelettes. Nous faisons quelques rappels sur la théorie des ondelettes en section 1.2, mais on peut déjà illustrer l'intérêt que présentent de telles bases dans notre problématique, comme dans la figure 1.4. Celle ci est à mettre en parallèle avec 1.3 et représente tous les coefficients de "détail" de l'analyse multirésolution de la fonction 'Bumps' déjà présentée. Contrairement à la décomposition de Fourier, on a un nombre réduit de grands coefficients d'ondelettes, qui sont localisés aux endroits de l'intervalle où 'Bumps' varie beaucoup, et qui contiennent l'essentiel de l'information contenue dans la fonction. On comprend aisément que le problème de débruitage sera beaucoup plus facile dans ce cas que dans le précédent : il suffit de ne garder que les coefficients supérieurs à un seuil choisi suffisamment grand pour que les coefficients "oubliés" ne représentent essentiellement que du bruit.
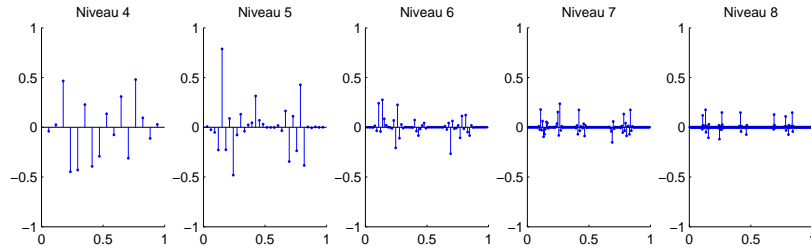
FIG. 1.4 – Coefficients de détail d'ondelettes de la fonction 'Bumps'

L'approche WVD repose donc sur l'hypothèse suivante sur l'opérateur. Il existe une base d'ondelettes (ψ_λ) et une base (w_λ) telles que pour une suite $\beta_j > 0$ (qui dépend typiquement de l'ill posedness) :

$$\forall l = (j,k), \quad K^* w_l = \beta_j \psi_l$$

et (w_l) soit une famille de vaguelettes, c'est à dire une famille de fonctions possédant des propriétés similaires à celles des ondelettes, comme la localisation, mais ne sont pas forcément orthogonales ni issues d'une fonction mère présentant toutes les caractéristiques d'une vraie ondelette. Tout ceci est détaillé par Donoho [35] et Meyer [68].

La méthode consiste à choisir $u = \psi$ et $v = w$. Comme dans la SVD le modèle séquentiel est très simple. Pour $l = (j,k)$:

$$y_{l'} = (K \sum_l c_l \psi_l, w_{l'}) + \varepsilon \xi(w_{l'}) = \sum c_l (K \psi_l, w_{l'}) + \varepsilon \xi(w_{l'})$$
$$= \sum c_l (\psi_l, K^* w_{l'}) + \varepsilon \xi(w_{l'}) = \sum c_l (\psi_l, \beta_j \psi_{l'}) + \varepsilon \xi(w_{l'}) = \beta_j c_{l'} + \varepsilon \xi(w_{l'}).$$

Donc la solution du problème sans bruit est :

$$\widetilde{c}_l = \frac{y_l}{\beta_j},$$

et enfin on débruite par un seuillage doux :

$$\hat{c}_l = sgn(\widetilde{c}_l)(|\widetilde{c}_l| - t_j)_+,$$

ou dur :

$$\hat{c}_l = \widetilde{c}_l I\{|\widetilde{c}_l| > t_j\}.$$

Avec un bon choix d'une suite de seuils t_j, l'estimateur obtenu est asymptotiquement optimal sur des boules d'espaces de Besov et pour une perte $L^2(dx)$.

Mentionnons ici également la décomposition Vaguelette-Wavelet (VWD) qui est une méthode jumelle de la WVD et qui a été développée par Abramovich et Silverman [1]. Notons $K^{-1} : Im(K) \to \mathbb{H}$ "l'inverse" de K et supposons que l'on dispose d'une base d'ondelettes $\psi_{j,k}$ appartenant à $Im(K)$ et telle que pour une suite $\beta_{j,k}$ bien choisie la famille $w_{j,k} = K^{-1}\psi_{j,k}/\beta_{j,k}$ soit une famille de vaguelettes. Alors à l'inverse de WVD, VWD consiste à utiliser les bases $u = w$ et $v = \psi$ ce qui donne :

$$y_{l'} = (K \sum_l c_l w_l, \psi_{l'}) + \varepsilon\xi(\psi_{l'}) = c_{l'}/\beta_{l'} + \varepsilon\xi(w_{l'}).$$

D'où :

$$\widetilde{c}_l = \beta_l y_l,$$

puis on débruite comme précédemment par seuillage doux ou dur.

Bien entendu, la condition imposée sur l'opérateur restreint les champs d'application de WVD et VWD. WVD s'applique à de nombreux opérateurs homogènes (par rapport à la dilatation) tels que l'intégration, l'intégration fractionnelle et la transformée de Radon. Il peut aussi être utilisé dans le cas de certains opérateurs non homogènes, comme la convolution. En revanche, il ne s'applique pas par exemple au problème de Wicksell (cf Antoniadis et al. [6]). De même VWD nécessite des restrictions similaires à celles de WVD.

Ondelettes et projection de Galerkin

Les méthodes SVD et de vaguelettes nécessitent l'utilisation de bases fortement liées à l'opérateur K. Ainsi, leur implémentation est difficile, voire impossible dans certains cas comme les opérateurs intégraux dont les noyaux ont une structure compliquée.

Pour pallier à cet inconvénient, plusieurs méthodes ont été développées dans Cohen et al. [24]. L'idée principale est d'adapter au cadre statistique le principe de projection de Galerkin, qui consiste, à l'origine, à résoudre des problèmes linéaires sans bruit en se ramenant à un problème discrétisé de dimension finie de forme matricielle.

Les méthodes sont développées dans le cas $\mathbb{H} = \mathbb{K}$ (mais avec une généralisation simple au cas $\mathbb{H} \neq \mathbb{K}$). Une première méthode non adaptative consiste à effectuer l'étape (i) avec $u = v = \psi$ où ψ est une base d'ondelettes dont le choix est entièrement libre. Le débruitage se fait avant l'inversion en appliquant un algorithme de seuillage dur aux observations y_k, et enfin l'étape (ii) se fait grâce à la méthode de Galerkin, avec un choix des ensembles finis d'indices I_ε et J_ε dépendant de la régularité de f. Une méthode adaptative est également proposée avec une évaluation du coût de calcul de la procédure en fonction de ε et une application concrète sur un opérateur à noyau.

Les estimateurs, ainsi obtenus, sont optimaux du point de vue minimax dans un cadre similaire à celui de WVD et VWD, à savoir pour f appartenant à une boule d'espace de Besov et pour un risque mesuré avec la norme Hibertienne sur $\mathbb{H}$.

1.1.4 Problèmes inverses à opérateurs aléatoires

Toutes les méthodes décrites à la section précédente traitent des problèmes inverses modélisés par 1.2 avec un opérateur K déterministe et connu. Récemment, des travaux ont également été réalisés dans le cas où K lui même est aléatoire. Nous traiterons d'un modèle de ce type dans le chapitre 6. Pour illustrer les motivations, donnons ici deux exemples de modélisation.

Premièrement, plusieurs travaux ont traité récemment la généralisation du modèle 1.2 au cas où l'on a deux erreurs de mesures indépendantes qui se superposent : l'une d'amplitude ε sur Kf (comme dans 1.2), et une autre d'amplitude δ sur K. Le système est donc régi par un opérateur déterministe inconnu dont on n'observe qu'une approximation aléatoire : $K_\delta = K(f) + \delta\zeta$, et on souhaite estimer f en fonction des observations $(Y_\varepsilon, K_\delta)$. Ces problèmes, appelés modèles à opérateurs bruités, ont fait l'objet de développement de procédures spécifiques tant par l'approche SVD (Cavalier et Hengartner [19]), que par l'approche Galerkin (Cohen et al. [23]). Une étude du risque minimax pour de tels problèmes a été faite dans Efromovich et Koltchinskii [38].

Dans une optique complètement différente, la modélisation par un opérateur aléatoire apparaît naturellement, par exemple, lorsque l'évolution future d'un système étudié dépend de son évolution passée. Ceci regroupe de nombreuses situations pratiques, dont notamment celles modélisées par les équations stochastiques avec retard qui sont données par :

$$dX_n(t) = \left(\int_0^r X_n(t-s)f(s)ds \right)dt + \sigma n^{-1/2}dW(t) \quad \forall t \geq 0,$$
$$X_n(t) = F(t) \quad \forall t \in [-r, 0].$$

On a ici un opérateur aléatoire lié au passé du processus. De nombreux résultats sur l'estimation de f dans ce type de problème sont donnés dans Reiss [83] et Reiss [82]. Nous verrons que ce modèle se rapproche de celui étudié au chapitre 6.

Pour notre part, nous introduirons, au chapitre 6, une modélisation nouvelle de problèmes à opérateurs aléatoires.

1.2   Quelques notions de statistique non paramétrique

1.2.1   L'approche minimax

Dans cette section, nous rappelons un point de vue théorique classique pour mesurer la performance d'une procédure d'estimation, à savoir le point de vue minimax.

Supposons que l'on dispose de n observations $X_1, \ldots, X_n$ issues d'un modèle statistique noté $(\mathcal{X}^n, \mathcal{A}^n, \mathbb{P}_f^n, f \in \mathcal{F}(\mathbb{R}^d, \mathbb{R}^{d'}))$ où $\mathcal{F}(\mathbb{R}^d, \mathbb{R}^{d'})$ désigne l'ensemble des applications de $\mathbb{R}^d$ dans $\mathbb{R}^{d'}$. Soit $\hat{f}_n$ un estimateur construit à partir $X_1, \ldots, X_n$, et soit ρ une fonction de perte (par exemple une perte de type L^p, ou issue des normes associées aux espaces de Sobolev, Hölder ou Besov). Alors le risque de l'estimateur $\hat{f}_n$ est défini par :

$$R_n^\rho(\hat{f}_n, f) = E(\rho(\hat{f}_n, f)).$$

Il représente l'erreur moyenne que l'on commet en estimant f par $\hat{f}_n$. L'approche minimax asymptotique consiste à étudier le comportement de cette erreur en fonction de n lorsque celui ci tend vers l'infini, et lorsque l'on considère la plus grande erreur possible quand f appartient à un espace $V \subset \mathcal{F}(\mathbb{R}^d, \mathbb{R}^{d'})$. Sous cet angle, la difficulté du problème d'estimation est représentée par le risque minimax :

$$\mathcal{R}_n^\rho(V) = \inf_{\hat{f}_n} \sup_{f \in V} E(\rho(\hat{f}_n, f)),$$

où l'infimum est pris sur l'ensemble des estimateurs. Bien entendu, l'idéal pour avoir une idée exhaustive de cette difficulté serait de poser $V = \mathcal{F}(\mathbb{R}^d, \mathbb{R}^{d'})$, mais il a été établi que l'on ne pouvait pas avoir de résultat de convergence dans un cadre aussi général. Ceci signifie grossièrement que tout estimateur sera forcément erroné, même avec une infinité d'observations, pour certaines fonctions f. On ne peut donc pas discriminer les estimateurs sous ces conditions.

Ainsi pour avoir un risque minimax convergent vers 0 et de façon quantifiable, on doit se restreindre à des espaces V qui imposent à f d'avoir un minimum de régularité, comme des boules d'espace de Sobolev, Hölder ou Besov. Dans ce cadre, on appelle vitesse minimax la suite r_n (si elle existe) telle que, avec c et C indépendantes de n :

$$cr_n \leq \mathcal{R}_n^\rho(V) \leq Cr_n,$$

et un estimateur $\hat{f}_n$ sera dit asymptotiquement optimal au sens minimax s'il existe C tel que :

$$\sup_{f \in V} E(\rho(\hat{f}_n, f)) \leq Cr_n.$$

Toute la théorie s'étend naturellement aux modèles de type bruit blanc tels que ceux introduits précédemment (voir la définition 1.2) avec $\varepsilon = \frac{1}{\sqrt{n}}$ remplaçant n.

1.2.2 Ondelettes

Nous faisons ici quelques rappels sommaires sur les ondelettes qui jouent un rôle fondamental en estimation non paramétrique, et auxquelles nous nous référons pour toutes les procédures d'estimation développées dans cette thèse. La construction de ces bases orthonormées repose sur l'analyse multirésolution.

Définition 1.2.3. *On appelle analyse multirésolution de $L^2(\mathbb{R})$ toute suite croissante de sous espaces fermés de $L^2(\mathbb{R})$, $(V_j)_{j \in \mathbb{Z}}$, vérifiant les propriétés suivantes :*

1. *$\bigcap_{j \in \mathbb{Z}} V_j = \{0\}$,*

2. *$\bigcup_{j \in \mathbb{Z}} V_j$ est dense dans $L^2(\mathbb{R})$,*

3. *$\forall f \in L^2(\mathbb{R}), \ \forall j \in \mathbb{Z}, \ f(x) \in V_j \Leftrightarrow f(2x) \in V_{j+1}$,*

4. *$\forall f \in L^2(\mathbb{R}), \ \forall k \in \mathbb{Z}, \ f(x) \in V_0 \Leftrightarrow f(x - k) \in V_0$,*

5. *il existe une fonction $\varphi \in V_0$, appelée fonction d'échelle de l'analyse multirésolution, telle que $\{\varphi(x - k), \ k \in \mathbb{Z}\}$ soit une base orthonormée de V_0.*

A chaque niveau de résolution j, l'espace V_j possède une base orthonormée obtenue par translations et dilatations de la fonction d'échelle $\varphi : \{\varphi_{j,k}(x) = 2^{j/2}\varphi(2^j x - k), \ k \in \mathbb{Z}\}$. La projection de toute fonction f de $L^2(\mathbb{R})$ sur l'espace V_j constitue une approximation de celle-ci au niveau de résolution j. Sa projection sur l'espace supplémentaire orthogonal W_j de V_j correspond à la différence d'approximation $P_{j+1}f - P_j f$ (où P_j représente l'opérateur de projection de $L^2(\mathbb{R})$ sur l'espace V_j) et représente les "détails" de f au niveau de résolution j. Il est alors possible de construire une fonction, appelée ondelette mère, de telle sorte que $\{\psi_{j,k}(x) = 2^{j/2}\psi(2^j x - k), \ k \in \mathbb{Z}\}$ soit une base orthonormée de W_j. Ainsi :

$$V_j = vect\{ \ \varphi_{j,k}, \ k \in \mathbb{Z}\}, \quad W_j = vect\{ \ \psi_{j,k}, \ k \in \mathbb{Z}\},$$

et pour tout entier naturel j_0, toute fonction f de $L^2(\mathbb{R})$ peut se décomposer comme suit :

$$f = \sum_{k \in \mathbb{Z}} \alpha_{j_0,k} \varphi_{j_0,k} + \sum_{j \geq j_0} \sum_{k \in \mathbb{Z}} \beta_{j,k} \psi_{j,k},$$

où les coefficients d'ondelettes sont définis par :

$$\alpha_{j,k} = \int f(x)\varphi_{j,k}(x)dx, \quad c_{j,k} = \int f(x)\psi_{j,k}(x)dx.$$

Comme nous le mentionnons à la section suivante, ces bases possèdent des propriétés particulièrement intéressantes dans le cadre des espaces de Besov. La régularité des fonctions φ et ψ y joue un rôle important. Pour des exemples de système d'ondelettes et la notion de régularité, on pourra se référer à Daubechies [26], Härdle et al. [49] ou Mallat [64].

1.2.3   Espaces de Besov

Nous donnons ici quelques éléments utiles sur les espaces de Besov forts. Ceux ci constituent une très grande classe d'espaces fonctionnels, incluant en particulier l'espace de Sobolev H_s ($H_s = B_{2,2}^s$) et l'espace de Hölder Λ^s ($\Lambda^s = B_{1,1}^s$ si $0 < s \neq \mathbb{N}$). Ils sont définis à partir d'un module de continuité comme suit.

Notons pour tout $(x, h) \in \mathbb{R}^2$, $\Delta_h f(x) = f(x - h) - f(x)$ et $\Delta_h^2 f = \Delta_h(\Delta_h(f))$. Pour tout $0 < s < 1, 1 \leq p \leq \infty, 1 \leq q < \infty$, on définit :

$$\gamma_{spq}(f) = \big[(\frac{\|\Delta_h f\|_p}{|h|^s})^q \frac{dh}{|h|}\big]^{1/q},$$

et

$$\gamma_{sp\infty}(f) = \sup_{h \in \mathbb{R}^*} \frac{\|\Delta_h f\|_p}{|h|^s}.$$

Lorsque $s = 1$, on pose

$$\gamma_{1pq}(f) = \big[(\frac{\|\Delta_h^2 f\|_p}{|h|})^q \frac{dh}{|h|}\big]^{1/q},$$

$$\gamma_{1p\infty}(f) = \sup_{h \in \mathbb{R}^*} \frac{\|\Delta_h^2 f\|_p}{|h|}.$$

Pour tout $0 < s \leq 1, 1 \leq p, q \leq \infty$, l'espace de Besov fort de paramètres s, p et q, noté $B_{p,q}^s$ est défini par :

$$B_{p,q}^s = \{f \in L^p(\mathbb{R}) : \gamma_{spq}(f) < \infty\},$$

muni de la norme :

$$\|f\|_{\Gamma_{spq}} = \|f\|_p + \gamma_{spq}(f).$$

Dès lors que $s = [s] + \alpha$, avec $[s] \in \mathbb{N}$ et $0 < \alpha \leq 1$, on dira que $f \in B_{p,q}^s$ si et seulement si $f^{(m)} \in B_{p,q}^\alpha$, pour tout $m \leq [s]$. Cet espace est muni de la norme :

$$\|f\|_{\Gamma_{spq}} = \|f\|_p + \sum_{m \leq [s]} \gamma_{\alpha pq}(f).$$

Plaçons nous maintenant dans un cadre d'analyse multirésolution comme décrit à la section précédente. On a alors le résultat suivant, qui donne une caractérisation des espaces de Besov forts à partir d'une notion de vitesse d'approximation.

Théorème 1.2.2. *Soient $N \in \mathbb{N}$, $0 < s < N + 1, 1 \leq p, q \leq \infty$ et (φ, ψ) un système "fonction d'échelle/ondelette" pour lequel il existe une fonction décroissante bornée H telle que :*

1. $\forall x, y, \quad |\sum_k \varphi(x - k)\varphi(y - k)| \leq H(|x - y|)$,

2. $\int H(u)|u|^{N+1}du < \infty$,

3. $\varphi^{(N+1)}$ existe et $\sup_{x \in \mathbb{R}} |\sum_k \varphi^{(N+1)}(x - k)| < \infty$.

Notons $P_j, j \geq 0$, les opérateurs de projection sur les espaces V_j. Alors f appartient à l'espace de Besov fort $B_{p,q}^s$ si et seulement si $f \in L^p(\mathbb{R})$ et s'il existe une suite de nombres positifs $(\varepsilon_j)_{j \in \mathbb{N}} \in L^q(\mathbb{N})$ telle que : $\forall j \in \mathbb{N}, \|f - P_j f\|_p \leq 2^{-js}\varepsilon_j$.

Les bases d'ondelettes sont donc très intéressantes pour décrire ce type d'espace. En effet (et ceci est probablement le point le plus important de ce paragraphe pour la suite) on peut montrer que l'on a la caractérisation suivante des espaces de Besov, et ce à l'aide de n'importe quelle base d'ondelettes suffisamment régulière.

Théorème 1.2.3. *Toute fonction $f \in L^p(\mathbb{R})$, dont les coefficients dans une base d'ondelettes fixée sont*

$$\alpha_{0,k} = \int f(x)\varphi_{0,k}(x)dx, \quad c_{j,k} = \int f(x)\psi_{j,k}(x)dx,$$

appartient à l'espace de Besov fort $B_{p,q}^s$ si et seulement si :

$$\|f\|_{B_{p,q}^s} = \|\alpha_{0,.}\|_{L^p} + \Big(\sum_{j \geq 0} 2^{jq(s-1/p+1/2)}\|c_{j,.}\|_{L^p}^q\Big)^{1/q} < \infty, \quad si \ q < \infty,$$

et

$$\|f\|_{B_{p,q}^s} = \|\alpha_{0,.}\|_{L^p} + \sup_{j \geq 0} 2^{j(s-1/p+1/2)}\|c_{j,.}\|_{L^p} < \infty, \quad si \ q = \infty.$$

De plus les normes $\|.\|_{B_{p,q}^s}$ et $\|.\|_{\Gamma_{spq}}$ sont équivalentes.

Chapitre 2

PRINCIPAUX RESULTATS ET PERSPECTIVES

Ce chapitre donne un premier aperçu des résultats de cette thèse, qui se trouvent dans leur intégralité dans les chapitres 3 à 7. Par souci de clarté, nous ne présentons pas ici chaque chapitre séparément, car les thèmes abordés se recoupent à plusieurs reprises. Essentiellement, la section 2.1 présente le principe général des méthodes d'estimation utilisées dans les chapitres 3 et 6. La section 2.2 donne les résultats d'optimalité minimax de celles ci, qui sont établies au cours des chapitres 4 et 6. La section 2.3 porte sur l'application au problème de Wicksell décrite au cours des chapitres 3 et 5. La section 2.4 porte sur l'application au modèle de convolution aléatoire du chapitre 6. Enfin la section 2.5 concerne le problème indépendant de régression du chapitre 7.

2.1 Principe général des méthodes d'estimation utilisées

Plaçons nous à nouveau dans l'optique du schéma général donné en 1.1.3 au chapitre 1. Nous allons décrire en parallèle la procédure du chapitre 3, appelée NeedVD, et celle dont s'inspire l'estimateur du chapitre 6, appelée WaveD, qui a été développée par Jonstone et al. [53]. Toutes les deux suivent le même principe. Pour simplifier, nous serons parfois amenés à regrouper les deux estimateurs sous le même nom, NeedVD, quitte à trahir un peu la terminologie.

L'objectif est d'avoir à la fois un problème d'inversion simple à résoudre, et une méthode de seuillage efficace. Ceci passe essentiellement par un bon choix de la famille de fonctions (u_l) servant à décomposer la fonction cible. L'idée principale est de construire des bases possédant des propriétés de localisation et présentant les avantages de l'analyse multirésolution, tout en s'exprimant simplement en fonction de la base SVD (e_l).

Parmi les trois approches décrites en 1.1.3, NeedVD se rapproche donc des méthodes de vaguelettes. Néanmoins la base localisée n'est pas quelconque, mais liée à l'opérateur, ce qui conduit à un autre choix de fonctions v que dans la méthode des vaguelettes. De plus NeedVD permet, par exemple, de traiter le problème de Wicksell, auquel WVD ne s'applique pas. Néanmoins comme les estimateurs SVD (et aussi souvent les estimateurs vaguelettes), NeedVD n'est pas implémentable dans le cas où les bases SVD sont trop difficiles à déterminer ou à manipuler.

2.1.1   Le scénario "ondelettes" et le scénario "jacobi"

Les résultats principaux du chapitre 3 sont établis dans deux cadres théoriques généraux qui correspondent à deux séries d'hypothèses sur le comportement de la famille de fonctions localisées servant à décomposer f.

On distingue ainsi le scénario "ondelettes", dans lequel la famille de needlets est supposée posséder des propriétés analogues à celles des ondelettes, et le scénario "jacobi" où leur comportement est sensiblement différent : il correspond notamment à une hétérogénéité des normes des needlets à résolution fixée suivant leur localisation, et de plus la famille de needlets peut ne pas être une base mais seulement une famille génératrice redondante.

Pour simplifier nous présentons dans ce chapitre les résultats dans les deux cadres plus restreints suivants, et qui correspondent aux cadres pour lesquels l'optimalité minimax des estimateurs a été établie.

Déconvolution

Le scénario "ondelettes" est illustré par le problème de déconvolution que nous avions déjà mentionné au chapitre 1. On se place dans le modèle de bruit blanc 1.2, avec :

1. $\mathbb{H} = \mathbb{K}$ est l'ensemble des fonctions $1-$ périodiques de carré intégrable pour la norme $\mathbb{L}^2([0,1], dx)$,

2. K est donné par

$$\forall f \in \mathbb{H},\ Kf(u) = \int_0^1 \gamma(u-t)f(t)dt \in \mathbb{H}$$

Le "filtre" γ est une fonction connue de $\mathbb{H}$, dont les caractéristiques déterminent la difficulté du problème d'estimation. Il intervient dans la décomposition en valeurs singulières au niveau des valeurs propres, qui sont égales aux coefficients de Fourier $\hat{\gamma}$ de γ :

$$b_k = \hat{\gamma}_k\cdot,$$

les fonctions propres étant, quant à elles, données par la base de Fourier : $\forall t \in [0,1],\ e_k = g_k = exp(2i\pi kt)$.

Modèle de type Jacobi

Nous donnerons les résultats du scénario "jacobi" pour le cadre suivant. On se place dans le modèle de bruit blanc 1.2, avec :

1. $\mathbb{H} = \mathbb{L}_2([-1,1], \mu)$, avec $d\mu(x) = c_{\alpha,\beta}\omega_{\alpha,\beta}(x)dx$ où

$$\omega_{\alpha,\beta}(x) = (1-x)^\alpha(1+x)^\beta; \quad \alpha, \beta > -1/2,$$

et $c_{\alpha,\beta}$ est une constante de normalisation : $\int_I d\mu(x) = 1$.

2. $K : \mathbb{H} \mapsto \mathbb{K}$ est un opérateur linéaire dont la première base SVD e_k vérifie :

$$e_k = P_k^{\alpha,\beta}$$

où $P_k^{\alpha,\beta}$ désigne le polynôme de Jacobi de type (α, β) et normalisé dans $L^2(d\mu)$ (voir par exemple Szegő [86]).

2.1.2   Inversion du modèle séquentiel et débruitage

Nous commençons par indiquer comment sont effectuées les étapes (ii) et (iii), qui sont très simples, et nous présentons le problème plus délicat du choix des bases à la section suivante.

La méthode diffère des méthodes citées au chapitre 1 notamment en ce que la famille u choisie n'est pas forcément libre, et donc il peut y avoir plusieurs solutions $\widetilde{c}$ au problème mis sous forme séquentielle. Mais dans les deux scénarios, u est au moins une frame. De plus on suppose qu'elle possède une structure "temps/fréquence" comme les ondelettes, donc nous noterons comme au chapitre 1 :

$$u_{j,k} = \psi_{j,k}.$$

On s'attache alors à la représentation suivante de f :

$$f = \sum_{j,k} c_{j,k}\psi_{j,k},$$

avec $c_{j,k} = (f, \psi_{j,k})_{\mathbb{H}}$. Deuxièmement, on choisit

$$(v_i)_{i\in\mathbb{N}} = (g_i)_{i\in\mathbb{N}}.$$

Alors, en utilisant la relation de Parseval, on vérifie qu'on a la solution suivante du problème séquentiel :

$$\widetilde{c}_{j,k} = \sum_i \frac{y_i}{b_i}(\psi_{j,k}, e_i).$$

Dans un deuxième temps, comme la base ψ est localisée, on peut débruiter ces coefficients simplement en effectuant un seuillage dur du type :

$$\hat{c}_{j,k} = \widetilde{c}_{j,k}I\{|\widetilde{c_{j,k}}| > \kappa 2^{\nu j}\varepsilon\sqrt{\log(\frac{1}{\varepsilon})}\},$$

pour tout j inférieur à un degré de résolution maximal J :

$$2^J = (\varepsilon\sqrt{\log(\frac{1}{\varepsilon})})^{-\frac{2}{1+2\nu}}.$$

Ainsi avec le choix des familles de fonctions u et v décrit dans ce que suit, on a à la fois un problème d'inversion facile à résoudre et une méthode de débruitage simple et efficace similaire au seuillage d'ondelettes.

2.1.3   Choix de base

Pour comprendre le principe de construction des fonctions $\psi_{j,k}$ regardons sous quelles conditions l'estimateur est performant, ce qui passe en particulier par une étude des erreurs faites sur chaque composante de f à l'étape (ii) :

$$(\widetilde{c}_{j,k} - c_{j,k})\psi_{j,k}(x) = \varepsilon\sum_i \xi_i\frac{(\psi_{j,k}, e_i)}{b_i}\psi_{j,k}(x).$$

Pour contrôler facilement la somme d'erreurs de ce type, il faut d'abord que la base
soit suffisamment localisée pour disposer d'inégalités de type ondelettes pour les normes L^p.
D'autre part, il faut un contrôle des produits scalaires du type suivant :

$$\sum_i [\frac{(\psi_{j,k}, e_i)}{b_i}]^2 \leq C 2^{2j\nu},$$

ce qui implique que les coefficients de $\psi_{j,k}$ dans e_i se concentrent essentiellement sur les
indices d'ordre j. L'inégalité est vraie en particulier si $|(\psi_{j,k}, e_i)|$ est majoré par une constante
pour tout i et :

$$\{i : \psi_{j,k}^i \neq 0\} \subset \{C_1 2^j, \ldots, C_2 2^j\}.$$

L'objectif est donc de construire des frames localisés satisfaisant cette condition.

Déconvolution

Dans le cas de la déconvolution, on peut utiliser les needlets construites à partir de
la base de Fourier en suivant le principe général que nous décrivons plus loin dans le cas
Jacobi, mais ce n'est pas indispensable. En effet, il existe directement une base d'ondelettes
présentant toutes les propriétés voulues, à savoir les ondelettes de Meyer périodisées (voir
Meyer [68] ou Mallat [64]). Celles ci sont construites à partir de fonctions père et mère
(définies sur $\mathbb{R}$) possédant toutes les deux des transformées de Fourier à support compact.
Ainsi les ondelettes périodisées $\psi_{j,k}$, données par $\psi_{j,k}(x) = \sum_{l \in \mathbb{Z}} \Psi_{j,k}(x+l)$, ont un nombre
fini de coefficients de Fourier non nuls, et qui se concentrent autour de 2^j comme l'exige
la condition donnée précédemment. Dans la suite, on suppose donc que l'on implémente
NeedVD avec cette base.

Jacobi

L'idée principale est d'utiliser la construction de frames localisés (appelés needlets) qui
a été développée par Petrushev et Xu [81]. Comme les ondelettes, les needlets ont une
structure dyadique permettant de faire une analyse temps / fréquence des fonctions de $\mathbb{H}$.

Sans entrer dans les détails, indiquons simplement que l'on introduit d'abord une analyse
en "fréquence" de l'espace $\mathbb{H}$ à l'aide d'une décomposition de Calderón faisant intervenir une
base orthonormée (dans notre cas la base SVD e_k) et une fonction a régulière de support
$[\frac{1}{2}, 2]$ et à valeurs dans $[0, 1]$ comme représenté dans la figure 2.1.

Dans un deuxième temps, on discrétise chaque sous-espace de fréquence fixée à l'aide
d'une formule de quadrature (dans notre cas une formule de quadrature par polynômes de
Jacobi), ce qui fait intervenir les racines η des polynômes de Jacobi et des coefficients de
quadrature $b_{j,\eta}$. L'expression des needlets en fonction de la base de départ est alors très
simple. Soit $\mathbb{Z}_j = \{\eta_1, \ldots, \eta_{2^j}\}$ l'ensemble des racines du polynôme de Jacobi de degré 2^j,
triées par ordre décroissant. Alors on a pour $j \geq 0$ et $k \in \{1, \ldots, 2^j\}$:

$$\psi_{j,k} = \sum_{l \in \mathbb{N}} a(l/2^{j-1}) P_l(x) P_l(\eta_k) \sqrt{b_{j,\eta_k}}.$$
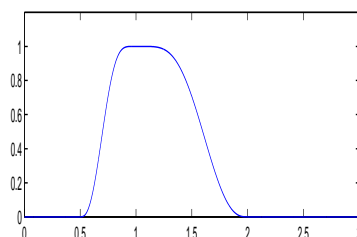
FIG. 2.1 – Fonction a servant à la décomposition de Calderón

Etant donné le support de a, ces fonctions satisfont la condition mentionnée plus haut sur les indices. De plus, pour tout $f \in \mathbb{H}$, on a la représentation suivante (mais ce n'est pas la seule), ainsi que la propriété de frame pour les normes L^2 :

$$f = \sum_{j \in \mathbb{N}, \, \eta_k \in \mathbb{Z}_j} \langle f, \psi_{j,k} \rangle \psi_{j,k},$$

$$\|f\|^2 = \sum_{j \in \mathbb{N}, \, \eta_k \in \mathbb{Z}_j} |\langle f, \psi_{j,k} \rangle|^2.$$

Par ailleurs, les needlets possèdent des propriétés de concentration intéressantes, qui permettent notamment comme les ondelettes de manipuler facilement les normes L^p des combinaisons linéaires de needlets de résolution fixe. Par contre elles sont localisées aux environs des racines η et non pas uniformément sur l'intervalle. Notons que certaines needlets ressemblent fortement à l'ondelette de Meyer périodisée : dans la figure 2.2 on a mis côte à côte une needlet de Legendre (c'est à dire Jacobi de type $(0,0)$) localisée au centre de $[-1,1]$, et une needlet de Meyer périodisée (de période 2).
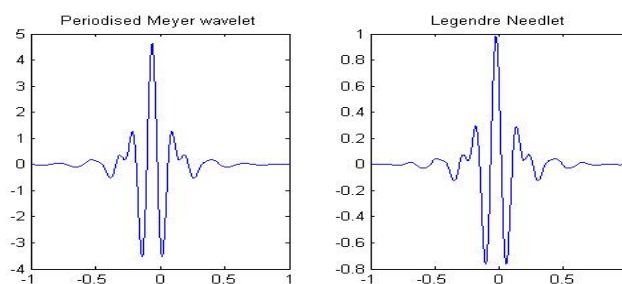
FIG. 2.2 – L'ondelette de Meyer périodisée et une needlet de Legendre

En revanche, on introduit des dissymétries quand $\alpha \neq \beta$ (voir figure 2.3) ou quand la needlet est localisée près des bords de l'intervalle. Notons en particulier que les normes L^p ne sont pas constantes à résolution fixée (voir figure 2.4).
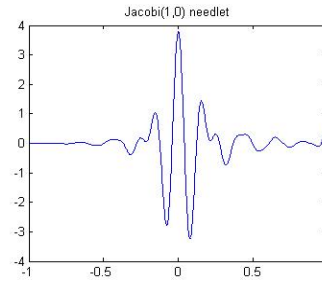
FIG. 2.3 – Needlet de Jacobi $(1,0)$
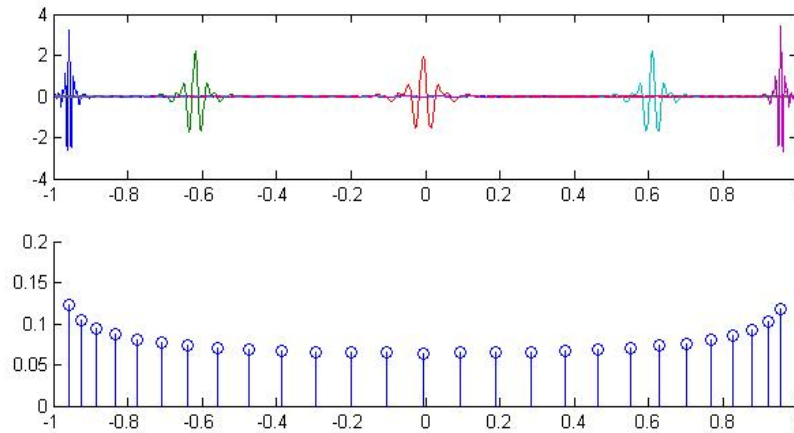
FIG. 2.4 – A résolution fixée : quelques needlets en haut, et les valeurs des normes L^3 en bas

2.2 Performances de NeedVD

Dans le scénario "ondelettes", on utilise la base des ondelettes de Meyer. Alors la procédure décrite à la section précédente se confond pratiquement avec WaveD développé dans Johnstone et al. [53]. Les vitesses de convergence dans ce cas sont donc les mêmes que celles établies dans leur article. En revanche NeedVD possède des vitesses entièrement nouvelles dans le scénario Jacobi, et offre des possibilités d'applications à un problème concret très éloigné des problèmes de type Fourier.

2.2.1 Vitesses de convergence

Nous nous plaçons dans un cadre minimax plus général que la majeure partie des méthodes citées en introduction, en supposant à la fois que f appartient à un espace de régularité très général de type Besov, et que le risque des estimateurs est mesuré en norme L^p et non plus L^2. Dans cette configuration, on voit apparaître des effets "coude" dans les vitesses de convergence de NeedVD, c'est à dire que l'on a plusieurs vitesses différentes selon les valeurs des paramètres du modèle. Cet effet coude a déjà été décrit dans le cas de l'observation directe dans Härdle et al. [49].

Scénario "ondelettes"

Dans le cas de la déconvolution on se place sur une boule d'un espace de Besov, que l'on décrit à partir des coefficients $c_{j,k}$ dans la base des ondelettes de Meyer périodisées $\psi_{j,k}$.

Pour $\pi \geq 1$, $s \geq 1/\pi$, $r \geq 1$, f appartient à l'espace $B_{\pi,r}^s(M)$ donné par :

$$\|f\|_{B_{\pi,r}^s} := \|(2^{js}(\sum |c_{j,k}|^\pi \|\psi_{j,k}\|_\pi^\pi)^{1/\pi})_{j \geq -1}\|_{L^r} < \infty, \quad \text{et}$$
$$f \in B_{\pi,r}^s(M) \iff \|f\|_{B_{\pi r}^s} \leq M.$$

On a alors les vitesses de convergence ci-dessous pour l'estimateur NeedVD :

Théorème 2.2.4. *Si $1 < p < \infty$, $2\nu + 1 > 0$ et $b_k \asymp k^{-\nu}$, pour $\kappa^2 \geq 16p$ on a pour tout $f \in B_{\pi,r}^s(M)$ avec $\pi \geq 1$, $s \geq 1/\pi$, $r \geq 1$ (avec la restriction $r \leq \pi$ si $s = (\nu + \frac{1}{2})(\frac{p}{\pi} - 1)$) :*

$$\mathbb{E}\|\hat{f} - f\|_p^p \leq C \log(1/\varepsilon)^{p-1}[\varepsilon\sqrt{\log(1/\varepsilon)}]^{\mu p},$$

où

$$\mu = \frac{s}{s + \nu + 1/2}, \quad si \ s \geq (\nu + \frac{1}{2})(\frac{p}{\pi} - 1)$$
$$\mu = \frac{s - 1/\pi + 1/p}{s + \nu + 1/2 - 1/\pi}, \quad si \ \frac{1}{\pi} \leq s < (\nu + \frac{1}{2})(\frac{p}{\pi} - 1).$$

On obtient donc une vitesse "regular" $\mu = \frac{s}{s+\nu+1/2}$ et une vitesse "sparse" $\mu = \frac{s-1/\pi+1/p}{s+\nu+1/2-1/\pi}$, et on peut cartographier les zones correspondantes pour (p, π) comme dans la figure 2.5 (où la zone du bas correspond aux paramètres π exclus par $s \geq 1/\pi$).
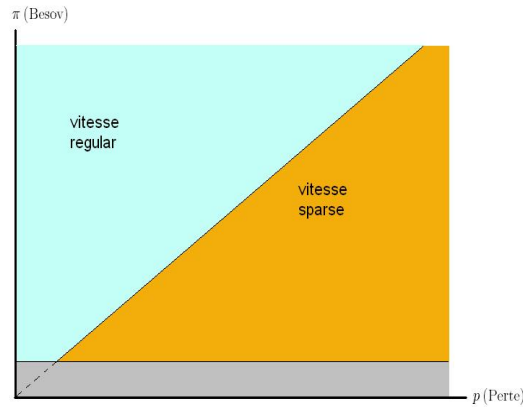
FIG. 2.5 – Distinction des zones dans le scénario "ondelettes"

Scénario "Jacobi"

Dans le cas Jacobi, on s'attache à la représentation suivante de f dans le frame $\psi_{j,k}$:

$$f = \sum_{j \geq -1} \sum_{\eta \in \mathbb{Z}_j} c_{j,k} \psi_{j,k},$$

où $c_{j,k}$ est défini par le produit scalaire :

$$c_{j,k} = (f, \psi_{j,k})_{\mathbb{H}}.$$

Pour $\pi \geq 1$, $s \geq 1/\pi$, $r \geq 1$, on suppose alors que f appartient à l'espace $\widetilde{B}^s_{\pi,r}(M)$ donné par :

$$\|f\|_{\widetilde{B}^s_{\pi,r}} := \|(2^{js}(\sum |c_{j,k}|^\pi \|\psi_{j,k}\|^\pi_\pi)^{1/\pi})_{j \geq -1}\|_{L^r} < \infty, \quad \text{et}$$
$$f \in \widetilde{B}^s_{\pi,r}(M) \iff \|f\|_{\widetilde{B}^s_{\pi r}} \leq M.$$

Dans le modèle de type Jacobi, l'évaluation du risque est plus difficile, notamment parce que les needlets (à résolution fixée) ont des comportements très différents selon leur localisation, contrairement aux ondelettes. On a par exemple le résultat suivant sur les normes (alors que dans le cas d'une ondelette $\|\psi_{j,k}\|^p_p \asymp 2^{j(p-2)/2}$ pour tout k) :

Pour tout $j \geq 0$ et $k \in \{1, \ldots, 2^j\}$,

$$\|\psi_{j,k}\|^p_p \asymp 2^{j(p-2)(\alpha+1)} k^{-(p-2)(\alpha+1/2)}, \quad k < 2^{j-1},$$
$$\|\psi_{j,k}\|^p_p \asymp 2^{j(p-2)(\beta+1)} k'^{-(p-2)(\beta+1/2)}, \quad k' = 2^j - k < 2^{j-1}.$$

L'étude des différentes erreurs d'estimation nécessite donc de distinguer de nombreux cas. Premièrement deux erreurs se superposent : celle faite sur l'intervalle $[0, 1]$ (qui fait intervenir α) et celle faite sur $[-1, 0]$ (qui a la même expression, mais en remplaçant α par β). Deuxièmement les majorations optimales des différents termes d'erreur sur $[0, 1]$ sont différentes suivant les signes de trois quantités, à savoir $\pi - p$, $(p - 2)(\alpha + 1/2) - 1$ et $s[(p - 2)(\alpha + 1/2) - 1] - (2\nu + 1)(\alpha + 1)(\frac{\pi-p}{\pi})$.

Toutefois, les vitesses obtenues se résument très simplement comme représentées dans la figure 2.6 en fonction de π et p, en supposant les autres paramètres fixés. Suivant la disposition des quantités $x = p - 2\frac{\alpha+1}{\alpha+1/2}$ et $y = \frac{\pi-p}{\pi}$ par rapport à une droite critique $y = \frac{s(\alpha+1/2)}{(2\nu+1)(\alpha+1)}x$, on obtient la vitesse "regular" bien connue ($\mu(s) = \frac{s}{s+\nu+\frac{1}{2}}$) ou une vitesse que nous continuons d'appeler "sparse", comme dans le scénario ondelettes, mais qui est totalement nouvelle et dépend de α : $\mu(s, \alpha) = \frac{s-2(1+\alpha)(\frac{1}{\pi}-\frac{1}{p})}{s+\nu+2(1+\alpha)(\frac{1}{2}-\frac{1}{\pi})}$.

Tout ceci est à superposer à l'erreur commise sur $[-1, 0]$, d'où le théorème général suivant.
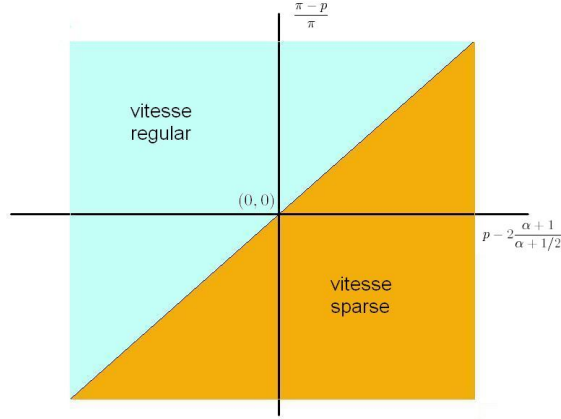
FIG. 2.6 – Distinction des zones dans le cas Jacobi

Théorème 2.2.5. *Soit* $1 < p < \infty$, $\alpha \geq \beta > -\frac{1}{2}$, *supposons* $b_i \sim i^{-\nu}$, $\nu > -\frac{1}{2}$, *et posons :*

$$\kappa^2 \geq 16p[1 + 4\{(\frac{\alpha}{2} - \frac{\alpha+1}{p})_+ \vee (\frac{\beta}{2} - \frac{\beta+1}{p})_+\}].$$

Alors pour $f \in \widetilde{B}^s_{\pi,r}(M)$ *avec* $s > \max_{\gamma \in \{\alpha,\beta\}}\{\frac{1}{2} - 2(\gamma+1)(\frac{1}{2} - \frac{1}{\pi}) \vee 2(\gamma+1)(\frac{1}{\pi} - \frac{1}{p}) \vee 0\}$,
on a

$$\mathbb{E}\|\hat{f} - f\|^p_p \leq C[\log(1/\varepsilon)]^{p-1+a}[\varepsilon\sqrt{\log(1/\varepsilon)}]^{\mu p},$$

avec

$$\mu = \min\{\mu(s),\ \mu(s,\alpha),\ \mu(s,\beta)\} \quad et \quad a = \max\{a(\alpha),\ a(\beta)\} \leq 2 \quad avec$$
$$\mu(s) = \frac{s}{s + \nu + \frac{1}{2}},$$
$$\mu(s,\gamma) = \frac{s - 2(1+\gamma)(\frac{1}{\pi} - \frac{1}{p})}{s + \nu + 2(1+\gamma)(\frac{1}{2} - \frac{1}{\pi})},$$

$$et\ a(\gamma) = \begin{cases} I\{\delta_p = 0\} & si\ [p-\pi][1 - (p-2)(\gamma+1/2)] \geq 0, \\ \frac{(\gamma+\frac{1}{2})(\pi-p)}{(\pi-2)(\gamma+1/2)-1} + I\{\delta_s = 0\} & si\ [p-\pi][1 - (p-2)(\gamma+1/2)] < 0, \end{cases}$$
$$où\ \delta_p = 1 - (p-2)(\gamma+1/2)\ et\ \delta_s = s[1 - (p-2)(\gamma+1/2)] - p(2\nu+1)(\gamma+1)(\frac{1}{\pi} - \frac{1}{p}).$$

Il est intéressant de voir que toutes ces vitesses coincident exactement avec celles de l'estimateur NeedVD dans le scénario "ondelettes" quand on se place dans le cas limite $\alpha = \beta = -\frac{1}{2}$. On peut ainsi mettre en parallèle la figure 2.5 avec la figure 2.7 qui délimite les zones dans le cas Jacobi où $\alpha = \beta$. Remarquons que la vitesse regular n'est jamais optimale quand p franchit un certain seuil $p_{\alpha,s}$:

$$p_{\alpha,s} = 2 + \frac{s + (2\nu+1)(\alpha+1)}{s(\alpha + \frac{1}{2})}.$$
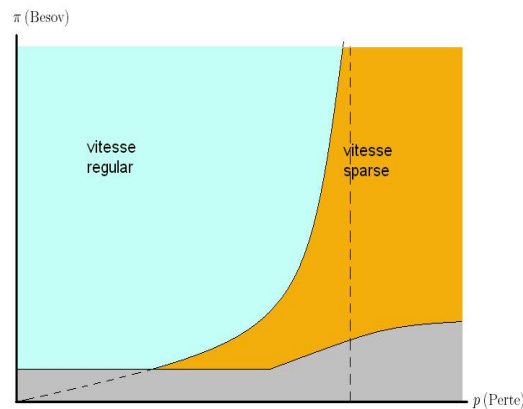
FIG. 2.7 – Distinction des zones dans le scénario "jacobi"

2.2.2 Optimalité minimax des procédures

On montre que les vitesses atteintes par l'estimateur NeedVD détaillées ci dessus sont optimales (ou quasi optimales) dans les deux cas suivants, dans lesquels nous nous étions placés depuis le début de ce chapitre :
- les problèmes de déconvolution
- tous les problèmes où la base SVD (e_i) est constituée de polynômes de Jacobi (dont par exemple le problème de Wicksell fait partie)

Dans les deux cas, le problème est d'établir des bornes inférieures pour le risque minimax en fonction de ε. Pour cela il s'agit de trouver une famille de fonctions $V = \{f_\lambda, \quad \lambda \in \Lambda\}$ de l'espace $\mathbb{H}$ de telle sorte que $V \subset B$ (où B désigne l'espace sur lequel le risque de l'estimateur NeedVD a été évalué), et V reflète l'essentiel des difficultés contenues dans B auxquelles on est confrontées quand on cherche à identifier la fonction f à partir de la loi du processus $Y_\varepsilon = Kf + \varepsilon\dot{W}$.

En d'autres termes il faut que les fonctions soient suffisamment distantes les unes des autres en norme L^p, et qu'en même temps les lois correspondantes du processus Y soient suffisamment proches les unes des autres. On voit bien que cette problématique conduit naturellement à utiliser des fonctions telles que leurs normes à la fois Besov et L^p soient facilement manipulables, et d'autre part liées à l'opérateur pour contrôler les lois des processus associés. Ainsi, les ondelettes de Meyer et les needlets de Jacobi s'avèrent à nouveau être des outils intéressants.

Déconvolution

Dans le cas de la déconvolution on a à nouveau recours aux ondelettes de Meyer périodisées notées $\psi_{j,k}$, et l'on se place sur une boule d'un espace de Besov que l'on décrit à

partir des coefficients $c_{j,k}$ comme précédemment, pour $\pi \geq 1$, $s \geq 1/\pi$, $r \geq 1$. On établit alors le théorème suivant qui découle des résultats principaux du chapitre 6 (ceux ci sont établis dans un cadre plus général avec un filtre aléatoire), pour le risque minimax $\mathcal{R}_\varepsilon$ (voir le chapitre 1 pour l'approche minimax).

Théorème 2.2.6. *Soit* $1 < p < \infty$ $\pi \geq 1$, $s \geq 1/\pi$, $r \geq 1$, *et supposons que* $b_i \asymp i^{-\nu}$, $\quad \nu > -\frac{1}{2}$. *Posons* $\vartheta = \frac{s+\nu+\frac{1}{2}}{p} - \frac{\nu+\frac{1}{2}}{p}$. *Alors on a :*

$$\mathcal{R}_\varepsilon(B^s_{\pi,r}(M), \mathbb{L}^p(dx)) \asymp \varepsilon^{p\frac{s}{s+\nu+\frac{1}{2}}} \quad si \ \vartheta > 0,$$

$$\mathcal{R}_\varepsilon(B^s_{\pi,r}(M), \mathbb{L}^p(dx)) \asymp \left(\varepsilon\sqrt{\log(\frac{1}{\varepsilon})}\right)^{p\frac{s-1/p+1/\rho}{s+\nu+\frac{1}{2}-\frac{1}{p}}} \quad si \ \vartheta < 0,$$

$$c\left(\varepsilon\sqrt{\log(\frac{1}{\varepsilon})}\right)^{p\frac{s-1/p+1/\rho}{s+\nu+\frac{1}{2}-\frac{1}{p}}} \leq \mathcal{R}_\varepsilon(B^s_{\pi,r}(M), \mathbb{L}^p(dx)) \leq C\left(\varepsilon\sqrt{\log(\frac{1}{\varepsilon})}\right)^{p\frac{s-1/p+1/\rho}{s+\nu+\frac{1}{2}-\frac{1}{p}}} \log(\frac{1}{\varepsilon})^{(1-\frac{p}{\rho q})+} \quad si \ \vartheta = 0.$$

Il est à noter que les bornes inférieures indiquées ici, dans le cadre des pertes L^p générales, sont nouvelles (à notre connaissance). Sans entrer dans les détails, mentionnons simplement que les familles utilisées pour montrer chacune des deux minorations sont les suivantes, pour des paramètres j et γ à ajuster en fonction de ε :

$$V_{sparse} = \{f_0 = 0\} \cup \{f_{j,k} = \gamma\psi_{j,k}, \text{ pour } k \in R_j\},$$

$$V_{regular} = \{f_{j,\varepsilon} = \gamma \sum_{k \in R_j} \varepsilon_k \psi_{j,k} \text{ pour } \varepsilon \in \{-1, +1\}^{R_j},$$

où l'on a posé $R_j = \{0, \dots, 2^j - 1\}$.

Les bornes supérieures sont quant à elles obtenues en utilisant un estimateur par ondelettes avec un algorithme de seuillage non adaptatif. Les vitesses de convergence de cet estimateur coincident exactement avec les bornes inférieures du risque minimax, sauf dans le cas critique où il reste un facteur logarithmique dont on ne sait pas s'il est améliorable ou non.

Problèmes inverses de type Jacobi

On se place sur l'espace $B = \widetilde{B}^s_{\pi,r}$ défini à partir des needlets de Jacobi $\psi_{j,k}$ comme à la section indiquant les performances de Needvd. Comparé à la déconvolution, le traitement de ce type de problèmes pose quelques difficultés supplémentaires.

Premièrement la condition d'appartenance à l'espace B nécessite d'étudier en détail le comportement des produits scalaires entre les needlets $\langle \psi_{j,k}, \psi_{j',l} \rangle$. Deuxièmement l'hétérogénéité des normes L^p des needlets à résolution fixée nécessite d'introduire une certaine pondération dépendant de la localisation dans les combinaisons linéaires de needlets. Enfin la condition d'espacement entre les fonctions de V nécessite d'établir un résultat de minoration des combinaisons linéaires de needlets. Une relation aussi générale que celle valable pour les ondelettes est impossible, mais on montre l'inégalité suivante pour des needlets à résolution fixée avec des indices de localisation suffisamment espacés :

Théorème 2.2.7. *Soit* $p \in 2\mathbb{N}^*$. *Alors il existe* $c_p > 0$ *et un entier* n_p *telle que toute collection de réels* $\{\lambda_k : k \in I_j\}$, $j \geq 0$, *où* $I_j \subset \{1, 2, \ldots, 2^j\}$ *et* $k, l \in I_j, k \neq l \Longrightarrow |k - l| \geq n_p$,

$$\| \sum_{k \in I_j} \lambda_k \psi_{j,\eta_k} \|^p_{\mathbb{L}^p(\mu)} \geq c_p \sum_{k \in I_j} |\lambda_k|^p \|\psi_{j,\eta_k}\|^p_{\mathbb{L}^p(\mu)}.$$

Le résultat principal est alors le suivant :

Théorème 2.2.8. *Soit* $1 < p < \infty$ *et* α, $\beta > -\frac{1}{2}$ *et supposons que*

$$b_i \asymp i^{-\nu}, \quad \nu > -\frac{1}{2}.$$

Alors on a :

$$\mathcal{R}_\varepsilon(B^s_{\pi,r}(M), \mathbb{L}^p(\mu)) \geq C\varepsilon^{\mu p}, \tag{2.1}$$

où

$$\mu = \min\{\mu(s), \ \mu(s,\alpha), \ \mu(s,\beta)\},$$

$$avec : \quad \mu(s) = \frac{s}{s + \nu + \frac{1}{2}}, \quad \mu(s,\gamma) = \frac{s - 2(1+\gamma)(\frac{1}{\pi} - \frac{1}{p})}{s + \nu + 2(1+\gamma)(\frac{1}{2} - \frac{1}{\pi})}.$$

Et indiquons aussi les familles utilisées pour montrer chacune des trois minorations, pour des paramètres j, γ et δ à ajuster en fonction de ε :

$$V_{sparse(\alpha)} = \{f_0 = 0, \quad f_1 = \gamma \psi_{j,1}\},$$

$$V_{sparse(\beta)} = \{f_0 = 0, \quad f_1 = \gamma \psi_{j,2^j}\},$$

$$V_{regular} = \{f_\varepsilon = \gamma \sum_{k=1}^{2^j} \varepsilon_k k^\delta \psi_{j,\eta_k}, \quad \varepsilon \in E_j\}\},$$

où $E_j \subset \{0,1\}^{2^j}$ est choisi de sorte d'avoir un espacement suffisant à la fois entre les localisations des needlets et entre les fonctions f_ε.

Ceci nous permet de conclure que NeedVD est au moins quasi optimal dans cette configuration, et que les exposants de ε du risque minimax sont donc égales à celles du théorème 9. Mais contrairement à la déconvolution, la détermination des facteurs logarithmiques exacts du risque minimax reste une question ouverte.

2.3 Application au problème de Wicksell

L'algorithme analogue à NeedVD dans le cas de la déconvolution et utilisant les bases de Meyer a déjà été étudié en pratique, en particulier sur un problème de traitement d'images, dans Johnstone et al. [53]. Aussi nous nous sommes concentrés sur l'étude pratique du scénario "Jacobi", pour lequel NeedVD offre des perspectives nouvelles. En particulier elle

permet de porter un regard neuf sur le problème de Wicksell. Pour l'instant les résultats ont été surtout établis dans un modèle de type bruit blanc. L'adaptation au modèle initial de densité est à l'étude, seule une étude sommaire des performances numériques est présentée à la fin du chapitre 5.

Rappelons l'opérateur apparaissant dans ce problème et donnons sa décomposition en valeurs singulières, telle que présentée dans Johnstone et Silverman [54] :

$$\mathbb{H} = \mathbb{L}^2([0,1], d\mu), \ d\mu(x) = (4x)^{-1}dx, \quad \mathbb{K} = \mathbb{L}^2([0,1], d\lambda), \ d\lambda(x) = 4\pi^{-1}(1 - y^2)^{1/2}dy,$$

et

$$Kf(y) = \frac{\pi}{4}y(1 - y^2)^{-1/2} \int_y^1 (x^2 - y^2)^{-1/2}f(x)d\mu.$$

Les bases SVD sont :

$$e_k(x) = 4(k+1)^{1/2}x^2 P_k^{0,1}(2x^2 - 1),$$
$$g_k(y) = U_{2k+1}(y).$$

où $P_k^{0,1}$ est le polynôme de Jacobi de degré k de type $(0,1)$, et U_k est le polynôme de Chebishev de deuxième type de degré k. Et les valeurs singulières sont :

$$b_k = \frac{\pi}{16}(1+k)^{-1/2}.$$

2.3.1 Modèle de bruit blanc

Nous considérons dans un premier temps le modèle sous forme bruit blanc (voir définition 1.2), pour lequel :
  – on obtient des vitesses minimax nouvelles,
  – on propose un estimateur optimal (à des facteurs logarithmiques près),
  – on développe une procédure d'estimation facilement implémentable et qui s'avère performante en pratique.
Le modèle est donc :
$$Y_\varepsilon = Kf + \varepsilon\dot{W}.$$

Les étapes de la transformation de f en Y sont illustrées dans la figure 2.8 : la fonction initiale est lissée par l'opérateur, puis on ajoute du bruit gaussien à la fonction résultante. Dans cet exemple l'étude de la performance de la procédure consiste à appliquer l'algorithme aux données bruitées de droite et à mesurer l'erreur commise en sortie par rapport à la fonction initiale de gauche. On comprend aisément ici que la tâche est difficile en cas de bruit trop fort : les détails de f deviennent invisibles au niveau de l'observation Y.

A un changement de variable près, la SVD du problème de Wicksell montre que l'on se trouve dans le scénario "Jacobi" avec $\alpha = 0$, $\beta = 1$, $b_k \sim k^{-1/2}$. On peut donc implémenter NeedVD en utilisant le frame $(\widetilde{\psi}_{j,k})$ suivant, défini à partir des needlets de Jacobi $\psi_{j,k}$:

$$\forall x \in [0,1], \quad \widetilde{\psi}_{j,k}(x) = 4\sqrt{2}x^2\psi_{j,k}(2x^2 - 1).$$
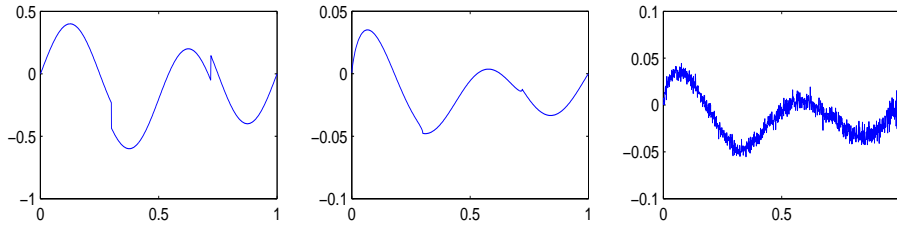
FIG. 2.8 – La fonction Heavisine, son image par Wicksell avec et sans bruit

L'estimateur NeedVD est comparé avec l'estimateur SVD non adaptatif de trocature spectrale, et l'estimateur SVD adaptatif par blocs de Cavalier et Tsybakov [16] (tous les deux sont détaillés au chapitre 1) pour plusieurs fonctions de perte, niveaux de bruit et fonctions cibles. Comme l'illustre le tableau suivant, NeedVD s'avère plus performant que les deux autres méthodes.

	SVD par troncature			SVD par blocs			NeedVD		
	low	**med**	**high**	**low**	**med**	**high**	**low**	**med**	**high**
Blocks	0.0714	0.0790	0.0959	0.0665	0.0743	0.0900	0.0606	0.0673	0.0816
Bumps	0.0489	0.0577	0.0706	0.0453	0.0508	0.0617	0.0378	0.0416	0.0523
Heavisine	0.0278	0.0327	0.0422	0.0266	0.0317	0.0418	0.0235	0.0288	0.0379
Doppler	0.1092	0.1200	0.1378	0.1042	0.1114	0.1258	0.0969	0.0999	0.1071

TAB. 2.1 – Erreur quadratique moyenne pour 4 fonctions test (une par ligne), trois niveaux de bruit et chacun des trois estimateurs (par colonne)

2.3.2   Modèle de densité

A la fin du chapitre 5, on cherche à appliquer directement l'algorithme précédent au problème de Wicksell d'origine, qui présente deux différences avec le modèle étudié ci dessus. Premièrement, l'opérateur et les espaces $\mathbb{H}$ et $\mathbb{K}$ sont définis différemment (les pondérations dans Johnstone et Silverman [54] ont été introduites pour écrire la SVD de façon simple). Deuxièmement, le problème suit un modèle de densité (voir la définition 1.3).

On s'attache tout d'abord au premier point et on étudie les performances de NeedVD, avec les modifications qui s'imposent, si l'on suppose une perturbation de type bruit blanc dans le modèle initial (et non plus dans le modèle SVD). Alors la procédure reste performante, comme l'atteste la figure 2.9, où elle est comparée aux deux mêmes estimateurs SVD que précédemment.

Puis au lieu de perturber par un bruit blanc additif, on simule des échantillons de variables iid, suivant les densités image, par K, de diverses densités initiales. On adapte alors les estimateurs des coefficients de Needvd. De plus on adapte la technique de seuillage en estimant les seuils asymptotiques de chacun des coefficients de needlets, car le seuillage homogène de type bruit blanc s'avère inadapté, étant donnée l'hétérogénéité des normes des
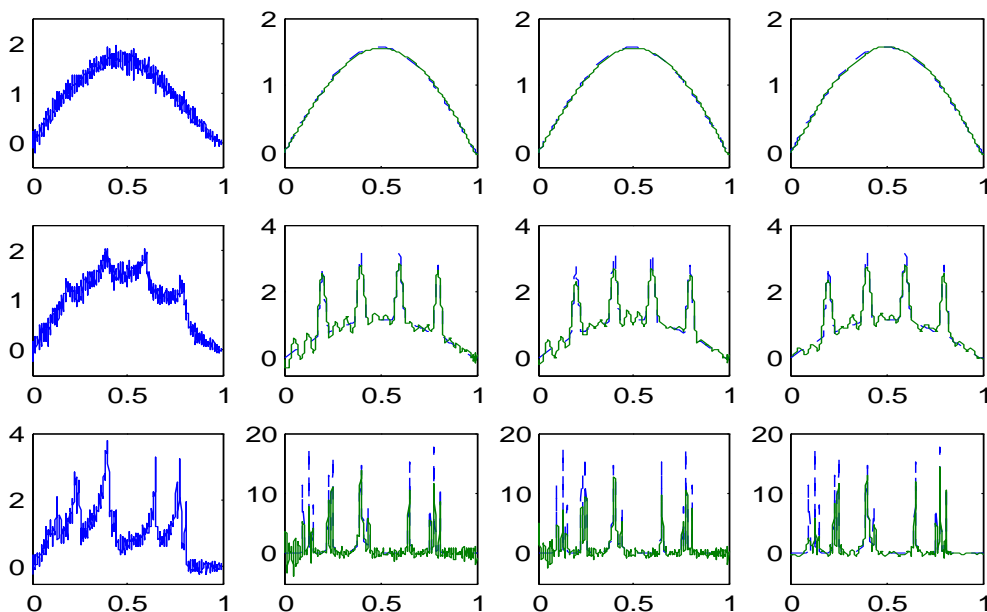
FIG. 2.9 – De gauche à droite : $K(f)$ perturbé par un bruit blanc additif ; estimateur SVD non adaptatif de troncature spectrale ; estimateur SVD adaptatif par blocs ; la fonction f est en pointillés

erreurs gaussiennes sur les coefficients. Toutefois l'estimation de fonctions cibles possédant quelques niveaux de détail s'avère difficile. Une comparaison avec les autres estimateurs disponibles pour le problème de Wicksell est en cours d'étude.

2.4 Déconvolution d'un signal brouillé par un filtre aléatoire

2.4.1 Motivation

Nous avons cité en introduction plusieurs approches où le modèle inverse fait apparaître un opérateur aléatoire, comme par exemple le cas des opérateurs observés avec une certaine erreur faible par rapport à un opérateur déterministe inconnu (voir par exemple Efromovich et Koltchinskii [38]).

Une approche originale qui n'a pas encore été envisagée, à notre connaissance, est de considérer des opérateurs "instables", qui varient en suivant une certaine loi de probabilité dans toute une gamme d'opérateurs possibles, et ceci indépendamment de l'erreur de mesure représentée par le bruit blanc gaussien. Cette modélisation parait utile par exemple dans le cas où l'opérateur n'a pas une expression explicite entièrement déterminée à l'avance, mais qu'il dépend de certains paramètres imprévisibles (voir les exemples du chapitre 6). Dans ce type de scénario, on a besoin de développer des techniques d'estimation robustes, qui sont efficaces pour toute une gamme d'opérateurs.

Nous nous plaçons ici dans le cadre de l'opérateur de déconvolution. Le modèle est donc le même que celui de la déconvolution classique, mais en remplaçant le filtre déterministe γ

par un filtre aléatoire X. De plus l'application à des données réelles nous conduit à changer la notation du niveau de bruit en utilisant un paramètre $n \in \mathbb{N}^*$ (lié en pratique à un niveau de discrétisation des observations) équivalent à ε donné par $\varepsilon = \frac{1}{\sqrt{n}}$. Le modèle est donc le suivant :

$$\begin{cases} dY_n(t) & = (\int_0^1 f(t-s)X(s)ds)dt + \sigma n^{-1/2}dW(t), \quad \forall t \in [0,1], \\ Y_n(0) & = y_0, \end{cases} \tag{2.2}$$

où y_0 est une condition initiale déterministe et σ est une constante positive connue. On suppose que X est indépendant de l'erreur W.

Bien entendu, les techniques adaptées aux filtres déterministes, dont l'estimateur décrit dans la section 2.1, sont applicables à ce cadre si le filtre vérifie des conditions très restrictives sur les coefficients de Fourier $|X_l|$ de X, comme :

$$c2^{-\nu l} \leq |X_l| \leq C2^{-\nu l},$$

presque sûrement pour des constantes c et C déterministes.

Cependant dès que l'on se donne un cadre plus large autorisant les coefficients à être à n'importe quelle proximité de 0 (mais en gardant bien sûr un certain contrôle de la probabilité de tels événements), des difficultés intéressantes apparaissent, qui conduisent à adapter la technique de seuillage.

2.4.2 Résultats minimax et estimation adaptative

Un premier objectif est d'établir les vitesses minimax pour un tel problème. On se place dans le même cadre que pour l'étude de NeedVD, à savoir avec des pertes L^ρ et pour f appartenant à une boule de Besov, que nous décrivons à partir des coefficients $c_{j,k}$ de f dans la base de Meyer $\psi_{j,k}$:

$$M(s,p,q,R) = \{f \in B^s_{p,q}([0,1]) \quad | \quad \|f\|_{s,p,q} \leq R\},$$

avec :

$$B^s_{p,q}([0,1]) = \{f \in L^p([0,1]) \quad | \quad \|f\|_{s,p,q} := \big(\sum_{j \leq 0} 2^{j(s+1/2-1/p)q}\big(\sum_{0 \leq k \leq 2^j} |c_{j,k}|^p\big)^{q/p}\big)^{1/q} < R\}.$$

On établit que les vitesses minimax sont alors exactement les mêmes que celles du cas déterministe, sous les conditions suivantes sur le filtre, qui remplacent la condition usuelle du cas déterministe $b_i \asymp i^{-\nu}$:

Définition 2.4.4. *Soient L_j^X et U_j^X les deux quantités suivantes :*

$$L_j^X = \frac{\sum_{l=2^j}^{2^{j+1}-1} |X_l|^2}{2^j}, \quad et \quad U_j^X = \frac{\sum_{l=0}^{2^{j+1}-1} |X_l|^{-2}}{2^j}.$$

Alors on a les vitesses minimax données dans la section 2.2 (avec les changements de notations), si les deux conditions suivantes, servant respectivement pour les bornes inférieures et pour les bornes supérieures, sont vérifiées :

C_{low} : *Il existe $\nu \geq 0$ telle que, pour tout $j \in \mathbb{N}$:*

$$E(L_j^X) \leq C 2^{-2\nu j}.$$

C_{up} : *$\forall l \in \mathbb{Z}, X_l \neq 0$ presque sûrement , et il existe $\nu \geq 0, c > 0, \alpha > 0$ tels que, pour tout $j \in \mathbb{N}$:*

$$\forall t \geq 0, \quad P\big(U_j^X \geq t 2^{2\nu j}\big) \lesssim e^{-ct^{\alpha}}.$$

Quand on cherche à construire un estimateur adaptatif atteignant ces vitesses, on s'aperçoit que le seuillage utilisé dans le cas déterministe peut s'avérer nettement sous optimal. On montre qu'une première possibilité pour gagner en performance est d'adapter les seuils et la résolution maximale, de façon à corriger l'effet aléatoire du filtre, comme suit :

$$2^{j_1} = \{n/(\log n)^{1+\frac{1}{\alpha}}\}^{1/(1+2\nu)},$$

$$t_j = \eta 2^{\nu j} \sqrt{(\log n)^{1+\frac{1}{\alpha}}/n},$$

où η est une constante suffisamment grande.

Alors en utilisant les mêmes estimateurs des coefficients d'ondelettes que dans le cas où X est déterministe, on définit l'estimateur suivant :

$$\hat{f}_n^D = \sum_{(j,k) \in \Lambda_n} \hat{\beta}_{j,k} I_{\{|\hat{\beta}_{j,k}| \geq t_j\}} \psi_{j,k}, \tag{2.3}$$

où $\Lambda_n = \{(j,k) \in \mathbb{Z}^2 \mid j \in \{-1, \ldots, j_1\}, \ k \in R_j\}$.

Celui ci atteint les vitesses quasi optimales suivantes :

Théorème 2.4.9. *Sous la condition C_{up} :*

$$\sup_{f \in M(s,p,q,R)} E_f(\|\hat{f}_n^D - f\|_\rho) \leq C \big(\frac{\log(n)^{1+\frac{1}{\alpha}}}{n}\big)^{\frac{s}{2s+2\nu+1}} \quad \textit{dans le cas regular,}$$

$$\sup_{f \in M(s,p,q,R)} E_f(\|\hat{f}_n^D - f\|_\rho) \leq C \big(\frac{\log(n)^{1+\frac{1}{\alpha}}}{n}\big)^{\frac{s-1/p+1/\rho}{2s+2\nu+1-2/p}} \quad \textit{dans les cas critiques et sparse.}$$

Le facteur logarithmique dépendant de α semble être le prix à payer sur la performance si l'on s'autorise à n'utiliser qu'un seuillage déterministe. En revanche l'utilisation d'autres seuillages permet d'apporter des améliorations. Ainsi on introduit dans un deuxième temps un seuillage aléatoire, car dépendant de X, déjà utilisé dans Johnstone et al. [53]. Ainsi on peut éliminer le facteur logarithmique dépendant de α. On pose :

$$2^{j_2} = \{n/\log n\}^{1/(1+2\nu)},$$

$$\tau_j = \eta' \sqrt{U_j^X \log n/n},$$

ce qui donne l'estimateur $\hat{f}_n^R$ obtenu comme $\hat{f}_n^D$ en remplaçant j_1 et t_j par j_2 et τ_j.

2.4.3   Performances pratiques

Sur le plan pratique, nous analysons d'abord sommairement le comportement des estimateurs sur des données réelles de sismologie. Puis nous évaluons les performances sur des données simulées, pour différents paramètres du système comme le niveau de bruit et la fonction inconnue, prise parmi les fonctions Blocks, Bumps, Heavisine et Doppler, très fréquemment utilisées.

On s'attache tout particulièrement à étudier l'effet des caractéristiques aléatoires du filtre (que nous modélisons par des fonctions gamma dont les paramètres aléatoires dépendent d'un niveau α) et de son "ill−posedness" (paramétrée par ν) pour comparer les performances de l'estimateur à seuil déterministe et celui à seuil aléatoire. Un exemple d'estimateurs obtenus est donné dans la figure 2.10, où l'on a aussi mis tout à droite la courbe que l'on obtiendrait si l'on appliquait directement l'estimateur valide dans le cas d'un filtre déterministe (c'est à dire avec des seuils : $t_j = \eta 2^{\nu j} \sqrt{\log n / n}$).
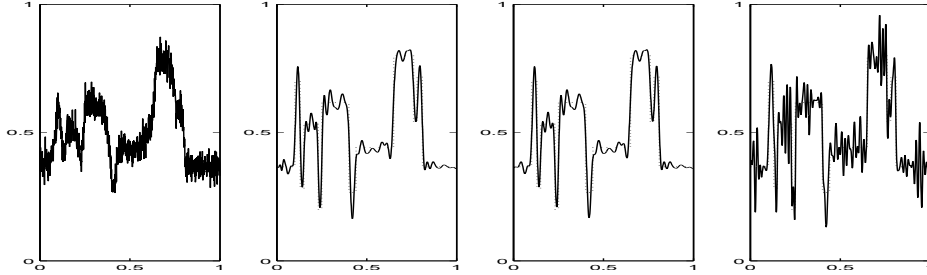
FIG. 2.10 – Données bruitées, estimateurs $\hat{f}_n^R$, $\hat{f}_n^D$ et celui issu du cadre déterministe

Des résultats plus complets sur l'erreur quadratique moyenne sont illustrés dans la figure 2.14. L'estimateur à seuil aléatoire y apparaît plus robuste par rapport aux variations du filtre, et aussi plus facile à utiliser que le seuillage déterministe qui nécessite un calibrage en fonction de α.

2.5   Régression en design aléatoire

Dans le chapitre 7 nous traitons d'un problème différent des problèmes inverses étudiés dans le reste de la thèse, et qui concerne l'étude des performances numériques d'une procédure de régression en design aléatoire.

On peut toutefois établir un parallèle avec la procédure décrite en section 2.1, en ce que la motivation à l'origine de l'estimateur de régression est la même que celle de la procédure NeedVD : trouver une base intéressante telle que l'on dispose d'estimateurs naturels des coefficients de f dans cette base, et telle que l'on puisse facilement débruiter ces estimateurs préliminaires par une procédure de seuillage classique, quitte à ce que la base en question perde quelques propriétés par rapport aux "bonnes" bases usuelles. En d'autres termes, on adopte à nouveau dans cette procédure une approche originale où l'on fait porter l'essentiel des difficultés (liées au caractère aléatoire du design) sur des problèmes d'analyse, résolus
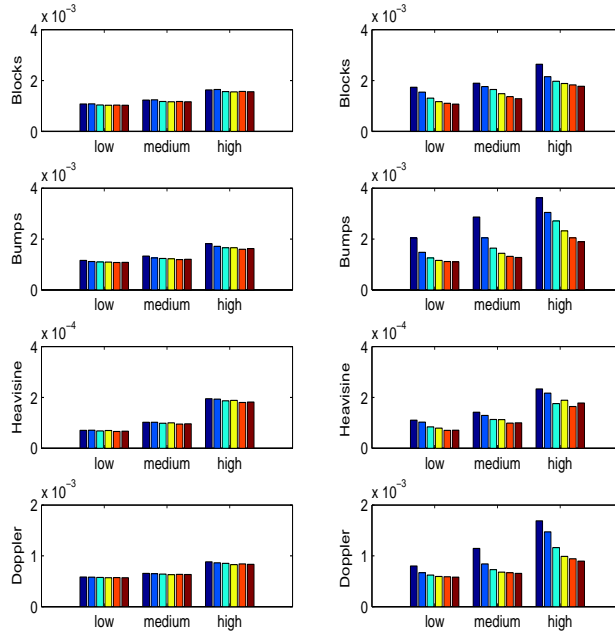
FIG. 2.11 – Effet de α sur la MSE de $\hat{f}_n^R$ (à gauche) et $\hat{f}_n^D$ (à droite) pour différentes valeurs de f, s et $\alpha \in \{0.5, 0.6, 0.7, 0.8, 0.9, 1\}$

grâce à des techniques nouvelles, afin de gagner au maximum en simplicité et en efficacité du point de vue de l'estimation.

Des résultats très complets sur les performances théoriques de l'estimateur en question sont donnés dans Kerkyacharian et Picard [57]. Dans la suite nous donnons un aperçu des performances numériques de cette procédure, qui sont détaillées au chapitre 7.

2.5.1 Motivation

Le modèle de régression avec design aléatoire est le suivant. Supposons que l'on observe des couples $(Y_1, X_1), ..., (Y_n, X_n)$ où $(Y_i)_{i=1,...,n}$ est donné par :

$$Y_i = f(X_i) + s\varepsilon_i, \quad i = 1, ..., n, \tag{2.4}$$

où les ε_i sont i.i.d centrés gaussiens de variance 1, s est un niveau de bruit fixé, et les X_i sont des variables i.i.d de densité g représentant les endroits où l'on a une observation bruitée de la valeur de f. Le but est d'estimer $f : [0, 1] \mapsto \mathbb{R}$ à partir des observations.

Par rapport au modèle déterministe uniforme (correspondant à $X_i = \frac{i}{n}$) qui a été très largement étudié, et pour lequel les résultats minimax sont bien connus (Korostelev et Tsybakov [61] et Tsybakov [89]), le modèle à design aléatoire pose quelques difficultés supplémentaires. Si l'on se place dans le cadre des méthodes d'ondelettes, ces difficultés sont résolues la plupart du temps en complexifiant la méthode d'estimation des coefficients et le débruitage. En effet le schéma suivant revient de manière récurrente :

1. On construit une fonction préliminaire $Y(x)$ de la forme :

$$Y(x) = \sum_m w_m(x) Y_m$$

   où $w_m(x)$ est une suite de fonctions bien choisies.

2. Dans un deuxième temps, on décompose la fonction Y sur une base d'ondelettes usuelle et on applique un algorithme de seuillage dur. Dans chacune des techniques citées plus haut, on est contraint de faire dépendre les seuils du design, généralement via la quantité $\max_t \frac{1}{g(t)}$.

Par exemple dans Hall et Turlach [47] les w_m sont des polynômes dépendant des points $(X_i)_{i=1,\ldots,n}$; dans Cai et Brown [14], ainsi que dans Maxim [66], ce sont des fonctions d'échelle déformées par G ; et dans Antoniadis et al. [5] les X_i sont d'abord transformées en données equi$-$espacées par une méthode de binning et les w_m correspondent alors à des fonctions d'échelle. Dans de telles approches, des difficultés peuvent apparaître en pratique lorsque la densité g est inconnue, ou surtout quand cette densité s'annule en certains points de l'intervalle. Ceci correspond au cas où l'on dispose de peu d'observations à certains endroits où l'estimation est donc difficile. Dans ce cadre on ne peut pas établir de résultats de type minimax pour ce genre d'estimateurs.

2.5.2 L'estimateur à bases déformées

La procédure développée dans Kerkyacharian et Picard [57], que nous appelons procédure à "bases déformées", permet de surmonter cette difficulté en construisant un estimateur robuste à un manque local d'informations.

L'idée est d'exploiter les avantages de la théorie des poids de Muckenhoupt (voir [70]) en s'autorisant une décomposition sur une base atypique qui permette d'une part d'estimer et de seuiller très simplement les coefficients dans cette base, et d'autre part d'avoir des bonnes performances théoriques et pratiques dans le cas où g s'annule. Cette base particulière est obtenue par déformation d'une base d'ondelette usuelle par la fonction de répartition $G(x) = \mathbb{P}(X_1 \leq x) = \int_0^x g(t)dt, \quad x \in [0,1]$. Plus précisément, on considère la décomposition suivante de f :

$$f(t) = \sum_{j,k} c_{j,k} \psi_{j,k}(G(t)), \quad t \in [0,1],$$

dont on estime les coefficients par :

$$\hat{c}_{j,k} = \frac{1}{n} \sum_{i=1}^n Y_i \psi_{j,k}(G(X_i)),$$

pour (j,k) appartenant à $\Lambda_n = \{(j,k) | -1 \leq j \leq j_1(n), \ 0 \leq k \leq 2^j - 1\}$, où $2^{j_1(n)} \asymp \sqrt{\frac{n}{\ln(n)}}$, auxquels on applique un algorithme de seuillage dur en utilisant simplement le seuil universel t :
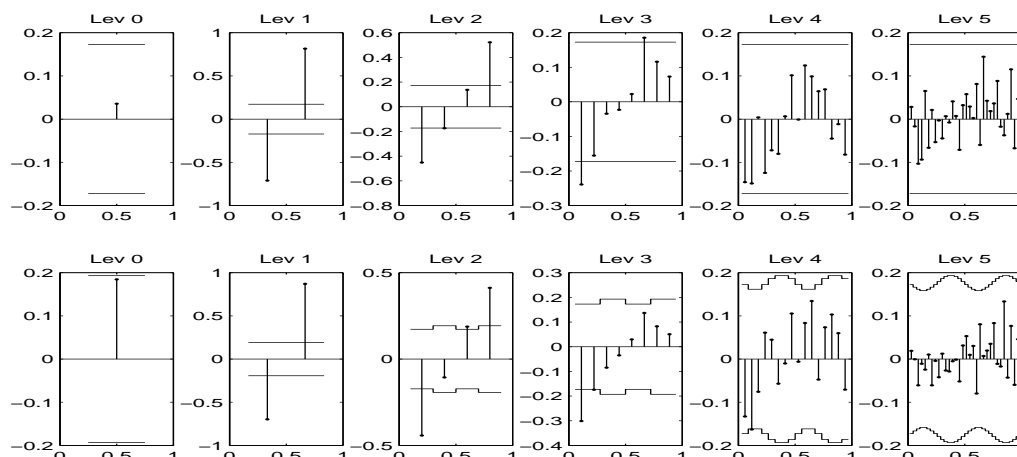
FIG. 2.12 – Coefficients (verticalement) et les seuils associés (horizontalement) pour l'estimateur 1 (en haut), et l'estimateur 2 (en bas) à chaque niveau de résolution j

$$t = s\sqrt{\frac{2\log(n)}{n}}.$$

On a donc un algorithme de seuillage très simple par rapport à ceux utilisés par les méthodes d'ondelettes citées précédemment. Ceci est illustré dans la figure 2.12 où l'on a représenté en haut, pour un modèle donné, les coefficients estimés $\hat{c}_{j,k}$ (barres verticales) et la zone exclue par le seuillage (horizontalement) par cette méthode, et en bas la même chose pour l'estimateur développé dans Cai et Brown [14]. Dans ce dernier cas on a besoin de calculer un seuil spécifique dépendant de g pour chaque coefficient, d'où les variations des deux courbes quand g n'est pas uniforme (ici g a été prise sinusoïdale).

Notons aussi que l'implémentation du calcul des estimateurs peut aussi se faire très simplement puisqu'en remplaçant G par la fonction de répartition empirique $\hat{G}_n(x) = \frac{1}{n}\sum_{i=1}^n 1_{\{X_i \le x\}}$, ceux ci deviennent :

$$\hat{c}_{j,k} = \frac{1}{n}\sum_{i=1}^n Y_i \psi_{j,k}(\frac{i}{n}),$$

dont on dispose directement d'une approximation en appliquant l'algorithme de transformée en ondelettes discrète au vecteur Y (Härdle et al. [49]).

2.5.3 Performances pratiques

On compare les performances de l'estimateur à bases déformées (estimateur 1 dans les figures) avec celui à bases usuelles (estimateur 2) développé par Cai et Brown [14]. On les applique sur deux bases de données réelles fréquemment utilisées dans ce genre de problèmes, et dans un cadre plus général, sur un grand nombre de données simulées correspondant à plusieurs possibilités pour n, s, f, g et le choix de la base d'ondelettes.
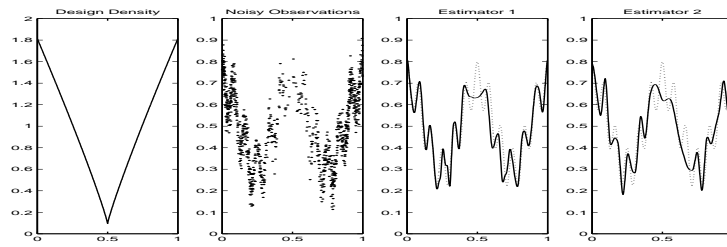
FIG. 2.13 – De gauche à droite : la densité du design, les observations, l'estimateur à bases déformées et celui à bases classiques ; La fonction cible est en pointillés
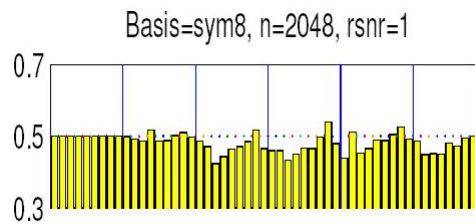
FIG. 2.14 – Erreur L^1 relative de l'estimateur 1 par rapport à l'estimateur 2 pour tous les choix de f et g

On observe des comportements similaires des estimateurs dans le cas de fonctions g suffisamment régulières et minorées par une valeur suffisament grande. En revanche des différences apparaissent dès que l'on étudie des design déséquilibrés, comme illustré par la figure 2.13 : l'estimateur 1 se montre plus robuste que l'estimateur 2 dans les zones de faible densité.

Quand on évalue l'erreur moyenne faite par chacun des estimateurs pour diverses pertes L^p, on s'aperçoit que pour une grande partie des paramètres du modèle considérés (qui contiennent notamment plusieurs fonctions de densité s'annulant plus ou moins abruptement) l'estimateur 1 est plus performant que l'estimateur 2. Par exemple dans la figure 2.14 on a mis bout à bout, pour des n et s fixés, la valeur de l'erreur moyenne de l'estimateur 1 relativement à l'estimateur 2 pour chaque choix du couple de paramètres (g, f). On obtient généralement des valeurs inférieures à 0.5 ce qui atteste d'une meilleure performance de l'estimateur 1, en particulier pour les densités s'annulant de façon de plus en plus prononcée (situées vers la droite de la figure).

On observe enfin que l'avantage de l'estimateur 1 s'accroît encore lorsque l'on se place dans le cadre d'un modèle où la densité g est inconnue. Dans ce cas l'estimateur 2 devient plus difficile à implémenter, surtout au niveau du seuillage qui est très sensible aux erreurs pour les indices k correspondant aux zones de faible densité. En revanche l'estimateur 1 s'étend très simplement à ce cadre, et est plus stable par rapport aux erreurs d'estimation faites sur g.

2.6 Perspectives

Généralisation de NeedVD

Nous avons étudié l'algorithme NeedVD (ou WaveD) dans deux cas d'opérateurs très distincts, suivant que la base SVD est constituée de la base de Fourier ou de la base des polynômes de Jacobi, et on a obtenu des liens frappants entre les résultats.

D'une part les résultats théoriques pour le scénario "ondelettes" apparaissent comme un cas limite des résultats pour le scénario "Jacobi". D'autre part comme cela a déjà été mentionné, il y a une forte ressemblance entre les familles localisées considérées, ou plus précisément entre les needlets de Legendre (construites à partir de polynômes) et l'ondelette de Meyer (construites à partir de la base de Fourier). Ces deux familles sont certes construites avec la même optique de départ, mais à partir de deux bases totalement différentes. Ceci signifie peut être que les constructions utilisées permettent de construire des frames indépendants du contexte, c'est à dire qui s'éloignent des bases SVD de départ pour converger vers un système de fonctions stable par rapport à l'opérateur. On peut donc espérer que ce type de frame puisse s'appliquer à d'autres problèmes inverses que ceux traités ici, au moins sur le plan pratique.

Sur le même thème, il serait intéressant de chercher à traiter, toujours à l'aide des needlets ou d'autres ondelettes de seconde génération, des problèmes inverses faisant intervenir des bases SVD d'une nature autre que celles étudiées dans cette thèse. En effet la construction reste valable dans d'autres contextes, notamment dans le cadre des harmoniques sphériques. Ainsi elles ont déjà été introduites par exemple pour l'analyse du rayonnement cosmologique (Cosmic Microwave Background) dans Baldi et al. [9], et les perspectives à la fois théoriques et pratiques dans ce domaine sont nombreuses. Concernant les problèmes d'estimation sur la sphère, à l'aide de bases localisées, des méthodes d'estimation par ondelettes ont par ailleurs été développées par Pereverzev et Schock [79].

Par ailleurs, en nous inspirant de l'idée d'Abramovich et Silverman concernant la méthode "Vaguelette Wavelet Decomposition", on pourrait peut être essayer de développer une méthode jumelle à NeedVD : on commencerait par décomposer les observations Y sur une base localisée construite à partir des fonctions SVD (g), puis on chercherait à inverser le modèle séquentiel. Ceci pourrait fournir un champ d'application différent de celui de NeedVD, mais une telle méthode posséderait probablement des limites sur le plan minimax.

Affiner les résultats théoriques

Que ce soit pour l'étude des problèmes inverses du type Jacobi ou des problèmes de déconvolution avec filtre aléatoire, les procédures proposées constituent des premières approches pour traiter des problèmes nouveaux, et peuvent très probablement être affinées. En particulier nous nous sommes restreints dans la plupart des cas à un débruitage simple dérivé de l'algorithme de seuillage dur, mais on peut sûrement gagner en performances théoriques (au niveau des facteurs logarithmiques dans le risque des estimateurs) et numériques en utilisant des méthodes plus développées (voir par exemple Autin [7]). Par exemple le seuillage par bloc ou certains autres seuillages aléatoires pourraient s'avérer utiles, et notamment

pour envisager des conditions plus générales sur le filtre dans le problème de déconvolution aléatoire.

Par ailleurs l'étude des performances de la procédure NeedVD débouche sur des problèmes d'analyse qui demandent à être encore approfondis, notamment concernant l'étude de l'espace considéré pour l'évaluation du risque minimax. Etant données les bonnes propriétés de localisation des needlets, et leurs similitudes avec la base de Meyer, on peut s'attendre à ce que l'espace de régularité en question soit de type Besov. Des résultats dans ce domaine ont été obtenus dans Narcowich et al. [72].

Sur le même thème, il serait intéressant d'effectuer une étude "maxiset" (Kerkyacharian et Picard [59]) de la procédure NeedVD, en essayant notamment de généraliser le résultat obtenu pour WaveD dans Johnstone et al. [53]. De premiers résultats maxisets, pour des problèmes inverses plus généraux, ont par ailleurs été établis par Loubes et Rivoirard [63].

Approfondir l'étude des opérateurs aléatoires

Nous n'avons pas traité ici des modèles à opérateurs aléatoires au sens usuel, c'est à dire bruités par une erreur d'amplitude réduite, comme décrit en introduction, et il serait intéressant de voir si la procédure NeedVD se généralise à ce cas.

Pour ce qui est des opérateurs aléatoires répondant à l'optique du chapitre 6, l'objectif principal est bien entendu de généraliser, sous deux points de vue :
  – en considérant d'autres opérateurs que celui de la déconvolution,
  – ou en restant dans le cadre de la déconvolution, mais en enlevant l'hypothèse d'indépendance entre le filtre et le bruit gaussien, ce qui permettrait par exemple de traiter les équations stochastiques avec retard (Reiss [82]).

Par ailleurs l'approche que nous avons donnée ici, face à la complexification du modèle initial, a été d'adapter la procédure dont nous disposions dans le cas déterministe (NeedVD ou WaveD) en travaillant sur le seuillage, sans toucher à la base. En nous replaçant dans l'optique générale de cette thèse, une deuxième possibilité serait peut être de chercher à altérer la base pour avoir un débruitage plus simple.

Chapter 3

NEED-VD: a second-generation wavelet algorithm for estimation in inverse problems

Ce chapitre est une version légèrement différente d'un article écrit en collaboration avec Gérard Kerkyacharian, Pencho Petrushev et Dominique Picard, et soumis à une revue.

<u>*Abstract:*</u> We provide a new algorithm for the treatment of inverse problems which combines the traditional SVD inversion with an appropriate thresholding technique in a well chosen new basis. Our goal is to devise an inversion procedure which has the advantages of localization and multiscale analysis of wavelet representations without losing the stability and computability of the SVD decompositions. To this end we utilize the construction of localized frames (termed "needlets") built upon the SVD bases.

We consider two different situations : the "wavelet" scenario, where the needlets are assumed to behave similarly to true wavelets, and the "Jacobi-type" scenario, where we assume that the properties of the frame truly depend on the SVD basis at hand (hence on the operator). To illustrate each situation, we apply the estimation algorithm respectively to the deconvolution problem and to the Wicksell problem. In the latter case, where the SVD basis is a Jacobi polynomial basis, we show that our scheme is capable of achieving rates of convergence which are optimal, and we give a simulation study showing that the NEED-VD estimator outperforms SVD algorithms in almost all situations.

3.1   Introduction

We consider the problem of recovering a function f from a blurred (by a linear operator) and noisy version of f: $Y_\varepsilon = Kf + \varepsilon\dot{W}$. It is important to note that, in general, for a problem like this there exists a basis which is fully adapted to the problem, and as a consequence, the inversion remains stable; this is the Singular Value Decomposition (SVD) basis. The SVD basis, however, might be difficult to determine and handle numerically. Also, it might not be appropriate for accurate description of the solution with a small number of parameters. Furthermore, in many practical situations, the signal exhibits inhomogeneous regularity, and its local features are particularly interesting to recover. In such cases, other bases or frames (in particular, localized wavelet type bases) might be much more appropriate for representation of the object at hand.

Our goal is to devise an inversion procedure which has the advantages of localization and multiscale analysis of wavelet representations without losing the stability and computability of the SVD decompositions. To this end we utilize the construction (due to Petrushev and his co-authors) of localized frames (termed "needlets") built upon particular bases - here the SVD bases. This construction uses a Calderón type decomposition combined with an appropriate quadrature (cubature) formula. It has the big advantage of producing frames which are close to wavelet bases in terms of dyadic properties and localization, but because of their compatibility with the SVD bases provide stable and easily computable schemes.

NEED-VD is an algorithm combining the traditional SVD inversion with an appropriate thresholding technique in a well chosen new basis. It enables one to approximate the targeted functions with excellent rates of convergence for any $\mathbb{L}_p$ loss function, and over a wide range of Besov spaces.

Our main idea is by combining the thresholding algorithm with SVD-based frames to create an effective and practically feasible algorithm for solving the inverse problem described above. The properties of the localized frame to be constructed depend on the underlying SVD basis. We will consider two different behaviors, the first corresponds to a "wavelet" behavior in the sense that the properties of the system are equivalent (as far as we are concerned) to the properties of a true wavelet basis. This case typically arises in the deconvolution setting. In the second case, the properties of the frame may differ from wavelet bases and truly depend on the SVD basis at hand (hence on the operator K). We will explore in detail a case typically arising when the SVD basis is a Jacobi polynomial basis. It is illustrated by the Wicksell problem. We show that our scheme is capable of achieving interesting rates of convergence, which are optimal and new in the literature. We also give a simulation study for the Wicksell problem which shows that the NEED-VD algorithm applied in combination with SVD based frames is valuable since it outperforms other standard algorithms.

The chapter is organized in the following way: the second section introduces the model, the classical SVD methods, and the two basic examples considered in this paper, i.e. the deconvolution and Wicksell's problem. The third section introduces the needlet construction, gives some basic properties of needlets and introduces the NEED-VD algorithm. The fourth section explores its properties in the wavelet scenario. The main motivation for the NEED-VD algorithm is given there after. The fifth section is devoted to the results in

a Jacobi scenario. The sixth section is devoted to simulation results. The proofs of the main results from sections 4–5 are given in sections 7–8, respectively. The last section is an appendix which contains the definition and basic properties of the Jacobi needlets.

3.2 Inverse Models

Suppose $\mathbb{H}$ and $\mathbb{K}$ are two Hilbert spaces and let $K : \mathbb{H} \mapsto \mathbb{K}$ be a linear operator. The standard linear ill-posed inverse problem consists in recovering a good approximation f_ε of the solution f of

$$g = Kf \tag{3.1}$$

when only a perturbation Y_ε of g is observed. In this paper, we will consider the case when this perturbation is an additive stochastic white noise. Namely, we observe Y_ε defined by the following identity:

$$Y_\varepsilon = Kf + \varepsilon \dot{W}, \tag{3.2}$$

where ε is the amplitude of the noise. It is supposed to be a small parameter which tends to 0. The error will be measured in terms of this small parameter. Here $\dot{W}$ is a $\mathbb{K}$-white noise, i.e. for any $g, h \in \mathbb{K}$, $\xi(g) := (\dot{W}, g)_\mathbb{K}$, $\xi(h) := (\dot{W}, h)_\mathbb{K}$ form random Gaussian vectors (centered) with marginal variance $\|g\|_\mathbb{K}^2$, $\|h\|_\mathbb{K}^2$, and covariance $(g, h)_\mathbb{K}$ (with the obvious extension when one considers k functions instead of 2).

Equation (3.2) means that for any $g \in \mathbb{K}$, we observe $Y_\varepsilon(g) := (Y_\varepsilon, g)_\mathbb{K} = (Kf, g)_\mathbb{K} + \varepsilon \xi(g)$, where $\xi(g) \sim N(0, \|g\|^2)$, and $Y(g)$, $Y(h)$ are independent random variables for orthogonal functions g and h.

Let us first recall the Singular Value Decomposition method. Under the assumption that K is compact, there exist two orthonormal bases (SVD bases) (e_k) of $\mathbb{H}$ and (g_k) of $\mathbb{K}$, and a sequence (b_k), $b_k \to 0$ as $k \to \infty$, such that

$$Ke_k = b_k g_k, \quad K^* g_k = b_k e_k,$$

with K^* being the adjoint operator of K.
The Singular Value Decomposition (SVD) of K

$$Kf = \sum_k b_k \langle f, e_k \rangle g_k$$

gives rise to approximation of the type

$$f_\varepsilon = \sum_{k=0}^{N} b_k^{-1} \langle Y_\varepsilon, g_k \rangle e_k,$$

where $N = N(\varepsilon)$ has to be properly selected. This SVD method is very attractive theoretically and can be shown to be asymptotically optimal in many situations (see Mathé and Pereverzev [65] together with their non linear counterparts Cavalier and Tsybakov [16], Cavalier et al. [17], Tsybakov [88], Goldenshluger and Pereverzev [43], Efromovich and Koltchinskii [38]). It also has the major advantage of performing a quick and stable inversion of the operator. However, it has serious limitations: First, the SVD bases might be

difficult to determine and handle numerically. Secondly, while these bases are fully adapted
to describe the operator K, they might not be appropriate for accurate description of the
solution with a small number of coefficients. Also in many practical situations, the signal has
inhomogeneous regularitiy, and its local features are particularly interesting to recover. In
such cases, other bases (in particular, localized wavelet type bases) are much more suitable
for representation of the object at hand.

In the last ten years, various nonlinear methods have been developed, especially in
the direct case with the objective of automatically adapting to the unknown smoothness
and local singular behavior of the solution. In the direct case, one of the most attractive
methods is probably wavelet thresholding, since it allies numerical simplicity to asymptotic
optimality on a large variety of functional classes such as Besov or Sobolev spaces.

To apply this approach to inverse problems, Donoho [35] introduced a wavelet-like de-
composition, specifically adapted to the operator K (Wavelet-Vaguelette-Decomposition)
and utilized a thresholding algorithm to this decomposition. In Abramovich and Silverman
[1], this method was compared with the similar vaguelette-wavelet decomposition. Other
wavelet schemes should be mentioned here, such as the ones from Antoniadis and Bigot [4],
Antoniadis et al. [6], Dicken and Maass [27], and especially for the deconvolution problem,
Pensky and Vidakovic [78], Fan and Koo [40], Kalifa and Mallat [55], Neelamani et al. [74].

Later on Cohen et al. [24] introduced an algorithm combining a Galerkin inversion with
a thresholding algorithm.

The approach developed here was greatly influenced by these works.

Deconvolution

The deconvolution problem is probably one of the most famous inverse problem, giving
rise to a great deal of investigations, specially in signal processing, and has an extensive
bibliography. In the deconvolution problem, we consider the following operator: Let in this
case $\mathbb{H} = \mathbb{K}$ be the set of square integrable periodic functions, with the standard $\mathbb{L}_2[0,1]$
norm, and consider

$$f \in \ \mathbb{H} \mapsto \ Kf = \int_0^1 \gamma(u - t)f(t)dt \in \mathbb{H}, \tag{3.3}$$

where γ is a known function in $\mathbb{H}$. It is generally assumed to be a regular function. A
standard example is the box-car function which plays an important role in extending this
model to image processing and specially to analysis of sequences of images.

In this case simple calculations show that the SVD bases e_k and g_k both coincide with
the Fourier basis. The singular values correspond to the Fourier coefficients of the function
γ:

$$b_k = \hat{\gamma}_k. \tag{3.4}$$

Wicksell's problem

Another typical example is the following classical Wicksell's problem (Wicksell [91]). Sup-
pose a population of spheres is embedded in a medium. The spheres have radii that may be
assumed to be drawn independently from a density f. A random plane slice is taken through
the medium and those spheres that are intersected by the plane furnish circles which radii

are the points of observation $Y_1, \ldots, Y_n$. The unfolding problem is then to determine the density of the sphere radii from the observed circle radii. This problem also arises in medicine, where the spheres might be tumors in an animal's liver (see Nychka et al. [76]), as well as in numerous other contexts (biological, engineering, etc.) see for instance Cruz-Orive [25].

The difficulty of estimating the target function is well illustrated by figure 3.1. The Wicksell operator has a smoothing effect, thus the local variations of the target function become almost invisible in the case of observations corrupted by noise. (Also compare the blurred and noised observations in figure 3.7 to the target functions of figure 3.5.)
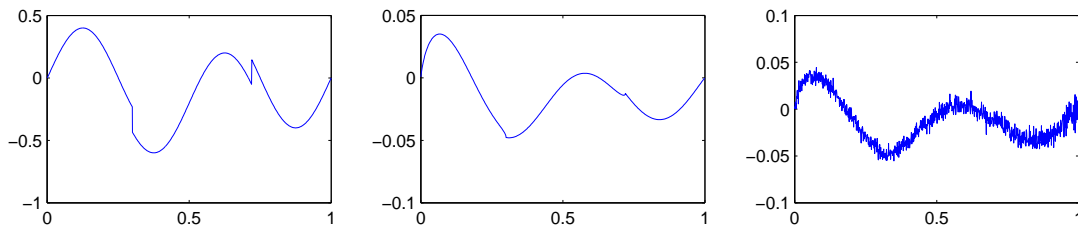
Figure 3.1: Heavisine function, its image by the Wicksell operator without and with gaussian noise with $rsnr = 5$

Following Johnstone and Silverman [54], the Wicksell's problem can be formulated using the following operator:

$$\mathbb{H} = \mathbb{L}_2([0,1], d\mu), \ d\mu(x) = (4x)^{-1}dx, \quad \mathbb{K} = \mathbb{L}_2([0,1], d\lambda), \ d\lambda(x) = 4\pi^{-1}(1-y^2)^{1/2}dy,$$

and

$$Kf(y) = \frac{\pi}{4}y(1-y^2)^{-1/2}\int_y^1 (x^2-y^2)^{-1/2}f(x)d\mu.$$

In this case, following Johnstone and Silverman [54], we have the following SVD bases:

$$e_k(x) = 4(k+1)^{1/2}x^2 P_k^{0,1}(2x^2-1)$$
$$g_k(y) = U_{2k+1}(y).$$

Here $P_k^{0,1}$ is the kth degree Jacobi polynomial of type $(0,1)$ and U_k is the second type Chebishev polynomial of degree k. The singular values are

$$b_k = \frac{\pi}{16}(1+k)^{-1/2}. \tag{3.5}$$

In this chapter, in order to avoid some additional technicalities, we consider this problem in the white noise framework, which is simpler than the original problem described above in density terms.

3.3 General scheme for construction of frames (Needlets) and thresholding

Frames were introduced in the 1950's by Duffin and Schaeffer [37] as a means for studying nonharmonic Fourier series. These are redundant systems which behave like bases and allow

for a lot of flexibility. Tight frame which are very close to orthonormal bases are particularly useful in signal and image processing.

In the following we present a general scheme for construction of frames due to Petrushev and his co-authors (Narcowich et al. [72], Petrushev and Xu [81, 80]). As will be shown this construction has the advantage of producing easily computable frame elements which are extremely well localized in all cases of interest. Following the aforementioned papers, we will term them "needlets".

Recall first the definition of a tight frame.

Definition 1. *Let $\mathbb{H}$ be a Hilbert space. A sequence (ψ_n) in $\mathbb{H}$ is said to be a tight frame if*

$$\|f\|^2 = \sum_n |\langle f, \psi_n \rangle|^2 \quad \forall f \in \mathbb{H}.$$

Let $(\mathcal{Y}, \mu)$ be a measure space with μ a finite positive measure. Suppose we have the following decomposition

$$\mathbb{L}_2(\mathcal{Y}, \mu) = \bigoplus_{k=0}^{\infty} H_k,$$

where the H_k's are finite dimensional spaces. For simplicity, we assume that H_0 is reduced to the constants.

Let $(e_i^k)_{i=1,\ldots,l_k}$ be an orthonormal basis of H_k. Then the orthogonal projector L_k onto H_k takes the form

$$L_k(f)(x) = \int_{\mathcal{Y}} f(y) L_k(x, y) d\mu(y), \quad \forall f \in \mathbb{L}_2(\mathcal{Y}, \mu),$$

where

$$L_k(x, y) = \sum_{i=1}^{l_k} e_i^k(x) \overline{e_i^k(y)}.$$

Note the obvious property of the orthogonal projectors:

$$\int_{\mathcal{Y}} L_k(x, y) L_m(y, z) d\mu(z) = \delta_{k,m} L_k(x, z). \tag{3.6}$$

The construction, inspired by the φ-transform of Frazier et al. [42], consists of two main steps: (i) Calderón type decomposition and (ii) Discretization, which are described in the following two subsections.

3.3.1   Calderón type decomposition

Let φ be a C^∞ function supported in $[-1, 1]$ such that $0 \le \varphi(\xi) \le 1$ and $\varphi(\xi) = 1$ if $|\xi| \le \frac{1}{2}$. Define $a(\xi) \ge 0$ from

$$a^2(\xi) = \varphi(\xi/2) - \varphi(\xi) \ge 0.$$

Then

$$\sum_{j \ge 0} a^2(\xi/2^j) = 1, \quad \forall |\xi| \ge 1. \tag{3.7}$$

We now introduce the operators

$$\Lambda_j = \sum_{k \geq 0} a^2(k/2^j) L_k$$

and their kernel

$$\Lambda_j(x,y) = \sum_{k \geq 0} a^2(k/2^j) L_k(x,y) = \sum_{2^{j-1} < k < 2^{j+1}} a^2(k/2^j) L_k(x,y).$$

The operators Λ_j provide a decomposition of $\mathbb{L}_2(\mathcal{Y}, \mu)$ which we record in the following proposition.

Proposition 1. *For all $f \in \mathbb{L}_2(\mathcal{Y}, \mu)$, we have*

$$f = L_0(f) + \sum_{j=0}^{\infty} \Lambda_j(f) \quad in \;\; \mathbb{L}_2(\mathcal{Y}, \mu). \tag{3.8}$$

Proof. By the definition of L_k and (3.7)

$$L_0 + \sum_{j=0}^{J} \Lambda_j = L_0 + \sum_{j=0}^{J} \sum_k a^2(k/2^j) L_k = \sum_k \varphi(k/2^{J+1}) L_k \tag{3.9}$$

and hence

$$\|f - L_0(f) - \sum_{j=0}^{J} \Lambda_j(f)\|^2 = \sum_{l \geq 2^{J+1}} \|L_l(f)\|^2 + \sum_{2^J \leq l < 2^{J+1}} \|L_l(f)(1 - \varphi(l/2^{J+1}))\|^2$$
$$\leq \sum_{l \geq 2^J} \|L_l(f)\|^2 \longrightarrow 0 \quad \text{as} \quad J \to \infty,$$

which completes the proof. $\qquad \square$

3.3.2 Discretization

Let us define

$$\mathcal{K}_k = \bigoplus_{m=0}^{k} H_m.$$

We make two additional assumptions which will enable us to discretize decomposition (3.8) from Proposition 1:

(a)
$$f \in \mathcal{K}_k, \; g \in \mathcal{K}_l \Longrightarrow fg \in \mathcal{K}_{k+l}.$$

(b) *Quadrature formula*: For any $k \in \mathbb{N}_0$ there exists $\mathcal{X}_k$ a finite subset of $\mathcal{Y}$ ($\#\mathcal{X}_0 = 1$) and positive numbers $\lambda_\eta > 0$, $\eta \in \mathcal{X}_k$, such that

$$\int_{\mathcal{Y}} f d\mu = \sum_{\eta \in \mathcal{X}_k} \lambda_\eta f(\eta) \quad \forall f \in \mathcal{K}_k. \tag{3.10}$$

We define

$$M_j(x,y) = \sum_k a(k/2^j) L_k(x,y) \quad \text{for} \quad j \geq 0. \tag{3.11}$$

Then as a consequence of (3.6), we have

$$\Lambda_j(x,y) = \int_{\mathcal{Y}} M_j(x,z) M_j(z,y) d\mu(z). \tag{3.12}$$

It is readily seen that $M_j(x,z) = \overline{M_j(z,x)}$ and

$$z \mapsto M_j(x,z) \in \mathcal{K}_{2^{j+1}-1} \quad \text{and hence} \quad z \mapsto M_j(x,z) M_j(z,y) \in \mathcal{K}_{2^{j+2}-2}.$$

Now, by (3.10)

$$\Lambda_j(x,y) = \int_{\mathcal{Y}} M_j(x,z) M_j(z,y) d\mu(z) = \sum_{\eta \in \mathcal{X}_{2^{j+2}-2}} \lambda_\eta M_j(x,\eta) M_j(\eta,y),$$

which implies

$$\begin{aligned}
\Lambda_j f(x) &= \int_{\mathcal{Y}} \Lambda_j(x,y) f(y) d\mu(y) = \int_{\mathcal{Y}} \sum_{\eta \in \mathcal{X}_{2^{j+2}-2}} \lambda_\eta M_j(x,\eta) M_j(\eta,y) f(y) d\mu(y) \\
&= \sum_{\eta \in \mathcal{X}_{2^{j+2}-2}} \sqrt{\lambda_\eta} M_j(x,\eta) \int_{\mathcal{Y}} f(y) \overline{\sqrt{\lambda_\eta} M_j(y,\eta)} d\mu(y).
\end{aligned} \tag{3.13}$$

We are now prepared to introduce the desired frame. Let $\mathbb{Z}_j = \mathcal{X}_{2^{j+2}-2}$ for $j \geq 0$ and $\mathbb{Z}_{-1} = \mathcal{X}_0$. We define the frame elements (needlets) by

$$\psi_{j,\eta}(x) = \sqrt{\lambda_\eta} M_j(x,\eta), \quad \eta \in \mathbb{Z}_j, \quad j \geq -1. \tag{3.14}$$

Notice that $\mathbb{Z}_{-1}$ consists of a single point and $\psi_0 = \psi_{-1,\eta}$, $\eta \in \mathbb{Z}_{-1}$, is the $\mathbb{L}_2$-normalized positive constant. Now (3.13) becomes

$$\Lambda_j f(x) = \sum_{\eta \in \mathbb{Z}_j} \langle f, \psi_{j,\eta} \rangle \psi_{j,\eta}(x). \tag{3.15}$$

Proposition 2. *The family* $(\psi_{j,\eta})_{\eta \in \mathbb{Z}_j, j \geq -1}$ *is a tight frame for* $\mathbb{L}_2(\mathcal{Y}, \mu)$.

Proof. As

$$f = \lim_{J \to \infty} L_0(f) + \sum_{j=0}^{J} \Lambda_j(f)$$

we have

$$\|f\|^2 = \lim_{J \to \infty} \langle L_0(f), f \rangle + \sum_{j=0}^{J} \langle \Lambda_j(f), f \rangle.$$

But by (3.15)

$$\langle \Lambda_j(f), f \rangle = \sum_{\eta \in \mathbb{Z}_j} \langle f, \psi_{j,\eta} \rangle \langle \psi_{j,\eta}, f \rangle = \sum_{\eta \in \mathbb{Z}_j} |\langle f, \psi_{j,\eta} \rangle|^2, \quad j \geq 0,$$

and since ψ_0 is the normalized constant $\langle L_0(f), f \rangle = |\langle f, \psi_0 \rangle|^2$. Hence

$$\|f\|^2 = |\langle f, \psi_0 \rangle|^2 + \sum_{j \in \mathbb{N}_0, \, \eta \in \mathbb{Z}_j} |\langle f, \psi_{j,\eta} \rangle|^2,$$

which shows that $(\psi_{j,\eta})$ is a tight frame. $\qquad\square$

3.3.3 Localization properties

The critical property of the frame construction above which makes it so attractive is the excellent localization of the frame elements (needlets) $(\psi_{j,\eta})$ in various settings of interest (see Narcowich et al. [71, 72], Petrushev and Xu [81, 80]).
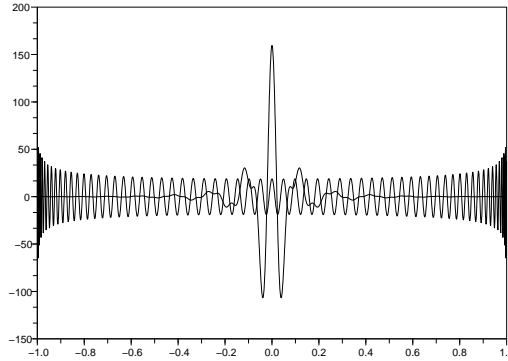
Figure 3.2: A Legendre polynomial (oscillating function) and a Legendre needlet of the same degree

Figure 3.2 is an illustration of this phenomenon. The rapidly oscillating function is the Legendre polynomial of degree 2^8, whereas the localized one is a needlet constructed as explained above using Legendre polynomials of degree $\leq 2^8$ and centered approximately at zero. Its localization is remarkable taking into account that both functions are polynomials of the same degree.

In the case of the unit sphere in $\mathbb{R}^{d+1}$, where H_k are the spaces of spherical harmonics, the following localization property of the needlets is established in Narcowich et al. [71, 72]: For any k there exists a constant C_k such that :

$$|\psi_{j\eta}(\xi)| \leq \frac{C_k 2^{dj/2}}{[1 + 2^j \arccos < \eta, \xi >]^k}.$$

In the case of Jacobi polynomials on $[-1, 1]$, the localization of the needlets proved in Petrushev and Xu [81] takes the form: For any k there exists a constant C_k such that

$$|\psi_{j\eta}(\cos\theta)| \leq \frac{C_k 2^{j/2}}{(1 + 2^j|\theta - \arccos\eta|)^k \sqrt{w_{\alpha,\beta}(2^j, \cos\theta)}}, \quad |\theta| \leq \pi,$$

where $w_{\alpha,\beta}(n, x) = (1 - x + n^{-2})^{\alpha+1/2}(1 + x + n^{-2})^{\beta+1/2}$ and $\alpha, \beta > -1/2$.

The almost exponential localization of the needlets and their semi-orthogonal structure allows to use them for characterization of spaces other than L_2, in particular the more general Triebel-Lizorkin and Besov spaces (see Narcowich et al. [72], Petrushev and Xu [81]).

3.3.4 NEED-VD algorithm: thresholding needlet coefficients

We describe here the general idea of the method. The first step is to construct a needlet system (frame) $\{\psi_{j\eta} : \eta \in \mathbb{Z}_j, j \geq -1\}$ as described in section 3, where H_k is simply the space spanned by the k-th vector e_k of the SVD basis.

The needlet decomposition of any $f \in \mathbb{H}$ takes the form

$$f = \sum_j \sum_{\eta \in \mathbb{Z}_j} (f, \psi_{j\eta})_{\mathbb{H}} \psi_{j\eta}.$$

Using Parseval's identity, we have $\beta_{j\eta} = (f, \psi_{j\eta})_{\mathbb{H}} = \sum_i f_i \psi_{j\eta}^i$ with $f_i = (f, e_i)_{\mathbb{H}}$ and $\psi_{j\eta}^i = (\psi_{j\eta}, e_i)_{\mathbb{H}}$. If we put $Y_i = (Y_\varepsilon, g_i)_{\mathbb{K}}$, then

$$Y_i = (Kf, g_i)_{\mathbb{K}} + \varepsilon \xi_i = (f, K^* g_i)_{\mathbb{K}} + \varepsilon \xi_i = \left(\sum_j f_j e_j, K^* g_i \right)_{\mathbb{H}} + \varepsilon \xi_i = b_i f_i + \varepsilon \xi_i,$$

where $\xi_i = (\dot{W}, g_i)_{\mathbb{K}}$ form a sequence of centered Gaussian variables with variance 1. Thus

$$\hat{\beta}_{j\eta} = \sum_i \frac{Y_i}{b_i} \psi_{j\eta}^i$$

is an unbiased estimate of $\beta_{j\eta}$. Notice that from the needlet construction (see the previous section) it follows that the sum above is finite. More precisely, $\psi_{j\eta}^i \neq 0$ only for $2^{j-1} < i < 2^{j+1}$.

Let us consider the following estimate of f:

$$\hat{f} = \sum_{j=-1}^J \sum_{\eta \in \mathbb{Z}_j} t(\hat{\beta}_{j\eta}) \psi_{j\eta},$$

where t is a thresholding operator defined by

$$t(\hat{\beta}_{j\eta}) = \hat{\beta}_{j\eta} I\{|\hat{\beta}_{j\eta}| \geq \kappa t_\varepsilon \sigma_j\} \quad \text{with} \tag{3.16}$$

$$t_\varepsilon = \varepsilon \sqrt{\log \frac{1}{\varepsilon}}. \tag{3.17}$$

Here κ is a tuning parameter of the method which will be properly selected later on. Notice that the thresholding depends on the resolution level j through the constant σ_j which will also be specified later on, and the same with regard to the upper level of details J.

We will particularly focus on two situations (corresponding to the two examples discussed above). In the first case (see subsection 3.4), the needlets have very nice properties and behave exactly like wavelets. This is for instance the case of the deconvolution, where the SVD basis is the Fourier basis. However, more complicated problems e.g. the Wicksell's problem exhibit more delicate concentration properties for the needlets giving rise to different behaviors in terms of rates of convergence for the estimators.

3.4   NEED-VD in wavelet scenario

In this section, we assume that the needlet system has the following properties: For any $1 \leq p < \infty$, there exist positive constants c_p, C_p, and D_p such that

$$\text{Card } \mathbb{Z}_j \leq C 2^j, \tag{3.18}$$

$$c_p 2^{j(\frac{p}{2}-1)} \leq \|\psi_{j\eta}\|_p^p \leq C_p 2^{j(\frac{p}{2}-1)}, \tag{3.19}$$

$$\| \sum_{\eta \in \mathbb{Z}_j} u_\eta \psi_{j\eta} \|_p^p \leq D_p \sum_{\eta \in \mathbb{Z}_j} |u_\eta|^p \|\psi_{j\eta}\|_p^p, \quad \text{for any any collection } (u_\eta). \tag{3.20}$$

We define the space $B_{\pi,r}^s$ as the collection of all functions f with $f = \sum_{j\geq 0}\sum_{\eta\in\mathbb{Z}_j}\beta_{j\eta}\psi_{j\eta}$ such that

$$\|f\|_{B_{\pi,r}^s} := \|(2^{j[s+\frac{1}{2}-\frac{1}{\pi}]}\|(\beta_{j\eta})_{\eta\in\mathbb{Z}_j}\|_{l_\pi})_{j\geq 0}\|_{l_r} < \infty, \quad \text{and} \tag{3.21}$$

$$f \in B_{\pi,r}^s(M) \iff \|f\|_{B_{\pi,r}^s} \leq M. \tag{3.22}$$

Theorem 1. *Let $1 < p < \infty$, $2\nu + 1 > 0$, and*

$$\sigma_j^2 := \sum_i [\frac{\psi_{j\eta}^i}{b_i}]^2 \leq C2^{2j\nu}, \ \forall \ j \geq 0. \tag{3.23}$$

Suppose $\kappa^2 \geq 16p$ and $2^J = [t_\varepsilon]^{\frac{-2}{2\nu+1}}$ with t_ε as in (3.16).
    Then for $f \in B_{\pi,r}^s(M)$ with $\pi \geq 1$, $s \geq 1/\pi$, $r \geq 1$ (with the restriction $r \leq \pi$ if $s = (\nu + \frac{1}{2})(\frac{p}{\pi} - 1)$), we have

$$\mathbb{E}\|\hat{f} - f\|_p^p \leq C \log(1/\varepsilon)^{p-1}[\varepsilon\sqrt{\log(1/\varepsilon)}]^{\mu p}, \tag{3.24}$$

where

$$\mu = \frac{s}{s+\nu+1/2}, \quad if \ s \geq (\nu + \frac{1}{2})(\frac{p}{\pi} - 1)$$

$$\mu = \frac{s-1/\pi+1/p}{s+\nu+1/2-1/\pi}, \quad if \ \frac{1}{\pi} \leq s < (\nu + \frac{1}{2})(\frac{p}{\pi} - 1).$$

  The proof of this theorem is given in section 7.
  Remarks :

1. These results are essentially minimax (see Chapter 6) up to logarithmic factors. We find back here the elbow, which was already observed in the direct problem, as well as in the deconvolution setting (see Johnstone et al. [53], for instance).

2. Condition (3.23) is essential in this problem. In the deconvolution case, the SVD basis is the *Fourier* basis and hence $\psi_{j\eta}^i$ are simply the Fourier coefficients of $\psi_{j\eta}$. Then assuming that we are in the so-called "regular" case ($b_k \sim k^{-\nu}$, for all k), it is easy to show that (3.23) is true for the needlet system as constructed above (see also the discussion in the following subsection). A similar remark can be made regarding conditions (3.19) and (3.20). In the deconvolution setting, the needlet construction is not strictly needed and, as is shown in Johnstone et al. [53], the periodized Meyer wavelet basis (see Meyer [69] and Mallat [64]) can replace the needlet construction. Condition (3.23) also holds in more general cases such as the box-car deconvolution, see Johnstone et al. [53], Kerkyacharian et al. [58] where this algorithm is applied using Meyer's wavelets. $\diamond$

Condition (3.23) and the needlet construction
    The following lines are intended to a posteriori motivate our decision to built upon the needlet construction. As was mentioned above condition (3.23) is very important for our algorithm. The proof will reveal that it is essential, since σ_j^2 is exactly the variance of our estimator of $\beta_{j\eta}$, so in a sense no other thresholding strategy can be better.

Let us now examine how condition (3.23) links the frame $(\psi_{j\eta})$ with the SVD basis (e_k). To see this clearly let us suppose that $(\psi_{j\eta})$ is an arbitrary frame and let us place ourselves in the regular case:

$$b_i \sim i^{-\nu}$$

(this means that there exist two positive constants c and c' such that $c'i^{-\nu} \leq b_i \leq ci^{-\nu}$). If condition (3.23) holds true, we have

$$C2^{2j\nu} \geq \sum_m \sum_{2^m \leq i \leq 2^{m+1}-1} [\frac{\psi_{j\eta}^i}{b_i}]^2.$$

Hence, $\forall\, m \geq j$,

$$\sum_{2^m \leq i \leq 2^{m+1}-1} [\psi_{j\eta}^i]^2 \leq c2^{2\nu(j-m)}.$$

This means that the energy of $\psi_{j\eta}^i$ decays exponentially for $i \geq 2^j$, which reviles the role of the Littlewood Paley decomposition in the previous construction, replacing the exponential discrepancy by a cut-off.

The following proposition establishes a kind of converse property: The construction of needlet systems always implies that condition (3.23) is satisfied in the regular case.

Proposition 3. *If $(\psi_{j,\eta})$ is a frame such that $\{i : \psi_{j\eta}^i \neq 0\}$ is contained in a set $\{C_1 2^j, \ldots, C_2 2^j\}$, and $b_i \sim i^{-\nu}$, then*

$$\sigma_j^2 := \sum_i [\frac{\psi_{j\eta}^i}{b_i}]^2 \leq C2^{2j\nu}.$$

Proof. Since the elements of an arbitrary frame are bounded in norm and $\psi_{j\eta}^i \neq 0$ only for $C_1 2^j \leq i \leq C_2 2^j$, we have

$$\sum_i [\frac{\psi_{j\eta}^i}{b_i}]^2 \leq C2^{2j\nu}\|\psi_{j,\eta}\|^2 \leq C'2^{2j\nu}.$$

$\square$

3.5 NEED-VD in a Jacobi-type case

Properties (3.19)-(3.20) are not necessarily valid for an arbitrary needlet system, since as mentioned above the localization properties of the frame elements depend on the initial underlying basis, and hence on the problem at hand. We will consider here a particular case motivated by Wicksell's problem.

We consider the space $\mathbb{H} = \mathbb{L}_2(I, d\gamma(x))$, where $I = [-1, 1]$, $d\gamma(x) = \omega_{\alpha,\beta}(x)dx$,

$$\omega_{\alpha,\beta}(x) = c_{\alpha,\beta}(1 - x)^\alpha(1 + x)^\beta, \quad \alpha, \beta > -1/2,$$

and $c_{\alpha,\beta}$ is selected so that $\int_I d\gamma_{\alpha,\beta}(x) = 1$. We will assume that $\alpha \geq \beta$ (otherwise we can interchange the roles of α and β).

Let $(P_k)_{k \geq 0}$ be the $\mathbb{L}_2(I, d\gamma(x))$ normalized Jacobi polynomials. We assume that the Jacobi polynomials appear as an SVD basis of the operator K. This is the case of Wicksell's problem, where $\beta = 0$, $\alpha = 1$, $b_k \sim k^{-1/2}$.

In the Jacobi case, the needlets have been introduced and studied in Petrushev and Xu [81]. See also the appendix, where the definition and some important properties of Jacobi needlets are given.

We will state our results in a more general setting, assuming that only a few conditions on the needlet system are valid. Note that these conditions are obeyed by the needlet system (Jacobi needlets) constructed using the Jacobi polynomials $(P_k)_{k \geq 0}$. The proofs are given in the appendix.

We will consider two sets of conditions. The first one (which only depends on α) is the following:

$$\text{Card } \mathbb{Z}_j \leq 2^j, \tag{3.25}$$

$$\sum_{\eta \in \mathbb{Z}_j} \|\psi_{j\eta}\|_p^p \leq C_p 2^{jp/2} \vee 2^{j(p-2)(1+\alpha)}, \quad \forall j, \ \forall\, p \neq 2 + \frac{1}{\alpha + 1/2}, \tag{3.26}$$

$$\|\sum_{\eta \in \mathcal{X}_j} \beta_\eta \psi_{j,\eta}\|_p \leq C \left(\sum_{\eta \in \mathcal{X}_j} |\beta_\eta|^p \|\psi_{j,\eta}\|_p^p\right)^{1/p}. \tag{3.27}$$

We define the space $\widetilde{B}_{\pi,r}^s$ as the collection of all functions f on $[-1, 1]$ with representation

$$f = \sum_{j \geq -1} \sum_{\eta \in \mathbb{Z}_j} \beta_{j\eta} \psi_{j\eta}$$

such that

$$\|f\|_{\widetilde{B}_{\pi,r}^s} := \|(2^{js}(\sum |\beta_{j,\eta}|^\pi \|\psi_{j,\eta}\|_\pi^\pi)^{1/\pi})_{j \geq -1}\|_{l_r} < \infty, \quad \text{and} \tag{3.28}$$

$$f \in \widetilde{B}_{\pi,r}^s(M) \iff \|f\|_{\widetilde{B}_{\pi r}^s} \leq M. \tag{3.29}$$

Theorem 2. *Let* $1 < p < \infty$ *and* $\alpha \geq \beta > -\frac{1}{2}$. *Suppose*

$$t_\varepsilon = \varepsilon \sqrt{\log 1/\varepsilon} \quad and \quad 2^J = t_\varepsilon^{-\frac{2}{1+2\nu}}.$$

Let $\kappa^2 \geq 16p[1 + 4\{(\frac{\alpha}{2} - \frac{\alpha+1}{p})_+ \vee (\frac{\beta}{2} - \frac{\beta+1}{p})_+\}]$ *and assume that we are in the regular case, i.e.*

$$b_i \sim i^{-\nu}, \quad \nu > -\frac{1}{2}.$$

Then for $f \in \widetilde{B}_{p,r}^s(M)$ *with* $s > [\frac{1}{2} - 2(\alpha + 1)(\frac{1}{2} - \frac{1}{p})]_+$, *we have*

$$\mathbb{E}\|\hat{f} - f\|_p^p \leq C[\log(1/\varepsilon)]^{p-1}[\varepsilon\sqrt{\log(1/\varepsilon)}]^{\mu p},$$

where

(i) *if* $p < 2 + \frac{1}{\alpha+1/2}$, *then*

$$\mu = \frac{s}{s + \nu + \frac{1}{2}};$$

(ii) *if* $p > 2 + \frac{1}{\alpha+1/2}$, *then*

$$\mu = \frac{s}{s + \nu + (\alpha + 1)(1 - \frac{2}{p})}.$$

Remarks :

1. In the case $p < 2 + \frac{1}{\alpha + 1/2}$, the rate obtained here is the usual one, and can be proved to be minimax (see Chapter 4). The case $p > 2 + \frac{1}{\alpha + 1/2}$ introduces a new rate of convergence, which is always better than in the first case.

2. Conditions (3.25)–(3.27) enabled us to estimate the rates of convergence of our scheme, whenever the index π of the Besov space is the same as the index of the loss function ($p = \pi$). In the sequel, we will study the case where p and π are independently chosen. This requires, however, some additional assumptions. $\diamond$

If in addition to properties (3.25)–(3.27), we now assume that the following conditions are fulfilled: For any $\eta \in \mathbb{Z}_j$, $j \geq 0$,

$$\|\psi_{j\eta}\|_p^p \asymp 2^{j(p-2)(\alpha+1)} k(\eta)^{-(p-2)(\alpha+1/2)}, \quad k(\eta) < 2^{j-1}, \qquad (3.30)$$

$$\|\psi_{j\eta}\|_p^p \asymp 2^{j(p-2)(\beta+1)} k'(\eta)^{-(p-2)(\beta+1/2)}, \quad k'(\eta) = 2^j - k(\eta) < 2^{j-1}, \qquad (3.31)$$

where $k(\eta) \in \{1, \dots, 2^j\}$ is the index of $\eta \in \mathbb{Z}_j$. Here we assume that the points in $\mathbb{Z}_j$ are ordered so that $\eta_1 > \eta_2 > \cdots > \eta_{2^j}$. Note that in the case of Jacobi needlets $\mathbb{Z}_j$ consists of the zeros of the Jacobi polynomial $P_{2^j}^{\alpha,\beta}$ (see the appendix). In the following we will briefly write k instead of $k(\eta)$ and k' instead of $k'(\eta)$. Of course, (3.26) is now a consequence of conditions (3.30)–(3.31).

Observe the important fact that properties (3.30)–(3.31) are valid in the case of Jacobi Polynomials (see the appendix).

Theorem 3. *Let $1 < p < \infty$ and $\alpha \geq \beta > -\frac{1}{2}$. Suppose that conditions $(3.25) - (3.27)$ and $(3.30) - (3.31)$ are fulfilled. Let*

$$2^J = t_\varepsilon^{-\frac{2}{1+2\nu}} \quad and \quad \kappa^2 \geq 16p[1 + 4\{(\frac{\alpha}{2} - \frac{\alpha+1}{p})_+ \vee (\frac{\beta}{2} - \frac{\beta+1}{p})_+\}]$$

and suppose that we are in the regular case, i.e.

$$b_i \sim i^{-\nu}, \quad \nu > -\frac{1}{2}.$$

Then for $f \in \widetilde{B}_{\pi,r}^s(M)$ with $s > \max_{\gamma \in \{\alpha,\beta\}}\{\frac{1}{2} - 2(\gamma+1)(\frac{1}{2} - \frac{1}{\pi}) \vee 2(\gamma+1)(\frac{1}{\pi} - \frac{1}{p}) \vee 0\}$, we have

$$\mathbb{E}\|\hat{f} - f\|_p^p \leq C[\log(1/\varepsilon)]^{p-1+a}[\varepsilon\sqrt{\log(1/\varepsilon)}]^{\mu p}, \qquad (3.32)$$

where

$$\mu = \min\{\mu(s), \mu(s,\alpha), \mu(s,\beta)\} \quad and \quad a = \max\{a(\alpha), a(\beta)\} \leq 2 \quad with$$

$$\mu(s) = \frac{s}{s + \nu + \frac{1}{2}},$$

$$\mu(s,\gamma) = \frac{s - 2(1+\gamma)(\frac{1}{\pi} - \frac{1}{p})}{s + \nu + 2(1+\gamma)(\frac{1}{2} - \frac{1}{\pi})}$$

and, $a(\gamma) = \begin{cases} I\{\delta_p = 0\} & \text{if } [p-\pi][1 - (p-2)(\gamma+1/2)] \geq 0, \\ \frac{(\gamma+\frac{1}{2})(\pi-p)}{(\pi-2)(\gamma+1/2)-1} + I\{\delta_s = 0\} & \text{if } [p-\pi][1 - (p-2)(\gamma+1/2)] < 0, \end{cases}$

with $\delta_p = 1 - (p-2)(\gamma+1/2)$ *and* $\delta_s = s[1 - (p-2)(\gamma+1/2)] - p(2\nu+1)(\gamma+1)(\frac{1}{\pi} - \frac{1}{p})$.

The proofs of Theorems 2 and 8 are relegated to section 8.

Remarks :

1. Naturally, Theorem 2 follows by Theorem 8. We stated these two theorems separately because the hypotheses of Theorem 2 are less restrictive than the conditions in Theorem 8 and hence Theorem 2 potentially has wider range of application than Theorem 8.

2. It is interesting to notice that the convergence rates in (8) depend only on three distinctive regions for the parameters (which are actually present in Theorem 2, but hidden in the condition $\alpha \geq \beta$), which depends on a very subtle interrelation between the parameters s, α, β, p, π. These rates are essentially minimax (see Chapter 4).

3. It is also interesting to note that the usual rates of convergence obtained e.g. in the wavelet scenario are realized in the extreme case $\alpha = \beta = -\frac{1}{2}$. $\diamond$

3.6 Simulation study

In this section we investigate the numerical performances of the Need-VD estimator in the context of Wicksell's problem described previously. We compare the results for simulated datasets to those obtained with several SVD methods.

3.6.1 The estimators

Singular value decomposition estimators

With the notations introduced before, f can be naturally estimated by the following linear estimator based on the singular value decomposition of operator K:

$$\hat{f} = \sum_i \lambda_i \frac{Y_i}{b_i} e_i,$$

where $(\lambda_i)_{i \in \mathbb{N}}$ is a deterministic filter.

In the simulations a first SVD estimator with projection weights was used:

$$\begin{cases} \lambda_i & = 1 \quad \text{if } i \leq N, \\ \lambda_i & = 0 \quad \text{if } i > N, \end{cases}$$

where the parameter N was fitted for each setting so as to minimize the root mean square error ($RMSE$) of the estimator.

We also use the SVD estimator developed in Cavalier and Tsybakov [16], which is completely adaptive with a data driven choice of the filter and thus much more convenient than the former in practice. The values of λ_i are constant in blocs $I_j = [\kappa_{j-1}, \kappa_j - 1]$ with limits $\kappa_0 = 1$ and $\kappa_J = N + 1$ determined further:

$$\begin{cases} \lambda_i = \left(1 - \frac{\sigma_j^2 (1 + \Delta_j^\gamma)}{\|\bar{Y}\|_{(j)}^2}\right)_+ & \text{if } i \in I_j, \; j = 1, \ldots J, \\ \lambda_i = 0 & \text{if } i > N, \end{cases}$$

where:

$$\bar{Y}_i = \frac{Y_i}{b_i}, \quad \|\bar{Y}\|_{(j)}^2 = \sum_{i \in I_j} \bar{Y}_i^2, \quad \sigma_j^2 = \varepsilon^2 \sum_{i \in I_j} b_i^{-2}, \quad \Delta_j = \frac{\max_{i \in I_j} b_i^{-2}}{\sum_{i \in I_j} b_i^{-2}}, \quad 0 < \gamma < 1/2,$$

and we used the notation $x_+ = \max(0, x)$.

The blocks are determined by the following procedure. Let $\nu_\varepsilon \sim \max(5, \log\log(1/\varepsilon))$ and $\rho_\varepsilon = \frac{1}{\log(\nu_\varepsilon)}$, we define:

$$\begin{cases} \kappa_j = 1 & \text{if } j = 0, \\ \kappa_j = \nu_\varepsilon & \text{if } j = 1, \\ \kappa_j = \kappa_{j-1} + \lfloor \nu_\varepsilon \rho_\varepsilon (1 + \rho_\varepsilon)^{j-1} \rfloor & \text{if } j = 2, \ldots, J, \end{cases}$$

where J is large enough such that: $\kappa_J > \max\{m : \sum_{i=1}^m b_i^{-2} \le \varepsilon^{-2} \rho_\varepsilon^{-3}\}$.

In the simulation settings considered further the value taken by $\kappa_J = N + 1$ is too large compared to the level n of the discretization resolution, thus the estimation was performed at the level $N_0 = \min\left(\frac{n}{2}, N\right)$ instead of N.

Construction of the needlet basis

Every needlet ψ_{j,η_k} defined on $I = [-1, 1]$ is a linear combination of Jacobi polynomials as described in section 3, with weights depending on some filter a. This function is chosen as:

$$a(x) = \sqrt{\varphi(x/2) - \varphi(x)}, \quad \forall x \ge 0$$

where $\varphi(x) = I\{x < 0.5\} + P(x)I\{0.5 \le x \le 1\}$ and P is a polynomial adjusted such that the corresponding needlet is sufficiently regular. In practice this choice seems to be slightly better than a C^∞ filter with exponential shape.

The shape of a is given by figure 3.3, and some examples of needlets are given in figure 3.4. Their amplitudes and supports fit automatically to the location of η: the needlets located near the edges of I are much sharper than those located in the middle.
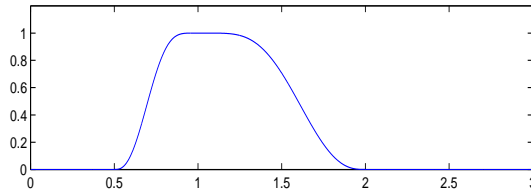
Figure 3.3: Filter a with polynomial shape

Finally NeedVD is performed by using the following basis $(\widetilde{\psi}_{j,\eta})$ adapted to the Wicksell problem:

$$\forall x \in [0, 1], \quad \widetilde{\psi}_{j,\eta}(x) = 4\sqrt{2}x^2 \psi_{j,\eta}(2x^2 - 1).$$
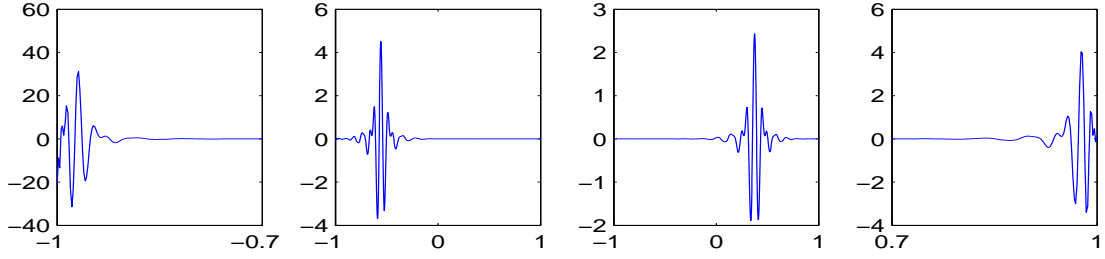
Figure 3.4: Examples of needlets: $\psi_{7,\eta_{10}}$, $\psi_{7,\eta_{40}}$, $\psi_{7,\eta_{80}}$ and $\psi_{7,\eta_{120}}$ (from left to right)

With such a basis we have for all $i \in \mathbb{N}$:

$$\widetilde{\psi}_{j,\eta}^{i} = a(i/2^{j-1})P_i(\eta)\sqrt{b_{j,\eta}},$$

thus the estimated coefficients of f in the frame are very easy to compute.

3.6.2 Parameters of the simulation

We consider the four commonly used target functions f represented in figure 3.5, and three levels of noise σ corresponding to three values of the root signal to noise ratio of $K(f)$: $rsnr \in \{3, 5, 7\}$. The discretization resolution level is set to $n = 1024$, and the constant η in the thresholds of NeedVD is set to $\eta = 0.75\sqrt{2}$.
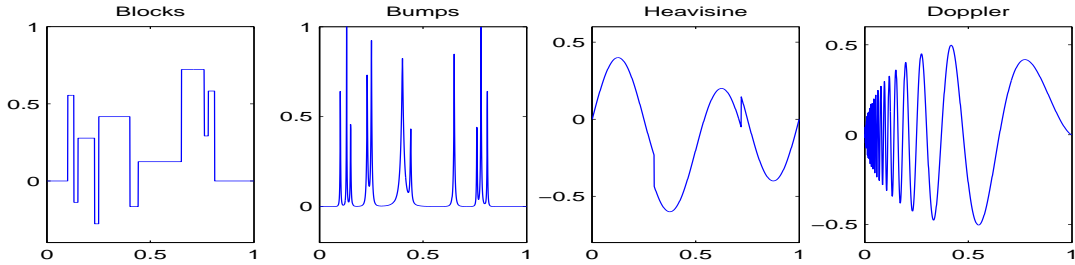
Figure 3.5: Target functions

The estimation error is evaluated by a Monte Carlo approximation of several $L_p(\mu)$ losses:

- $L1$ is computed as the average over 20 runs of $\frac{1}{n} \sum\limits_{i=1}^{n} |f(\frac{i}{n}) - \hat{f}(\frac{i}{n})|/(\frac{4i}{n})$.

- $RMSE$ is computed as the average over 20 runs of $\sqrt{\frac{1}{n} \sum\limits_{i=1}^{n} (f(\frac{i}{n}) - \hat{f}(\frac{i}{n}))^2/(\frac{4i}{n})}$.

In each run, the gaussian noise component is simulated independently of its values in the other runs.
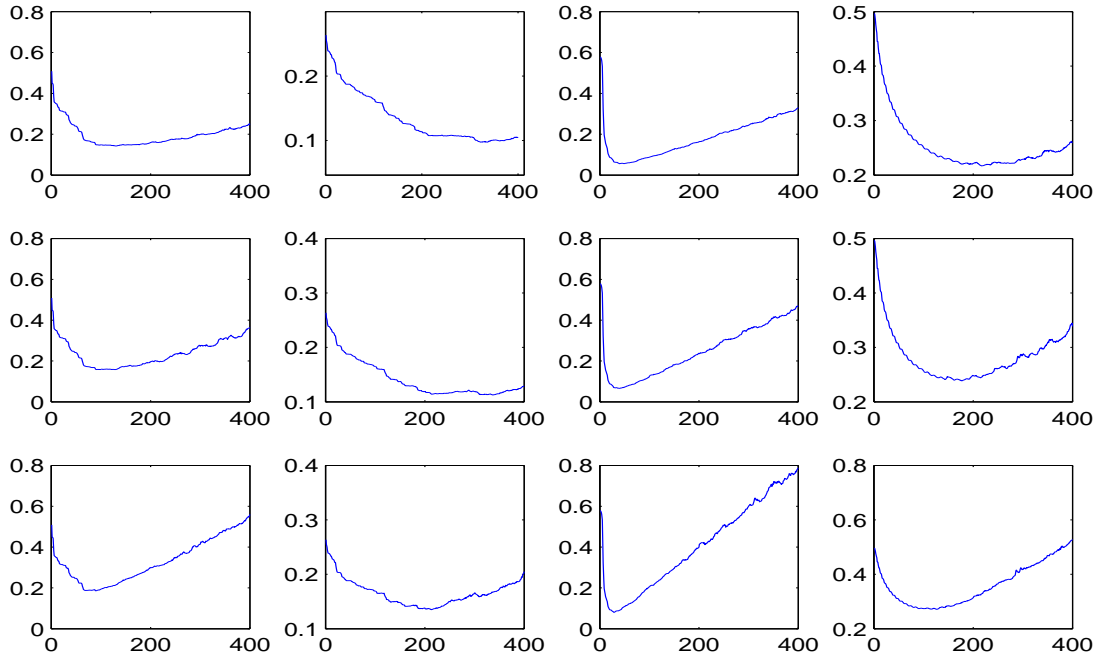
Figure 3.6: Value of the mean square error of the non adaptive SVD estimator (y-axis) for each value of N (x-axis) for $rsnr = 7$ to $rsnr = 3$ (from top to bottom) and for the target function Blocks, Bumps, Heavisine and Doppler (from left to right)

3.6.3   Analysis of the results

The performance of the non adaptive SVD estimator depends very strongly on the choice of N (see figure 3.6). A large N is needed in the case of small noise (first row of the figure) and in the case of very oscillating functions such as Doppler and Bumps. However even with this optimal *a posteriori* choice of N, the adaptive filter leads to better results than the non adaptive projection weights as shown in tables 3.1 and 3.2. Indeed the former is more adapted to the ill posed nature of the problem and to the variations of the noise, by adjusting over the singular values (b_k) and the data (y_k).

Moreover the NeedVD estimator generally outperforms both SVD estimators. As can be seen on figure 3.7, the differences are obvious in high noise for the Bumps and Doppler targets, where the SVD estimators are very noisy (in fact all the estimators happen to leave some noise unfiltered near the right edge of the interval, which is given lesser importance

	SVD			Adaptive SVD			NeedVD		
	low	**med**	**high**	**low**	**med**	**high**	**low**	**med**	**high**
Blocks	0.0452	0.0495	0.0677	0.0399	0.0465	0.0591	0.0347	0.0404	0.0511
Bumps	0.0324	0.0388	0.0463	0.0258	0.0295	0.0361	0.0180	0.0206	0.0270
Heavisine	0.0257	0.0305	0.0402	0.0248	0.0299	0.0401	0.0205	0.0254	0.0321
Doppler	0.1032	0.1138	0.1307	0.1002	0.1085	0.1230	0.0858	0.0909	0.1007

Table 3.1:   Error L1 for each target, each noise level and each estimator
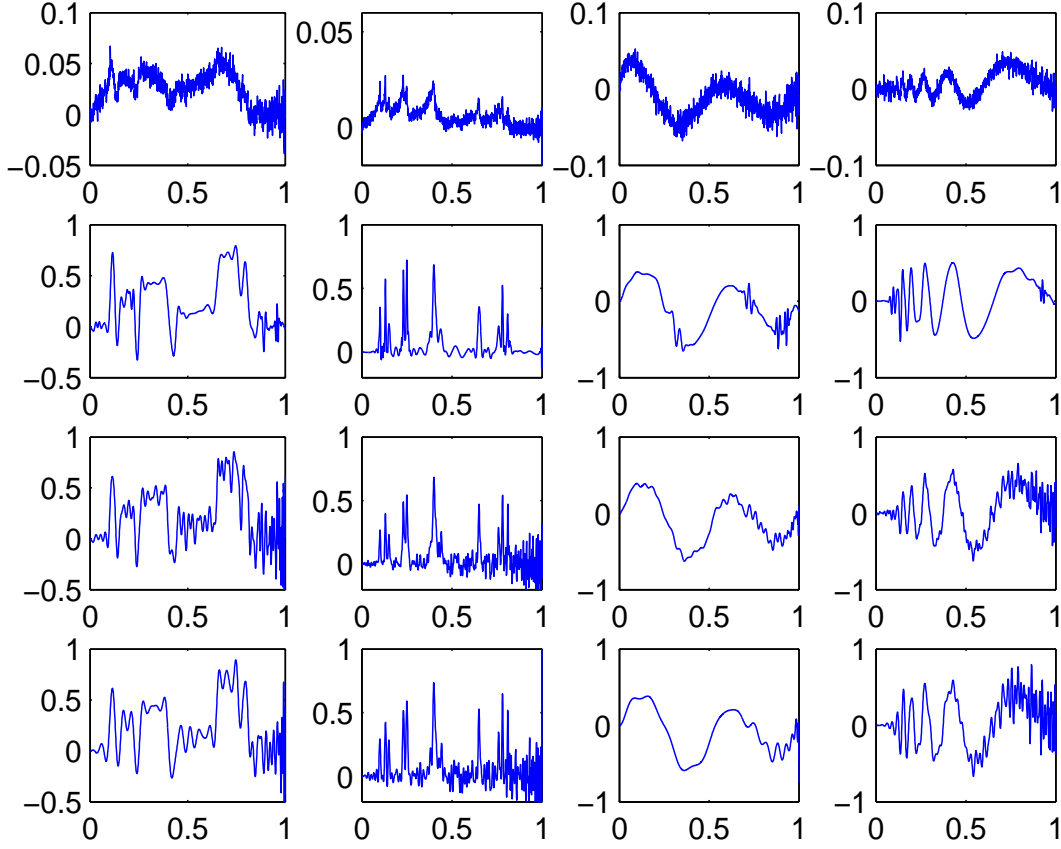
Figure 3.7: From top to bottom: observed data, NeedVD estimator, adaptive SVD estimator and non adaptive SVD estimator for high noise (rsnr=3)

by errors measured with the weight $\mu(x) = 1/(4x)$, for $x \in]0, 1]$.) This order of comparison is confirmed by the lower values of $L1$ and $RMSE$ for NeedVD than for SVD in all the settings (see tables 3.1 and 3.2).

3.7 Proof of Theorem 1

In this proof, C will denote an absolute constant which may change from one line to the other.

First we have the following decomposition :

$$
\mathbb{E}\|\hat{f} - f\|_p^p \leq 2^{p-1}\{\mathbb{E}\|\sum_{j=-1}^{J}\sum_{\eta \in \mathbb{Z}_j}(t(\hat{\beta_{j\eta}}) - \beta_{j\eta})\psi_{j\eta}\|_p^p + \|\sum_{j>J}\sum_{\eta \in \mathbb{Z}_j}\beta_{j\eta}\psi_{j\eta}\|_p^p\}
$$
$$
=: I + II
$$

The term II is easy to analyze, as follows: Since f belongs to $B_{\pi,r}^s(M)$, using standard embedding results (which in this case simply follows from direct comparisons between l_q

	SVD			Adaptive SVD			NeedVD		
	low	**med**	**high**	**low**	**med**	**high**	**low**	**med**	**high**
Blocks	0.0714	0.0790	0.0959	0.0665	0.0743	0.0900	0.0606	0.0673	0.0816
Bumps	0.0489	0.0577	0.0706	0.0453	0.0508	0.0617	0.0378	0.0416	0.0523
Heavisine	0.0278	0.0327	0.0422	0.0266	0.0317	0.0418	0.0235	0.0288	0.0379
Doppler	0.1092	0.1200	0.1378	0.1042	0.1114	0.1258	0.0969	0.0999	0.1071

Table 3.2: Error L2 for each target, each noise level and each estimator

norms) we have that f also belong to $B_{p,r}^{s-(\frac{1}{\pi}-\frac{1}{p})+}(M')$, for some constant M'. Hence

$$\|\sum_{j>J}\sum_{\eta\in\mathbb{Z}_j}\beta_{j\eta}\psi_{j\eta}\|_p \leq C2^{-J[s-(\frac{1}{p}-\frac{1}{p})+]}.$$

Then we only need to verify that $\frac{s-(\frac{1}{\pi}-\frac{1}{p})+}{\nu+1/2}$ is always larger that μ, which is not difficult.

Bounding the term I is more involved. Using the triangular inequality together with Hölder inequality, and property (3.20) for the second line, we get

$$I \leq 2^{p-1}J^{p-1}\sum_{j=-1}^{J}\mathbb{E}\|\sum_{\eta\in\mathbb{Z}_j}(t(\hat{\beta_{j\eta}})-\beta_{j\eta})\psi_{j\eta}\|_p^p$$

$$\leq 2^{p-1}J^{p-1}C\sum_{j=-1}^{J}\sum_{\eta\in\mathbb{Z}_j}\mathbb{E}|t(\hat{\beta_{j\eta}})-\beta_{j\eta}|^p\|\psi_{j\eta}\|_p^p.$$

Now, we separate four cases :

$$\sum_{j=-1}^{J}\sum_{\eta\in\mathbb{Z}_j}\mathbb{E}|t(\hat{\beta_{j\eta}})-\beta_{j\eta}|^p\|\psi_{j\eta}\|_p^p = \sum_{j=-1}^{J}\sum_{\eta\in\mathbb{Z}_j}\mathbb{E}|t(\hat{\beta_{j\eta}})-\beta_{j\eta}|^p\|\psi_{j\eta}\|_p^p\Big\{I\{|\hat{\beta_{j\eta}}|\geq\kappa t_\varepsilon\sigma_j\}$$

$$+I\{|\hat{\beta_{j\eta}}|<\kappa t_\varepsilon\sigma_j\}\Big\}$$

$$\leq \sum_{j=-1}^{J}\sum_{\eta\in\mathbb{Z}_j}\Big[\mathbb{E}|\hat{\beta_{j\eta}}-\beta_{j\eta}|^p\|\psi_{j\eta}\|_p^pI\{|\hat{\beta_{j\eta}}|\geq\kappa t_\varepsilon\sigma_j\}$$

$$\Big\{I\{|\beta_{j\eta}|\geq\frac{\kappa}{2}t_\varepsilon\sigma_j\}+I\{|\beta_{j\eta}|<\frac{\kappa}{2}t_\varepsilon\sigma_j\}\Big\}$$

$$+|\beta_{j\eta}|^p\|\psi_{j\eta}\|_p^pI\{|\hat{\beta_{j\eta}}|<\kappa t_\varepsilon\sigma_j\}\Big\{I\{|\beta_{j\eta}|\geq2\kappa t_\varepsilon\sigma_j\}$$

$$+I\{|\beta_{j\eta}|<2\kappa t_\varepsilon\sigma_j\}\Big\}\Big]$$

$$\leq \;: Bb+Bs+Sb+Ss.$$

If we notice that $\hat{\beta_{j\eta}}-\beta_{j\eta}=\sum_i\frac{Y_i-b_if_i}{b_i}\psi_{j\eta}^i=\varepsilon\sum_i\xi_i\frac{\psi_{j\eta}^i}{b_i}$ is a gaussian random variable centered, and with variance $\varepsilon^2\sum_i[\frac{\psi_{j\eta}^i}{b_i}]^2$, we have using standard properties of the gaussian distribution, for any $q\geq1$, if we recall that we set $\sigma_j^2=:\sum_i[\frac{\psi_{j\eta}^i}{b_i}]^2\leq C2^{2j\nu}$, and denote by s_q the qth absolute moment of the gaussian distribution when centered and with variance 1:

$$\mathbb{E}|\hat{\beta_{j\eta}} - \beta_{j\eta}|^q \leq s_q \sigma_j^q \varepsilon^q$$

$$\mathbb{P}\{|\hat{\beta_{j\eta}} - \beta_{j\eta}| \geq \frac{\kappa}{2} t_\varepsilon \sigma_j\} \leq 2\varepsilon^{\kappa^2/8}$$

Hence,

$$Bb \leq \sum_{j=-1}^{J} \sum_{\eta \in \mathbb{Z}_j} \sigma_j^p \varepsilon^p \|\psi_{j\eta}\|_p^p I\{|\beta_{j\eta}| \geq \frac{\kappa}{2} t_\varepsilon \sigma_j\}$$

$$Ss \leq \sum_{j=-1}^{J} \sum_{\eta \in \mathbb{Z}_j} |\beta_{j\eta}|^p \|\psi_{j\eta}\|_p^p I\{|\beta_{j\eta}| < 2\kappa t_\varepsilon \sigma_j\}.$$

And,

$$Bs \leq \sum_{j=-1}^{J} \sum_{\eta \in \mathbb{Z}_j} [\mathbb{E}|\hat{\beta_{j\eta}} - \beta_{j\eta}|^{2p}]^{1/2} [\mathbb{P}\{|\hat{\beta_{j\eta}} - \beta_{j\eta}| \geq \frac{\kappa}{2} t_\varepsilon \sigma_j\}]^{1/2} \|\psi_{j\eta}\|_p^p I\{|\beta_{j\eta}| < \frac{\kappa}{2} t_\varepsilon \sigma_j\}$$

$$\leq \sum_{j=-1}^{J} \sum_{\eta \in \mathbb{Z}_j} s_{2p}^{1/2} \sigma_j^p \varepsilon^p 2^{1/2} \varepsilon^{\kappa^2/16} \|\psi_{j\eta}\|_p^p I\{|\beta_{j\eta}| < \frac{\kappa}{2} t_\varepsilon \sigma_j\}$$

$$\leq C \sum_{j=-1}^{J} 2^{jp(\nu+\frac{1}{2})} \varepsilon^p \varepsilon^{\kappa^2/16} \leq C\varepsilon^{\kappa^2/16}.$$

Now, if we remark that the $\beta_{j\eta}$ are necessarily all bounded by some constant (depending on M) since f belongs to $B_{\pi,r}^s(M)$, and using (3.19),

$$Sb \leq \sum_{j=-1}^{J} \sum_{\eta \in \mathbb{Z}_j} |\beta_{j\eta}|^p \|\psi_{j\eta}\|_p^p \mathbb{P}\{|\hat{\beta_{j\eta}} - \beta_{j\eta}| \geq 2\kappa t_\varepsilon \sigma_j\} I\{|\beta_{j\eta}| \geq 2\kappa t_\varepsilon \sigma_j\}$$

$$\leq \sum_{j=-1}^{J} \sum_{\eta \in \mathbb{Z}_j} |\beta_{j\eta}|^p \|\psi_{j\eta}\|_p^p 2\varepsilon^{\kappa^2/8} I\{|\beta_{j\eta}| \geq 2\kappa t_\varepsilon t_\varepsilon \sigma_j\}$$

$$\leq C \sum_{j=-1}^{J} 2^{j\frac{p}{2}} \varepsilon^{\kappa^2/8} \leq C\varepsilon^{\frac{\kappa^2}{8} - \frac{p}{(2\nu+1)}}.$$

It is easy to check that in any cases if $\kappa^2 \geq 16p$ the terms Bs and Sb are smaller than the rates announced in the theorem.

If we recall that:

$$t_\varepsilon = \varepsilon \sqrt{\log \frac{1}{\varepsilon}}$$

We have using (3.19) and condition (3.23) for any $z \geq 0$:

$$Bb \leq C\varepsilon^p \sum_{j=-1}^{J} 2^{j(\nu p + \frac{p}{2} - 1)} \sum_{\eta \in \mathbb{Z}_j} I\{|\beta_{j\eta}| \geq \frac{\kappa}{2} t_\varepsilon \sigma_j\}$$

$$\leq C\varepsilon^p \sum_{j=-1}^{J} 2^{j(\nu p + \frac{p}{2} - 1)} \sum_{\eta \in \mathbb{Z}_j} |\beta_{j\eta}|^z [t_\varepsilon \sigma_j]^{-z}$$

$$\leq C t_\varepsilon^{p-z} \sum_{j=-1}^{J} 2^{j[\nu(p-z) + \frac{p}{2} - 1]} \sum_{\eta \in \mathbb{Z}_j} |\beta_{j\eta}|^z$$

Also, for any $p \geq z \geq 0$

$$Ss \leq C \sum_{j=-1}^{J} 2^{j(\frac{p}{2} - 1)} \sum_{\eta \in \mathbb{Z}_j} |\beta_{j\eta}|^z \sigma_j^{p-z} [t_\varepsilon]^{p-z}$$

$$\leq C [t_\varepsilon]^{p-z} \sum_{j=-1}^{J} 2^{j(\nu(p-z) + \frac{p}{2} - 1)} \sum_{\eta \in \mathbb{Z}_j} |\beta_{j\eta}|^z$$

So in both cases we have the same bound to investigate. We will write this bound on the following form (forgetting the constant) :

$$I + II = t_\varepsilon^{p-z_1} [\sum_{j=-1}^{j_0} 2^{j[\nu(p-z_1) + \frac{p}{2} - 1]} \sum_{\eta \in \mathbb{Z}_j} |\beta_{j\eta}|^{z_1}] + t_\varepsilon^{p-z_2} [\sum_{j=j_0+1}^{J} 2^{j[\nu(p-z_2) + \frac{p}{2} - 1]} \sum_{\eta \in \mathbb{Z}_j} |\beta_{j\eta}|^{z_2}]$$

The constants z_i and j_0 will be chosen depending on the cases, with the only constraint $p \geq z_i \geq 0$.

Notice first, that we only need to investigate the case $p \geq \pi$, since when $p \leq \pi$, $B^s_{\pi r}(M) \subset B^s_{pr}(M')$.

Let us first consider the case where $s \geq (\nu + \frac{1}{2})(\frac{p}{\pi} - 1)$, put

$$q = \frac{p(2\nu + 1)}{2(s + \nu) + 1}$$

and observe that on the considered domain, $q \leq \pi$ and $p > q$. In the sequel it will be useful to observe that we have $s = (\nu + \frac{1}{2})(\frac{p}{q} - 1)$. Now, taking $z_2 = \pi$, we get :

$$II \leq t_\varepsilon^{p-\pi} [\sum_{j=j_0+1}^{J} 2^{j[\nu(p-\pi) + \frac{p}{2} - 1]} \sum_{\eta \in \mathbb{Z}_j} |\beta_{j\eta}|^\pi]$$

Now, as

$$\frac{p}{2q} - \frac{1}{\pi} + \nu(\frac{p}{q} - 1) = s + \frac{1}{2} - \frac{1}{\pi}$$

and

$$\sum_{\eta \in \mathbb{Z}_j} |\beta_{j\eta}|^\pi = 2^{-j\pi(s + \frac{1}{2} - \frac{1}{\pi})} \tau_j^\pi$$

with $(\tau_j)_j \in l_r$ (this last thing is a consequence of the fact that $f \in B^s_{\pi,r}(M)$ and item (5)), we can write :

$$II \leq t_\varepsilon{}^{p-\pi} \sum_{j=j_0+1} 2^{jp(1-\frac{\pi}{q})(\nu+\frac{1}{2})} \tau_j^\pi$$

$$\leq C t_\varepsilon{}^{p-\pi} 2^{j_0 p(1-\frac{\pi}{q})(\nu+\frac{1}{2})}$$

The last inequality is true for any $r \geq 1$ if $\pi > q$ and for $r \leq \pi$ if $\pi = q$. Notice that $\pi = q$ is equivalent to $s = (2\nu + 1)(\frac{p}{2\pi} - \frac{1}{2})$. Now if we choose j_0 such that $2^{j_0 \frac{p}{q}(\nu+\frac{1}{2})} \sim t_\varepsilon{}^{-1}$ we get the bound

$$t_\varepsilon{}^{p-q}$$

which exactly gives the rate announced in the theorem for this case.

As for the first part of the sum (before j_0), we have, taking now $z_1 = \tilde{q}$, with $\tilde{q} \leq \pi$, so that $[\frac{1}{2^j} \sum_{\eta \in \mathbb{Z}_j} |\beta_{j\eta}|^{\tilde{q}}]^{\frac{1}{\tilde{q}}} \leq [\frac{1}{2^j} \sum_{\eta \in \mathbb{Z}_j} |\beta_{j\eta}|^\pi]^{\frac{1}{\pi}}$, and using again (3.7),

$$I \leq t_\varepsilon{}^{p-\tilde{q}} [\sum_{-1}^{j_0} 2^{j[\nu(p-\tilde{q})+\frac{p}{2}-1]} \sum_{\eta \in \mathbb{Z}_j} |\beta_{j\eta}|^{\tilde{q}}]$$

$$\leq t_\varepsilon{}^{p-\tilde{q}} [\sum_{-1}^{j_0} 2^{j[\nu(p-\tilde{q})+\frac{p}{2}-\frac{\tilde{q}}{\pi}]} [\sum_{\eta \in \mathbb{Z}_j} |\beta_{j\eta}|^\pi]^{\frac{\tilde{q}}{\pi}}]$$

$$\leq t_\varepsilon{}^{p-\tilde{q}} \sum_{-1}^{j_0} 2^{j[(\nu+\frac{1}{2})p(1-\frac{\tilde{q}}{q})]} \tau_j^{\tilde{q}}$$

$$\leq C t_\varepsilon{}^{p-\tilde{q}} 2^{j_0[(\nu+\frac{1}{2})p(1-\frac{\tilde{q}}{q})]}$$

$$\leq C t_\varepsilon{}^{p-q}$$

The last two lines are valid if $\tilde{q}$ is chosen strictly smaller than q (this is possible since $\pi \geq q$). Let us now consider the case where $s < (2\nu + 1)(\frac{p}{2\pi} - \frac{1}{2})$, and choose now

$$q = \frac{p}{2(s + \nu - \frac{1}{\pi}) + 1}.$$

In such a way that we easily verify that $p - q = 2\frac{s-1/\pi+1/p}{1+2(\nu+s-1/\pi)}$, $q - \pi = \frac{(p-\pi)(1+2\nu)}{2(s+\nu-\frac{1}{\pi})+1} > 0$, because s is supposed to be larger that $\frac{1}{\pi}$. Furthermore we also have $s + \frac{1}{2} - \frac{1}{\pi} = \frac{p}{2q} - \frac{1}{q} + \nu(\frac{p}{q} - 1)$.

Hence taking $z_1 = \pi$ and using again the fact that f belongs to $B^s_{\pi,r}(M)$,

$$I \leq t_\varepsilon{}^{p-\pi} [\sum_{-1}^{j_0} 2^{j[\nu(p-\pi)+\frac{p}{2}-1]} \sum_{\eta \in \mathbb{Z}_j} |\beta_{j\eta}|^\pi]$$

$$\leq t_\varepsilon{}^{p-\pi} \sum_{-1}^{j_0} 2^{j[(\nu+\frac{1}{2}-\frac{1}{p})\frac{p}{q}(q-\pi)]} \tau_j^\pi$$

$$\leq C t_\varepsilon{}^{p-\pi} 2^{j_0[(\nu+\frac{1}{2}-\frac{1}{p})\frac{p}{q}(q-\pi)]}$$

This is true since $\nu + \frac{1}{2} - \frac{1}{p}$ is also strictly positive because of our constraints. If we now take $2^{j_0 \frac{p}{q}(\nu + \frac{1}{2} - \frac{1}{p})} \sim t_\varepsilon^{-1}$ we get the bound

$$t_\varepsilon^{p-q}$$

which is the rate announced in the theorem for this case.

Again, for II, we have, taking now $z_2 = \widetilde{q} > q(> \pi)$

$$
\begin{aligned}
II &\leq t_\varepsilon^{p-\widetilde{q}}\Big[\sum_{j=j_0+1}^{J} 2^{j[\nu(p-\widetilde{q})+\frac{p}{2}-1]} \sum_{\eta \in \mathbb{Z}_j} |\beta_{j\eta}|^{\widetilde{q}}\Big] \\
&\leq C t_\varepsilon^{p-\widetilde{q}} \sum_{j=j_0+1} 2^{j[(\nu+\frac{1}{2}-\frac{1}{p})\frac{p}{q}(q-\widetilde{q})]} z_j^{\frac{\widetilde{q}}{\pi}} \\
&\leq C t_\varepsilon^{p-\widetilde{q}} 2^{j_0[(\nu+\frac{1}{2}-\frac{1}{p})\frac{p}{q}(q-\widetilde{q})]} \\
&\leq C t_\varepsilon^{p-q}
\end{aligned}
$$

3.8   Proof of the Theorems 2 and 8

The proof essentially follows the same steps as in the previous section. However, the following proposition will be helpful in the sequel.

Proposition 4. *Let us suppose that the following estimates are verified : Under the conditions (3.30) and (3.31), we have*

 1.
$$\pi \geq p \Rightarrow (\sum_\eta |\beta_{j\eta}|^p \|\psi_{j,\eta}\|_p^p)^{1/p} \leq (\sum_\eta |\beta_{j\eta}|^\pi \|\psi_{j,\eta}\|_\pi^\pi)^{1/\pi}$$

 2.
$$\pi < p \Rightarrow (\sum_{\eta,k(\eta)<2^{j-1}} |\beta_{j\eta}|^p \|\psi_{j,\eta}\|_p^p)^{1/p} \leq (\sum_{\eta,k(\eta)<2^{j-1}} |\beta_{j\eta}|^\pi \|\psi_{j,\eta}\|_\pi^\pi)^{1/\pi} 2^{2j(\alpha+1)(1/\pi-1/p)}$$
$$\pi < p \Rightarrow (\sum_{\eta,k(\eta)\geq 2^{j-1}} |\beta_{j\eta}|^p \|\psi_{j,\eta}\|_p^p)^{1/p} \leq (\sum_{\eta,k(\eta)\geq 2^{j-1}} |\beta_{j\eta}|^\pi \|\psi_{j,\eta}\|_\pi^\pi)^{1/\pi} 2^{2j(\beta+1)(1/\pi-1/p)}$$

Proof. • If $\pi \geq p$ clearly, because, $\text{Card}Z_j \leq 2^j$,

$$(\sum_{\eta \in Z_j} |\beta_{j\eta}|^p \|\psi_{j,\eta}\|_p^p)^{1/p} \leq 2^{j(1/p-1/\pi)}(\sum_{\eta \in Z_j} |\beta_{j\eta}|^\pi \|\psi_{j,\eta}\|_p^\pi)^{1/\pi}$$

But, using (3.30) and (3.31),

$$\pi \geq p \Rightarrow \|\psi_{j,\eta}\|_p \leq C\|\psi_{j,\eta}\|_\pi 2^{j(1/\pi-1/p)}.$$

So

$$(\sum_\eta |\beta_{j\eta}|^p \|\psi_{j,\eta}\|_p^p)^{1/p} \leq (\sum_\eta |\beta_{j\eta}|^\pi \|\psi_{j,\eta}\|_\pi^\pi)^{1/\pi}$$

- If $\pi \leq p$, clearly

$$(\sum_{\eta,k(\eta)<2^{j-1}} |\beta_{j\eta}|^p \|\psi_{j,\eta}\|_p^p)^{1/p} \leq (\sum_{\eta,k(\eta)<2^{j-1}} |\beta_{j\eta}|^\pi \|\psi_{j,\eta}\|_p^\pi)^{1/\pi}$$

But

$$\|\psi_{j,\eta}\|_p \leq C\|\psi_{j,\eta}\|_\pi 2^{j2(\alpha+1)(1/\pi-1/p)}, \ \forall \eta \ k(\eta) < 2^{j-1}$$

Hence, $(\sum_{\eta,k(\eta)<2^{j-1}} |\beta_{j\eta}|^p \|\psi_{j,\eta}\|_p^p)^{1/p} \leq (\sum_{\eta,k(\eta)<2^{j-1}} |\beta_{j\eta}|^\pi \|\psi_{j,\eta}\|_\pi^\pi)^{1/\pi} 2^{2j(\alpha+1)(1/\pi-1/p)}$

The proof of the inequality with β instead of α obviously is identical.

$\square$

Going back to the main stream of the proof, we first decompose :

$$\mathbb{E}\|\hat{f} - f\|_p^p \leq 2^{p-1}\{\mathbb{E}\| \sum_{j=-1}^{J} \sum_{\eta \in \mathbb{Z}_j} (t(\hat{\beta}_{j\eta}) - \beta_{j\eta})\psi_{j\eta}\|_p^p + \| \sum_{j>J} \sum_{\eta \in \mathbb{Z}_j} \beta_{j\eta}\psi_{j\eta}\|_p^p \}$$
$$=: \ I + II$$

- For II, using (3.27),

$$\| \sum_{j>J} \sum_{\eta \in \mathbb{Z}_j} \beta_{j\eta}\psi_{j\eta}\|_p^p \leq (\sum_{j>J} \| \sum_{\eta \in \mathbb{Z}_j} \beta_{j\eta}\psi_{j\eta}\|_p)^p \leq C[\sum_{j>J}(\sum_{\eta \in \mathbb{Z}_j} \|\beta_{j\eta}\psi_{j\eta}\|_p^p)^{1/p}]^p$$

If $\pi \geq p$, if we put $\delta = \frac{2}{1+2\nu}$, using $f \in \widetilde{B}_{p,r}^s(M)$,

$$II \leq C2^{-Jsp} = Ct_\varepsilon^{\delta sp}$$

If $\pi < p$, we decompose II in the following way
$II \leq C\{[\sum_{j>J}(\sum_{\eta,k(\eta)<2^{j-1}} |\beta_{j\eta}|^p\|\psi_{j\eta}\|_p^p)^{1/p}]^p + [\sum_{j>J}(\sum_{\eta,k(\eta)\geq 2^{j-1}} |\beta_{j\eta}|^p\|\psi_{j\eta}\|_p^p)^{1/p}]^p\} :=$
$II(\alpha) + II(\beta)$.

Now, using (4), and $f \in \widetilde{B}_{p,r}^s(M)$,

$$II(\alpha) \leq C[\sum_{j>J} 2^{-js} 2^{j2(\alpha+1)(1/\pi-1/p)}]^p$$

If $s > 2(\alpha+1)(1/\pi - 1/p)$

$$II(\alpha) \leq C2^{-J(s-2(\alpha+1)(1/\pi-1/p))p} = Ct_\varepsilon^{\delta(s-2(\alpha+1)(1/\pi-1/p))p}.$$

The term $II(\beta)$ can be treated in the same way.

- For I

Using the triangular inequality together with Hölder inequality, and (3.27) for the second line, we get

$$\begin{aligned} I &\leq 2^{p-1}J^{p-1} \sum_{j=-1}^{J} \mathbb{E}\| \sum_{\eta \in \mathbb{Z}_j} (t(\hat{\beta}_{j\eta}) - \beta_{j\eta})\psi_{j\eta}\|_p^p \\ &\leq 2^{p-1}J^{p-1}C \sum_{j=-1}^{J} \sum_{\eta \in \mathbb{Z}_j} \mathbb{E}|t(\hat{\beta}_{j\eta}) - \beta_{j\eta}|^p\|\psi_{j\eta}\|_p^p \\ &\leq 2^{p-1}J^{p-1}C[I(\alpha) + I(\beta)] \end{aligned}$$

In the last line we separated as previously, in the sum $\eta \in \mathbb{Z}_j$, the indices $k(\eta) < 2^{j-1}$ and $k(\eta) \geq 2^{j-1}$. We will only investigate in the sequel $I(\alpha)$, since the argument for $I(\beta)$ goes in the same way.

Now, we separate four cases :

$$
\begin{aligned}
\sum_{j=-1}^{J} \sum_{\eta, k(\eta)<2^{j-1}} \mathbb{E}|t(\hat{\beta_{j\eta}}) - \beta_{j\eta}|^p \|\psi_{j\eta}\|_p^p \;=\; & \sum_{j=-1}^{J} \sum_{\eta, k(\eta)<2^{j-1}} \mathbb{E}|t(\hat{\beta_{j\eta}}) - \beta_{j\eta}|^p \|\psi_{j\eta}\|_p^p \Big\{ I\{|\hat{\beta_{j\eta}}| \geq \kappa t_\varepsilon \sigma_j\} \\
& + I\{|\hat{\beta_{j\eta}}| < \kappa t_\varepsilon \sigma_j\} \Big\} \\
\leq\; & \sum_{j=-1}^{J} \sum_{\eta, k(\eta)<2^{j-1}} \Big[\mathbb{E}|\hat{\beta_{j\eta}} - \beta_{j\eta}|^p \|\psi_{j\eta}\|_p^p I\{|\hat{\beta_{j\eta}}| \geq \kappa t_\varepsilon \sigma_j\} \\
& \Big\{ I\{|\beta_{j\eta}| \geq \tfrac{\kappa}{2} t_\varepsilon \sigma_j\} + I\{|\beta_{j\eta}| < \tfrac{\kappa}{2} t_\varepsilon \sigma_j\} \Big\} \\
& + |\beta_{j\eta}|^p \|\psi_{j\eta}\|_p^p I\{|\hat{\beta_{j\eta}}| \geq \kappa t_\varepsilon \sigma_j\} \Big\{ I\{|\beta_{j\eta}| \geq 2\kappa t_\varepsilon \sigma_j\} \\
& + I\{|\beta_{j\eta}| < 2\kappa t_\varepsilon \sigma_j\} \Big\} \Big] \\
\leq:\; & Bb + Bs + Sb + Ss
\end{aligned}
$$

If we notice, as before, that $\hat{\beta_{j\eta}} - \beta_{j\eta} = \sum_i \frac{Y_i - b_i f_i}{b_i} \psi_{j\eta}^i = \varepsilon \sum_i \xi_i \frac{\psi_{j\eta}^i}{b_i}$ is a gaussian random variable centered, and with variance $\varepsilon^2 \sum_i (\frac{\psi_{j\eta}^i}{b_i})^2$, we have using standard properties of the gaussian distribution, for any $q > 0$:

$$
\mathbb{E}|\hat{\beta_{j\eta}} - \beta_{j\eta}|^q \leq s_q [\varepsilon^2 \sum_i (\frac{\psi_{j\eta}^i}{b_i})^2]^{q/2} \leq s_q \sigma_j^q \varepsilon^q \leq C 2^{j\nu q} \varepsilon^q
$$

$$
\mathbb{P}\{|\hat{\beta_{j\eta}} - \beta_{j\eta}| \geq \tfrac{\kappa}{2} \varepsilon \sqrt{\log \tfrac{1}{\varepsilon}} \sigma_j\} \leq c \varepsilon^{\kappa^2/8}
$$

Hence,

$$
\begin{aligned}
Bb \;\leq\; & \sum_{j=-1}^{J} \sum_{\eta, k(\eta)<2^{j-1}} \sigma_j^p \varepsilon^p \|\psi_{j\eta}\|_p^p I\{|\beta_{j\eta}| \geq \tfrac{\kappa}{2} \varepsilon \sqrt{\log \tfrac{1}{\varepsilon}} \sigma_j\} \\
Ss \;\leq\; & \sum_{j=-1}^{J} \sum_{\eta, k(\eta)<2^{j-1}} |\beta_{j\eta}|^p \|\psi_{j\eta}\|_p^p I\{|\beta_{j\eta}| < 2\kappa \varepsilon \sqrt{\log \tfrac{1}{\varepsilon}} \sigma_j\}
\end{aligned}
$$

And,

$$
\begin{aligned}
Bs \;\leq\; & \sum_{j=-1}^{J} \sum_{\eta,k(\eta)<2^{j-1}} [\mathbb{E}|\hat{\beta_{j\eta}} - \beta_{j\eta}|^{2p}]^{1/2}[\mathbb{P}\{|\hat{\beta_{j\eta}} - \beta_{j\eta}| \geq \frac{\kappa}{2}\varepsilon\sqrt{\log\frac{1}{\varepsilon}}\sigma_j\}]^{1/2} \\
& \|\psi_{j\eta}\|_p^p I\{|\beta_{j\eta}| < \frac{\kappa}{2}\varepsilon\sqrt{\log\frac{1}{\varepsilon}}\sigma_j\} \\
\leq\; & \sum_{j=-1}^{J} \sum_{\eta,k(\eta)<2^{j-1}} \sigma_{2p}^{1/2}\sigma_j^p\varepsilon^p c^{1/2}\varepsilon^{\kappa^2/16}\|\psi_{j\eta}\|_p^p I\{|\beta_{j\eta}| < \frac{\kappa}{2}\varepsilon\sqrt{\log\frac{1}{\varepsilon}}\sigma_j\} \\
\leq\; & c'\varepsilon^p\varepsilon^{\kappa^2/16} \sum_{j=-1}^{J} 2^{jp\nu} \sum_{\eta\in\mathbb{Z}_j} \|\psi_{j\eta}\|_p^p \\
\leq\; & c'\varepsilon^p\varepsilon^{\kappa^2/16} 2^{J(\nu p + (p/2)\vee(p-2)(1+\alpha))}
\end{aligned}
$$

using (3.26). Now, if we remark that the $\beta_{j\eta}$ are necessarily all bounded by some constant M, since $f \in \widetilde{B}_{p,r}^s(M)$,

$$
\begin{aligned}
Sb \;\leq\; & \sum_{j=-1}^{J} \sum_{\eta,k(\eta)<2^{j-1}} |\beta_{j\eta}|^p \|\psi_{j\eta}\|_p^p \mathbb{P}\{|\hat{\beta_{j\eta}} - \beta_{j\eta}| \geq 2\kappa\varepsilon\sqrt{\log\frac{1}{\varepsilon}}\sigma_j\} I\{|\beta_{j\eta}| \geq 2\kappa\varepsilon\sqrt{\log\frac{1}{\varepsilon}}\sigma_j\} \\
\leq\; & \sum_{j=-1}^{J} \sum_{\eta,k(\eta)<2^{j-1}} |\beta_{j\eta}|^p \|\psi_{j\eta}\|_p^p c\varepsilon^{\kappa^2/8} I\{|\beta_{j\eta}| \geq 2\kappa\varepsilon\sqrt{\log\frac{1}{\varepsilon}}\sigma_j\} \\
\leq\; & c\varepsilon^{\kappa^2/8} \sum_{j=-1}^{J} \sum_{\eta\in\mathbb{Z}_j} \|\psi_{j\eta}\|_p^p \\
\leq\; & c''\varepsilon^{\frac{\kappa^2}{8}} 2^{J(p/2\vee(p-2)(1+\alpha))}
\end{aligned}
$$

It is easy to check that in any cases for κ^2 large enough, the terms Bs and Sb are smaller than the rates announced in the two theorems.

Now we focus on the bounds of Bb and Ss. Let $q \in [0,p]$, we always have:

$$
\begin{aligned}
\varepsilon^p \sum_{j=-1}^{J} \sum_{\eta,k(\eta)<2^{j-1}} \sigma_j^p \|\psi_{j\eta}\|_p^p I\{\frac{|\beta_{j\eta}|}{\sigma_j} \geq \frac{\kappa}{2}t_\varepsilon\} \quad & \leq \varepsilon^p \sum_{j=-1}^{J} \frac{\sum_{\eta,k(\eta)<2^{j-1}} \sigma_j^p\|\psi_{j\eta}\|_p^p|\beta_{j\eta}|^q}{(\kappa\sigma_j t_\varepsilon/2)^q} \\
& \leq \varepsilon^p(\kappa t_\varepsilon/2)^{-q} \sum_{j=-1}^{J} \sum_{\eta,k(\eta)<2^{j-1}} \sigma_j^{p-q}\|\psi_{j\eta}\|_p^p|\beta_{j\eta}|^q
\end{aligned}
$$

And

$$
\begin{aligned}
\sum_{j=-1}^{J} \sum_{\eta,k(\eta)<2^{j-1}} |\beta_{j\eta}|^p\|\psi_{j\eta}\|_p^p I\{|\beta_{j\eta}| < 2\kappa t_\varepsilon\sigma_j\} \quad & \leq \sum_{j=-1}^{J} (2\kappa t_\varepsilon\sigma_j)^{p-q} \sum_{\eta,k(\eta)<2^{j-1}} |\beta_{j\eta}|^q\|\psi_{j\eta}\|_p^p \\
& \leq (2\kappa t_\varepsilon)^{p-q} \sum_{j=-1}^{J} \sum_{\eta,k(\eta)<2^{j-1}} \sigma_j^{p-q}\|\psi_{j\eta}\|_p^p|\beta_{j\eta}|^q.
\end{aligned}
$$

So like in the wavelet scenario we have the same bound to investigate:

$$Bb + Ss \leq \sum_{j=-1}^{J} \sum_{\eta, k(\eta) < 2^{j-1}} (t_\varepsilon \sigma_j)^{p-q} \|\psi_{j\eta}\|_p^p |\beta_{j\eta}|^q,$$

then we use (3.30) and we separate as before the bound obtained in two terms A and B with some parameters j_0, z_1 and z_2 determined later, depending on the cases :

$$A := \sum_{j=-1}^{j_0} (t_\varepsilon \sigma_j)^{p-z_1} 2^{j(p-2)(\alpha+1)} \sum_{\eta, k(\eta) < 2^{j-1}} |\beta_{j\eta}|^{z_1} k^{-(p-2)(\alpha+1/2)}$$

$$B := \sum_{j=j_0+1}^{J} (t_\varepsilon \sigma_j)^{p-z_2} 2^{j(p-2)(\alpha+1)} \sum_{\eta, k(\eta) < 2^{j-1}} |\beta_{j\eta}|^{z_2} k^{-(p-2)(\alpha+1/2)}.$$

Let us first suppose that $p \leq \pi$ and $(p-2)(\alpha+1/2) \leq 1$, or that $p \geq \pi$ and $(p-2)(\alpha+1/2) \geq 1$.

Then we take $z_1 = 0$ and $z_2 = p$, and let us denote $\delta_p = 1 - (p-2)(\alpha+\frac{1}{2})$. We have:

$$
\begin{aligned}
A &= \sum_{j=-1}^{j_0} (t_\varepsilon \sigma_j)^p 2^{j(p-2)(\alpha+1)} \sum_{\eta, k(\eta) < 2^{j-1}} k^{-(p-2)(\alpha+1/2)} \\
&= \sum_{j=-1}^{j_0} (t_\varepsilon \sigma_j)^p 2^{j(p/2) \vee (p-2)(\alpha+1)} j^{I(\delta_p=0)} \\
&\leq C (t_\varepsilon \sigma_{j_0})^p 2^{j_0(p/2) \vee (p-2)(\alpha+1)} (\log \frac{1}{\varepsilon})^{I(\delta_p=0)}.
\end{aligned}
$$

And by treating B as was done previously with the term $II(\alpha)$, we obtain:

$$
\begin{aligned}
B &= \sum_{j=j_0+1}^{J} 2^{j(p-2)(\alpha+1)} \sum_{\eta, k(\eta) < 2^{j-1}} |\beta_{j\eta}|^p k^{-(p-2)(\alpha+1/2)} \\
&\leq C 2^{-j_0 p [s-2(\alpha+1)(\frac{1}{\pi}-\frac{1}{p})+]}.
\end{aligned}
$$

So if $p \leq \pi$ and $(p-2)(\alpha+1/2) \leq 1$ we set $2^{j_0} = t_\varepsilon^{-1/[s+\nu+\frac{1}{2}]}$, which yields:

$$A + B \leq C t_\varepsilon^{p \frac{s}{s+\nu+\frac{1}{2}}} (\log \frac{1}{\varepsilon})^{I(\delta_p=0)},$$

and if $p \geq \pi$ and $(p-2)(\alpha+1/2) \geq 1$ we take $2^{j_0} = t_\varepsilon^{-1/[s+\nu+(\alpha+1)(1-\frac{2}{\pi})]}$, which yields:

$$A + B \leq C t_\varepsilon^{p \frac{s-2(\alpha+1)(\frac{1}{\pi}-\frac{1}{p})}{s+\nu+(\alpha+1)(1-\frac{2}{\pi})}} (\log \frac{1}{\varepsilon})^{I(\delta_p=0)}.$$

In the other cases: $p < \pi$ and $(p-2)(\alpha+1/2) > 1$, or $p > \pi$ and $(p-2)(\alpha+1/2) < 1$, let us set $q = \frac{(p-2)(\alpha+1/2)-1}{(\pi-2)(\alpha+1/2)-1} \pi$, which satisfies:

$$p - q = \frac{2(\alpha+1)(\pi-p)}{(\pi-2)(\alpha+1/2)-1}, \quad \text{and} \quad \pi - q = \frac{\pi(\alpha+1/2)(\pi-p)}{(\pi-2)(\alpha+1/2)-1},$$

so $q \in]0, p \wedge \pi[$ under the assumptions made above.

Let us bound the quantity $\sum_{\eta, k(\eta) < 2^{j-1}} |\beta_{j\eta}|^q k^{-(p-2)(\alpha+1/2)}$. We define:

$$\delta_1 = -\frac{q}{\pi}(\pi - 2)(\alpha + 1/2), \quad \text{and} \quad \delta_2 = -(p-2)(\alpha + 1/2) - \delta_1.$$

Using Hölder inequality, (3.30), and the fact that $f \in \widetilde{B}_{p,r}^s(M)$, we have:

$$\sum_{\eta, k(\eta) < 2^{j-1}} |\beta_{j\eta}|^q k^{-(p-2)(\alpha+1/2)} = \sum_{\eta \in \mathbb{Z}_j} |\beta_{j\eta}|^q k^{\delta_1} k^{\delta_2}$$

$$\leq [\sum_{\eta, k(\eta) < 2^{j-1}} |\beta_{j\eta}|^\pi k^{-(\pi-2)(\alpha+1/2)}]^{\frac{q}{\pi}} [\sum_{\eta, k(\eta) < 2^{j-1}} k^{\frac{\delta_2}{1-\frac{q}{\pi}}}]^{1-\frac{q}{\pi}}$$

$$\leq C 2^{-jsq - j\frac{q}{\pi}(\pi-2)(\alpha+1)} [\sum_{\eta, k(\eta) < 2^{j-1}} k^{\frac{\pi\delta_2}{\pi-q}}]^{1-\frac{q}{\pi}}$$

$$= C 2^{-j(p-2)(\alpha+1)} 2^{j(-sq + \frac{p-q}{2})} j^{1-\frac{q}{\pi}}.$$

In the last line we used the fact that :

$$(p-2)(\alpha+1) - sq - \frac{q}{\pi}(\pi-2)(\alpha+1) = -sq + \frac{p-q}{2}, \quad \text{and} \quad \frac{\pi\delta_2}{\pi - q} = -1.$$

1. Let us assume that:
$$-sq + (p-q)(\nu + \frac{1}{2}) < 0,$$

i.e. that:
$$\frac{-s\pi[(p-2)(\alpha+1/2) - 1] + (\alpha+1)(\pi-p)(2\nu+1)}{(\pi-2)(\alpha+1/2) - 1} < 0.$$

Then we take $z_1 = 0$ and $z_2 = q$:

$$A = \sum_{j=-1}^{j_0} (t_\varepsilon \sigma_j)^p 2^{j(p-2)(\alpha+1)} \sum_{\eta, k(\eta) < 2^{j-1}} k^{-(p-2)(\alpha+1/2)}$$

$$\leq (t_\varepsilon \sigma_{j_0})^p 2^{j_0(p/2) \vee (p-2)(\alpha+1)},$$

$$B = \sum_{j=j_0+1}^{J} (t_\varepsilon \sigma_j)^{p-q} 2^{j(p-2)(\alpha+1)} \sum_{\eta, k(\eta) < 2^{j-1}} |\beta_{j\eta}|^q k^{-(p-2)(\alpha+1/2)}$$

$$\leq C[\sum_{j=j_0+1}^{J} (t_\varepsilon \sigma_j)^{p-q} 2^{j(-sq + \frac{p-q}{2})}] J^{1-\frac{q}{\pi}}$$

$$\leq C(t_\varepsilon \sigma_{j_0})^{p-q} 2^{j_0(-sq + \frac{p-q}{2})} (\log \frac{1}{\varepsilon})^{1-\frac{q}{\pi}}.$$

If $(p-2)(\alpha+1/2) > 1$ we take $2^{j_0} = t_\varepsilon^{-1/[s+\nu+(\alpha+1)(1-\frac{2}{\pi})]}$, which yields:

$$A + B \leq C t_\varepsilon^{p\frac{s - 2(\alpha+1)(\frac{1}{\pi} - \frac{1}{p})}{s+\nu+(\alpha+1)(1-\frac{2}{\pi})}} (\log \frac{1}{\varepsilon})^{1-\frac{q}{\pi}},$$

and if $(p-2)(\alpha+1/2) < 1$ we take $2^{j_0} = t_\varepsilon^{-1/[s+\nu+\frac{1}{2}]}$, which yields:

$$A + B \leq C t_\varepsilon^{p \frac{s}{s+\nu+\frac{1}{2}}} (\log \frac{1}{\varepsilon})^{1-\frac{q}{\pi}}.$$

Notice that, because of our conditions on s, we always have $j_0 \leq J$.

2. Let us now assume that:

$$\frac{-s\pi[(p-2)(\alpha+1/2)-1] + (\alpha+1)(\pi-p)(2\nu+1)}{(\pi-2)(\alpha+1/2)-1} > 0.$$

Then we take $z_1 = q$ and $z_2 = p$:

$$
\begin{aligned}
A &\leq C[\sum_{j=-1}^{j_0} (t_\varepsilon \sigma_j)^{p-q} 2^{j(-sq+\frac{p-q}{2})}] J^{1-\frac{q}{\pi}} \\
&\leq C(t_\varepsilon \sigma_{j_0})^{p-q} 2^{j_0(-sq+\frac{p-q}{2})} (\log \frac{1}{\varepsilon})^{1-\frac{q}{\pi}},
\end{aligned}
$$

and as before with the bias term $II(\alpha)$:

$$
\begin{aligned}
B &\leq \sum_{j=j_0+1}^{J} 2^{j(p-2)(\alpha+1)} \sum_{\eta, k(\eta)<2^{j-1}} |\beta_{j\eta}|^p k^{-(p-2)(\alpha+1/2)} \\
&\leq C 2^{-j_0 p[s-2(\alpha+1)(\frac{1}{\pi}-\frac{1}{p})+]}.
\end{aligned}
$$

If $\pi > p$ we take $2^{j_0} = t_\varepsilon^{-1/[s+\nu+\frac{1}{2}]}$, which yields:

$$A + B \leq C t_\varepsilon^{p \frac{s}{s+\nu+\frac{1}{2}}} (\log \frac{1}{\varepsilon})^{1-\frac{q}{\pi}},$$

and if $\pi < p$ we take $2^{j_0} = t_\varepsilon^{-1/[s+\nu+(\alpha+1)(1-\frac{2}{\pi})]}$, which yields:

$$A + B \leq C t_\varepsilon^{p \frac{s-2(\alpha+1)(\frac{1}{\pi}-\frac{1}{p})}{s+\nu+(\alpha+1)(1-\frac{2}{\pi})}} (\log \frac{1}{\varepsilon})^{1-\frac{q}{\pi}}.$$

3. Let us finally assume that:

$$-s\pi[(p-2)(\alpha+1/2)-1] + (\alpha+1)(\pi-p)(2\nu+1) = 0.$$

We take $z_1 = q$ and $z_2 = p$ as previously:

$$A+B \leq C \sum_{j=-1}^{j_0} t_\varepsilon^{p-q} j^{1-\frac{q}{\pi}} + C 2^{-j_0 p[s-2(\alpha+1)(\frac{1}{\pi}-\frac{1}{p})+]} \leq C t_\varepsilon^{p-q} (\log \frac{1}{\varepsilon})^{2-\frac{q}{\pi}} + C 2^{-j_0 p[s-2(\alpha+1)(\frac{1}{\pi}-\frac{1}{p})+]}.$$

We proceed exactly like in the previous case, and we obtain the same rate whether $\pi \geq p$ or $\pi < p$:

$$A + B \le Ct_\varepsilon^{p\frac{s}{s+\nu+\frac{1}{2}}} (\log \frac{1}{\varepsilon})^{2-\frac{q}{\pi}}.$$

We can sum up all the results for Bb and Ss (and thus on $I(\alpha)$) very simply:

if $2(\alpha+1)(\frac{1}{\pi} - \frac{1}{p}) < s$ and $s[1 - (p-2)(\alpha+1/2)] \le p(2\nu+1)(\alpha+1)(\frac{1}{\pi} - \frac{1}{p})$ then:

$$Bb + Ss \le Ct_\varepsilon^{p\frac{s+2(\alpha+1)(\frac{1}{p}-\frac{1}{\pi})}{s+\nu+(\alpha+1)(1-\frac{2}{\pi})}} (\log \frac{1}{\varepsilon})^a,$$

if $s[1 - (p-2)(\alpha+1/2)] > p(2\nu+1)(\alpha+1)(\frac{1}{\pi} - \frac{1}{p})$ then:

$$Bb + Ss \le Ct_\varepsilon^{p\frac{s}{s+\nu+\frac{1}{2}}} (\log \frac{1}{\varepsilon})^a,$$

where the power of the log factor depends on the parameters:

$$a = \begin{cases} I\{\delta_p = 0\} & \text{if } [p-\pi][1-(p-2)(\alpha+1/2)] \ge 0, \\ \frac{(\alpha+\frac{1}{2})(\pi-p)}{(\pi-2)(\alpha+1/2)-1} + I\{\delta_s = 0\} & \text{if } [p-\pi][1-(p-2)(\alpha+1/2)] < 0, \end{cases}$$

with $\delta_p = 1 - (p-2)(\alpha+1/2)$ and $\delta_s = s[1 - (p-2)(\alpha+1/2)] - p(2\nu+1)(\alpha+1)(\frac{1}{\pi} - \frac{1}{p})$.

Note that the first term in the second case is bounded by 1, so we have $a \le 2$ whatever the case.

3.9 Appendix: Needlets induced by Jacobi polynomials

3.9.1 Jacobi needlets: Definition and basic properties

In this section we apply the general scheme from §3.3 for the construction of Jacobi needlets. We begin by introducing some necessary notation. We denote $I = [-1, 1]$ and $d\gamma_{\alpha,\beta}(x) = c_{\alpha,\beta}\omega_{\alpha,\beta}(x)dx$, where

$$\omega_{\alpha,\beta}(x) = (1-x)^\alpha(1+x)^\beta; \quad \alpha, \beta > -1/2,$$

and $c_{\alpha,\beta}$ is defined by $\int_I d\gamma_{\alpha,\beta}(x) = 1$. Assume $P^{\alpha,\beta}$ are the classical Jacobi polynomials (cf. e.g. Szegő [86]). Let $\Pi_k^{\alpha,\beta}$ be the Jacobi polynomial of degree k, normalized in $L_2(d\gamma_{\alpha\beta})$, i.e.

$$\int_I \Pi_k^{\alpha,\beta}\Pi_n^{\alpha,\beta} d\gamma_{\alpha,\beta} = \delta_{m,n}.$$

Let $a(\xi)$ be as in §3.3.1 with the additional condition: $a(\xi) > c > 0$ for $3/4 \le \xi \le 7/4$. Note that $\operatorname{supp} a \subset [1/2, 2]$. We define as as in §3.3.1

$$\Lambda_j(x, y) = \sum_k a(k/2^j)\Pi_k^{\alpha,\beta}(x)\Pi_k^{\alpha,\beta}(y).$$

Let $\eta_\nu = \cos\theta_{j,\nu}$, $\nu = 1, 2, \ldots, 2^j$, be the zeros of the Jacobi polynomial P_{2^j} ordered so that $\eta_1 > \eta_2 > \cdots > \eta_{2^j}$ and hence $0 < \theta_{j,1} < \theta_{j,2} < \cdots < \theta_{j,2^j} < \pi$. It is well known that (cf. Szegő [86])

$$\theta_{j,\nu} \sim \frac{\nu\pi}{2^j}. \tag{3.33}$$

We set

$$\mathcal{X}_j = \{\eta_\nu : \nu = 1, 2, \ldots, 2^j\}.$$

Let Π_n denote the space of all polynomials of degree $\leq n$. As is well known Szegő [86] the zeros of the Jacobi polynomial P_{2^j} serve as knots of the Gaussian quadrature which is exact for all polynomials from $\Pi_{2^{j+1}-1}$, that is,

$$\int_I P d\gamma_{\alpha,\beta} = \sum_{\eta_\nu \in \mathcal{X}_j} b_{j,\eta_\nu} P(\eta_\nu), \quad \forall P \in \Pi_{2^{j+1}-1},$$

where the coefficients $b_{j,\eta_\nu} > 0$ are the Christoffel numbers Szegő [86] and $b_{j,\eta_\nu} \sim 2^{-j}\omega_{\alpha,\beta}(2^j; \eta_\nu)$ with

$$\omega_{\alpha,\beta}(2^j; x) := (1 - x + 2^{-2j})^{\alpha+1/2}(1 + x + 2^{-2j})^{\beta+1/2}.$$

We now define the Jacobi needlets by

$$\psi_{j,\eta_\nu}(x) = \sqrt{b_{j,\eta_\nu}}\Lambda_{2^j}(x, \eta_\nu), \quad \nu = 1, 2, \ldots, 2^j; \; j \geq 0,$$

and we set $\psi_0(x) = \psi_{-1,\eta}(x) = 1$, $\eta \in \mathcal{X}_{-1}$ with $\mathcal{X}_{-1}$ consisting of only one point $\eta = 0$. From Proposition 2, (ψ_{j,η_ν}) is a tight frame of $\mathbb{L}_2(d\gamma_{\alpha\beta})$, i.e.

$$\|f\|_2^2 = \sum_{j \geq -1} \sum_{\eta \in \mathcal{X}_j} |\langle f, \psi_{j,\eta}\rangle|^2, \quad \forall f \in \mathbb{L}_2(d\gamma_{\alpha\beta}).$$

Hence

$$\|\psi_{j,\eta_\nu}\|_2 \leq 1, \tag{3.34}$$

which cannot be an equality since otherwise the needlet system (ψ_{j,η_ν}) would be an orthonormal basis and this is impossible because

$$\sum_\nu \sqrt{b_{j,\eta_\nu}}\psi_{j,\eta_\nu} = \sum_\nu b_{j,\eta_\nu}L_{2^j}(x, \eta_\nu) = \int_I L_{2^j}(x, y)d\gamma(x) = 0.$$

We now recall the two main results from Petrushev and Xu [81] which will be essential steps in our development.

Theorem 4. *For any $l \geq 1$ there exists a constant $C_l > 0$ such that*

$$|\psi_{j,\eta_\nu}(\cos\theta)| \leq C_l \frac{1}{\sqrt{\omega_{\alpha,\beta}(2^j, \cos\theta)}} \frac{2^{j/2}}{(1 + 2^j|\theta - \frac{\pi\nu}{2^j}|)^l}, \quad 0 \leq \theta \leq \pi. \tag{3.35}$$

Obviously

$$\omega_{\alpha,\beta}(2^j; \cos\theta) = (2\sin^2(\theta/2) + 2^{-2j})^{\alpha+1/2}(2\cos^2(\theta/2) + 2^{-2j})^{\beta+1/2}. \tag{3.36}$$

Therefore, $0 \leq \theta \leq \pi/2 \Longrightarrow \omega_{\alpha,\beta}(2^j, \cos\theta) \sim ((2^j\theta + 1)^{2\alpha+1}2^{-j(2\alpha+1)}$ and hence

$$|\psi_{j,\eta_\nu}(\cos\theta)| \leq C_l \frac{2^{j(1+\alpha)}}{(1 + 2^j|\theta - \frac{\nu\pi}{2^j}|)^l} \frac{1}{(2^j\theta + 1)^{\alpha+1/2}}, \quad 0 \leq \theta \leq \pi/2. \tag{3.37}$$

Similarly, from (3.36)

$$\pi/2 \leq \theta \leq \pi \Longrightarrow \omega_{\alpha,\beta}(2^j, \cos\theta) \sim (2^j(\pi - \theta) + 1)^{2\beta+1}2^{-j(2\beta+1)}$$

and hence

$$|\psi_{j,\eta_\nu}(\cos\theta)| \leq C_l \frac{2^{j(1+\beta)}}{(1 + 2^j|\theta - \frac{\nu\pi}{2^j}|)^l} \frac{1}{(2^j(\pi - \theta) + 1)^{\beta+1/2}}, \quad \pi/2 \leq \theta \leq \pi. \tag{3.38}$$

Theorem 5. *Let $0 < p \leq \infty$. Then*

$$\|\psi_{j,\eta_\nu}\|_p = \Big(\int_I |\psi_{j,\eta_\nu}(x)|^p d\gamma_{\alpha,\beta}\Big)^{1/p} \leq C_p \Big(\frac{2^j}{\omega_{\alpha,\beta}(2^j; \eta_\nu)}\Big)^{1/2-1/p}.$$

Using (4.2) and (3.36), we infer $\omega_{\alpha,\beta}(j; \eta_\nu) \sim 2^{-j(2\alpha+1)}\nu^{2\alpha+1}$ if $1 \leq \nu \leq 2^{j-1}$ and $\omega_{\alpha,\beta}(j; \eta_\nu) \sim 2^{-j(2\beta+1)}(2^j - \nu + 1)^{2\beta+1}$ if $2^{j-1} < \nu \leq 2^j$. Consequently,

$$1 \leq \nu \leq 2^{j-1} \Longrightarrow \quad \|\psi_{j,\eta_\nu}\|_p \leq C_p \left(\frac{2^{j(\alpha+1)}}{\nu^{\alpha+1/2}}\right)^{1-2/p}, \tag{3.39}$$

$$2^{j-1} < \nu \leq 2^j \Longrightarrow \quad \|\psi_{j,\eta_\nu}\|_p \leq C_p \left(\frac{2^{j(\beta+1)}}{(2^j - \nu + 1)^{\beta+1/2}}\right)^{1-2/p}. \tag{3.40}$$

3.9.2 Estimation of the $\mathbb{L}_p$ norms of the needlets

Here we establish estimates (3.30)–(3.31) for the norms of the Jacobi needlets. In fact we only need to prove the lower bounds because the upper bounds are given above, see Theorem 5 and (3.39)–(3.40). We record these bounds in the following theorem. We want to express our thanks to Yuan Xu for communicating to us another proof of this result.

Theorem 6. $\forall\, 0 < p \leq \infty, \ \forall j \in \mathbb{N}$,

$$\forall\, \nu = 1, \dots, 2^{j-1}, \quad c_p \left(\frac{2^{j(\alpha+1)}}{\nu^{\alpha+1/2}}\right)^{1-2/p} \leq \|\psi_{j,\eta_\nu}\|_p \leq C_p \left(\frac{2^{j(\alpha+1)}}{\nu^{\alpha+1/2}}\right)^{1-2/p}$$

$$\forall\, 2^{j-1} < \nu \leq 2^j, \quad c_p \left(\frac{2^{j(\beta+1)}}{(1 + (2^j - \nu))^{\beta+1/2}}\right)^{1-2/p} \leq \|\psi_{j,\eta_\nu}\|_p \leq C_p \left(\frac{2^{j(\beta+1)}}{(1 + (2^j - \nu))^{\beta+1/2}}\right)^{1-2/p}$$

The following proposition will play a critical role in the proof of this theorem.

Proposition 5. *Let $c^\diamond$ be an arbitrary positive constant. Then there exists a constant $c > 0$ such that*

$$\sum_{k=N}^{2N-1} [P_k^{\alpha,\beta}(\cos\theta)]^2 \geq c\,\omega_{\alpha,\beta}(N; \cos\theta)^{-1} \quad for \quad c^\diamond N^{-1} \leq \theta \leq \pi - c^\diamond N^{-1}, \quad N \geq 2. \tag{3.41}$$

Proof. The proof will rely on the well known asymptotic representation of Jacobi polynomials (sf. [86, Theorem 8.21.12, p. 195]): For any constants $c > 0$ and $\varepsilon > 0$

$$\left(\sin\frac{\theta}{2}\right)^\alpha \left(\cos\frac{\theta}{2}\right)^\beta P_n^{\alpha,\beta}(\cos\theta) = N^{-\alpha}\frac{\Gamma(n+\alpha+1)}{n!}\left(\frac{\theta}{\sin\theta}\right)^{1/2} J_\alpha(N\theta) + \theta^{1/2}\mathcal{O}(n^{-3/2})$$
(3.42)

for $cn^{-1} \le \theta \le \pi - \varepsilon$, where $N = n + (\alpha + \beta + 1)/2$ and J_α is the Bessel function. Further, using the well known asymptotic identity

$$J_\alpha(z) = \left(\frac{2}{\pi z}\right)^{1/2}\cos(z+\gamma) + \mathcal{O}(z^{-3/2}), \quad z \to \infty \quad (\gamma = -\alpha\pi/2 - \pi/4),$$
(3.43)

one obtains (sf. [86, Theorem 8.21.13, p. 195])

$$P_n^{\alpha,\beta}(\cos\theta) = (\pi n)^{-1/2}\left(\sin\frac{\theta}{2}\right)^{-\alpha-1/2}\left(\cos\frac{\theta}{2}\right)^{-\beta-1/2}\{\cos(N\theta+\gamma) + (n\theta)^{-1}\mathcal{O}(1)\} \quad (3.44)$$

for $cn^{-1} \le \theta \le \pi - cn^{-1}$.

As is well known the Jacobi polynomials $P_k^{\alpha,\beta}$ and $P_{k+1}^{\alpha,\beta}$ have no common zeros and hence it suffices to prove (3.41) only for sufficiently large N. Also, $P_k^{\alpha,\beta}(-x) = (-1)^k P_k^{\beta,\alpha}(x)$ and therefore it suffices to prove (3.41) only in the case $c^\diamond N^{-1} \le \theta \le \pi/2$.

Denote by $F_N(\theta)$ the left-hand side quantity in (3.41). Then by (3.44), applied with $c = 1/2$, it follows that

$$F_N(\theta) \ge N^{-1}\theta^{-2\alpha-1}\sum_{k=N}^{2N-1}\left(c_1\cos^2(k\theta + h(\theta)) - c_2(k\theta)^{-2}\right)$$

$$\ge c' N^{-1}\theta^{-2\alpha-1}\sum_{k=N}^{2N-1}\cos^2(k\theta + h(\theta)) - c''\theta^{-2\alpha-1}(N\theta)^{-2},$$

for $N^{-1} \le \theta \le \pi/2$, where $h(\theta) = (\alpha + \beta + 1)\theta/2 - \pi\alpha/2 - \pi/4$. It is easy to verify that for $\pi N^{-1} \le \theta \le \pi/2$

$$\sum_{k=N}^{2N-1}\cos^2(k\theta + h) = \frac{N}{2} + \frac{\sin N\theta}{2\sin\theta}\cos((3N-1)\theta + 2h) \ge \frac{N}{2}\left(1 - \frac{\pi}{2N\theta}\right) \ge \frac{N}{4}.$$

Therefore,

$$F_N(\theta) \ge \theta^{-2\alpha-1}(c'/4 - c''(N\theta)^{-2}) \ge (c'/8)\theta^{-2\alpha-1} \ge c\omega_{\alpha,\beta}(N;\theta) \quad \text{for} \quad c^* N^{-1} \le \theta \le \pi/2,$$
(3.45)

where $c^* = \max\{\pi, (8c''/c')^{1/2}\} > 0$.

It remains to establish (3.41) for $c^\diamond N^{-1} \le \theta \le c^* N^{-1}$. Denote $\delta = (\alpha + \beta + 1)/2$. We now apply (3.42) with $c = c^\diamond$ and $\varepsilon = \pi/2$ to obtain using that $\Gamma(n + \alpha + 1)/n! \sim n^\alpha$, $\sin\theta \sim \theta$, and (3.43)

$$\left[P_k^{\alpha,\beta}(\cos\theta)\right]^2 \ge \theta^{-2\alpha}\left(c_1[J_\alpha((k+\delta)\theta)]^2 - c_2 k^{-3/2}\theta^{1/2}|J_\alpha((k+\delta)\theta)|\right)$$

$$\ge c_1\theta^{-2\alpha}[J_\alpha((k+\delta)\theta)]^2 - c\theta^{-2\alpha}k^{-2}.$$

Choose λ so that $\theta = \frac{\lambda}{N}$ and $c^\diamond \le \lambda \le c^*$. Summing up above we get

$$F_N(\theta) \ge c_1 \theta^{-2\alpha} \sum_{k=N}^{2N-1} [J_\alpha((k+\delta)\theta)]^2 - c\theta^{-2\alpha} N^{-1}$$

$$= c_1 \theta^{-2\alpha} N \sum_{k=N}^{2N-1} \frac{1}{N} \Big[J_\alpha\Big(\frac{(k+\delta)\lambda}{N} \Big) \Big]^2 - c\theta^{-2\alpha} N^{-1}$$

$$= c_1 \theta^{-2\alpha} N \sum_{j=0}^{N-1} \frac{1}{N} \Big[J_\alpha\Big(\frac{j\lambda}{N} + \lambda + \frac{\delta\lambda}{N} \Big) \Big]^2 - c\theta^{-2\alpha} N^{-1}.$$

Obviously, the last sum above involves only values of the Bessel function $J_\alpha(\theta)$ for $c^\diamond \le \theta \le c^*(2+\delta)$ and hence uniformly in $\lambda \in [c^\diamond, c^*]$

$$\Big| \sum_{j=0}^{N-1} \frac{1}{N} \Big[J_\alpha\Big(\frac{j\lambda}{N} + \lambda + \frac{\delta\lambda}{N} \Big) \Big]^2 - \sum_{j=0}^{N-1} \frac{1}{N} \Big[J_\alpha\Big(\frac{j\lambda}{N} + \lambda \Big) \Big]^2 \Big| \longrightarrow 0, \quad N \longrightarrow \infty.$$

The second sum above can be viewed as a Riemann sum of the integral $\int_0^1 J_\alpha^2(\lambda(\theta+1))d\theta$, which is a continuous function of $\lambda \in [c^\diamond, c^*]$ and hence $\min_{\lambda \in [c^\diamond, c^*]} \int_0^1 J_\alpha^2(\lambda(\theta+1))d\theta \ge \widetilde{c} > 0$. Consequently, for sufficiently large N

$$F_N(\theta) \ge \theta^{-2\alpha}(\widetilde{c} c_1 N/2 - cN^{-1}) \ge c\theta^{-2\alpha} N \ge c\omega_{\alpha,\beta}(N;\theta) \quad \text{for} \quad c^\diamond N^{-1} \le \theta \le c^* N^{-1}.$$

From this and (3.45) it follows that (3.41) holds for sufficiently large N and this completes the proof of Proposition 5. $\qquad\square$

Proof of Theorem 6. We first note that (sf. Szegő [86]) $\Pi_k^{\alpha,\beta}(x) \sim k^{1/2} P_k^{\alpha,\beta}(x)$ and hence

$$\|\psi_{j,\eta_\nu}\|_2^2 = b_{j,\nu} \sum_{2^{j-2} < k < 2^j} a^2(k/2^j)(\Pi_k^{\alpha,\beta}(\cos\theta_{j,\nu}))^2$$

$$\ge c\omega_{\alpha,\beta}(2^j; \eta_\nu) \sum_{2^{j-2} < k < 2^j} a^2(k/2^j)(P_k^{\alpha,\beta}(\cos\theta_{j,\nu}))^2$$

$$\ge c\omega_{\alpha,\beta}(2^j; \eta_\nu) \sum_{\frac{3}{4}2^j \le k \le \frac{7}{4}2^j} (P_k^{\alpha,\beta}(\cos\theta_{j,\nu}))^2.$$

Observe also that there exists a constant $c^\diamond > 0$ such that $c^\diamond/2^j \le \theta_{j,\nu} \le \pi - c^\diamond/2^j$, $\nu = 1, 2, \ldots, 2^j$. We now employ Proposition 5 and (3.34) to conclude that

$$0 < c \le \|\psi_{j,\eta_\nu}\|_2 \le 1. \tag{3.46}$$

We need to establish only the lower bound in Theorem 6. Recall first the upper bound from Theorem 5

$$\|\psi_{j,\eta_\nu}\|_p \le C_p \Big(\frac{2^j}{\omega_{\alpha,\beta}(2^j; \eta_\nu)} \Big)^{1/2 - 1/p}, \quad 0 < p \le \infty. \tag{3.47}$$

Suppose $2 < p < \infty$ and let $1/p + 1/q = 1$. By (4.5) and Hölder's inequality we have

$$0 < c \le \|\psi_{j,\eta_\nu}\|_2^2 \le \|\psi_{j,\eta_\nu}\|_p \|\psi_{j,\eta_\nu}\|_q \le c\|\psi_{j,\eta_\nu}\|_p \Big(\frac{2^j}{\omega_{\alpha,\beta}(2^j; \eta_\nu)} \Big)^{1/2 - 1/q}$$

which yields

$$\|\psi_{j,\eta_\nu}\|_p \geq c\Big(\frac{2^j}{\omega_{\alpha,\beta}(2^j;\eta_\nu)}\Big)^{1/2-1/p}. \tag{3.48}$$

The case $p=\infty$ is similar. In the case $0 < p < 2$, we have using (4.5)

$$0 < c \leq \|\psi_{j,\eta_\nu}\|_2^2 \leq \|\psi_{j,\eta_\nu}\|_p^p\|\psi_{j,\eta_\nu}\|_\infty^{2-p} \leq c\|\psi_{j,\eta_\nu}\|_p^p\Big(\frac{2^j}{\omega_{\alpha,\beta}(2^j;\eta_\nu)}\Big)^{1-p/2},$$

which implies (3.48). The lower bound estimates in Theorem 6 follow by (3.48).   □

3.9.3   Bounding for the norm of a linear combination of needlets

Our goal is to prove estimate (3.27), which we record in the following theorem:

Theorem 7. *Let $0 < p < \infty$. Then there exists a constant $C_p > 0$ such that for any collection of numbers $\{\lambda_\nu : \nu = 1, 2, \ldots, 2^j\}$, $j \geq 0$,*

$$\|\sum_{\nu=1}^{2^j} \lambda_\nu \psi_{j,\eta_\nu}\|_{\mathbb{L}_p(\gamma_{\alpha,\beta})}^p \leq C_p \sum_{\nu=1}^{2^j} |\lambda_\nu|^p\|\psi_{j,\eta_\nu}\|_{\mathbb{L}_p(\gamma_{\alpha,\beta})}^p. \tag{3.49}$$

Proof. Consider the maximal operator

$$(M_s f)(x) = \sup_{J \ni x} \Big(\frac{1}{|J|}\int_J |f(u)|^s du\Big)^{1/s}, \quad s > 0,$$

where the supremum is taken over all intervals $J \subset [-1,1]$ which contain x and $|J|$ denotes the length of J. As elsewhere, let $\alpha \wedge \beta > -1/2$. It is well known the weight $\omega_{\alpha,\beta}(x) = (1-x)^\alpha(1+x)^\beta$ on $[-1,1]$ belongs to the Muckenhoupt class A_p with $p > 1$ if $\alpha \vee \beta \leq p-1$. Then in the weighted case the Fefferman-Stein maximal inequality (see Fefferman and Stein [41] and Andersen and John [2]) can be stated as follows: If $1 < p, r < \infty$ and $\omega_{\alpha,\beta} \in A_p$, then for any sequence of functions (f_k) on $[-1,1]$

$$\Big\|\Big(\sum_k (M_1 f_k)^r\Big)^{1/r}\Big\|_{\mathbb{L}_p(\gamma_{\alpha,\beta})} \leq C_{p,r}\Big\|\Big(\sum_k |f_k|^r\Big)^{1/r}\Big\|_{\mathbb{L}_p(\gamma_{\alpha,\beta})}.$$

Using that $M_1|f|^s = (M_s f)^s$ one easily infers from above that the following maximal inequality holds: If $0 < p, r < \infty$ and $0 < s < \min\{p, r, \frac{p}{\alpha\vee\beta+1}\}$, then for any sequence of functions (f_k) on $[-1,1]$

$$\Big\|\Big(\sum_k (M_s f_k)^r\Big)^{1/r}\Big\|_{\mathbb{L}_p(\gamma_{\alpha,\beta})} \leq C\Big\|\Big(\sum_k |f_k|^r\Big)^{1/r}\Big\|_{\mathbb{L}_p(\gamma_{\alpha,\beta})}. \tag{3.50}$$

As in §3.9.1, let $\eta_\nu = \cos\theta_{j,\nu}$, $\nu = 1, 2, \ldots, 2^j$, be the zeros of the Jacobi polynomial $P_{2^j}^{\alpha,\beta}$. Set $\eta_0 = 1$, $\eta_{2^j+1} = -1$ and $\theta_{j,0} = 0$, $\theta_{j,2^j+1} = \pi$, respectively. Denote $I_\nu = [\frac{\eta_\nu+\eta_{\nu+1}}{2}, \frac{\eta_\nu+\eta_{\nu-1}}{2}]$ and put

$$H_\nu = h_\nu 1_{I_\nu} \quad \text{with} \quad h_\nu = \Big(\frac{2^j}{\omega_{\alpha,\beta}(2^j;\eta_\nu)}\Big)^{1/2},$$

where 1_{I_ν} is the indicator function of I_ν.

We next show that for any $s > 0$

$$|\psi_{j,\eta_\nu}(x)| \le c(M_s H_\nu)(x), \quad x \in [-1,1], \quad \forall \nu = 1, 2, \ldots, 2^j, \; j \ge 0. \tag{3.51}$$

Obviously, $(M_s 1_{I_\nu})(x) = 1_{I_\nu}(x)$ for $x \in I_\nu$. Let $x \in [-1,1] \setminus I_\nu$ and set $\cos\theta = x$, $\theta \in [0,\pi]$. Then

$$
\begin{aligned}
[(M_s 1_{I_\nu})(x)]^s \;\; &\sim \;\; \frac{|I_\nu|}{|x - \eta_\nu|} \sim \frac{\eta_{\nu-1} - \eta_{\nu+1}}{|x - \eta_\nu|} \sim \frac{\sin\frac{1}{2}(\theta_{j,\nu+1} - \theta_{j,\nu-1})\sin\frac{1}{2}(\theta_{j,\nu+1} + \theta_{j,\nu-1})}{\sin\frac{1}{2}|\theta - \theta_{j,\nu}|\sin\frac{1}{2}(\theta + \theta_{j,\nu})} \\
&\sim \;\; \frac{2^{-j}\theta_{j,\nu}}{|\theta - \theta_{j,\nu}|(\theta + \theta_{j,\nu})}.
\end{aligned}
$$

Using that $\theta_{j,\nu} \ge c_* 2^{-j}$ for some constant $c_* > 0$, one easily verifies the inequality

$$\frac{\theta_{j,\nu}}{\theta + \theta_{j,\nu}} \ge \frac{1}{(2 + c_*^{-1})(1 + 2^j|\theta - \theta_{j,\nu}|)}.$$

From above it follows that

$$(M_s 1_{I_\nu})(\cos\theta) \ge \frac{c}{(1 + 2^j|\theta - \theta_{j,\nu}|)^{2/s}}, \quad \theta \in [0,\pi],$$

which along with (3.35) (applied with $l \ge 2/s$) yields (4.6).

Combining (4.6) and (3.50) we get

$$\Big\| \sum_{\nu=1}^{2^j} \lambda_\nu \psi_{j,\eta_\nu} \Big\|_{\mathbb{L}_p(\gamma_{\alpha,\beta})}^p \le c \sum_{\nu=1}^{2^j} |\lambda_\nu|^p \|H_\nu\|_{\mathbb{L}_p(\gamma_{\alpha,\beta})}^p. \tag{3.52}$$

Straightforward calculation show that $\|1_{I_\nu}\|_{\mathbb{L}_p(\gamma_{\alpha,\beta})} \sim \left(2^{-j}\omega_{\alpha,\beta}(2^j;\eta_\nu)\right)^{1/p}$ and hence, using Theorem 6,

$$\|H_\nu\|_{\mathbb{L}_p(\gamma_{\alpha,\beta})} \sim \left(\frac{2^j}{\omega_{\alpha,\beta}(2^j;\eta_\nu)}\right)^{1/2 - 1/p} \sim \|\psi_{j,\eta_\nu}\|_{\mathbb{L}_p(\gamma_{\alpha,\beta})}.$$

This coupled with (4.4) implies (4.3). $\qquad\qquad\square$

Chapter 4

New minimax rates for inverse problems

Ce chapitre est une version légèrement différente d'un article soumis à une revue.

Abstract: We consider inverse problems where one wishes to recover an unknown function from the observation of a linear transformation of it, corrupted by an additive white noise perturbation. We assume that the singular value decomposition of the linear operator consists of Jacobi polynomials, which includes, as an application, the well known Wicksell's problem. We determine the asymptotic rate of the minimax risk for this model in a wide framework, considering $(L^p)_{1<p<\infty}$ losses, and Besov-like regularity spaces. We draw a comparison with the rate corresponding to the more standard deconvolution problem which appears as a critical case of the Jacobi-type rate. We also establish some new results on the needlets introduced by Petrushev and Xu [81, 80] which appear as essential tools in this setting.

4.1　Introduction

4.1.1　Motivation

We consider the problem of recovering a function f from a blurred (by a linear operator) and noisy version of f: $Y_\varepsilon = Kf + \varepsilon\dot{W}$, where $\dot{W}$ is a $\mathbb{K}$-white noise and K is a compact linear operator between two Hilbert spaces: $K : \mathbb{H} \mapsto \mathbb{K}$. We assume that K admits a singular value decomposition, ie there exists an orthonormal basis (called SVD basis) formed by the eigenfunctions of the self-adjoint operator K^*K where K^* is the adjoint of K. Moreover we assume that $\mathbb{H} = L^2([-1,1],\mu)$ with $d\mu(x) \asymp (1-x)^\alpha(1+x)^\beta$;　$\alpha,\beta > -1/2$, and that the SVD basis of K consists of the classical Jacobi polynomials of type (α,β) (see Szegő [86]). In practice, an application of such an inverse model is the well known Wicksell's problem (Wicksell [91]) which concerns the recovery of the density of the radii of spherical particles, when a sample of planar cuts is given.

The main motivation of this article is to establish the asymptotic minimax rates of this problem in a wide framework, considering $L^p([-1,1],\mu)$ losses and a Besov like regularity space. We will draw a parallel between our results and the rates of more standard inverse models such as deconvolution, for which the minimax rates for $L^p([0,1],dx)$ losses and over Besov spaces were established in Johnstone et al. [53] and Chapter 6. We consider all kinds of values for p: $1 < p < \infty$. Thus, in comparison to the standard L^2 framework, we observe the well known elbow effects. This means that the rates take several expressions depending on the parameters of the model, see Härdle et al. [49] for an example in a direct observation model. However, the cartography of the rates is more implied than in the deconvolution setting, for which the "critical" case corresponds to a simple linear relation between p and the index π of the Besov. We show that the rates of the risk in the Jacobi-type model appear as a critical case of the rates of the risk in the deconvolution model.

This chapter is closely linked to Chapter 3, where an estimation algorithm called NeedVD was developed for several inverse problems, including Jacobi-type models. This procedure consists in estimating coefficients of the unknown function f in a tight frame consisting of localized functions termed needlets, which are built upon the SVD basis. Here we prove that NeedVD is nearly optimal for Jacobi-type models, since the lower bounds established here turn to match with the convergence rates of the procedure. So the upper bound of the minimax risk needs no inquiry, and our main concern here is the lower bound. However the same kind of problematic arises in both problems, so we give first the main ideas which motivated the NeedVD procedure, and afterwards some explanations on the lower bounds.

4.1.2　The NeedVD algorithm

The NeedVD procedure must be understood in the context of wavelet multiresolution analysis, which turned to be a very useful tool in non parametric estimation problems. For example in many direct observation problems such as density estimation or regression, wavelet bases provide interesting non linear adaptive estimators, based on coefficients thresholding, which enjoy near minimax properties in a wide variety of settings as established in a series of papers Donoho et al. [32, 33, 36, 34]. In comparison linear estimators can be far from optimal in many situations.

In more complex models such as inverse problems, several methods have been proposed to take the advantages provided by wavelets in direct observation problems to good account. This approach was pioneered in Donoho [35] with the well known Wavelet-Vaguelette decomposition (WVD) procedure. While enjoying very general minimax properties, WVD requires some hypotheses on the operator. Those can be easily checked in the cases of homogeneous operators (see Kolaczyk [60] for a list of examples) and of convolution operators, but are more implied for other operators.

One may wonder, in this context, if we could avoid some of the limitations of WVD by allowing some flexibility in the decomposition basis, and requiring it to possess only "essential" wavelet properties. In others words could one use bases with weaker properties than wavelets, keeping only those essential for the minimax study, with a view to providing a simpler denoising algorithm, and another field of applications among inverse problems?

Seen from this point of view, the results of Chapter 3 yield some answers. Two particular situations were investigated: the deconvolution model, which can be treated by numerous wavelet methods (including WVD), and the Jacobi-type models treated in this paper, which include Wicksell's problem for which only one wavelet procedure (to our knowledge) was developed in Antoniadis et al. [6]. In that case NeedVD consists in expanding the unknown function in a frame presenting the advantages of multiscale analysis of wavelet representations, and having at the same time close connections with the SVD basis of the operator K. As mentioned previously, the minimax rates for deconvolution problems have already been established. So in this paper we focus on the second scenario, which leads to new results for inverse models such as Wicksell's problem.

4.1.3 Lower bounds of the minimax rates

Establishing the lower bound amounts to solving problems similar to the ones encountered in the construction of NeedVD. Indeed the main concern is to find a family of "hypotheses" $V = \{f_\lambda, \quad \lambda \in \Lambda\} \subset \mathbb{H}$, such that V contains some of the most difficult functions to estimate inside the regularity space considered for the risk. This means that the functions f_λ must be chosen such that:

- the $L^p(\mu)$ distance between the f_λ's is as large as possible,

- and in the same time the distributions of the associated processes $Y_\varepsilon = K f_\lambda + \varepsilon \dot{W}$ are as close as possible (in a Kullback sense, for example).

A natural way to build such hypotheses is to use functions which enjoy localization properties and whose images by K can be easily studied, which is exactly the motivation at the heart of the construction of the NeedVD procedure. Thus here again needlets are an essential tool: the hypotheses are built as linear combinations of such functions, with some parameters left free, which we adjust optimally with respect to the two constraints cited above. Then the $L^p(\mu)$ distance between the hypotheses yields the lower bound on the whole regularity space.

In this context several additional difficulties must be treated in comparison to more standard inverse problems such as deconvolution, which stem from the non orthogonality of

the needlets and from the heterogeneity of their $L^p(\mu)$ norms. We also have to establish a wavelet-like lower bound for the $L^p(\mu)$ norms of linear combinations of needlets.

The chapter is organized as follows. In section 2 we describe the model and state the main result, section 3 gives the basic properties of the needlets that we use to prove the main result. The fourth section gives the proofs of the lower bounds and the fifth section gives the proofs of the preliminary results from section 3.

4.2   Main result

4.2.1   The model

In this paper we use the framework of "Jacobi-type" inverse models, which we define as follows. This setting may be a bit unusual for inverse problems, but it will enable us to turn the singular value decomposition of some operators to good account, as will be seen later.

Let K be a linear operator between two Hilbert spaces $K : \mathbb{H} \mapsto \mathbb{K}$, with weights μ and λ:

$$\mathbb{H} = \mathbb{L}_2([-1,1], \mu(x)dx),$$

$$\mathbb{K} = \mathbb{L}_2(I, \lambda(x)dx),$$

with $\mu(x) = c_{\alpha,\beta}\omega_{\alpha,\beta}(x)dx$, where

$$\omega_{\alpha,\beta}(x) = (1-x)^\alpha(1+x)^\beta; \quad \alpha, \beta > -1/2,$$

and $c_{\alpha,\beta}$ is such that $\int_{[-1,1]} d\mu(x) = 1$. Moreover I is an interval of $\mathbb{R}$.

We assume that K is injective and admits a singular value decomposition (which is for example true if K is compact), ie there exist two orthonormal bases (SVD bases) (P_k) of $\mathbb{H}$ and (U_k) of $\mathbb{K}$, and a sequence of values $b_k > 0$ such that:

$$KP_k = b_k U_k, \quad K^*U_k = b_k P_k,$$

with K^* being the adjoint operator of K. We assume that the first SVD basis (P_k) consists of the Jacobi polynomials of type (α, β) normalized in $L^2(d\mu)$ (see Szegő [86] for details), ie P_k is the polynomial of degree k such that:

$$\int_{-1}^{1} P_k P_l d\mu = \delta_{k,l}.$$

The problem consists in recovering a good approximation of the function f from the observation of a realization of the process Y_ε defined by the following identity:

$$Y_\varepsilon = Kf + \varepsilon\dot{W}, \tag{4.1}$$

where ε is the amplitude of the noise and $\dot{W}$ is a $\mathbb{K}$-white noise, i.e. for any $g, h \in \mathbb{K}$, $\xi(g) := (\dot{W}, g)_{\mathbb{K}}$, $\xi(h) := (\dot{W}, h)_{\mathbb{K}}$ form random Gaussian vectors (centered) with marginal variance $\|g\|_{\mathbb{K}}^2$, $\|h\|_{\mathbb{K}}^2$, and covariance $(g, h)_{\mathbb{K}}$ (with the obvious extension when one considers k functions instead of 2).

4.2.2 Minimax rates

We establish the minimax rates in a wide setting with $\mathbb{L}^p(\mu)$ losses (for any $1 < p < +\infty$) and over balls of a Besov-like space $\widetilde{B}^s_{\pi,r}$ that we describe here.

Details on Besov spaces (denoted by $B^s_{\pi,r}$) can be found in Härdle et al. [49]. We recall simply that they are very general regularity spaces including as particular cases Sobolev and Hölder spaces, and which can be described very simply, thanks to any regular enough wavelet basis $(\psi_{j,k})_{j \geq -1, \, k \in \mathbb{Z}}$. Indeed if $f \in L^p(\mathbb{R}, dx)$ we have the decomposition:

$$f = \sum_{j \geq -1} \sum_{k \in \mathbb{Z}} \beta_{j,k} \psi_{j,k}, \quad \text{where } \beta_{j,k} = \int f(x)\psi_{j,k}(x)dx,$$

if we define:

$$\|f\|_{B^s_{\pi,r}} := \|(2^{js}(\sum |\beta_{j,k}|^\pi \|\psi_{j,k}\|_\pi^\pi)^{1/\pi})_{j \geq -1}\|_{L^r} < \infty,$$

then we have:

$$f \in B^s_{\pi,r}(M) \iff \|f\|_{B^s_{\pi r}} \leq M.$$

We adapt this approach to the framework of Jacobi-type models. Let $(\psi_{j\eta})_{j \geq 0, \, \eta \in \mathbb{Z}_j}$ denote the tight frame of needlets described in the next section. For any $f \in \mathbb{H}$, we have the following decomposition:

$$f = \sum_{j \geq 0} \sum_{\eta \in \mathbb{Z}_j} \beta_{j\eta} \psi_{j\eta}, \quad \text{where } \beta_{j\eta} = (f, \psi_{j\eta})_\mathbb{H}.$$

Then for $\pi \geq 1$, $s \geq 1/\pi$, $r \geq 1$, we define $\widetilde{B}^s_{\pi,r}(M)$ by:

$$\|f\|_{\widetilde{B}^s_{\pi,r}} := \|(2^{js}(\sum_{\eta \in \mathbb{Z}_j} |\beta_{j,\eta}|^\pi \|\psi_{j,\eta}\|_\pi^\pi)^{1/\pi})_{j \geq -1}\|_{L^r} < \infty, \quad \text{and}$$

$$f \in \widetilde{B}^s_{\pi,r}(M) \iff \|f\|_{\widetilde{B}^s_{\pi r}} \leq M.$$

In this framework the minimax risk is defined by:

$$R_\varepsilon(\widetilde{B}^s_{\pi,r}(M), \mathbb{L}^p(\mu)) := \inf_{\hat{f}_\varepsilon} \sup_{f \in \widetilde{B}^s_{\pi,r}(M)} \mathbb{E}_f(\|\hat{f}_\varepsilon - f\|_{\mathbb{L}^p(\mu)})^p,$$

where the infimum is taken over all $\sigma(Y_\varepsilon(t))_{t \geq 0}$−measurable estimators $\hat{f}_\varepsilon$.

The following theorem is an immediate consequence of the results of chapter 3, establishing the rates of convergence of the NeedVD estimator:

Theorem 8. *Let* $1 < p < \infty$*,* α*,* $\beta > -\frac{1}{2}$ *and suppose that*

$$b_k \asymp k^{-\nu}, \quad \nu > -\frac{1}{2}.$$

Then for $\pi \geq 1$, $r \geq 1$ and $s > \max_{\gamma \in \{\alpha,\beta\}}\{\frac{1}{2} - 2(\gamma+1)(\frac{1}{2} - \frac{1}{\pi}) \vee 2(\gamma+1)(\frac{1}{\pi} - \frac{1}{p}) \vee 0\}$ we have:

$$R_\varepsilon(\widetilde{B}^s_{\pi,r}(M), \mathbb{L}^p(\mu)) \leq C[\log(1/\varepsilon)]^{p+1}[\varepsilon\sqrt{\log(1/\varepsilon)}]^{\mu p},$$

where

$$\mu = \min\{\mu(s),\ \mu(s,\alpha),\ \mu(s,\beta)\}$$

$$\text{with:} \quad \mu(s) = \frac{s}{s+\nu+\frac{1}{2}}, \quad \mu(s,\gamma) = \frac{s - 2(1+\gamma)(\frac{1}{\pi} - \frac{1}{p})}{s+\nu+2(1+\gamma)(\frac{1}{2} - \frac{1}{\pi})}.$$

Our aim is to prove that these rates coincide to the rates of the minimax risk up to log factors. We will prove the following theorem:

Theorem 9. *Let $1 < p < \infty$, α, $\beta > -\frac{1}{2}$ and suppose that*

$$b_k \asymp k^{-\nu}, \quad \nu > -\frac{1}{2}.$$

Then for $\pi \geq 1$, $r \geq 1$ and $s \geq 1/\pi$, we have:

$$R_\varepsilon(\widetilde{B}^s_{\pi,r}(M), \mathbb{L}^p(\mu)) \geq C\varepsilon^{\mu p},$$

where

$$\mu = \min\{\mu(s),\ \mu(s,\alpha),\ \mu(s,\beta)\}$$

$$\text{with:} \quad \mu(s) = \frac{s}{s+\nu+\frac{1}{2}}, \quad \mu(s,\gamma) = \frac{s - 2(1+\gamma)(\frac{1}{\pi} - \frac{1}{p})}{s+\nu+2(1+\gamma)(\frac{1}{2} - \frac{1}{\pi})}.$$

It is interesting to compare these results with those obtained in the deconvolution case (see Johnstone et al. [53] and chapter 6). In this context, for $\pi \geq 1$, $s \geq 1/\pi$, $r \geq 1$, the rates for the $L^p(dx)$ loss ($1 < p < \infty$) and over a ball of Besov space $B^s_{\pi,r}(M)$ are as above (up to the logarithmic factors) with μ replaced by:

$$\mu = \min\{\mu_{regular},\ \mu_{sparse}\},$$

with:

$$\mu_{regular} = \frac{s}{s+\nu+1/2}, \quad \mu_{sparse} = \frac{s - 1/\pi + 1/p}{s+\nu+1/2 - 1/\pi}.$$

Then the deconvolution setting appears as a critical case of the Jacobi-type model: we obtain exactly the same regular and sparse rates if we set $\alpha = \beta = -\frac{1}{2}$. More generally if we set $\alpha = \beta > -\frac{1}{2}$ we can draw the cartography of the regular and sparse zones with respect to (p,π) (see figure 4.1), as was done in Härdle et al. [49] in the direct observation case. In the deconvolution case (ie the "wavelet scenario") the separation between the zones is linear whereas in the "Jacobi scenario" the critical case corresponds to a convex curve, and notice that in this case the regular rate is never optimal when:

$$p > p_{\alpha,s} := p_{\alpha,s} = 2 + \frac{s + (2\nu+1)(\alpha+1)}{s(\alpha+\frac{1}{2})}.$$

Let us also mention that unlike in the deconvolution case, the exact logarithmic factors of the minimax risk are not established yet. In this paper we have focused only on the main rate ε^μ, so our results prove that NeedVD is "quasi optimal" in the Jacobi-type models.
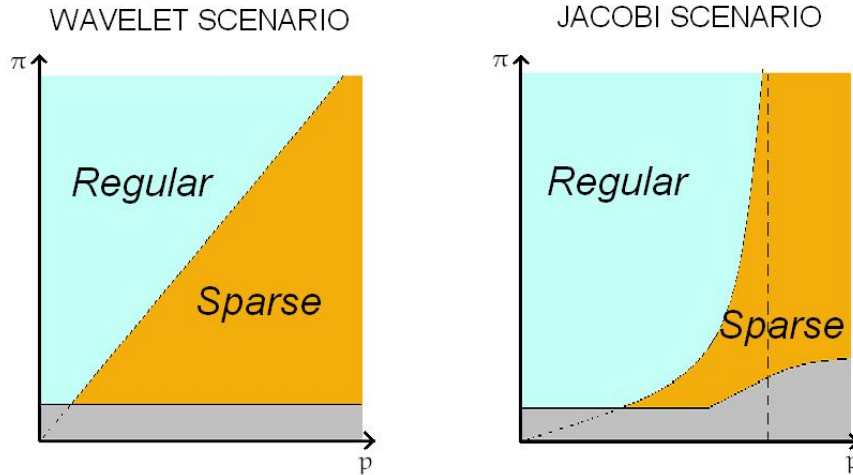
Figure 4.1: Cartography of the regular and sparse zones with respect to (p, π) in the deconvolution case (left) and in the Jacobi case (right)

4.2.3 Application to the Wicksell problem

The main practical motivation of introducing the Jacobi-type inverse models is to investigate the rates of the minimax risk and to propose an optimal estimation procedure in a well known inverse model: the Wicksell's problem (Wicksell [91]), which corresponds to the following situation.

Suppose a population of spheres is embedded in a medium. The spheres have radii that may be assumed to be drawn independently from a density f. A random plane slice is taken through the medium, and some the spheres intersected by it. They furnish circles, the radii of which yield the points of observation $Y_1, \ldots, Y_n$. The unfolding problem is then to determine the density of the sphere radii from the observed circle radii. This problem also arises in medicine, where the spheres might be tumors in an animal's liver (Nychka et al. [76]), as well as in numerous other contexts (biological, engineering, etc.) see for instance Cruz-Orive [25].

In this article we consider this problem in the white noise framework. Some comments about the application to the density framework are made in Chapter 5, but a more thorough investigation is still under study. We use the singular value decomposition established in Johnstone and Silverman [54], where the Wicksell's problem corresponds to the following operator:

$$\mathbb{H} = \mathbb{L}^2([0, 1], d\mu^*), \ d\mu^*(x) = (4x)^{-1}dx, \quad \mathbb{K} = \mathbb{L}^2([0, 1], d\lambda), \ d\lambda(x) = 4\pi^{-1}(1 - y^2)^{1/2}dy,$$

and

$$Kf(y) = \frac{\pi}{4}y(1 - y^2)^{-1/2} \int_y^1 (x^2 - y^2)^{-1/2}f(x)d\mu^*.$$

In this case we have the following SVD bases:

$$e_k(x) = 4(k+1)^{1/2} x^2 P_k^{0,1}(2x^2-1)$$
$$g_k(y) = U_{2k+1}(y).$$

Here $P_k^{0,1}$ is the kth degree Jacobi polynomial of type $(0,1)$ and U_k is the second type Chebishev polynomial of degree k. The singular values are

$$b_k = \frac{\pi}{16}(1+k)^{-1/2}.$$

Thus the results of theorem 9 establish rates for the minimax risk $R_\varepsilon^{Wicksell}$ of the Wicksell problem, considered in the framework of Johnstone and Silverman [54], with white noise perturbations. Then the NeedVD estimator is quasi optimal in this context:

$$R_\varepsilon^{Wicksell}(\widetilde{B}_{\pi,r}^s(M), \mathbb{L}^2(\mu^*)) \asymp \varepsilon^{\mu p}, \text{ (up to } \log(1/\varepsilon) \text{ factors)}$$

where

$$\mu = \min\{\frac{s}{s+1}, \frac{s-2(\frac{1}{\pi}-\frac{1}{2})}{s+\frac{3}{2}-\frac{2}{\pi}}, \frac{s-4(\frac{1}{\pi}-\frac{1}{2})}{s+\frac{5}{2}-\frac{4}{\pi}}\}.$$

For other values of the loss p, the picture is a bit more complex. An analysis of the results can be found in the second section of Chapter 5. The rates we obtain seem to be new in the literature. However other formulations of the Wicksell problem have been proposed, with some other results: a minimax study can be found in Golubev and Levit [46] for the estimation of the distribution function associated to f, and in Antoniadis et al. [6] convergence rates are established for the estimation of a probability distribution function closely related to f.

4.3   Localized functions adapted to the operator

4.3.1   Construction of needlets

In this section we recall briefly the construction of Jacobi needlets introduced by Petrushev and Xu [81]. We denote by (P_k) the classical Jacobi polynomials of type (α, β) normalized in $L^2(d\mu_{\alpha\beta})$. Let $a(\xi)$ be a C^∞ function supported in $[-2, -\frac{1}{2}] \cup [\frac{1}{2}, 2]$ such that

$$\sum_{j\geq 0} a^2(\xi/2^j) = 1, \quad \forall|\xi| \geq 1.$$

Moreover we add the condition: $a(\xi) > c > 0$ for $3/4 \leq \xi \leq 7/4$.

We define:

$$\Lambda_j(x,y) = \sum_k a(k/2^j) P_k(x) P_k(y).$$

Let $\eta_k = \cos\theta_{j,k}$, $k = 1, 2, \ldots, 2^j$, be the zeros of the Jacobi polynomial P_{2^j} ordered so that $\eta_1 > \eta_2 > \cdots > \eta_{2^j}$ and hence $0 < \theta_{j,1} < \theta_{j,2} < \cdots < \theta_{j,2^j} < \pi$. It is well known that (cf Szegő [86])

$$\theta_{j,k} \sim \frac{k\pi}{2^j}. \tag{4.2}$$

We set

$$\mathbb{Z}_j = \{\eta_k : k = 1, 2, \ldots, 2^j\}.$$

Let Π_n denote the space of all polynomials of degree inferior to n. As is well known (Szegő [86]) the zeros of the Jacobi polynomial P_{2^j} serve as knots of the Gaussian quadrature which is exact for all polynomials from $\Pi_{2^{j+1}-1}$, that is,

$$\int_I P d\mu = \sum_{\eta_k \in \mathbb{Z}_j} b_{j,\eta_k} P(\eta_k), \quad \forall P \in \Pi_{2^{j+1}-1},$$

where the coefficients $b_{j,\eta_k} > 0$ are the Christoffel numbers (Szegő [86]) and $b_{j,\eta_k} \sim 2^{-j} \omega_{\alpha,\beta}(2^j; \eta_k)$ with

$$\omega_{\alpha,\beta}(2^j; x) := (1 - x + 2^{-2j})^{\alpha+1/2}(1 + x + 2^{-2j})^{\beta+1/2}.$$

We now define the Jacobi needlets by

$$\psi_{j,\eta_k}(x) = \sqrt{b_{j,\eta_k}} \Lambda_{2^j}(x, \eta_k), \quad k = 1, 2, \ldots, 2^j; j \geq 0.$$

So the needlets depend on the Jacobi polynomials in the following way:

$$\psi_{j,\eta} = \sum_{l \in \mathbb{N}} a(l/2^{j-1}) P_l(x) P_l(\eta) \sqrt{b_{j,\eta}},$$

where the support of a is included in $[\frac{1}{2}, 2]$. So we have

$$\psi_{j,\eta}(x) = \sum_{l=2^{j-2}+1}^{2^j-1} c_{j,\eta,l} P_l(x),$$

with coefficients $c_{j,\eta,l} = a(l/2^{j-1}) P_l(\eta) \sqrt{b_{j,\eta}}$.

Some examples of needlets are given in figure 4.2. Note that setting $\alpha \neq \beta$ introduces some dissymmetry in the function, which presents more variations in the interval corresponding to the highest parameter $\max(\alpha, \beta)$.
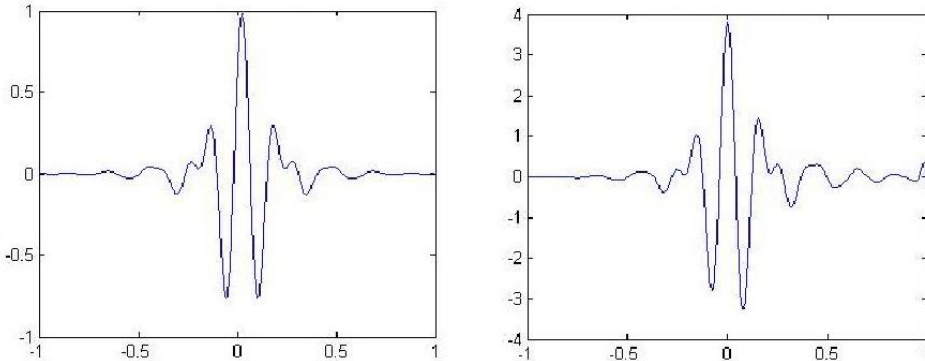

Figure 4.2: A Jacobi needlet of type $(\alpha, \beta) = (0, 0)$ (left) and $(\alpha, \beta) = (1, 0)$ (right)

4.3.2   Properties of needlets in the Jacobi case

In this section we give a list of some useful results on the needlets established in previous papers, and we give two new results that will be needed to establish the lower bounds for the Wicksell problem.

First of all, the needlets obtained this way form a tight frame: for any $f \in \mathbb{H}$,

$$f = \sum_{j \in \mathbb{N} \eta \in \mathbb{Z}_j} \langle f, \psi_{j,\eta} \rangle \psi_{j,\eta},$$

$$\|f\|^2 = \sum_{j \in \mathbb{N} \eta \in \mathbb{Z}_j} |\langle f, \psi_{j,\eta} \rangle|^2.$$

Unlike the first generation wavelets, they do not form an orthonormal basis: they form a redundant system. However they still enjoy "wavelet like" properties as detailed hereafter.

Concentration property

The interesting localization properties of the needlets stem essentially from the following concentration inequality, which is the main result established in Petrushev and Xu [81]:

Theorem 10. *For any $l \geq 1$ there exists a constant $C_l > 0$ such that*

$$|\psi_{j,\eta_k}(\cos\theta)| \leq C_l \frac{1}{\sqrt{\omega_{\alpha,\beta}(2^j, \cos\theta)}} \frac{2^{j/2}}{(1 + 2^j|\theta - \frac{\pi k}{2^j}|)^l}, \quad 0 \leq \theta \leq \pi.$$

This inequality enables to establish wavelet-like inequalities for the L^p norms of linear combinations of needlets, as detailed in the next section. However it also highlights major differences with respect to wavelets. First the energy of each needlet ψ_{j,η_k} is concentrated on a small interval centered on η. Moreover for a given resolution level j, needlets behave quite differently depending on their locations η in the interval, which is due to the variations of the function $\omega_{\alpha,\beta}(2^j, .)$. This is illustrated in figure 4.3: for a given resolution j, "edge" needlets have different shapes than "middle" needlets, and the L^3 norms are not constant with respect to η (the L^2 norms are more or less invariant though).

More precisely concerning L^p norms, the following bounds have been established in Petrushev and Xu [81] (for the upper bounds) and in Chapter 3 (for the lower bounds):

Theorem 11. $\forall\, 0 < p \leq \infty, \forall j \in \mathbb{N}$,

$$\forall\, k = 1, \ldots, 2^{j-1}, \; c_p \left(\frac{2^{j(\alpha+1)}}{k^{\alpha+1/2}} \right)^{1-2/p} \leq \|\psi_{j,\eta_k}\|_p \leq C_p \left(\frac{2^{j(\alpha+1)}}{k^{\alpha+1/2}} \right)^{1-2/p},$$

$$\forall\, 2^{j-1} < k \leq 2^j, \; c_p \left(\frac{2^{j(\beta+1)}}{(1+(2^j-k))^{\beta+1/2}} \right)^{1-2/p} \leq \|\psi_{j,\eta_k}\|_p \leq C_p \left(\frac{2^{j(\beta+1)}}{(1+(2^j-k))^{\beta+1/2}} \right)^{1-2/p}.$$
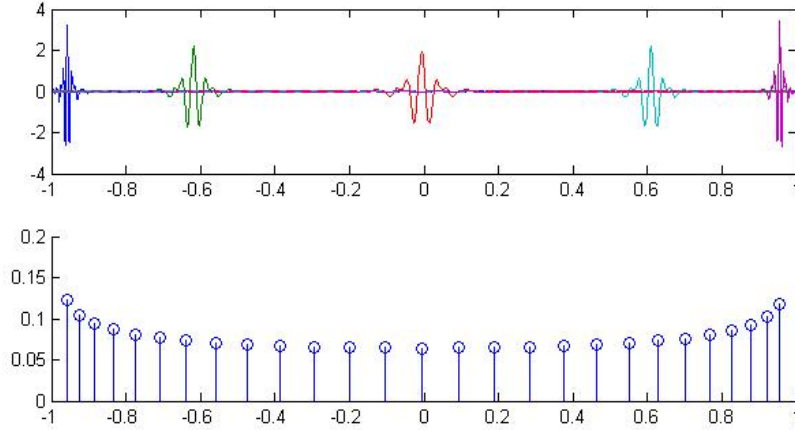
Figure 4.3: For a given resolution j: the shape of the needlet ψ_{j,η_k} (above), and the values of its L^3 norm (below) for several η_k

Inequalities for L^p norms of linear combinations of needlets

An important result for linear combinations of needlets was established in Chapter 3, showing that needlets have wavelet-like properties for the L^p norm:

Theorem 12. *Let $0 < p < \infty$. Then there exists a constant $C_p > 0$ such that for any collection of numbers $\{\lambda_k : k = 1, 2, \ldots, 2^j\}$, $j \geq 0$,*

$$\|\sum_{k=1}^{2^j} \lambda_k \psi_{j,\eta_k}\|_{\mathbb{L}^p(\mu)}^p \leq C_p \sum_{k=1}^{2^j} |\lambda_k|^p \|\psi_{j,\eta_k}\|_{\mathbb{L}^p(\mu)}^p. \tag{4.3}$$

Note that establishing the corresponding lower bound for linear combinations of needlets is impossible in general. For instance with the coefficients $\sqrt{b_{j,\eta_k}}$ introduced in the definition of the needlets, one can check that:

$$\sum_{k=1}^{2^j} \sqrt{b_{j,\eta_k}} \psi_{j,\eta_k} = 0.$$

However we will establish the following result for needlets with a large enough distance between the indexes of the η's, in the case where p is an even integer:

Theorem 13. *Let $p \in 2\mathbb{N}^*$. Then there exists a constant $c_p > 0$ and an integer n_p such that for any collection of numbers $\{\lambda_k : k \in I_j\}$, $j \geq 0$, where $I_j \subset \{1, 2, \ldots, 2^j\}$ and $k, l \in I_j, k \neq l \Longrightarrow |k - l| \geq n_p$,*

$$\|\sum_{k \in I_j} \lambda_k \psi_{j,\eta_k}\|_{\mathbb{L}^p(\mu)}^p \geq c_p \sum_{k \in I_j} |\lambda_k|^p \|\psi_{j,\eta_k}\|_{\mathbb{L}^p(\mu)}^p. \tag{4.4}$$

Finally we also establish the following bounds for scalar products of needlets:

Lemma 1. *We have:*

1. $\forall j, j', k, l$ such that $|j' - j| \geq 2$,

$$\langle \psi_{j,\eta_k}, \psi_{j',\eta_l} \rangle = 0.$$

2. $\forall \zeta > 0$, $\exists c_\zeta$ such that $\forall j, j', k, l$ with $|j' - j| \leq 1$:

$$|\langle \psi_{j,\eta_k}, \psi_{j',\eta_l} \rangle| \leq \frac{c_\zeta}{(1 + |k - 2^{j-j'}l|)^\zeta}.$$

The proofs of that theorem and of that lemma are given in the appendix.

4.4   Proof of the main result

4.4.1   Scheme of the proof

The proof of theorem (9) requires lemma (2), which is a consequence of Fano's lemma adapted from Birge [11]. It uses the Kullback-Leibler divergence $\mathcal{K}(P, Q)$ between two probability measures P and Q, defined by:

$$\mathcal{K}(P, Q) = \begin{cases} \int \ln(\frac{dP}{dQ}) dP, & \text{if } P \ll Q; \\ +\infty, & \text{otherwise.} \end{cases}$$

Lemma 2. *Let A be a sigma algebra on the space Ω and $m \in \mathbb{N}^*$. Let $A_i \in A$, $i \in \{0, 1, \ldots, m\}$ such that $\forall i \neq j, A_i \cap A_j = \emptyset$. Let P_i, $i \in \{0, 1, \ldots, m\}$ be $m + 1$ probability measures on (Ω, A). Then*

$$\sup_{i \in \{0,1,\ldots,m\}} P_i(A_i^c) \geq \min(2^{-1}, \sqrt{m} \exp(-3e^{-1}) \exp(-\chi_m)),$$

where

$$\chi_m = \inf_{i \in \{0,1,\ldots,m\}} \frac{1}{m} \sum_{j \neq i} \mathcal{K}(P_j, P_i).$$

We use this lemma by building several sets of hypotheses f_i, $i \in \{0, 1, \ldots, m\}$ such that:

- *(i) f_i belongs to the set considered for the upper bound (denoted by $\widetilde{B}_{\pi,r}^s(M)$)*

- *(ii) for all $i \neq j$, $\|f_i - f_j\|_p^p \geq \delta$ for some $\delta > 0$.*

- *(iii) $\sqrt{m} \exp[-\inf_{i \in \{0,1,\ldots,m\}} \frac{1}{m} \sum_{j \neq i} K(P_{f_j}, P_{f_i})] \geq \pi_0$ where P_{f_i} denotes the probability distribution of the process Y_ε under the hypothesis f_i and π_0 is a positive constant.*

Using Chebychev's inequality for any estimator $\hat{f}$ we have:

$$\delta^{-1} \sup_{f \in B^s_{\pi,r}(R)} E_f(\|\hat{f} - f\|_p^p) \geq \sup_{i \in \{0,1,\dots,m\}} P_{f_i}(A_i^c),$$

where the sets A_i are defined by $A_i = \{\|\hat{f} - f_i\|_p^p < \frac{\delta}{2^p}\}$ and satisfy $A_i \cap A_j = \emptyset$ for $i \neq j$. Then using the lemma we obtain:

$$\sup_{f \in \widetilde{B}^s_{\pi,r}(R)} E_f(\|\hat{f} - f\|_p^p) \geq \pi_1 \delta,$$

where $\pi_1 = 2^p \min(2^{-1}, \pi_0 \exp(-3e^{-1}))$ is a strictly positive constant. With an appropriate choice of f_i and m depending on the level of noise ε, δ yields the expected rates.

A simple preliminary lemma will also be needed concerning the Kullback divergence for our model.

Lemma 3. *Under model* (4.1) *if P_f denotes the probability distribution of the process $Y_\varepsilon = Kf + \varepsilon\dot{W}$ then for all $f, g \in \mathbb{L}^2([-1,1], \mu)$:*

$$\mathcal{K}(P_f, P_g) \leq c\|\frac{K(f-g)}{\varepsilon}\|^2_{L^2(\lambda)}.$$

Proof of lemma 3. Using for example theorem 7.18 from Lipster and Shiryaev [62], for all $f, g \in \mathbb{H}$ P_f is absolutely continuous with respect to P_g, and if we denote by $\Lambda_\varepsilon(f,g) := \frac{dP_f}{dP_g}(X)$ the likelihood ratio, then under the hypothesis g and for $\dot{W}$ given by $Y_\varepsilon = Kg + \varepsilon\dot{W}$ we have:

$$\Lambda_\varepsilon(f,g) = \exp\Big[-\int_0^1 \frac{K(f-g)(t)}{\varepsilon} d\dot{W}(t) - \frac{1}{2} \int_0^1 \big(\frac{K(f-g)(t)}{\varepsilon}\big)^2 d\lambda(t) \Big].$$

Thus:

$$\mathcal{K}(P_f, P_g) = E_f \ln(\Lambda_\varepsilon(f,g)) = -E_f \ln(\Lambda_\varepsilon(g,f)) = \frac{1}{2} \int_0^1 \big(\frac{K(f-g)(t)}{\varepsilon}\big)^2 d\lambda(t).$$

$\square$

4.4.2 Sparse cases

The sparse rate $\mu(\alpha)$ is obtained by applying lemma (2) to the following set of functions:

$$f_0 = 0,$$

and

$$f_1 = \gamma \psi_{j_0, \eta_1},$$

for some parameters γ and j_0 chosen so as to satisfy conditions *(i)* to *(iii)*.

Condition *(i)*

The function $f_1 = \gamma \psi_{j_0,\eta_1}$ belongs to $\widetilde{B}^s_{\pi,r}(M)$ if $u_j := 2^{js}(\sum_{\eta \in \mathbb{Z}_j} |\langle f_1, \psi_{j,\eta}\rangle|^\pi \|\psi_{j,\eta}\|^\pi_\pi)^{1/\pi}$ belongs to $L^r(M)$.

Using the first part of lemma (1), $u_j = 0$ whenever $|j - j_0| \geq 2$. So in the sequel we assume that $j \in \{j_0 - 1, j_0, j_0 + 1\}$, and the L^r norm of (u_j) is bounded by a constant M (independent of $\gamma > 0$ and j_0) if for instance $u_j \leq 3^{-\frac{1}{r}}M$.

We have:
$$u_j^\pi = 2^{j\pi s}\gamma^\pi \sum_{\eta \in \mathbb{Z}_j} |\langle \psi_{j_0,\eta_1}, \psi_{j,\eta}\rangle|^\pi \|\psi_{j,\eta}\|^\pi_\pi \leq c(I_1 + I_2)$$

with, using the bound of theorem (4.3):

$$I_1 = 2^{j[\pi s + (\pi-2)(\alpha+1)]}\gamma^\pi \sum_{k=1}^{2^{j-1}} |\langle \psi_{j_0,\eta_1}, \psi_{j,\eta}\rangle|^\pi k^{-(\pi-2)(\alpha+1/2)},$$

$$I_2 = 2^{j[\pi s + (\pi-2)(\beta+1)]}\gamma^\pi \sum_{k=2^{j-1}+1}^{2^j} |\langle \psi_{j_0,\eta_1}, \psi_{j,\eta}\rangle|^\pi (2^j - k + 1)^{-(\pi-2)(\beta+1/2)}.$$

Using the second part of lemma (1), we have for any ζ:

$$|\langle \psi_{j_0,\eta_1}, \psi_{j,\eta_k}\rangle| \leq c\frac{1}{k^\zeta}$$

Thus choosing any $\zeta > \frac{-(\pi-2)(\alpha+1/2)+1}{\pi}$, we obtain:

$$I_1 \leq c2^{j[\pi s+(\pi-2)(\alpha+1)]}\gamma^\pi.$$

Moreover
$$\sum_{k=1}^{2^{j-1}} \frac{(2^j - k + 1)^{-(\pi-2)(\beta+1/2)}}{k^{\zeta\pi}} \leq c2^{-\zeta\pi j}2^{j[1-(\pi-2)(\beta+1/2)]_+},$$

so

$$I_2 \leq c2^{j(\pi s+(\pi-2)(\beta+1)-\zeta\pi+[1-(\pi-2)(\beta+1/2)]_+)}\gamma^\pi \leq cI_1$$

for a large enough ζ.

Thus we have for all $j \in \{j_0 - 1, j_0, j_0 + 1\}$,

$$u_j^\pi \leq c2^{j[\pi s+(\pi-2)(\alpha+1)]}\gamma^\pi,$$

and f_1 belongs to $\widetilde{B}^s_{\pi,r}(M)$ if

$$\gamma \leq c2^{-j[s+(1-\frac{2}{\pi})(\alpha+1)]},$$

with a small enough c depending on M.

Condition *(ii)*

Using theorem 11, condition *(ii)* is fulfilled with: $\delta \asymp \gamma^p 2^{j_0(p-2)(\alpha+1)}$.

Condition *(iii)*

Using lemma (3) *(iii)* is satisfied if:

$$\int_I \left(\frac{K(\gamma\psi_{j_0,\eta_1})(t)}{\varepsilon}\right)^2 d\lambda(t) \le C.$$

We have:

$$\psi_{j_0,\eta}(x) = \sum_{l=2^{j-2}+1}^{2^j-1} c_{j,\eta,l} P_l(x),$$

so:

$$K\psi_{j_0,\eta}(x) = \sum b_l c_{j,\eta,l} U_l(x),$$

and:

$$\|K(\psi_{j_0,\eta_1})\|^2_{\mathbb{L}_2(I,\lambda)} = \sum_l [b_l c_{j,\eta,l}]^2 \asymp 2^{-2\nu j_0} \sum_l [c_{j,\eta,l}]^2 = 2^{-2\nu j_0} \|\psi_{j_0,\eta_1}\|^2_{\mathbb{L}_2(I,\mu)} \le C 2^{-2\nu j_0}.$$

So *(iii)* is satisfied if: $\frac{\gamma 2^{-\nu j_0}}{\varepsilon} \le c$.

Sparse rate $\mu(\alpha)$

Finally we set: $\gamma \asymp \varepsilon 2^{\nu j_0}$, and $2^{j_0} \asymp \varepsilon^{-\frac{1}{s+\nu+(1-\frac{2}{\pi})(\alpha+1)}}$, and we obtain the lower bound:

$$\delta \asymp \varepsilon^{\frac{p[s+2(\frac{1}{p}-\frac{1}{\pi})(\alpha+1)]}{s+\nu+(1-\frac{2}{\pi})(\alpha+1)}}.$$

Sparse rate $\mu(\beta)$

Similarly we obtain $\mu(\beta)$ by using the set:

$$f_0 = 0,$$

and

$$f_1 = \gamma\psi_{j_0,\eta_{2^{j_0}}}.$$

Obviously conditions *(ii)* and *(iii)* are valid under the same constraints as before, with α replaced by β. For *(i)* we also proceed the same way as before. This time we have:

$$|\langle \psi_{j_0,\eta_{2^{j_0}}}, \psi_{j,\eta_k}\rangle| \le c\frac{1}{(1+|k-2^{j-j_0}2^{j_0}|)^\zeta} = c\frac{1}{(2^j-k+1)^\zeta},$$

so

$$I_2 = 2^{j[\pi s+(\pi-2)(\beta+1)]}\gamma^\pi \sum_{k=2^{j-1}+1}^{2^j} \frac{(2^j-k+1)^{-(\pi-2)(\beta+1/2)}}{(2^j-k+1)^{\zeta\pi}} \le c2^{j[\pi s+(\pi-2)(\beta+1)]}\gamma^\pi,$$

$$I_1 = 2^{j[\pi s + (\pi-2)(\alpha+1)]} \gamma^\pi \sum_{k=1}^{2^{j-1}} \frac{k^{-(\pi-2)(\alpha+1/2)}}{(2^j - k + 1)^{\zeta\pi}} \leq c 2^{j(\pi s + (\pi-2)(\alpha+1) - \zeta\pi + [1-(\pi-2)(\alpha+1/2)]_+)} \gamma^\pi \leq c I_2,$$

for a large enough ζ. Thus condition *(i)* is also valid under the same constraint as before, with α replaced by β, and we obtain the expected rate with $\gamma \asymp \varepsilon 2^{\nu j_0}$ and $2^{j_0} \asymp \varepsilon^{-\frac{1}{s+\nu+(1-\frac{2}{\pi})(\beta+1)}}$.

4.4.3   Regular case

Let m be an integer such that $2^m \geq n_2$, where n_2 is the integer from theorem 4.4 in the case $p = 2$. For some parameters γ and $j_0 \geq m + 1$ chosen further, we consider for $\varepsilon \in \{0,1\}^{2^{j_0-m-1}}$ the $2^{2^{j_0-m-1}}$ functions:

$$f_\varepsilon = \gamma \sum_{k=1}^{2^{j_0-m-1}} \varepsilon_k k^\delta \psi_{j_0, \eta_{2^m k}},$$

for a large enough δ:

$$\delta > \max[1, \alpha + 1/2, (1 - \frac{2}{\pi})(\alpha + \frac{1}{2}) - \frac{1}{\pi}].$$

We only keep some of these functions. By Varshamov-Gilbert theorem (see for instance Tsybakov [89]), there exists a subset $E_{j_0} = \{\varepsilon^0, \dots, \varepsilon^{T_{j_0}}\}$ of $\{0,1\}^{2^{j_0-m-1}}$ and two constants $c > 0$, $\rho > 0$ such that $\forall 0 \leq u < v \leq T_{j_0}$:

$$\sum_{k=1}^{2^{j_0-m-1}} |\varepsilon_k^u - \varepsilon_k^v| \geq c 2^{j_0},$$

and

$$T_{j_0} \geq exp(\rho 2^{j_0}).$$

In the sequel we consider the set $\{f_\varepsilon, \quad \varepsilon \in E_{j_0}\}$.

Condition *(i)*

For $\varepsilon \in E_{j_0}$, let:
$$u_j := 2^{js}(\sum_{\eta \in \mathbb{Z}_j} |\langle f_\varepsilon, \psi_{j,\eta}\rangle|^\pi \|\psi_{j,\eta}\|_\pi^\pi)^{1/\pi}.$$

We have:
$$u_j^\pi \leq c(I_1 + I_2),$$

with

$$I_1 = 2^{j[\pi s + (\pi-2)(\alpha+1)]} \gamma^\pi \sum_{k=1}^{2^{j-1}} k^{-(\pi-2)(\alpha+1/2)} (\sum_{l=1}^{2^{j_0-1}} l^\delta |\langle \psi_{j_0, \eta_l}, \psi_{j, \eta_k}\rangle|)^\pi,$$

$$I_2 = 2^{j[\pi s + (\pi-2)(\beta+1)]} \gamma^\pi \sum_{k=2^{j-1}+1}^{2^j} (2^j - k + 1)^{-(\pi-2)(\beta+1/2)} \Big(\sum_{l=1}^{2^{j_0}-1} l^\delta |\langle \psi_{j_0,\eta_l}, \psi_{j,\eta_k} \rangle| \Big)^\pi.$$

Once again $u_j = 0$ whenever $|j - j_0| \geq 2$, and for $j \in \{j_0 - 1, j_0, j_0 + 1\}$ we have:

$$|\langle \psi_{j_0,\eta_l}, \psi_{j,\eta_k} \rangle| \leq c \frac{1}{(1 + |l - 2^{j_0 - j}k|)^\varsigma}.$$

Let, for $x \in \mathbb{R}$, $E(x)$ denote the largest integer smaller than x. We have:

$$\sum_{l \leq E(2^{j_0-j}k)} \frac{l^\delta}{(1 + |l - 2^{j_0-j}k|)^\varsigma} \leq ck^\delta \sum_{l \leq E(2^{j_0-j}k)} \frac{1}{(1 + E(2^{j_0-j}k) - l)^\varsigma} \leq ck^\delta \sum_{l \geq 1} \frac{1}{l^\varsigma} \leq ck^\delta,$$

Moreover

$$\sum_{l \geq E(2^{j_0-j}k)+1} \frac{l^\delta}{(1 + |l - 2^{j_0-j}k|)^\varsigma} \leq \sum_{l \geq E(2^{j_0-j}k)+1} \frac{l^\delta}{(l - E(2^{j_0-j}k))^\varsigma}$$

$$= \sum_{l \geq 1} \frac{(l + E(2^{j_0-j}K))^\delta}{l^\varsigma}$$

$$\leq c \sum_{l \geq 1} \frac{l^\delta + E(2^{j_0-j}k)^\delta}{l^\varsigma} \leq ck^\delta,$$

for ς large enough. To obtain the last line, we used the fact that $\delta \geq 1$.

Thus $\sum_{l=1}^{2^{j_0}-1} \frac{l^\delta}{(1+|l-2^{j_0-j}k|)^\varsigma} \leq ck^\delta$, and:

$$I_1 \leq c 2^{j[\pi s + (\pi-2)(\alpha+1)]} \gamma^\pi \sum_{k=1}^{2^{j-1}} k^{-(\pi-2)(\alpha+1/2)} k^{\delta\pi} = c 2^{j[s+\delta+\frac{1}{2}]} \gamma.$$

For I_2 remark that for any $k \in \{2^{j-1} + 1, \ldots, 2^j\}$ and any $l \in \{1, \ldots, 2^{j_0}-1\}$, we have:

$$|\frac{k}{2^j} - \frac{l}{2^{j_0}}| = \frac{k}{2^j} - \frac{l}{2^{j_0}} \geq |\frac{2^j - k}{2^j} - \frac{l}{2^{j_0}}|.$$

So for such a k, as previously: $\sum_{l=1}^{2^{j_0}-1} \frac{l^\delta}{(1+|l-2^{j_0-j}k|)^\varsigma} \leq \sum_{l=1}^{2^{j_0}-1} \frac{l^\delta}{(1+|l-2^{j_0-j}(2^j-k)|)^\varsigma} \leq c(2^j - k)^\delta$, and:

$$I_2 \leq c 2^{j[\pi s + (\pi-2)(\beta+1)]} \gamma^\pi \sum_{k=2^{j-1}+1}^{2^j} (2^j - k + 1)^{-(\pi-2)(\beta+1/2)} (2^j - k + 1)^{\delta\pi} = c 2^{j[s+\delta+\frac{1}{2}]} \gamma.$$

So we have $u_j \leq c 2^{j[s+\delta+\frac{1}{2}]} \gamma$ and finally f_u belongs to $\widetilde{B}_{\pi,r}^s(M)$ if:

$$\gamma \leq c 2^{-j_0[s+\delta+\frac{1}{2}]},$$

with a small enough c depending on M.

Condition *(ii)*

For all $u, v \in E_{j_0}$ with $u \neq v$,

$$f_u - f_v = \sum_{k=1}^{2^{j_0-m-1}} \gamma(\varepsilon_k^u - \varepsilon_k^v)k^\delta \psi_{j_0, \eta_2 m_k}$$

So by theorems 4.4 and 11, we have:

$$\|f_u - f_v\|_{\mathbb{L}^2(\mu)}^2 \geq c\gamma^2 \sum_{k=1}^{2^{j_0-m-1}} (\varepsilon_k^u - \varepsilon_k^v)^2 k^{2\delta} = c\gamma^2 \sum_{\{k \,|\, \varepsilon_k^u \neq \varepsilon_k^v\}} k^{2\delta}.$$

Let $N_{u,v}$ denote the cardinal of the set $\{k \in \{1, \ldots, 2^{j_0-m-1}\} \mid \varepsilon_k^u \neq \varepsilon_k^v\}$, then we have $N_{u,v} \geq c2^{j_0}$ and, since $\delta > 0$:

$$\|f_u - f_v\|_{\mathbb{L}^2(\mu)}^2 \geq c\gamma^2 \sum_{k=1}^{N_{u,v}} k^{2\delta} = \gamma^2 N_{u,v}^{1+2\delta} \geq c\gamma^2 2^{j_0(1+2\delta)}. \tag{4.5}$$

Let us distinguish two cases. *Suppose $2 < p < \infty$* and let $1/p + 1/q = 1$. By 4.5 and Hölder's inequality we have:

$$c2^{j_0(1+2\delta)} \leq \|f_u - f_v\|_{\mathbb{L}^2(\mu)}^2 \leq \|f_u - f_v\|_{\mathbb{L}^p(\mu)}\|f_u - f_v\|_{\mathbb{L}^q(\mu)}.$$

Using 4.3 and the fact that, under our assumptions, $q\delta - (q-2)(\alpha + 1/2) > -1$:

$$\|f_u - f_v\|_{\mathbb{L}^q(\mu)} \leq c\gamma 2^{j\frac{(q-2)}{q}(\alpha+1)}\Big(\sum_{k=1}^{2^{j_0-m-1}} k^{q\delta-(q-2)(\alpha+1/2)}\Big)^{1/q} \leq c'\gamma 2^{j_0(\frac{1}{2}+\delta)}$$

thus:

$$\|f_u - f_v\|_{\mathbb{L}^p(\mu)}^p \geq c\gamma^p 2^{j_0 p(\frac{1}{2}+\delta)}.$$

Suppose now $1 < p < 2$, we have using (4.5)

$$c2^{j_0(1+2\delta)} \leq \|f_u - f_v\|_{\mathbb{L}^2(\mu)}^2 \leq \|f_u - f_v\|_{\mathbb{L}^p(\mu)}^p\|f_u - f_v\|_{\mathbb{L}^\infty(\mu)}^{2-p}.$$

From 10 we infer for all $0 \leq \theta \leq \pi/2$:

$$|\psi_{j_0, \eta_k}(\cos\theta)| \leq C\frac{2^{j_0(1+\alpha)}}{(1 + 2^{j_0}|\theta - \frac{k\pi}{2^{j_0}}|)^l} \frac{1}{(2^{j_0}\theta + 1)^{\alpha+1/2}},$$

so for l large enough:

$$|\psi_{j_0, \eta_k}(\cos\theta)| \leq C\frac{2^{j_0(1+\alpha)}}{k^{\alpha+1/2}} \frac{1}{(1 + 2^{j_0}|\theta - \frac{k\pi}{2^{j_0}}|)^2},$$

and, since $\delta - (\alpha + 1/2) \geq 0$:

$$|f_u(\cos\theta) - f_v(\cos\theta)| \leq c\gamma 2^{j_0(\alpha+1)} \sum_{k=1}^{2^{j_0}-m-1} k^{\delta-(\alpha+1/2)} \frac{1}{(1+2^{j_0}|\theta - \frac{k\pi}{2^{j_0}}|)^2} \leq c'\gamma 2^{j_0(\frac{1}{2}+\delta)},$$

where in the last line we used the fact that for any θ, $\sum_{k=1}^{2^{j_0}-m-1} \frac{1}{(1+2^{j_0}|\theta-\frac{k\pi}{2^{j_0}}|)^2} \leq c\sum_{l=1}^{+\infty} \frac{1}{l^2}$.

Similarly the same bound holds for any $\pi/2 \leq \theta \leq \pi$, thus we have:

$$\|f_u - f_v\|_{\mathbb{L}^\infty(\mu)} \leq c2^{j_0(\frac{1}{2}+\delta)},$$

and once again:

$$\|f_u - f_v\|_{\mathbb{L}^p(\mu)}^p \geq c\gamma^p 2^{j_0 p(\frac{1}{2}+\delta)}.$$

Condition *(iii)*

We have

$$\sqrt{T_{j_0}} \geq exp(\frac{\rho}{2}2^{j_0}),$$

so *(iii)* is satisfied if

$$\int_0^1 (\frac{K(f_u - f_v)(t)}{\varepsilon})^2 d\lambda(t) \leq C2^{j_0},$$

for a small enough constant C: $0 < C < \frac{\rho}{2}$.

For all $u, v \in E_{j_0}$ with $u \neq v$, we have:

$$f_u - f_v = \sum_{k=1}^{2^{j_0}-m-1} \beta_{j_0,k}\psi_{j_0,\eta_{2^m k}} = \sum_{k=1}^{2^{j_0}-m-1} \sum_{l\in\mathbb{N}} \beta_{j_0,k}c_{j_0,\eta_k,l}P_l(x),$$

with $\beta_{j_0,k} = \gamma(\varepsilon_k^u - \varepsilon_k^v)k^\delta$.

Thus:

$$\|K(f_u - f_v)\|_{\mathbb{L}_2(I,\lambda)}^2 = \sum_l [\sum_{k=1}^{2^{j_0}-m-1} \beta_{j_0,k}b_l c_{j_0,\eta_k,l}]^2 \asymp 2^{-2\nu j_0} \sum_l [\sum_{k=1}^{2^{j_0}-m-1} \beta_{j_0,k}c_{j_0,\eta_k,l}]^2$$

$$= 2^{-2\nu j_0}\|\sum_{k=1}^{2^{j_0}-m-1} \beta_{j_0,k}\psi_{j_0,\eta_{2^m k}}\|_{\mathbb{L}_2(I,\mu)}^2 \leq c2^{-2\nu j_0} \sum_{k=1}^{2^{j_0}-m-1} \beta_{j_0,k}^2$$

$$\leq c2^{-2\nu j_0}\gamma^2 \sum_{k=1}^{2^{j_0}-m-1} k^{2\delta} = c2^{-2\nu j_0}\gamma^2 2^{(2\delta+1)j_0}.$$

So finally we need:

$$\frac{2^{-\nu j_0}\gamma 2^{(\delta+\frac{1}{2})j_0}}{\varepsilon} \leq C2^{j_0/2},$$

i.e.

$$\frac{2^{(\delta-\nu)j_0}\gamma}{\varepsilon} \leq C,$$

with a small enough constant C.

All the conditions are satisfied with: $2^{j_0} \asymp \varepsilon^{-\frac{1}{s+\nu+\frac{1}{2}}}$ and $\gamma \asymp \varepsilon^{\frac{s+\delta+\frac{1}{2}}{s+\nu+\frac{1}{2}}}$, and we obtain the lower bound:

$$\delta \asymp \varepsilon^{\frac{ps}{s+\nu+\frac{1}{2}}}.$$

4.5   Appendix

Proof of theorem 4.4. Let $p \in 2\mathbb{N}^*$ and $I_j \subset \{1, 2, \ldots, 2^j\}$. We have:

$$\|(\sum_{k \in I_j} \lambda_k \psi_{j,\eta_k})\|_{\mathbb{L}^p(\mu)}^p = A + B,$$

where:

$$A = \sum_{k \in I_j} \lambda_k^p \|\psi_{j,\eta_k}\|_{\mathbb{L}^p(\mu)}^p,$$

$$B = \sum_{(p_k)_{k \in I_j} \in \Lambda} \frac{p! \prod_{k \in I_j} \lambda_k^{p_k}}{\prod_{k \in I_j} p_k!} \int_{-1}^1 (\prod_{k \in I_j} \psi_{j,\eta_k}^{p_k}(x))\mu(x)dx,$$

and $\Lambda = \{(p_k)_{k \in I_j} \mid p_k \in \mathbb{N}, \sum_{k \in I_j} p_k = p$ and $\exists u \neq v$ such that $p_u > 0$ and $p_v > 0\}$.

Let us introduce the functions:

$$\varphi_{j,k}(x) = \frac{1}{\sqrt{\omega_{\alpha,\beta}(2^j,x)}}\frac{2^{j/2}}{(1 + 2^j|\arccos x - \frac{\pi k}{2^j}|)^{\frac{2}{s}}}, \text{ for some } 0 < s < \min\{1, \frac{p}{\alpha \vee \beta + 1}\}.$$

For $(p_k)_{k \in I_j} \in \Lambda$, we use 10 with $l = \frac{2}{s} + 1$ for every ψ_{j,η_k}, $k \in I_j$. There exists C such that:

$$\prod_{k \in I_j} |\psi_{j,\eta_k}(\cos\theta)|^{p_k} \leq C \prod_{k \in I_j} \varphi_{j,k}(\cos\theta)^{p_k} \prod_{k \in I_j} \frac{1}{(1 + 2^j|\theta - \frac{\pi k}{2^j}|)^{p_k}}.$$

Let $u, v \in I_j, u \neq v$ such that $p_u > 0$ and $p_v > 0$, and let $n_{inf} = \min_{k,l \in I_j, k \neq l} |k - l|$. We have:

$$\prod_{k \in I_j} (1 + 2^j|\theta - \frac{\pi k}{2^j}|)^{p_k} \geq (1 + 2^j|\theta - \frac{\pi u}{2^j}|)(1 + 2^j|\theta - \frac{\pi v}{2^j}|) \geq c|u - v| \geq cn_{inf}.$$

Thus we obtain:

$$\sum_{(p_k)_{k\in I_j}\in\Lambda} \frac{p! \prod_{k\in I_j} |\lambda_k^{p_k}|}{\prod_{k\in I_j} p_k!} \prod_{k\in I_j} |\psi_{j,\eta_k}|^{p_k} \leq \frac{C}{n_{inf}} \sum_{(p_k)_{k\in I_j}\in\Lambda} \frac{p! \prod_{k\in I_j} |\lambda_k|^{p_k}}{\prod_{k\in I_j} p_k!} \prod_{k\in I_j} \varphi_{j,\eta_k}^{p_k}$$

$$\leq C \frac{(\sum_{k\in I_j} |\lambda_k|\varphi_{j,\eta_k})^p}{n_{inf}}.$$

Now we proceed similarly to the sketch of the proof of theorem 4.3 available in Chapter 3. Let us recall the two main tools.

First, consider the maximal operator

$$(M_s f)(x) = \sup_{J\ni x} \Big(\frac{1}{|J|} \int_J |f(u)|^s du\Big)^{1/s}, \quad s > 0,$$

where the supremum is taken over all intervals $J \subset [-1, 1]$ which contain x and $|J|$ denotes the length of J.

Then one can infer the following bound from the Fefferman-Stein maximal inequality (see Fefferman and Stein [41] and Andersen and John [2]). If $0 < p, r < \infty$ and $0 < s < \min\{p, r, \frac{p}{\alpha\vee\beta+1}\}$, then for any sequence of functions (f_k) on $[-1, 1]$

$$\Big\|\Big(\sum_k (M_s f_k)^r\Big)^{1/r}\Big\|_{\mathbb{L}^p(\mu)} \leq C \Big\|\Big(\sum_k |f_k|^r\Big)^{1/r}\Big\|_{\mathbb{L}^p(\mu)}.$$

Secondly set $\eta_0 = 1$, $\eta_{2^j+1} = -1$ and $\theta_{j,0} = 0$, $\theta_{j,2^j+1} = \pi$, respectively. Denote $I_k = [\frac{\eta_k+\eta_{k+1}}{2}, \frac{\eta_k+\eta_{k-1}}{2}]$ and put

$$H_k = h_k 1_{I_k} \quad \text{with} \quad h_k = \Big(\frac{2^j}{\omega_{\alpha,\beta}(2^j; \eta_k)}\Big)^{1/2},$$

where 1_{I_k} is the indicator function of I_k. Then $\|H_k\|_{\mathbb{L}^p(\mu)} \sim \|\psi_{j,\eta_k}\|_{\mathbb{L}^p(\mu)}$, and one shows in Chapter 3 that for any $s > 0$

$$\varphi_{j,\eta_k}(x) \leq c(M_s H_k)(x), \quad x \in [-1, 1], \quad \forall k = 1, 2, \ldots, 2^j, j \geq 0. \tag{4.6}$$

We use use these two results, with $f_k = H_k$ and $r = 1$. Noticing that the (H_k) have disjoint supports, we obtain:

$$\|\sum_{k=1}^{2^j} |\lambda_k|\varphi_{j,\eta_k}\|_{\mathbb{L}^p(\mu)}^p \leq C\|\sum_{k=1}^{2^j} |\lambda_k| H_k\|_{\mathbb{L}^p(\mu)}^p = C\sum_{k=1}^{2^j} |\lambda_k|^p \|H_k\|_{\mathbb{L}^p(\mu)}^p \leq C'\sum_{k=1}^{2^j} |\lambda_k|^p \|\psi_{j,\eta_k}\|_{\mathbb{L}^p(\mu)}^p.$$

So finally there exists $C > 0$ such that

$$|B| \leq C\frac{A}{n_{inf}},$$

and if we impose the following condition on I_j:

$$n_{inf} \geq 2C,$$

then we obtain $|B| \leq \frac{1}{2}A$, and thus:

$$\|(\sum_{k \in I_j} \lambda_k \psi_{j,\eta_k})\|_{\mathbb{L}^p(\mu)}^p \geq \frac{1}{2} \sum_{k \in I_j} \lambda_k^p \|\psi_{j,\eta_k}\|_{\mathbb{L}^p(\mu)}^p.$$

$\square$

Proof of lemma 1. As indicated previously, the needlets are defined as:

$$\psi_{j,\eta} = \sum_{l=2^{j-2}+1}^{2^j-1} c_{j,\eta,l} P_l(x),$$

with coefficients $c_{j,\eta,l} = a(l/2^{j-1})P_l(\eta)\sqrt{b_{j,\eta}}$.

If $|j'-j| \geq 2$ then $\{2^{j-2}+1,\ldots,2^j-1\} \cap \{2^{j'-2}+1,\ldots,2^{j'}-1\} = \emptyset$, thus

$$\langle \psi_{j,\eta_k}, \psi_{j',\eta_l} \rangle = 0, \quad \forall(k,l).$$

For the second part of the lemma we use theorem 10. For any δ there exists c_δ such that for all j,k:

$$|\psi_{j,\eta_k}(\cos\theta)| \leq c_\delta \frac{1}{\sqrt{\omega_{\alpha,\beta}(2^j,\cos\theta)}} \frac{2^{j/2}}{(1+2^j|\theta-\frac{\pi k}{2^j}|)^\delta}, \quad 0 \leq \theta \leq \pi,$$

with:

$$\omega_{\alpha,\beta}(x) = (1-x)^\alpha (1+x)^\beta,$$
$$\omega_{\alpha,\beta}(2^j;x) := (1-x+2^{-2j})^{\alpha+1/2}(1+x+2^{-2j})^{\beta+1/2}.$$

For a given $\zeta > 0$ and j,j',k,l such that $|j'-j| \leq 1$, we use this inequality for $|\psi_{j,\eta_k}|$ with $\delta = \zeta + 2$ and for $|\psi_{j',\eta_l}|$ with $\delta = \zeta$. Noticing that $\omega_{\alpha,\beta}(2^j,\cos\theta) \asymp \omega_{\alpha,\beta}(2^{j'},\cos\theta)$ we obtain:

$$|\langle \psi_{j,\eta_k}, \psi_{j',\eta_l} \rangle| \leq c2^j \int_0^\pi \frac{\omega_{\alpha,\beta}(\cos\theta)}{\omega_{\alpha,\beta}(2^j,\cos\theta)} \frac{\sin\theta d\theta}{(1+2^j|\theta-\frac{\pi k}{2^j}|)^{\zeta+2}(1+2^{j'}|\theta-\frac{\pi l}{2^{j'}}|)^\zeta}$$

$$\leq c\frac{I_{j,k,\alpha,\beta}}{(\min_{0\leq\theta\leq\pi} f_{j,j',k,l}(\theta))^\zeta},$$

with

$$f_{j,j',k,l}(\theta) = (1+2^j|\theta-\frac{\pi k}{2^j}|)(1+2^{j'}|\theta-\frac{\pi l}{2^{j'}}|), \quad 0 \leq \theta \leq \pi,$$

and

$$I_{j,k,\alpha,\beta} = 2^j \int_0^\pi \frac{\omega_{\alpha,\beta}(\cos\theta)}{\omega_{\alpha,\beta}(2^j,\cos\theta)} \frac{\sin\theta d\theta}{(1+2^j|\theta - \frac{\pi k}{2^j}|)^2}.$$

First we have:

$$\min_{0\leq\theta\leq\pi} f_{j,j',k,l}(\theta) = \min\{f_{j,j',k,l}(\frac{\pi k}{2^j}), f_{j,j',k,l}(\frac{\pi l}{2^{j'}})\}$$
$$\geq 1 + \frac{\pi}{2^{|j-j'|}}|k - 2^{j-j'}l|$$
$$\geq c(1 + |k - 2^{j-j'}l|).$$

Secondly let us divide $I_{j,k,\alpha,\beta}$ into two terms: $I_{j,k,\alpha,\beta} = I^1_{j,k,\alpha,\beta} + I^2_{j,k,\alpha,\beta}$, with:

$$I^1_{j,k,\alpha,\beta} = 2^j \int_0^{\frac{\pi}{2}} \frac{\omega_{\alpha,\beta}(\cos\theta)}{\omega_{\alpha,\beta}(2^j,\cos\theta)} \frac{\sin\theta d\theta}{(1+2^j|\theta - \frac{\pi k}{2^j}|)^2},$$

$$I^2_{j,k,\alpha,\beta} = 2^j \int_{\frac{\pi}{2}}^\pi \frac{\omega_{\alpha,\beta}(\cos\theta)}{\omega_{\alpha,\beta}(2^j,\cos\theta)} \frac{\sin\theta d\theta}{(1+2^j|\theta - \frac{\pi k}{2^j}|)^2}$$

$$= 2^j \int_0^{\frac{\pi}{2}} \frac{\omega_{\alpha,\beta}(-\cos\theta)}{\omega_{\alpha,\beta}(2^j,-\cos\theta)} \frac{\sin\theta d\theta}{(1+2^j|\pi - \theta - \frac{\pi k}{2^j}|)^2}$$

$$= 2^j \int_0^{\frac{\pi}{2}} \frac{\omega_{\beta,\alpha}(\cos\theta)}{\omega_{\beta,\alpha}(2^j,\cos\theta)} \frac{\sin\theta d\theta}{(1+2^j|\theta - \frac{\pi(2^j-k)}{2^j}|)^2}$$

$$= I^1_{j,2^j-k,\beta,\alpha}.$$

We have for $0 \leq \theta \leq \frac{\pi}{2}$:

$$\sin\theta\omega_{\alpha,\beta}(\cos\theta) = \sin\theta(2\sin^2(\theta/2))^\alpha(2\cos^2(\theta/2))^\beta \leq c_1\theta^{2\alpha+1},$$

and

$$\omega_{\alpha,\beta}(2^j;\cos\theta) = (2\sin^2(\theta/2) + 2^{-2j})^{\alpha+1/2}(2\cos^2(\theta/2) + 2^{-2j})^{\beta+1/2} \geq c_2\theta^{2\alpha+1}.$$

Thus

$$I^1_{j,k,\alpha,\beta} \leq c2^j \int_0^{\frac{\pi}{2}} \frac{d\theta}{(1+2^j|\theta - \frac{\pi k}{2^j}|)^2} \leq c \int_0^{\frac{\pi 2^j}{2}} \frac{d\theta}{(1+|\theta - \pi k|)^2} \leq C,$$

since $\int_{-\infty}^{+\infty} \frac{d\theta}{(1+\theta)^2}$ is finite, and the same goes for $I^2_{j,k,\alpha,\beta}$.

Thus there exists $C(\alpha,\beta) > 0$ such that for all (j,k): $I_{j,k,\alpha,\beta} \leq C(\alpha,\beta)$, which completes the proof of the lemma.

$\square$

Chapter 5

A classification of various estimation methods for inverse problems, illustrated by the Wicksell's problem

Abstract: The main purpose of this chapter is to describe various well known estimation methods for linear inverse problems by the means of two general principles, that we will name "Inversion-Denoising" and "Denoising-Inversion". Through this common description we highlight in particular the advantages of a second generation wavelet approach for inverse problems, in the case of compact operators with standard polynomial ill posedness. For such models SVD methods are appealing, but possess some limits that one may try to circumvent thanks to wavelet techniques. However because of their connections to Fourier analysis, such methods are not always easy to handle for some operators. In between the two techniques, one may wish to decompose in a localized, but also operator dependent basis consisting of either first or second generation wavelets. In a second part of the paper we give an illustration of the main points discussed in the first section by considering the well known Wicksell's problem. We recall the main methods used in this model and we give the theoretical properties of the second generation wavelet estimator "NeedVD". Then we make a simulation study of this procedure in the original density estimation problem.

5.1   Motivation

We consider the problem of recovering a function f from a blurred (by a linear operator) and noisy version: $Y = Kf + \varepsilon\xi$, where ξ is a white noise and where the problem is ill posed, with an unbounded (or non existent) operator K^{-1}. The purpose of this Chapter is give an overview of various estimation methods for these problems, through one common framework consisting in the choice of three parameters (at the cost of changing the presentations of the methods in the papers where they have been introduced.)

Moreover focusing on a new method, we pay particular attention to compact operators with standard ill posedness (ie with polynomial decrease of the singular values) and we wish to highlight the advantages of a operator based wavelet approach which finds applications in two kinds of models, that we will name Fourier type models and polynomial type models. Estimation procedures following this approach have been given in Chapter 3 (the Needvd procedure), and we try to put their ideas in parallel to the well known wavelet vaguelette decomposition estimator which was the pioneering wavelet method in inverse models introduced in Donoho [35].

The vaguelette approach consists in investigating under which conditions decompositions on standard wavelet basis can give rise to simple inversion schemes. Thus the procedure obtained is generally easy to handle if the operator at hand has well known Fourier characteristics (see examples in Kolaczyk [60]), as wavelet constructions are often based on Fourier analysis considerations (see Härdle et al. [49]). Moving away from the Fourier situation by considering for example polynomial type inverse models, an operator-based wavelet algorithm can present an interesting alternative. So we will pay particular attention to these problems, treated by the NeedVD procedure by using frames which are built directly upon the operator.

The principle of this new approach can be described very simply as follows. First let us recall the most well known technique, ie the Singular Value Decomposition (SVD) estimator where one expands f in an orthonormal basis e of eigenfunctions of K^*K:

$$f = \sum_{i\in\mathbb{N}} c_i e_i, \quad c_i = (f, e_i),$$

then one obtains estimators of the coefficients by decomposing the noisy observed function in the eigenfunctions g_i of KK^*, which involves singular values b_i:

$$\widetilde{c}_i = \frac{(Y, g_i)}{b_i} = c_i + \varepsilon\frac{(\xi, g_i)}{b_i}.$$

Then one performs some filtering on $\widetilde{c}$ so as to eliminate as much noise as possible.

A major drawback of the SVD estimators is that when the basis is not adapted to the target, numerous coefficients are needed to approximate that function properly. Then, since in ill posed problems gaussian noise with increasing amplitude contaminates the coefficients $\widetilde{c}$, it is not easy to recover high order coefficients for which one cannot efficiently discriminate between the signal and the noise.

To avoid this limitation, a natural idea is to reorganize the SVD expression in a localized frame (ψ_j) characterized by a set of coefficients $\gamma_{i,j} = (\psi_j, e_i)$:

$$f = \sum_{i \in \mathbb{N}} (f, e_i) e_i = \sum_{i \in \mathbb{N}} (f, e_i) \sum_j \gamma_{i,j} \psi_j = \sum_j (\sum_{i \in \mathbb{N}} \gamma_{i,j}(f, e_i)) \psi_j.$$

Then the SVD yields simple estimators of the coefficients d_j of f in the frame:

$$\widetilde{d}_j = \sum_{i \in \mathbb{N}} \frac{\gamma_{i,j}(Y, g_i)}{b_i},$$

which contain noise with amplitudes:

$$\mathbb{E}|\widetilde{d}_j - d_j|^2 = \sum_{i \in \mathbb{N}} \left(\frac{\gamma_{i,j} \varepsilon}{b_i} \right)^2.$$

So the main idea is to find a construction scheme γ which:

- is simple to compute in practice,

- yields a sufficiently localized frame,

- gives rise to a suitable control of the errors given above, in a noisy ill posed setting.

If such a construction exists, then we recover an approximation of f with coefficients corrupted by noise of the same order of amplitude than in the SVD decomposition, but this time with a parsimonious representations for a wide variety of target functions f. So it is much easy to denoise such a preliminary approximation, by using wavelet-type thresholding techniques.

Constructions of such frames have been developed for two simple cases, generating estimators optimal in wide minimax settings: the case when the basis e consists of the Fourier basis (see Chapter 6), and the case when it consists of the Jacobi polynomial basis (see Chapter 3 and 4). Of course this approach has strong connections to the various wavelet methods for inverse problems. However the frame is built upon a given preliminary given basis, and thus is not necessarily based on Fourier constructions: as a consequence one may use second generation wavelets, which do not possess a translation/dilatation structure.

Coming back to the general motivation, the chapter is organized as follows. In a first part we give an overview of several well known methods, by describing them through two general schemes for solving inverse problems. From this point of view, we draw first a comparison between SVD and wavelet methods, and then we distinguish three main approaches among wavelet procedures.

In a second part we illustrate the main ideas given in the first section thanks to an application to Wicksell's corpuscule problem, which proves very interesting here as it can be represented by several complementary inverse models. We also investigate the numerical performances of the operator based wavelet estimator in this model by performing a simulation study in the standard density formulation of the problem.

5.2   Classification of several methods of estimation in inverse models

Suppose $\mathbb{H}$ and $\mathbb{K}$ are two Hilbert spaces and let $K : \mathbb{H} \mapsto \mathbb{K}$ be an injective linear operator. The standard linear ill-posed inverse problem consists in recovering a good approximation f_ε of the solution f of

$$g = Kf$$

when only a perturbation Y_ε of g is observed. In this paper, we will consider the case when this perturbation is an additive stochastic white noise. Namely, we observe Y_ε defined by the following identity:

$$Y_\varepsilon = Kf + \varepsilon \xi, \tag{5.1}$$

where ε is the amplitude of the noise and ξ is a $\mathbb{K}$-white noise, i.e. for any $g, h \in \mathbb{K}$, $\xi(g) := (\xi, g)_\mathbb{K}$, $\xi(h) := (\xi, h)_\mathbb{K}$ form random Gaussian vectors (centered) with marginal variance $\|g\|_\mathbb{K}^2$, $\|h\|_\mathbb{K}^2$, and covariance $(g, h)_\mathbb{K}$ (with the obvious extension when one considers k functions instead of 2). Equation (5.1) means that for any $g \in \mathbb{K}$, we observe $Y_\varepsilon(g) := (Y_\varepsilon, g)_\mathbb{K} = (Kf, g)_\mathbb{K} + \varepsilon \xi(g)$, where $\xi(g) \sim N(0, \|g\|^2)$, and $Y(g)$, $Y(h)$ are independent random variables for orthogonal functions g and h. Two problems are intertwined here, namely inversion and denoising. Thus two strategies are possible: either invert first and then denoise, or vice versa. This is performed on a matrix representation of the inverse problem.

The inversion-denoising strategy is the most widespread one, and uses the following methodology.

Definition 2. *Inversion-Denoising Method (IDM): First, we choose a basis u_j of $\mathbb{H}$, usually an orthonormal basis, and decompose the target function in it: $f = \sum c_j u_j$. We estimate the coefficients c_j of f by the following procedure.*

- *(i) First choose a set of functions v_i of $\mathbb{K}$, and perform an inversion as if the observations $y_i := (Y, v_i)_\mathbb{K}$ contained no noise. Namely determine $\widetilde{c}$ satisfying:*

$$y_i = \sum_{j \in J_\varepsilon} (Ku_j, v_i) \widetilde{c}_j, \quad \forall i \in I_\varepsilon,$$

  where $I_\varepsilon \subset I$ and $J_\varepsilon \subset J$ are suitably chosen sets of indexes.

- *(ii) In fact the observations y_i are corrupted by noise $\xi_i := \xi(v_i)$:*

$$y_i = \sum_j (Ku_j, v_i) c_j + \varepsilon \xi_i.$$

  Thus one tries in a second step to filter the coefficients $\widetilde{c}$ thanks to a sequence of weights $\lambda = (\lambda_j)_{j \in \mathbb{N}}$ which yields more accurate coefficients $\hat{c}$:

$$\hat{c}_j = \lambda_j \widetilde{c}_j.$$

Coming back to the functional framework we obtain an estimator $\hat{f}$ of f:

$$\hat{f} = \sum \hat{c}_j u_j.$$

Given a basis u, the procedure is characterized by the choice of v to perform the inversion in (i), and of λ to perform the denoising in (ii). Two motivations generally guide the choice of the functions v. First one may wish to have a simple inversion problem (i) by diagonalizing the problem choosing $v = (K^*)^{-1}(u)$ (if this is possible), which yields: $y_k = c_k + \varepsilon \xi_k$. Secondly so as to have a simple denoising problem (ii) one may choose v such that the structure of the noise ξ_k is simple, which is for example the case if v consists of orthogonal functions with easily controllable norms in $\mathbb{K}$.

Concerning the filter λ, which can be either linear, or non linear (for wavelet techniques in particular), the main concern is to the shrink the most noisy coefficients $\widetilde{c}$. Thus it consists of weights adapted to the heteroscedasticity of the noise, whose amplitude tends to increase for high frequency coefficients as will be seen later.

A second strategy is to denoise first and then perform the inversion.

Definition 3. *Denoising-Inversion Method (DIM):* *First we choose an orthonormal basis (v_i) of $\mathbb{K}$ where we decompose the observations $Y = \sum y_i v_i$, with $y_i = (Y, v_i)_{\mathbb{K}}$. Then we follow the two steps:*

- *(i) The sequence $(y_i)_{i \in \mathbb{N}}$ consists of the coefficients of Kf in v corrupted by white noise $\xi_i = \xi(v_i)$: $y_i = (Kf, v_i) + \varepsilon \xi_i$, so we denoise them thanks to some filter $\lambda = (\lambda_i)_{i \in \mathbb{N}}$.*

- *(ii) Choose a basis u_j of $\mathbb{H}$, and estimate the unknown coefficients c_j of f in u by the solution $\hat{c}$ of the matricial equation:*

$$\lambda_i y_i = \sum_{j \in J_\varepsilon} (Ku_j, v_i) \hat{c}_j, \quad \forall j \in J_\varepsilon,$$

where $I_\varepsilon \subset I$ and $J_\varepsilon \subset J$ are finite sets.

Then we obtain an estimator $\hat{f}$ of f:

$$\hat{f} = \sum \hat{c}_j u_j.$$

Compared to the first procedure, this is in some sense some dual strategy. An advantage is that the denoising is performed in the observation domain $\mathbb{K}$, and thus does not have to take heteroscedastic noise structures into account.

We now distinguish two families of methods according to the choice of the orthonormal basis made in the beginning of the procedure (ie u for inversion-denoising methods and v for denoising-inversion methods). In the first family there is one natural way to invert the problem, but numerous denoising methods which are rarely adaptive and which are not efficient in some cases. On the contrary the second family of methods uses a very simple and adaptive denoising technique, which is efficient for a wide set of target functions. But this time the inversion problem is more implied and gives rise to three methods as will be seen in the corresponding subsection.

5.2.1   Operator based decomposition

As already briefly mentioned in introduction, the most well known estimation procedure is based on the singular value decomposition of the operator K. This means that, if K is a compact operator, there exist two orthonormal bases $(e_j)_{j\in\mathbb{N}}$ in $\mathbb{H}$ and $(g_i)_{i\in\mathbb{N}}$ in $\mathbb{K}$, and a decreasing sequence $(b_j)_{j\in\mathbb{N}}$, $b_j \to 0$ if $j \to \infty$, such that

$$Ke_i = b_i g_i, \quad K^* g_i = b_i e_i,$$

where K^* is the adjoint of K. Note that $b_i > 0$ for all i under the injectivity hypothesis on K.

The method is best described as an IDM as the first step is to introduce two bases u and v, which are chosen so as to obtain a very simple sequential model. It consists first in expanding the unknown function in the basis $u = e$. Then in step (i) a natural choice for v is $v = (K^*)^{-1}(u) = (g_i/b_i)_{i\in\mathbb{N}}$, which at the same time yields a diagonal representation and a simple noise structure:

$$y_i = c_i + \varepsilon \xi_i,$$

where $\xi_i = \xi(g_i)/b_i$ are independent centered gaussian variables with variance: $E(\xi_i^2) = \frac{1}{b_i^2}$.

In this simple setting we have coefficients $\widetilde{c}_j = y_j$ containing high amplitude noise for large j, so in step (ii) one applies weights λ_j penalizing the most noisy coefficients. Numerous methods were developed, generally non adaptive ones:

- spectral truncation:

$$\begin{cases} \lambda_j & = 1 \quad \text{if } j \leq N, \\ \lambda_j & = 0 \quad \text{if } j > N. \end{cases}$$

- Tikhonov regularization:

$$\lambda_j = \frac{b_j^2}{b_j^2 + \alpha^2},$$

- Tikhonov-Phillips filters:

$$\lambda_j = \frac{1}{1 + (j/\alpha)^\beta}$$

- Pinsker filters:

$$\lambda_j = (1 - (j/\alpha)^\beta)_+,$$

    where $x_+ = \max(0, x)$.

These filters generally require to fit parameters (N, α, β) with respect to the regularity of the target function and on the ill posedness of the operator, by minimization of an upper bound of the risk of the estimator.

There exists also an adaptive method developed in Cavalier and Tsybakov [16] where the filter depends only on the data (y_i). We recall its construction as the estimator will be used later in the simulation study. The values of λ_k are constant for all $k \in I_j = [\kappa_{j-1}, \kappa_j - 1]$ with $\kappa_0 = 1$ and $\kappa_J = N + 1$:

$$\begin{cases} \lambda_k = \left(1 - \frac{\sigma_j^2(1+\Delta_j^\gamma)}{\|y\|_{(j)}^2}\right)_+ & \text{if } k \in I_j, \ j = 1, \dots J, \\ \lambda_k = 0 & \text{if } k > N, \end{cases}$$

with:

$$\|y\|_{(j)}^2 = \sum_{k \in I_j} y_k^2, \quad \sigma_j^2 = \varepsilon^2 \sum_{k \in I_j} b_k^{-2}, \quad \Delta_j = \frac{\max_{k \in I_j} b_k^{-2}}{\sum_{k \in I_j} b_k^{-2}}, \quad 0 < \gamma < 1/2.$$

For $\nu_\varepsilon \sim \max(5, \log\log(1/\varepsilon))$ and $\rho_\varepsilon = \frac{1}{\log(\nu_\varepsilon)}$, the blocs are given by:

$$\begin{cases} \kappa_j = 1 & \text{if } j = 0, \\ \kappa_j = \nu_\varepsilon & \text{if } j = 1, \\ \kappa_j = \kappa_{j-1} + \lfloor \nu_\varepsilon \rho_\varepsilon (1 + \rho_\varepsilon)^{j-1} \rfloor & \text{if } j = 2, \dots, J, \end{cases}$$

for a large enough J satisfying: $\kappa_J > \max\{m : \sum_{k=1}^m b_k^{-2} \leq \varepsilon^{-2}\rho_\varepsilon^{-3}\}$.

These SVD methods are very attractive theoretically and can be shown to be asymptotically optimal in many situations (see Mathé and Pereverzev [65] together with their non linear counterparts Cavalier and Tsybakov [16], Cavalier et al. [17], Tsybakov [88], Goldenshluger and Pereverzev [43], Efromovich and Koltchinskii [38]). Nevertheless the minimax framework is somehow restricted by the properties of the decomposition basis $u = e$: one can only establish rates measured by the L^2 loss and over regularity spaces which are expressed thanks to e, and thus to K. However the target function should not a priori be assumed to depend on the operator at hand. So in fact these methods perform well in general for functions displaying homogeneous variations, but difficulties appear when e is not adapted to the description of the function f. More precisely, the denoising is not as efficient as one could hope when the energy of f is scattered over a large number of coefficients c.

To illustrate this in practice, let us consider the example of a convolution operator, for which the SVD bases are the Fourier bases, and of the spatially inhomogeneous 'Bumps' target function given in figure 5.1. Then the coefficients of the coefficients are scattered on a large scale of frequencies. In the ill posed convolution problem (we took a polynomial ill posedness $\nu = \frac{1}{2}$ in figure 5.2) we only possess a noisy version of this spectrum, with a noise amplitude increasing with the frequency. Let us imagine that we can separate in $\widetilde{c}$ the true coefficients c and the errors (the white bars respectively on the left and right part of the figure). Then the smoothing, performed here with a Tikhonov filter, aims at reducing the noise coefficients as much as possible without reducing too much the largest coefficients of the true function. This gives rise to the coefficients $\hat{c}$ which are the sum of smoothed "true signal" and "noise" components represented by the black bars. However for such a widespread spectrum, some information was lost in the end, especially for high frequency components. As a result, the estimator is either a slightly smoothed version the true function (as is the case in the figure here), or slightly too noisy, depending on the adjustment of the parameters of the filter.

Thus in such situations it would more convenient to have sparse decompositions of the signals to be estimated.
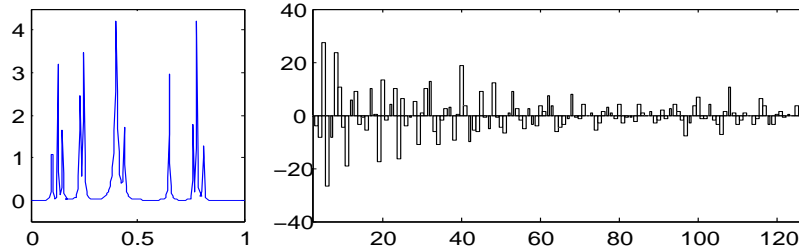
Figure 5.1:   The 'Bumps' function (left) and the real part of some of its Fourier coefficients (right)

5.2.2   Target based decomposition

So as to avoid the drawbacks of SVD methods, Donoho [35] proposed to use decompositions in wavelet bases. These are orthonormal bases which enable to represent a wide variety of functions by a parsimonious set of coefficients. Moreover these decompositions enjoy interesting localization (and thus L^p) properties, and can be easily linked to a wide class of regularity spaces, namely Besov spaces. Thus they appear as ideal tools in the context of inverse problems, yielding procedures that enjoy minimax rates in wider settings than for the SVD methods.

Indeed for example taking into account the Bumps function once again, we have the sparse representation given in figure 5.3 in an usual wavelet basis. So let us imagine an IDM with a situation similar to the one in figure 5.2, but this time in a wavelet case. Assume that we possess noisy versions $\widetilde{c}_{j,k}$ (j stands for resolution and k stands for time localization) of the wavelet coefficients c (left of the figure 5.4) plus gaussian noise (right of the figure 5.4) with an amplitude increasing with the resolution. Then one can denoise the coefficients $\widetilde{c}$ very efficiently by computing a threshold greater than most noise components (as shown on figure 5.4) and by keeping only the observed coefficients larger than this threshold. Then most of the noise is filtered and at the same time the local variations of the function are recovered by the estimator.

However, in this figure we exposed only the denoising step of the wavelet procedure, as the inversion step is more involved: in fact figure 5.4 has only an illustrative purpose as it was not drawn from the same experiment as figure 5.2. It may represent some ideal case for wavelet methods, and the closeness to this situation depends on whether v can be chosen such that we have a simple inversion step along with controllable errors on $\widetilde{c}$. However this time the choice of the matrix representation to perform the inversion is more implied. One can distinguish three strategies, depending somehow on the degree of diagonalization of the sequential model.

Vaguelettes methods

Wavelet methods for inverse problems were introduced by Donoho [35] with the well known wavelet-vaguelette decomposition (WVD) procedure. This method follows the inversion-denoising principle where:

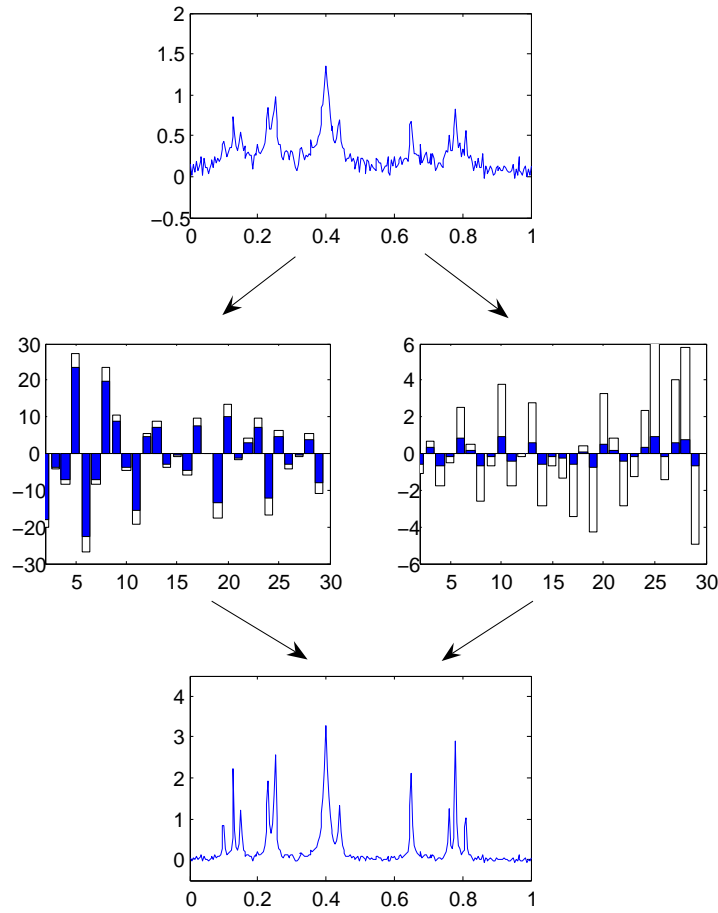- $(u_{j,k}) = (\psi_{j,k})$ where $\psi_{j,k}$ is an usual wavelet basis,

Figure 5.2: Top: A noisy version of a convolution of Bumps; Middle: in white, the coefficients c of Bumps (left) and the SVD errors $\widetilde{c} - c$ (right), and in black the effects of a Tikhonov filtering; Bottom: the SVD estimator obtained using the smoothed coefficients $\hat{c}$

- $v_{j,k} = (K^*)^{-1}(u_{j,k})$ so as to diagonalize the sequential model,

- The weights are given (among other possibilities) by hard thresholding rules:

$$\begin{cases} \lambda_{j,k} = 1 & \text{if } |\widetilde{c}_{j,k}| > t_{\varepsilon,j} \text{ and } j \leq J_\varepsilon, \\ \lambda_{j,k} = 0 & \text{in the other cases}, \end{cases}$$

with an adaptive choice of $t_{\varepsilon,j}$ and J_ε.

A kind of "dual" method was introduced by Abramovich and Silverman [1], who use a vaguelette-wavelet decomposition (VWD) procedure, which is an DIM with:

- $(v_{j,k}) = (\psi_{j,k})$ an usual wavelet basis,

- The weights are given by:

$$\begin{cases} \lambda_{j,k} = 1 & \text{if } |\widetilde{c}_{j,k}| > t_\varepsilon \text{ and } j \leq J_\varepsilon, \\ \lambda_{j,k} = 0 & \text{in the other cases}, \end{cases}$$
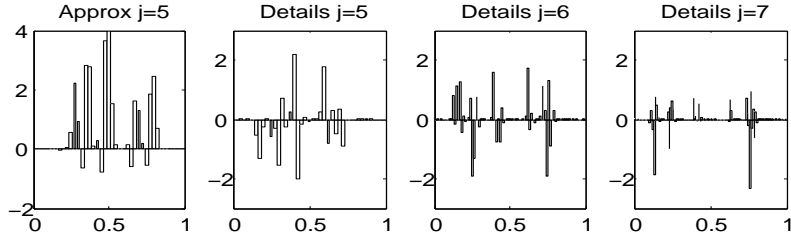
Figure 5.3:   The coefficients of Bumps in a Daubechies wavelet basis for every resolution level and localization parameter

- $u = (K^*)^{-1}(v)$.

Note that the VWD uses an homoscedastic filter, ie based on uniform thresholds t_ε, whereas WVD requires heteroscedastic thresholds $t_{\varepsilon,j}$ since the denoising is performed in the solution domain.

Of course these methods are only valid under hypotheses on the operator K. The price to pay for the simplicity of the inversion is that the noise structure of the sequential model is a bit complicated, as it depends on the properties of the diagonalization bases. Let us focus on WVD where $v = (K^*)^{-1}(\psi_{j,k})$ for WVD. Investigating the conditions required, the decompositions are valid in the functional setting if v forms a Riesz basis up to normalizations $\beta_{j,k} = \|(K^*)^{-1}(\psi_{j,k})\|_2$. This is true if the functions $(v_{j,k}/\beta_{j,k})$ enjoy vaguelette (ie weak wavelet) properties, hence the name of the method. Moreover minimax results can be obtained with easily described thresholding rules if these norms are homogeneous, ie: $\beta_{j,k} \asymp 2^{\nu j}$ for some $\nu > 0$.

Then minimax rates were established for WVD and VWD for the $L^2(dx)$ norm over Besov regularity spaces $B^s_{\pi,r}$ for thresholding rules of the kind:

$$t_\varepsilon = \kappa(\nu)\varepsilon\sqrt{\log\frac{1}{\varepsilon}},$$

$$t_{\varepsilon,j} = \kappa(K,\psi)2^{\nu j}\varepsilon\sqrt{\log\frac{1}{\varepsilon}}.$$

Note that in WVD the derivation of the constant κ must be done specifically in each case by determining an optimal upper bound of the L^2-norms of the vaguelettes, thus as indicated it has to be fitted according to K and ψ. Several examples were examined in Donoho [35] and Kolaczyk [60]. This is the main reason why WVD may be uneasy to describe, or to apply, for some operators whose action on usual wavelet bases is not well known. Most often the operators are required to be easily described from the Fourier analysis point of view.

In fact usual applications of the vaguelettes methods concern mainly homogeneous operators, or otherwise inhomogeneous convolution operators. Let us make some comments on these two categories of models, as compared to the SVD assumptions. First let us notice that the homogeneity assumption is generally incompatible with the cases treated by SVD
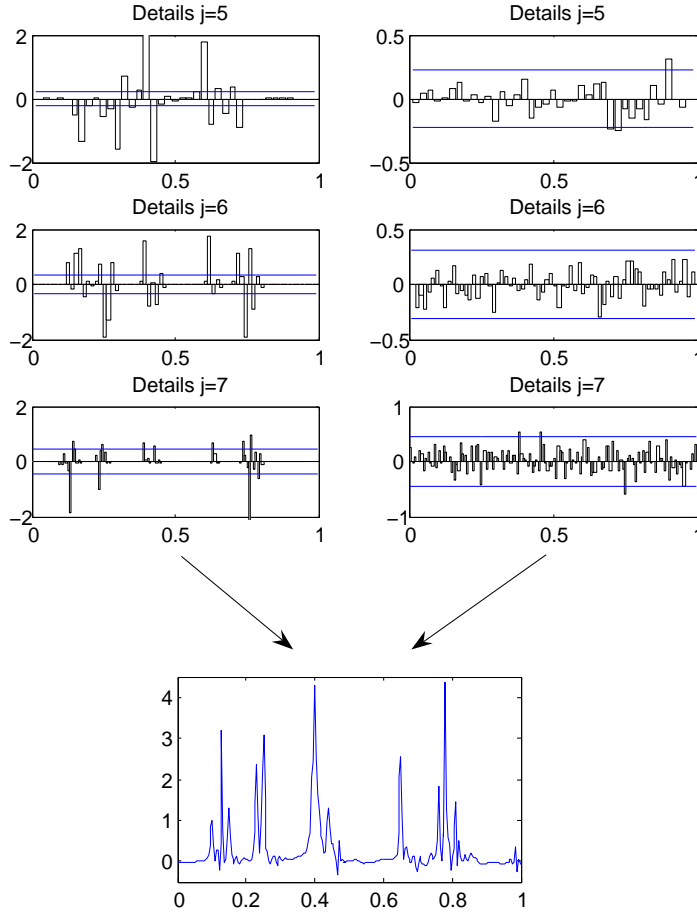
Figure 5.4: Coefficients $\tilde{c}$ as the sum of the wavelet coefficients c (left), plus gaussian noise (right), along with resolution dependent thresholds (horizontal lines); Bottom: the wavelet estimator obtained using the thresholded coefficients $\hat{c}$

methods. Indeed for example let us assume that $\mathbb{K} = \mathbb{H} = \mathbb{L}^2(dt)$, $f \in \mathbb{K}$ and K is an homogeneous operator of order $\nu \neq 0$. Then for $a > 0$ let $f_a(t) = f(at)$, $\forall t \in \mathbb{R}$ we have:

$$\frac{\|K(f_a)\|}{\|f_a\|} = a^\nu \frac{\|K(f)\|}{\|f\|},$$

so the operator is not bounded and the SVD relations given previously cannot hold.

Secondly focusing on compact operators, for which a convenient characterization of the ill-posedness is obtained by analysing the singular values (eg the standard hypothesis $b_i \asymp i^{-\nu}$), WVD can easily be applied if the functions $K\psi_{j,k}$ are vaguettes, up to homogeneous constants. However this hypothesis is difficult to check in general. For example concerning the homogeneity of the norms $\|K\psi_{j,k}\|^2$ we need for all (j,k):

$$\sum_{i \in \mathbb{N}} i^{-2\nu} |\langle \psi_{j,k}, e_i \rangle|^2 \asymp 2^{-2\nu j}.$$

For Fourier type models (ie if e is the Fourier basis) such as convolution models, this can be satisfied since the construction of wavelets is strongly connected to Fourier analysis.

For example Meyer and Daubechies wavelets are easily managed in the Fourier domain. Nevertheless little can be said for more general bases e.

Wavelet Galerkin methods

As established in Dicken and Maass [27], the WVD procedure can be seen as a particular Galerkin projection method. In the same domain Cohen et al. [24] proposed two other wavelet Galerkin methods, especially with a view to treating inverse problems with operators which are difficult to handle numerically. In such cases one can not resort to vaguelettes or singular functions which are too complicated to determine.

The methods are designed for self-adjoint positive operators, but with a natural extension to more general operators. The first procedure is non adaptive and uses an DIM methodology similar to the VWD, with the same choice of v and λ. The only difference is the inversion step (ii) in 3: one chooses $(u_{j,k}) = (\psi_{j,k})$ (just like v) instead of the vaguelettes. Then a matrix inversion has to be performed, corresponding to the system:

$$\lambda_{j,k} y_{j,k} = \sum_{j' \leq J_\varepsilon, k'} (K\psi_{j',k'}, \psi_{j,k})\hat{c}_{j',k'}, \quad \forall j \leq J_\varepsilon,$$

where J_ε depends on the regularity of the function f. In the end the estimator is the same as VWD, only with the vaguelettes $K^{-1}(\psi_{j,k})$ replaced by their Galerkin approximations in $Span\{\psi_{j,k}, \quad j \leq J_\varepsilon\}$.

The second procedure is adaptive, with the same choices as the first procedure for v, λ and u, but with a different inversion method: instead of inverting the matrix (which is very expensive when J_ε is chosen adaptively) one uses an algorithm combining in each iteration an inversion step consisting in a gradient correction, with a denoising step in the solution domain thanks to an heteroscedastic wavelet thresholding rule.

Under an ellipticity hypothesis on the operator, the two estimators have convergence rates for L^2 norms and Besov regularity spaces $B_{p,p}^s$, where p depends on s. In practice they allow to treat problems where WVD and SVD could not be applied. Thus, just like WVD as compared to SVD, they find specific applications outside of the scope of former methods.

Operator based wavelets

In WVD the main concern has been somehow to check under which conditions the wavelet thresholding procedure, which has proved very efficient in the case of direct observation (ie when K is the identity), could be easily extended to the case of more complex problems with ill posed K. One may adopt a slightly different point of view. Considering a given operator K, can one find an interesting decomposition basis such that a procedure similar to wavelet thresholding could be applied? From this point of view, let us now describe an operator-based wavelet procedure. It was already introduced in the SVD framework at the beginning of the chapter, now we wish to present it in a wavelet perspective.

We focus on compact operators with polynomial ill posedness of degree ν. The procedure consists in a technique similar to the WVD while aiming at avoiding its limitations in such a framework. We use an IDM where ones allows more flexibility in the choice of the basis,

which is not necessarily required to be a classical wavelet, but only to enjoy interesting concentration properties. So it will still possess some "frequency/time" structure, and we keep denoting $(u_{j,k}) = (\psi_{j,k})$. The main difference with WVD then stems from the choice of v for the sequential model. Indeed the IDM uses the three following parameters described hereafter:

- $(u_{j,k}) = (\psi_{j,k})$,

- $(v_i) = (g_i)$, ie the second SVD basis,

- and the filter is

$$\begin{cases} \lambda_{j,k} = 1 & \text{if } |\widetilde{c}_{j,k}| > t_{\varepsilon,j} \text{ and } j \leq J_\varepsilon \\ \lambda_{j,k} = 0 & \text{in the other cases.} \end{cases}$$

As in other wavelet methods the starting point is a decomposition in functions $(u_{j,k}) = (\psi_{j,k})$, localized in frequency and in time (but this time in an "operator-based" sense as seen later) so as to take advantage of the sparse representation of signals as detailed earlier. We will see later how the functions need to be chosen, for the moment they are only assumed to be a tight frame. This means that the two following properties are satisfied for all $f \in \mathbb{H}$:

$$f = \sum_{j \in \mathbb{N} \eta \in \mathbb{Z}_j} \langle f, \psi_{j,k} \rangle \psi_{j,k},$$

$$\|f\|^2 = \sum_{j \in \mathbb{N} k \in \mathbb{Z}_j} |\langle f, \psi_{j,k} \rangle|^2.$$

In comparison to the WVD strategy, the choice of v gives rise to a less simple relation between the observations y and the coefficients $\widetilde{c}$, but on the other hand we have a simpler noise structure. Still the inversion remains easy as one can check that, under the frame hypothesis, a solution is given by:

$$\widetilde{c_{j,k}} = \sum_i \frac{y_i}{b_i} (\psi_{j\eta}, e_i).$$

Just as in WVD, a simple thresholding algorithm will enable to denoise efficiently these coefficients under an homogeneity condition on their errors. Indeed let us assume that for all (j,k):

$$\sum_i [\frac{\psi_{j,k}^i}{b_i}]^2 \leq C 2^{2j\nu}, \tag{5.2}$$

then one can use an heteroscedastic non linear filter, with thresholds:

$$t_{\varepsilon,j} = \kappa(K) 2^{\nu j} \varepsilon \sqrt{\log \frac{1}{\varepsilon}},$$

for all $j \leq J_\varepsilon$ where $2^{J_\varepsilon} \asymp (\varepsilon \sqrt{\log \frac{1}{\varepsilon}})^{-\frac{2}{1+2\nu}}$.

So the crucial point in the procedure is to find a suitable frame satisfying condition 5.2, which requires that the coefficients of each $\psi_{j,k}$ in (e_i) be concentrated among the indexes of order $i \asymp 2^j$. This is true if, for some constants C_1, C_2:

$$\{i : \psi_{j\eta}^i \neq 0\} \subset \{C_1 2^j, \ldots, C_2 2^j\}. \tag{5.3}$$

Answers to this question can be given in two situations.

Application in two types of inverse models:

Suppose we have an inverse problem given by 3.2 with an operator K admitting a singular value decomposition. Let us define the two following models:

Definition 4.   • **_Fourier type model:_** $\mathbb{H}$ *is the space of 1-periodic functions with restrictions to* $[0,1]$ *belonging to* $L^2([0,1], dx)$, *and the SVD basis* e *of the operator consists of the Fourier basis:* $e_k(x) = \exp(i2\pi kx)$,

• **_Jacobi type model:_** $\mathbb{H} = L^2([-1,1], \mu)$ *with (up to a normalization constant)* $d\mu(x) = (1-x)^\alpha(1+x)^\beta$ *where* $\alpha, \beta > -1/2$, *and the SVD basis* e_k *of the operator consists of the Jacobi polynomials of degree* k *and of type* (α, β), *normalized in* $L^2(d\mu)$ *(see Szegő [86] for details).*

In the first case, it is very easy to find classical wavelet bases directly satisfying condition 5.3. The procedure can be implemented using for example the Meyer wavelet (Meyer [69]): for the deconvolution model, this is the WaveVD algorithm (Johnstone et al. [53]). Furthermore a quantity of other first generation wavelet techniques, including WVD, can also be used for deconvolution (see Chapter 6).

Searching for orthonormal wavelet bases in the second situation, several constructions have been proposed in the literature. However as far as we know they do not give rise to bases enjoying satisfying L^p-norm properties. Thus it seems necessary to resort to families possessing only the property of wavelets which is essential in our framework, namely a strong enough concentration property. As presented in Chapter 3, this is true for the "needlets" which are some kind of second generation wavelets. Unlike usual wavelets, they are neither orthonormal nor independent as they only form a tight frame of $\mathbb{H}$, and the shape of the function varies with respect to the time localization.

Details on the construction of the needlets are given in Chapter 3, let us just briefly recall the two main steps which are the frequency and the time decomposition of the Hilbert space $\mathbb{H}$. First the "frequency" discretization is performed thanks to the following family of operators:

$$\Lambda_j = \sum_{k \geq 0} a^2(k/2^j) L_k,$$

where L_k denotes the orthogonal projector on the SVD function e_k and a is a C^∞ function supported in $[-2, -\frac{1}{2}] \cup [\frac{1}{2}, 2]$ such that

$$\sum_{j \geq 0} a^2(\xi/2^j) = 1, \quad \forall |\xi| \geq 1.$$

Then For all $f \in \mathbb{H}$, one can show that:

$$f = L_0(f) + \sum_{j=0}^{\infty} \Lambda_j(f) \quad \text{in } \mathbb{H}.$$

Note that here the notion of frequency is not related to Fourier analysis, but is in some sense an "operator" frequency as it depends on the SVD of the operator.

Second, a quadrature formula is used so as to introduce a time localization (however not uniformly on the interval, but at the zeros η_k of a Jacobi polynomial). Thus we obtain for all f and j:

$$\Lambda_j f(x) = \sum_k (f, \psi_{j,\eta}) \psi_{j,k}(x).$$

where $\psi_{j,k}$ (the needlets) depend on the Jacobi polynomials e_l in the following way, involving quadrature weights $b_{j,k}$:

$$\psi_{j,k} = \sum_{l \in \mathbb{N}} a(l/2^{j-1}) e_l(x) e_l(\eta_k) \sqrt{b_{j,k}}.$$

Given the support of a, we have

$$\psi_{j,k} = \sum_{l=2^{j-2}+1}^{2^j-1} \gamma_{j,k,l} e_l(x),$$

with coefficients $\gamma_{j,\eta_k,l} = a(l/2^{j-1}) e_l(\eta) \sqrt{b_{j,\eta}}$. Then the needlets satisfy condition 5.3.

Remark 5.2.1. *In some sense, the adaptive SVD estimator developed in Cavalier and Tsybakov [16] uses the same kind of "operator based" frequency discretization as one pays interest to the components of f corresponding to the family of operators $\Lambda_j^{SVD} = \sum_{k \in I_j} L_k$, where (I_j) is the partition of $\mathbb{N}$ in blocs, as recalled in the section on the SVD methods. In a noisy setting, each estimated component of f in this decomposition is smoothed according to the level of noise it contains.*

However in the second generation wavelet approach, the frequency discretization consists in a smoothed sum of projectors on the elements of the SVD basis, and thus the family of operators Λ_j have overlapping ranges with respect to this basis. Moreover in a noisy setting, we have a filter functional depending only on the resolution like in the SVD, but which generates for each j a whole family of weights $\lambda_{j,k}$ adapted to the time discretization within each frequency level.

Grouping the Fourier and Jacobi models together, the procedure enjoys the following minimax properties. Let $f \in \mathbb{H}$ have the following representation in the family $\psi_{j,k}$:

$$f = \sum_{j \geq -1} \sum_{\eta \in \mathbb{Z}_j} c_{j,k} \psi_{j,k},$$

with:

$$c_{j,k} = (f, \psi_{j,k})_{\mathbb{H}}.$$

Then for $\pi \geq 1$, $s \geq 1/\pi$, $r \geq 1$, we define the space $B^s_{\pi,r}(M)$ by:

$$\|f\|_{B^s_{\pi,r}} := \|(2^{js}(\sum |c_{j,k}|^{\pi}\|\psi_{j,k}\|_{\pi}^{\pi})^{1/\pi})_{j \geq -1}\|_{L^r} < \infty, \quad \text{and}$$

$$f \in B^s_{\pi,r}(M) \iff \|f\|_{B^s_{\pi r}} \leq M.$$

Theorem 14. *Let $1 < p < \infty$, and assume $b_i \sim i^{-\nu}$, $\nu > 0$. Let the thresholds $t_{\varepsilon,j}$ be given as described previously, with κ larger than a constant depending on p and on the operator K of the inverse problem. Then for some parameters α' and β' depending on the type of model, and given just after the theorem, we have:*
$\forall f \in B^s_{\pi,r}(M)$ *with* $s > \max_{\gamma \in \{\alpha',\beta'\}}\{\frac{1}{2} - 2(\gamma+1)(\frac{1}{2} - \frac{1}{\pi}) \vee 2(\gamma+1)(\frac{1}{\pi} - \frac{1}{p}) \vee 0\}$:

$$\mathbb{E}\|\hat{f} - f\|_p^p \leq C[\log(1/\varepsilon)]^{p+1}\varepsilon^{\mu p},$$

with $\varsigma = \min\{\varsigma(s), \varsigma(s,\alpha'), \varsigma(s,\beta')\}$ *where:*

$$\varsigma(s) = \frac{s}{s + \nu + \frac{1}{2}},$$

$$\varsigma(s,\gamma) = \frac{s - 2(1+\gamma)(\frac{1}{\pi} - \frac{1}{p})}{s + \nu + 2(1+\gamma)(\frac{1}{2} - \frac{1}{\pi})}.$$

In the case of Fourier type operators, the theorem holds with $\alpha' = \beta' = -\frac{1}{2}$ and the regularity space for the target is the ball of a Besov space. In the case of Jacobi type operators, we have $\alpha' = \alpha$ and $\beta' = \beta$, and the regularity space is some Besov-type space (see Narcowich et al. [72] for connections between needlets and Besov spaces). In each one of these cases, the exponents ς in the rates are optimal from the minimax point of view as established in Chapter 6 for Fourier models (with also the exact logarithmic factors) and in Chapter 4 for Jacobi models.

It is worth noting that these theoretical performances were established in a wide setting, as one considers risks measured in all the L^p norms in the solution domain and over general "Besov type" regularity spaces $B^s_{\pi,r}$.

Generalizations to other situations

Only the Fourier and Jacobi type inverse models have been inquired in detail so far. However it is worth noting that the needlets can be built upon many other bases than Jacobi polynomials, such as other polynomial families (Petrushev and Xu [81]), spherical harmonics (Narcowich et al. [71], with applications to the study of the Cosmic Microwave Background Baldi et al. [9]), or the Fourier basis. Thus the scope of Needvd can probably be extended.

Furthermore it may be interesting to use the same estimation procedure with other second generation wavelets available in the literature. Secondly following the idea of Abramovich and Silverman [1] concerning the vaguelettes methods, one may try to develop "dual" methods for such procedures where the observed noisy function instead of the target would be decomposed in a localized basis adapted to the operator. Then minimax results would hold

in a narrower framework than for inversion-denoising techniques, but the thresholding would be simpler and the method would have other fields of application.

Moreover remark that the Legendre needlets show striking similarities to the Meyer wavelets used in Fourier type models, as can be seen in figure 5.5. Even though these two families are built upon specific bases, the end results are functions enjoying very interesting properties of approximation and localization. They enable to characterize wide functional spaces in a way the original bases could never hope to achieve. Thus, as might seem paradoxical, the aim of the operator-based wavelet approach is to build frames as distant as possible from the initial SVD basis, in terms of approximation properties. The frames must enjoy some universal properties, describing target spaces with no connection with the operator at hand.
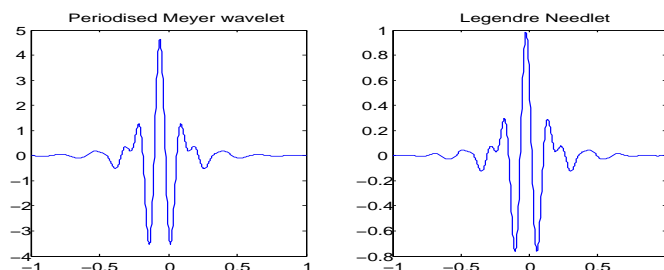
Figure 5.5: A periodized Meyer wavelet and a Legendre needlet

5.3 Application of NeedVD to the Wicksell's problem

This section has two main motivations. First we wish to illustrate the main points discussed in the first part of the paper, ie:

- the advantages of decompositions in localized bases over decompositions in singular bases,

- the complementarity of the fields of applications of the methods based on first generation wavelets, and those adapted to compact operators.

From this point of view, the well known Wicksell's problem is a very interesting inverse problem, as the original model can be turned either into a deconvolution type or into a polynomial type inverse problem. Thus, among wavelet methods, several first generation wavelet procedures can be used in the first case. On the contrary only the operator-based approach (here an adaptation of Needvd) can be used in the second case.

A second motivation here is to investigate the numerical performances of NeedVD in the original Wicksell's problem, which is in fact a density estimation problem, and not a white noise model of the type considered all through the first part of the chapter.

5.3.1   Estimation procedures for Wicksell's problem

Wicksell's corpuscule problem was introduced in Wicksell [91], and finds applications in medicine (see Nychka et al. [76]), as well as in numerous other contexts (biological, engineering, etc.) see for instance Cruz-Orive [25]. It corresponds to the following situation. Suppose a population of spheres is embedded in a medium as represented in figure 5.6. The spheres have radii that may be assumed to be drawn independently from a density f. A random plane slice is taken through the medium and the spheres intersected by the plane furnish circles which radii are the points of observation $Y_1, \ldots, Y_n$ which are independent identically distributed (iid). The unfolding problem is then to determine the density of the sphere radii from the observed circle radii.
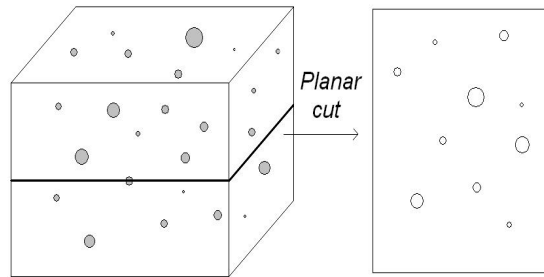
Figure 5.6: Wicksell's corpuscule problem

One generally assumes that the radii of the spheres have an upper bound, which can supposed to be equal to 1 without loss of generality. If the centers of the sphere are distributed with respect to a stationary Poisson point process then the density g of the discs radii depends on f through $g = Kf$, with:

$\mathbb{H} = \mathbb{K} = \mathbb{L}^2([0,1], dx)$ and $K : \mathbb{H} \mapsto \mathbb{K}$ is defined by: $\forall y \in [0,1]$

$$Kf(y) = \frac{y}{m} \int_y^1 \frac{f(x)}{(x^2 - y^2)^{1/2}} dx, \tag{5.4}$$

where $m = \int_0^1 x f(x) dx$.

Remark 5.3.1. *The factor m can be estimated by (see Hall and Smith [48]):*

$$\hat{m} = \frac{n\pi}{2} (\sum_l Y_l^{-1})^{-1}, \tag{5.5}$$

which enjoys an almost parametric convergence rate, so plugging it in the density estimators does not alter the rates of convergence. In the sequel we consider it as a constant and we treat K as a linear operator.

Focusing only on the density estimation (there are also other contexts), no minimax results for any kind of L^p-loss seem to have been established, as far as we know, directly in this model. However results have been found in a slightly transformed version of the problem, given hereafter.

Deconvolution model

Wicksell's problem can be turned into a deconvolution problem with a simple change of variables. If f_2 and g_2 denote respectively the densities of the squared radii of the spheres and of the discs, then $g_2 = K_2 f_2$ with:

$\mathbb{H} = \mathbb{K} = \mathbb{L}^2([0,1], dx)$ and $K_2 : \mathbb{H} \mapsto \mathbb{K}$ is defined by: $\forall y \in [0,1]$

$$K_2 f_2(y) = \frac{1}{m_2} \int_y^1 \frac{f_2(x)}{(x-y)^{1/2}} dx. \tag{5.6}$$

Several statistical procedures have been developed in this framework, enjoying explicit convergence rates. First concerning the problem of estimating the distribution function of the squared radii, minimax results can be found in Golubev and Levit [46] for risks measured with a wide class of loss functions. For the density estimation, Golubev and Enikeeva [45] also develop optimal estimators for the L^2 loss. Moreover first generation wavelet approaches can also be used: Antoniadis et al. [6] propose a non adaptive and an adaptive estimator, which are based on a wavelet decomposition combined with a Fourier deconvolution arguments. They obtained rates of convergence of the mean square error for an estimator of the density of the squared radii, when the function Kf has some Besov regularity. They also perform a simulation study of the estimator. Moreover vaguelettes techniques may also be used as in Champier and Grammont [20], but only if the radii are assumed to have no upper bound (which makes the operator homogeneous) and if the derivation of the thresholds and the computation of the vaguelettes is not too difficult. Otherwise one could also use Wavelet Galerkin techniques as mentioned in Cohen et al. [24].

However except of Antoniadis et al. [6], all these methods are designed for white noise perturbations. Whether the thresholding algorithm can be easily adapted to the density estimation framework needs further investigation. Indeed, as will be seen in the simulation study, the estimators may display heterogeneous variances incompatible with the homogeneous white noise thresholds. Moreover adapting the techniques by trying to estimate these variances is generally uneasy, as they depend on the wavelets is difficult way to handle (see for example Herrick et al. [51] for thresholding methods in the standard density estimation problem).

Jacobi type model

Lastly, Wicksell's problem can also be turned into a "Jacobi type" problem by using the following formulation.

Let

$\mathbb{H} = L^2([0,1], d\mu^*), \; d\mu^*(x) = (4x)^{-1} dx, \quad \mathbb{K} = L^2([0,1], d\lambda), \; d\lambda(y) = 4\pi^{-1}(1-y^2)^{1/2} dy.$

Then starting from f and g satisfying 5.4, let $f_3(x) = 4xf(x)$ and $g_3(y) = \frac{\pi}{4}(1-y^2)^{-1/2}g(y)$. Then f_3 and g_3 are respectively densities on $\mathbb{H}$ and $\mathbb{K}$, and are linked by: $g_3 = K_3 f_3$ with $K_3 : \mathbb{H} \mapsto \mathbb{K}$ defined for all $y \in [0,1]$ by:

$$K_3 f_3(y) = \frac{1}{m} \int_y^1 \frac{\pi}{4} y (1 - y^2)^{-1/2} \int_y^1 (x^2 - y^2)^{-1/2} f_3(x) d\mu^*(x). \tag{5.7}$$

Then Johnstone and Silverman [54] showed that this model admits a simple singular value decomposition, with the following SVD bases:

$$e_k(x) = 4\sqrt{2} x^2 P_k^{0,1}(2x^2 - 1)$$
$$g_k(y) = U_{2k+1}(y).$$

Here $P_k^{0,1}$ is the kth degree Jacobi polynomial of type $(0, 1)$ normalized in $\mathbb{L}^2([-1, 1], \mu)$ with $d\mu(x) = (1 + x)dx$ (we take another normalization than in Johnstone and Silverman [54]) and U_k is the second type Chebishev polynomial of degree k. Moreover the singular values are

$$b_k = \frac{\pi}{8}(1 + k)^{-1/2}.$$

Models 5.4 and 5.7 are closely linked, and unlike in model 5.6, first generation wavelet techniques do not seem very convenient for both of them. Considering for example vaguelettes methods, one can check that the operator K in the model 5.6 is not homogeneous either in frequency or in time. For example the image of an usual wavelet basis by K is not "wavelet-like" (figure 5.7), and the L^2-norms of the vaguelettes are not constant within each level (figure 5.8). Thus vaguelettes methods cannot be applied for the original model 5.4. Of course the situation is even worse for classical wavelets in model 5.7 where a non uniform weight has been introduced in the target space.
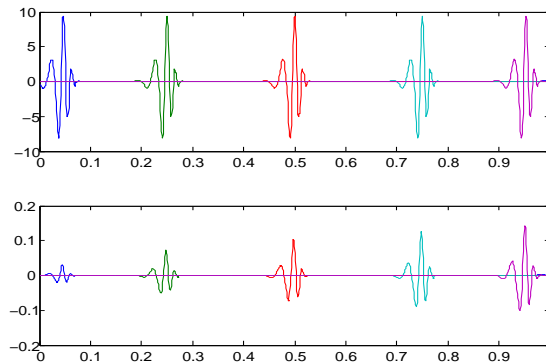

Figure 5.7: Top: several Daubechies wavelets with a fixed resolution level; Bottom: images of the wavelets by Wicksell's operator

On the contrary SVD and second generation wavelet methods based on polynomials can be used here. Then for white noise perturbations and for estimation errors measured in the $\mathbb{L}^2([0, 1], d\mu)$ loss, SVD estimators enjoy minimax rates over target spaces linked to the Jacobi polynomials, and NeedVD enjoys minimax rates over wide target spaces, as described previously.
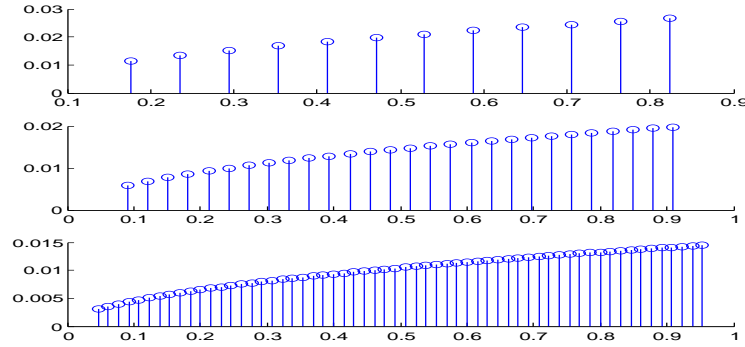
Figure 5.8: The $L^2(dx)$ norms of the images of several wavelets by Wicksell's operator, grouped by resolution level ($j = 4$ to $j = 6$ from top to bottom)

Let us examine more closely the theoretical performances of the NeedVD procedure, as the picture is a bit complicated for general L^p losses. It is based in fact on a preliminary estimator $\hat{f}_4$ of the function f_4 given by

$$f_3(x) = 4\sqrt{2}x^2 f_4(2x^2 - 1).$$

Then $\hat{f}_4$ enjoys optimal $L^p([-1, 1], \mu)$ rates $r(\varepsilon, \alpha, \beta, \nu, s, \pi, p)$, given by theorem 14 with $(\alpha, \beta, \nu) = (0, 1, 1/2)$, over Besov type regularity spaces $B^s_{\pi,r}$:

$$\sup_{f_4 \in B^s_{\pi,r}(M)} \mathbb{E}_{f_4} \int_{-1}^{1} |\hat{f}_4(y) - f_4(y)|^p (1 + y) dy \leq r(\varepsilon, \alpha, \beta, s, \pi, p).$$

Back to model 5.7 we use the estimator:

$$\hat{f}_3(x) = 4\sqrt{2}x^2 \hat{f}_4(2x^2 - 1).$$

Let us denote $e_4(y) = |\hat{f}_4(y) - f_4(y)|$ the estimation error on f_4 and $e_3(y)$ the error on f_3. We have:

$$\int_{-1}^{1} e_4(y)^p (1 + y) dy \asymp \int_{0}^{1} e_4(2x^2 - 1)^p x^3 dx \asymp \int_{0}^{1} e_3(x)^p x^{3-2p} dx,$$

so estimator we obtain has optimal rates in 5.7 for $p = 2$, and provide lower or upper bound results for the minimax risk in the other cases.

Interestingly the performances of NeedVD also yield information in the other settings, even though the noise structure is particular. For example in the standard model 5.4 where no minimax results have been established for the density setting (as far as we know) and $L^p(dx)$ losses, the estimator given by

$$\hat{f}_1(x) = \frac{\hat{f}_3(x)}{4x} = \sqrt{2}x\hat{f}(2x^2 - 1) \tag{5.8}$$

has errors linked to e_4, ie those of the initial NeedVD estimator $\hat{f}_4$, by the relation:

$$\int_0^1 e_1(x)^p x^{3-p} dx \asymp \int_{-1}^1 e_4(y)^p (1+y) dy,$$

so we obtain here an optimal estimator with $p = 3$, and information on the minimax risks in the other cases. In the next section we investigate the numerical performances of this estimator $\hat{f}_1$. The numerical performances in the white noise framework for model 5.7 were already studied in Chapter 3.

Our aim is to make a brief simulation investigation on whether Needvd can directly be applied in the density estimation setting. Comparison with other methods will be only made by investigating the behavior of Needvd in the the two models considered in Antoniadis et al. [6]. Of course a much more detailed investigation would be needed, both from the theoretical and the practical point of view. So a comparison of most wavelet and SVD methods mentioned previously is under study.

5.3.2   Simulation study of the NeedVD procedure

In this section we wish to apply the procedure to the standard model 5.4. First we give a few results in the white noise setting, then we turn to a more detailed study in the density model.

Preliminary algorithmic remarks

We recall the expression of the needlets in our case:

$$\psi_{j,k} = \sum_{l \in \mathbb{N}} a(l/2^{j-1}) P_l^{0,1}(x) P_l^{0,1}(\eta_k) \sqrt{b_{j,\eta_k}},$$

where η_k is the $k-th$ zero of $P_{2^j}^{0,1}$ and a is a function whose support is included in $[\frac{1}{2}, 2]$. As mentioned previously, one uses transformations of these needlets suited to the expression of the SVD basis e_i, but for the sake of simplicity we keep the same notation $\psi_{j,k}$ for this frame in the sequel.

Several possibilities can be used for a, but the resulting needlets do not depend drastically on this choice. In the simulations, we take an exponential shape function, then all the needlets are computed at a sufficiently precise grid and stored, along with their scalar products with the the first SVD basis:

$$(\psi_{j,k}, e_i) = a(i/2^{j-1}) P_i^{0,1}(\eta_k) \sqrt{b_{j,\eta_k}},$$

which are zero outside of $i \in \{2^{j-2} + 1, \ldots, 2^j - 1\}$.

Then the estimation procedure is implemented in various datasets: simulations are performed for different sample sizes, and using the four target functions represented in figure 5.9, which are densities on $L^2([01], dx)$.

Though the thresholds given in the first part of the chapter for the NeedVD estimator yield satisfactory theoretical (and practical) performances, one had better in practice try
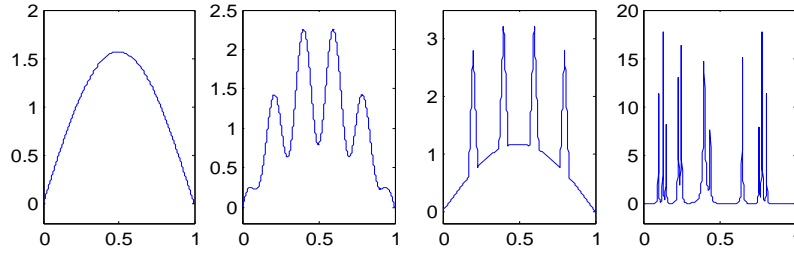
Figure 5.9: Target functions, taken as densities on $L^2([0,1], dx)$: Sine, Sine2, Sine3 and Bumps

to fit to the variance of the noise as precisely as possible. So we will use thresholds of the kind:

$$t_{j,k} = \kappa \sqrt{\frac{j \sum_{i \in \mathbb{N}} \left(\frac{(\psi_{j,k}, e_i)}{b_i}\right)^2}{n}}.$$

Note also that the singular values (b_i) include the estimator of the normalization constant for $K(f)$ given in 5.5.

White noise perturbations

We focus on the setting 5.4. First we investigate the performances of estimator $\hat{f}_1$, given by 5.8, if the perturbation is a white noise equivalent to the one of model 5.7. More precisely, discretizing the model in a large grid of equidistant points $(x_i)_{i=1...n}$, this model means basically that we observe the values $Kf(x_i)$ corrupted by independent centered gaussian variables ξ_i with an amplitude slightly decreasing near the right edge of the interval: $E(\xi_i^2) = (1 - x_i^2)^{1/2} n \varepsilon^2$. If $\sigma = n\varepsilon^2$ corresponds to a signal to signal to noise ratio $rsnr = 5$, figure 5.10 shows that we obtain satisfying results for the NeedVD estimator, as compared to the truncation SVD estimator with a non adaptive choice of the cutoff level, and to the bloc estimator of Cavalier and Tsybakov [16] which is recalled in the first section of the chapter.

These results are encouraging, as the target function seems to be well estimated by NeedVD all along the definition domain (except sometimes near the left edge of the interval) and this remains true for high noise. So the estimator may be robust with respect to the behaviour of the noise, and thus we investigate if an application to the density setting is possible.

Density estimation

We adapt the algorithm designed for the white noise setting to the density estimation model, where the noise amplitude ε is replaced by the number of observations n (with the parameter equivalence $\varepsilon = \frac{1}{\sqrt{n}}$). Then we use the following estimators of the coefficients:

$$\widetilde{c}_{j,k} = \frac{1}{n} \sum_{i \in \mathbb{N}, \, l=1,...,n} \frac{(\psi_{j,k}, e_i) g_i(Y_l)}{b_i},$$

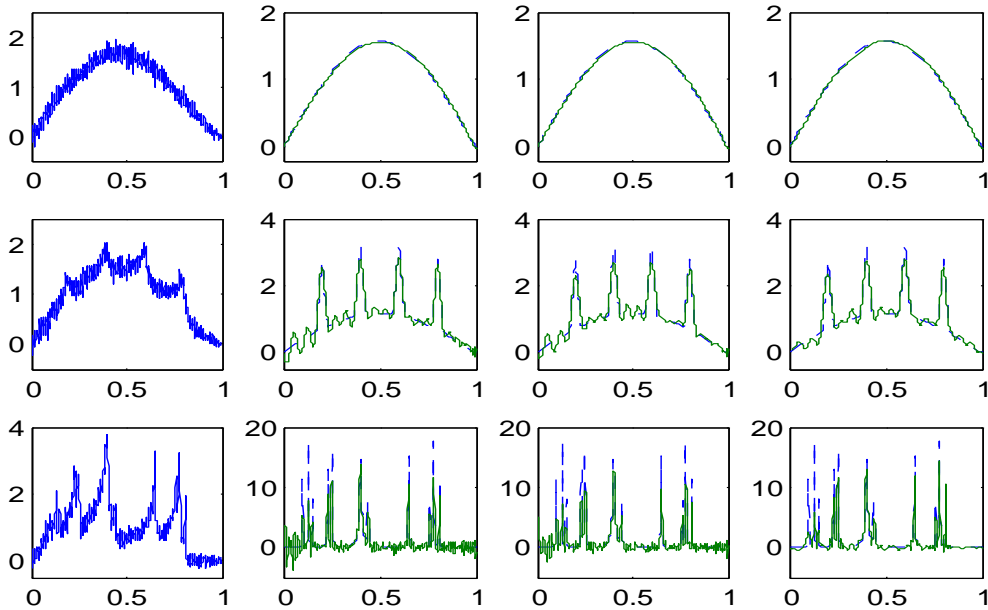and the filter is based on thresholds of the kind:

Figure 5.10: From left to right: blurred observed function, corrupted by white noise with $rsnr = 5$; truncation SVD estimator; adaptive SVD estimator; Adaptive NeedVD estimator, along with the true functions in dashed line

$$t_{j,k} = \kappa \sqrt{\frac{j \sum_{i \in \mathbb{N}} \left(\frac{(\psi_{j,k}, e_i)}{b_i}\right)^2}{n}},$$

but where κ may not be a universal constant, as scaling effects should be taken into account.

Applying this estimator, difficulties arise in fact whatever the scale parameter κ. Considering for instance samples of $n = 1000$ observations, it seems impossible to find a convenient constant κ enabling the procedure to discriminate the noise and the signal in relatively high resolution levels.

An obvious explanation to this problem could be that the variances of the coefficients $\widetilde{c}$ in the density model are too heterogeneous within each resolution level, and thus cannot be treated by the (relatively) constant white noise thresholds. Indeed figure 5.11 shows that the variances of the coefficients issued from the white noise representation (first row) do not fit to the asymptotic variances in the density model (second row).

A natural way to circumvent this problem is to estimate the asymptotic variances. Unlike in first generation wavelet algorithms for density estimation, this can be easily done here as we have simple explicit expressions of the way the coefficients depend on the observations:

$$\widetilde{c}_{j,k} = \frac{1}{n} \sum_{i \in \mathbb{N}, \, l=1,...,n} \frac{(\psi_{j,k}, e_i) g_i(Y_l)}{b_i} = \frac{1}{n} \sum_{l=1,...,n} A_l,$$
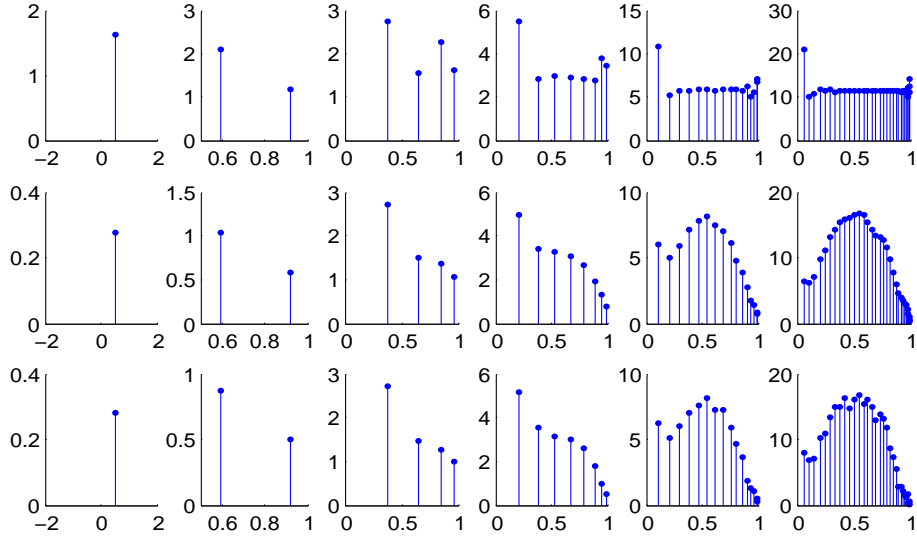
Figure 5.11: Variances (up to constant factors) of the needlet coefficients of the "Sine2" function in the white noise framework (top) and in the density framework (middle); Bottom: estimators of the variances in the density framework

with iid variables:

$$A_l = \sum_{l=1,\ldots,n} \frac{(\psi_{j,k}, e_i)g_i(Y_l)}{b_i},$$

so we have $\sqrt{n}(\widetilde{c}_{j,k} - c_{j,k}) \longrightarrow \mathcal{N}(0, \sigma_{j,k})$ with

$$\sigma_{j,k} = \int \Big(\sum_{i\in\mathbb{N}} \frac{(\psi_{j,k}, e_i)g_i(y)}{b_i}\Big)^2 Kf(y)dy - \Big(\int \sum_{i\in\mathbb{N}} \frac{(\psi_{j,k}, e_i)g_i(y)}{b_i} Kf(y)dy\Big)^2,$$

which can be estimated by:

$$\bar{\sigma}_{j,k} = \frac{1}{n} \sum_{l=1,\ldots,n} \Big(\sum_{i\in\mathbb{N}} \frac{(\psi_{j,k}, e_i)g_i(Y_l)}{b_i}\Big)^2 - \widetilde{c}_{j,k}^2.$$

Then we also investigate the performances of the NeedVD estimator using the thresholds:

$$\bar{t}_{n,j,k} = \kappa\sqrt{\frac{j\bar{\sigma}_{j,k}}{n}}.$$

Moreover the adaptive SVD estimator used in the white noise setting cannot be applied here for the same reason of non constant variances, and it is difficult to adapt it to this heterogeneity without changing completely the bloc structure of the filters. So we focus on needlets techniques, and instead of the truncation SVD procedure we also study non adaptive estimators based on projections on needlets (ie no thresholding is performed and the resolution level is fitted according to the target function), which yields better results and is more convenient to handle than the truncation SVD.

Checking the performances of these two procedures, it remains very difficult to capture details in the targets for samples containing 1000 observations. All we can do is estimate

simple functions, where the empirical threshold method is equivalent to the white noise method, since only a few low resolution coefficients are taken into account. Examples of results are given in figure 5.12. A convenient choice for κ consists of values close to 1 for the empirical thresholds estimator, whereas it has to depend on the target function at hand for the white noise thresholds. But both methods do not always yield very stable results (for Sine3).
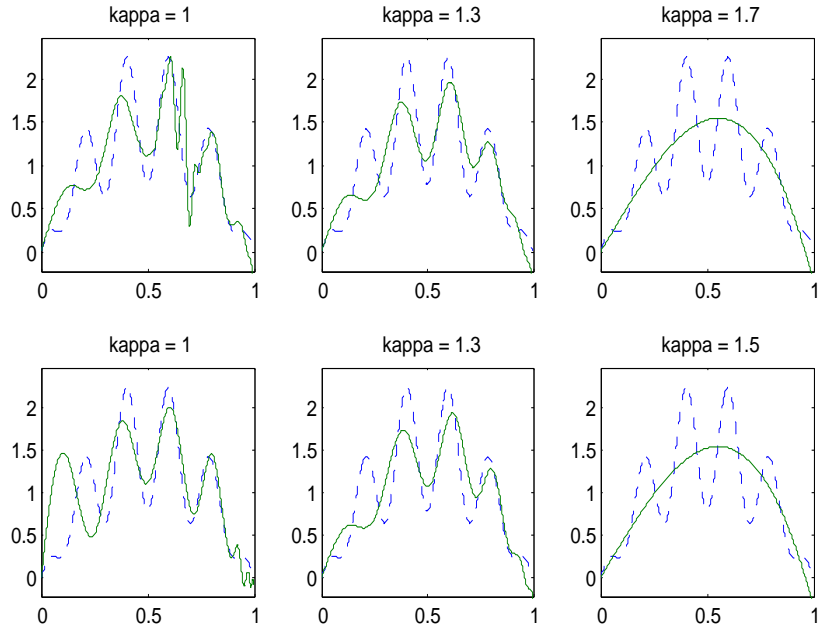

Figure 5.12: In solid line: adaptive NeedVD with white noise type thresholds (top) and with empirical variance thresholds (bottom) for $n = 1000$ and different choices of κ, and the true function in dashed line

Focusing on simple functions and on limited sample sizes, performances of the adaptive estimator are similar to those obtained with the non adaptive projection method, and we obtain the results given in figure 5.13 for the three sine target functions when $n = 1000$. We also investigate the performances of the estimators in the setting used by Antoniadis et al. [6] where $n = 270$ and f is given by a gamma pdf or a mixture of a gamma pdf, with a gaussian pdf. The procedures yield satisfying results (figure 5.14) as compared to those obtained by the three methods implemented in their paper.

Finally we focus on large samples so as to highlight the differences between the non adaptive and the adaptive estimator when applied to more inhomogeneous functions, such as Sine3. In fact a preliminary investigation reveals that a very large number of observations are needed so as to obtain satisfactory results. Indeed let us consider the optimal estimator (ie the NeedVD estimator with $\widetilde{c}_{j,k}$ replaced by the true coefficients $c_{j,k}$), which is given in the first row of figure 5.15. One can see that, with a reasonable filtering of the noise ($\kappa = 1$), one can hope to recover the details of the function only for very large sample sizes. Then the thresholding algorithm clearly outperforms the projection estimator which is either too smooth (as shown on figure 5.15), or too noisy.
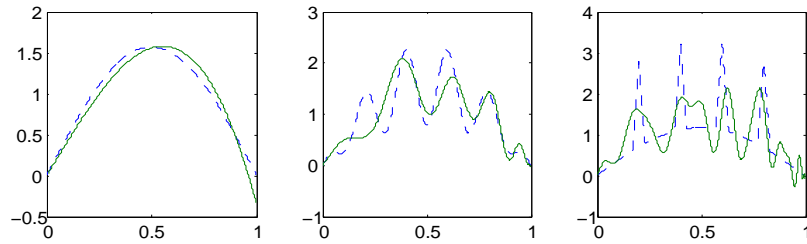
Figure 5.13: Non adaptive projection estimator (solid line) of three target functions (dashed line) for $n = 1000$
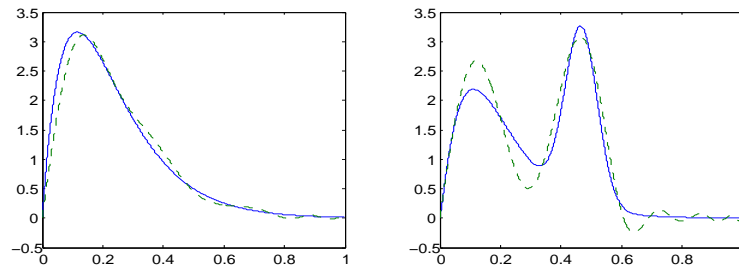

Figure 5.14: NeedVD estimator (dashed line) of two target functions (solid line) for a small sample $n = 270$

A way to improve the performances of the estimator would be perhaps to use more refined thresholding techniques, since the simple hard thresholding rule has been proved to be suboptimal in certain situations (especially from the maxiset point of view) as established by Autin [8].
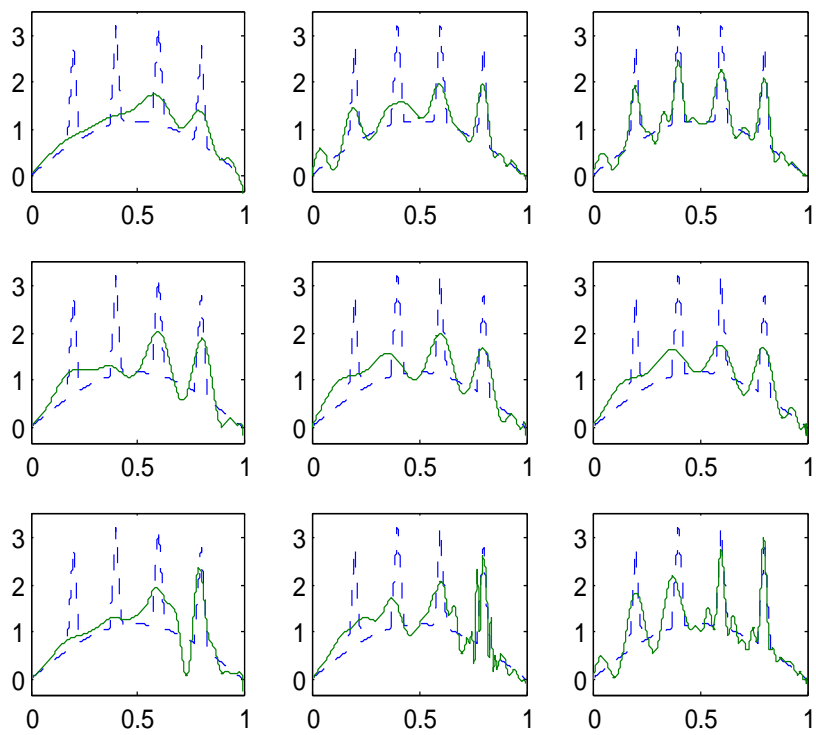
Figure 5.15: Top: "optimal" adaptive NeedVD; middle: non adaptive NeedVD; bottom: adaptive NeedVD, for sample sizes $n = 1000$, $n = 5000$ and $n = 15000$ (from left to right)

Chapter 6

Deconvolution in white noise with a random blurring effect

Ce chapitre est une version légèrement différente d'un article soumis à une revue.

Abstract: We consider the problem of denoising a function observed after a convolution with a random filter independent of the noise and satisfying some mean smoothness condition depending on an ill posedness coefficient. We establish the minimax rates for the L^p risk over balls of periodic Besov spaces with respect to the level of noise, and we provide an adaptive estimator achieving these rates up to log factors. The behavior of the estimator is examined in practice first in a simulation study with various distributions of the filter, and then in an application on a real dataset.

6.1   Motivations and preliminaries

6.1.1   Inverse problems in practice

Deconvolution is a particularly important case in a more general setting of problems, known as inverse problems. They consist in recovering an unknown object f from an observation h_n corresponding to $H(f)$ corrupted by a white noise ξ, for some operator H. The model is of the kind:

$$h_n = H(f) + \sigma n^{-1/2}\xi, \quad \forall n \geq 1. \tag{6.1}$$

Inverse problems appear in many scientific domains. Several applications can be found for example in OFTA [77] in various domains such as meteorology, thermodynamics and mechanics. Deconvolution, in particular, is a common problem in signal and image processing (see Bertero and Boccacci [10]). It appears notably in light detection and ranging devices, computing distances to an object by measuring the lapse of time between the emission of laser pulses and the detection of the pulses reflected by the object. In the underlying model f is a distance to an object measured up to small gaussian errors after being blurred by a convolution phenomenon due to the fact that the system response function of the device is longer than the time resolution interval of the detector. Several papers deal with this application of deconvolution methods, for example Harsdorf and Reuter [50] or Johnstone et al. [53].

In some cases, it is difficult to know *a priori* the underlying operator which transformed the object to be determined into the observed data. This problem appears notably when the operator is sensitive to even slight changes in the experimental conditions, or is affected by external random effects that cannot be controlled, and thus changes for every observation. In these conditions, a framework with a random operator is more adapted than a setting with a fixed deterministic operator.

As an example let us consider an inverse problem of reconstruction in a tomographic imagery system, borrowed from OFTA [77]. The problem is to find the density of activity f of a radioactive tracer by collecting the γ photons which it radiates on a detector. The framework is illustrated on figure 6.1. The setting is such that only the photons transmitted perpendicularly to the detector are taken into account. A given pixel A_d of the detector collects a number of photons that depends on the density of activity f along some segment $[FA_d]$, where F is the focal point towards which A_d is headed. Each point M of this segment transmits a contribution $f(M)$ towards A_d but the pixel detects only $a(M, A_d)f(M)$ photons from M because the radiation diminishes after it has gone across the fluid between M and A_d. So the following quantity is observed on the pixel A_d:

$$X_\mu f(F, A_d) = \int_{M \in [F, A_d]} f(M) a(M, A_d) dM,$$

and the function a can be put in the following form :

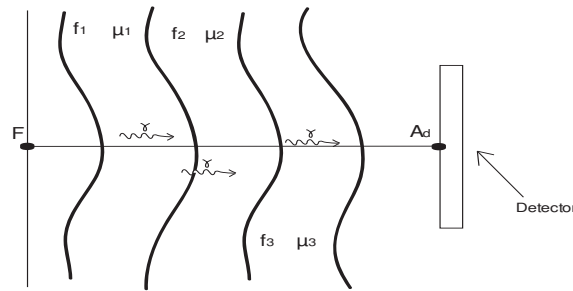$$a(M, A_d) = \exp\Big[- \int_{M' \in [M, A_d]} \mu(M') dM' \Big],$$

Figure 6.1: Reconstruction of a density of activity

where μ is a coefficient quantifying the radiation fading around M'. On figure 6.1 several zones characterized by different densities of activity and different coefficients μ are represented. If μ is constant along the segment $[FA_d]$, then recovering f is a deconvolution problem.

In practice the cartography of μ is not well known *a priori*. There is a different function for each pixel and this function depends on the characteristics of the fluid where the tracers were injected. Complementary measures and reconstruction algorithms are necessary to obtain it. In this context a probabilistic model is useful, where μ is a random function determined *a posteriori* thanks to additional measures.

6.1.2 Estimation in inverse problems with random operators

In the case of deterministic operators, inverse problems have been studied in many papers in a general framework where (6.1) holds with some linear operator H. Two main methods of estimation are generally used to recover f from the observation: singular value decomposition (SVD) and Galerkin projection methods. The former uses a decomposition of f on a basis of eigenfunctions of $H^T H$, which can be hard to perform if H is difficult to diagonalize. The latter uses a decomposition of f on a fixed basis adapted to the kind of functions to be estimated and then consists in solving a finite linear system to recover the coefficients of f. Wavelet decomposition is a very useful tool in such settings, see Donoho [29] and Abramovich and Silverman [1].

Among others, a method combining wavelet-vaguelettes decompositions and Galerkin projections can be found in Cohen et al. [24], whereas a sharp adaptive SVD estimator can be found in Cavalier and Tsybakov [16]. Concerning the deconvolution problem, wavelet-based estimation techniques were developed in Pensky and Vidakovic [78], Walter and Shen [90], Fan and J.S [39], Kalifa and Mallat [55] and Johnstone et al. [53]. Multidimensional situations have also been considered: minimax rates and estimation techniques can be found in Tsybakov [87].

Generalizations of inverse problems to the case of random operators have been made in several recent papers. First, random operators enable to treat situations where, in practice, the operator modifying the object to be estimated is not exactly known because of errors of measure. In such settings, equation (6.1) holds with an unknown deterministic operator H, and additional noisy observations provide a random operator H_δ where δ is a level

of noise : $H_\delta = H(f) + \delta\xi$. The problem is to build an estimator of f based on the data (h_n, H_δ) achieving minimax rates. Several adaptive estimation methods have been developed in this case. Some are based on SVD methods such as in Cavalier and Hengartner [19], whereas estimators based on Galerkin projection methods were developed in Efromovich and Koltchinskii [38] or Cohen et al. [23].

Random operators also appear quite naturally in models where the evolution of a random process is influenced by its past. For example let us consider the problem of estimating an unknown function f thanks to the observation of X_n ruled by the following equation (called stochastic delay differential equation, SDDE in short):

$$dX_n(t) = (\int_0^r X_n(t - s)f(s)ds)dt + \sigma n^{-1/2}dW(t) \quad \forall t \geq 0,$$
$$X_n(t) = F(t) \quad \forall t \in [-r, 0].$$

This problem is close to problem (6.2): a convolution of the unknown function with the random filter X_n is observed with small errors. However this filter is not independent from W so our results do not apply to this particular problem. Numerous estimation results in SDDEs can be found in Reiss [82] and in Reiss [83], with a different asymptotic framework.

The organization of the paper is as follows. Section 2, 3 and 4 present respectively the model, the estimator and the main results. Section 5 gives simulation results where the behavior of the estimator is investigated for several distributions of the random filter, and section 6 gives the proofs of the theorems.

6.2   The model

We consider the following deconvolution problem. Let $(\Omega, \mathcal{A}, P)$ be a probability space and W a standard Wiener process on this space. For a given $n \in \mathbb{N}^*$ we observe the realizations of two processes X_n and Y linked in the following way:

$$\begin{cases} dX_n(t) & = f \star Y(t)dt + \sigma n^{-1/2}dW(t), \quad \forall t \in [0, 1], \\ X_n(0) & = x_0, \end{cases} \tag{6.2}$$

where $\star$ denotes the convolution : $f \star Y(t) = \int_0^1 f(t - s)Y(s)ds$, x_0 is a deterministic initial condition and σ is a known positive constant.

The problem is to estimate the 1-periodic function f when Y is independent of W and satisfies some condition of smoothness.

6.2.1   The target function

We introduce functional spaces especially useful to describe the target functions. For a given $\rho > 1$, let us first denote by L^ρ the following space:

$$L^\rho([0, 1]) = \{f : \mathbb{R} \mapsto \mathbb{R} \quad | \quad f \text{ is } 1 - periodic, \quad \text{and} \int_0^1 |f|^\rho < \infty\}.$$

Secondly let us set $R_j = \{0, \ldots, 2^j - 1\}$ for all $j \in \mathbb{N}$, and let $(\Phi_{j,k}, \Psi_{j,k})_{j,k \in \mathbb{Z}}$ denote the periodized Meyer wavelet basis (see Meyer [68] or Mallat [64] for details). For convenience the following notations will be used further: $R_{-1} = \{0\}$ and $\Phi_{-1,0} = \Psi_{0,0}$. Then any $f \in L^\rho([0,1])$ has an expansion of the kind:

$$f = \sum_{j \geq -1, \, k \in R_j} \beta_{j,k} \Psi_{j,k}, \quad \text{where} \quad \beta_{j,k} = \int_0^1 f \Psi_{j,k}.$$

We assume that the targets satisfy some regularity condition by using periodic Besov spaces, which are defined thanks to the modulus of continuity in a similar way as in the non periodic case (see Johnstone et al. [53] for the exact definition). They have the advantage of being very general, including spatially unsmooth functions, and of being very well suited to wavelet decompositions. Indeed, the following characterization holds under several conditions on the wavelet basis similar to the conditions in the general case (which can be found in Härdle et al. [49]):

$$B_{p,q}^s([0,1]) = \{f \in L^p([0,1]) \quad | \quad \|f\|_{s,p,q} := \Big(\sum_{j \geq 0} 2^{j(s+1/2-1/p)q} \Big(\sum_{k \in R_j} |\beta_{j,k}|^p\Big)^{q/p}\Big)^{1/q} < \infty\}.$$

We investigate the maximal error when f can be any function in a ball of a periodic Besov space $B_{p,q}^s([0,1])$ of radius R and when the estimation error is measured by the L^ρ-loss. We suppose that $s > \frac{1}{p}$ so that f is continuous and hence its L^ρ-norm exists.

Definition 5. *For given $R > 0$, $p > 1$, $q > 1$ and $s > \frac{1}{p}$, define :*

$$M(s, p, q, R) = \{f \in B_{p,q}^s([0,1]) \quad | \quad \|f\|_{s,p,q} \leq R\}.$$

Our aim is to determine the rate of the following minimax risk for $\rho > 1$:

$$R_n := \inf_{\hat{f}_n} \sup_{f \in M(s,p,q,R)} E_f(\|\hat{f}_n - f\|_\rho),$$

where the infimum is taken over all $\sigma((X_n(t), Y(t))_{t \in [0,1]})$−measurable estimators $\hat{f}_n$.

6.2.2 The filter

We assume that the blurring function Y is a random process independent of n, f, and (in probabilistic terms) of the process W, and taking its values in $L^2([0,1])$.

Throughout this paper, we will use the following notations for two functions A and B depending on parameters p :

- $A \lesssim B$ means that there exists a positive constant C such that for all p, $\quad A(p) \leq CB(p)$,

- $A \gtrsim B$ means that $B \lesssim A$,

- $A \asymp B$ means that $A \lesssim B$ and $A \gtrsim B$.

For $j \in \mathbb{N}$ we introduce two random variables L_j^Y and U_j^Y (whenever they exist) linked to the smoothness of the process Y:

$$L_j^Y = \frac{\sum_{l=2^j}^{2^{j+1}-1} |Y_l|^2}{2^j}, \quad \text{and} \quad U_j^Y = \frac{\sum_{l=0}^{2^{j+1}-1} |Y_l|^{-2}}{2^j},$$

where $(Y_l)_{l \in \mathbb{Z}}$ are the Fourier coefficients of $(Y(t))_{t \in [0,1]}$.

To establish the lower (resp upper) bound of the minimax risk, we impose the following control on the distribution of L_j^Y (resp U_j^Y), which implies that the Fourier coefficients are not too large (resp small):

C_{low}: *There exists a constant $\nu \geq 0$ such that, for all $j \in \mathbb{N}$:*

$$E(L_j^Y) \lesssim 2^{-2\nu j}.$$

C_{up} : *$\forall l \in \mathbb{Z}, Y_l \neq 0$ almost surely, and there exist $\nu \geq 0, c > 0, \alpha > 0$ such that, for all $j \in \mathbb{N}$:*

$$\forall t \geq 0, \quad P\big(U_j^Y \geq t 2^{2\nu j}\big) \lesssim e^{-ct^\alpha}.$$

All those conditions are satisfied if the Fourier Transform $\hat{Y}$ of the process Y has the following form: $|\hat{Y}(w)| = \frac{T(w)}{(1+w^2)^{\nu/2}}$, where T is a positive random process with little probability of taking small or high values (for example bounded almost surely by deterministic constants). This case includes for example gamma probability distribution functions with some random scale parameter, which will be used further. On the contrary, condition C_{up} does not hold for filters with realizations belonging to supersmooth functions, ie Y such that $|\hat{Y}(w)| = T(w)\frac{e^{-B|w|^\beta}}{(1+w^2)^{\nu/2}}$, for some constants $B, \beta > 0$ and with T as before. Results on deconvolution of supersmooth functions can be found in Butucea [13].

6.3   Adaptive estimators

We build an adaptive estimator, nearly achieving the minimax rates exposed in the next section, which is close to the one developed in Johnstone et al. [53] in the case of a deterministic filter Y. The method combines elements of the SVD methods (deconvolution thanks to the Fourier basis) and of the projection methods (decomposition on a wavelet basis adapted to the target functions).

Let us consider a target function f belonging to $M(s, p, q, R)$ and denote its wavelet coefficients by $(\beta_{j,k})$. We estimate f by estimating those coefficients. Let $(e_l(t)) = (\exp(2\pi ilt))_{l \in \mathbb{Z}}$ denote the Fourier basis, and let $(\Psi_{j,k,l})_{l \in \mathbb{Z}}$, $(f_l)_{l \in \mathbb{Z}}$ and $(Y_l)_{l \in \mathbb{Z}}$ be the Fourier coefficients of the functions $\Psi_{j,k}$, f and Y. Set also: $W_l = \int_0^1 e_l(t)dW(t)$ and $X_l^n = \int_0^1 e_l(t)dX_n(t)$. Then by Plancherel's identity we have:

$$\beta_{j,k} = \sum_{l \in \mathbb{Z}} f_l \Psi_{j,k,l}.$$

Moreover $\int_0^1 (f \star Y)\bar{e}_l = f_l Y_l$, so equation (6.2) yields:

$$X_l^n = f_l Y_l + \sigma n^{-1/2} W_l,$$

and thus if we suppose that $Y_l \neq 0$ almost surely for all l, f_l can naturally be estimated by $\frac{X_l^n}{Y_l}$ and we set:

$$\hat{\beta}_{j,k} = \sum_{l \in \mathbb{Z}} \frac{X_l^n}{Y_l} \Psi_{j,k,l}.$$

Thresholding is then needed to denoise these coefficients. A well known technique in the case of white noise or equivalent models is hard thresholding with a threshold t of the kind: $t = \eta\sqrt{\log n/n}$. Here the ill posed nature of the problem at hand requires an additional factor, and the randomness of the filter requires some dependency on the parameter α. Namely we set the following values for the thresholds λ_j and the highest resolution level j_1:

$$\lambda_j = \eta 2^{\nu j} \sqrt{(\log n)^{1+\frac{1}{\alpha}}/n}, \quad 2^{j_1} = \{n/(\log n)^{1+\frac{1}{\alpha}}\}^{1/(1+2\nu)},$$

where η is a positive constant larger than a threshold (which is determined in section 6).

Finally the following estimator achieves the minimax rates up to log factors when the filter satisfies condition C_{up}:

$$\hat{f}_n^D = \sum_{(j,k) \in \Lambda_n} \hat{\beta}_{j,k} I_{\{|\hat{\beta}_{j,k}| \geq \lambda_j\}} \Psi_{j,k}, \tag{6.3}$$

where $\Lambda_n = \{(j,k) \in \mathbb{Z}^2 \mid j \in \{-1, \dots, j_1\}, k \in R_j\}$.

Nevertheless our choice of remaining close to white-noise thresholds has some cost, as some extra log factors involving α appear in the minimax rates presented in the next section. A probable solution to this issue is to use alternative thresholds depending directly on the filter Y, namely by replacing λ_j and j_1 by the following τ_j and j_2:

$$\tau_j = \eta'\sqrt{U_j^Y \log n/n}, \quad 2^{j_2} = \{n/\log n\}^{1/(1+2\nu)},$$

where η' is a large enough constant. Let us denote by $\hat{f}_n^R$ the estimator defined that way, using random thresholds instead of deterministic ones (hence the superscript R instead of D). Its theoretical performances will be studied in a separate publication, here only a simulation study is provided.

6.4   Main results

Let $\rho > 1$, $R > 0$, $p > 1$, $q > 1$ and $s > 1/p$. We distinguish three cases for the regularity parameters characterizing the target functions according to the sign of $\varepsilon = \frac{2s+2\nu+1}{\rho} - \frac{2\nu+1}{p}$:

the sparse case ($\varepsilon < 0$), the critical case ($\varepsilon = 0$) and the regular case ($\varepsilon > 0$).

Let us introduce the two following rates:

$$r_n(s,\nu) = \Big(\frac{1}{n}\Big)^{\frac{s}{2s+2\nu+1}}, \quad s_n(s,p,\rho,\nu) = \Big(\frac{\log(n)}{n}\Big)^{\frac{s-1/p+1/\rho}{2s+2\nu+1-2/p}}.$$

Theorem 15. *Under condition C_{low} on Y:*

$$r_n(s,\nu)^{-1}R_n \gtrsim 1 \quad \text{in the regular case,}$$
$$s_n(s,p,\rho,\nu)^{-1}R_n \gtrsim 1 \quad \text{in the sparse and critical cases.}$$

Theorem 16. *Under condition C_{up} on Y:*

$$r_n(s,\nu)^{-1}R_n \lesssim 1 \quad \text{in the regular case,}$$
$$s_n(s,p,\rho,\nu)^{-1}R_n \lesssim 1 \quad \text{in the sparse case,}$$
$$s_n(s,p,\rho,\nu)^{-1}R_n \lesssim \log(n)^{(1-\frac{p}{\rho q})+} \quad \text{in the critical case.}$$

Theorem 17. *Under condition C_{up} on Y, for estimator $\hat{f}_n^D$ defined in (6.3) and if $q \leq p$ in the critical case:*

$$\sup_{f \in M(s,p,q,R)} E_f(\|\hat{f}_n^D - f\|_\rho) \lesssim \Big(\frac{\log(n)^{1+\frac{1}{\alpha}}}{n}\Big)^{\frac{s}{2s+2\nu+1}} \quad \text{in the regular case,}$$

$$\sup_{f \in M(s,p,q,R)} E_f(\|\hat{f}_n^D - f\|_\rho) \lesssim \Big(\frac{\log(n)^{1+\frac{1}{\alpha}}}{n}\Big)^{\frac{s-1/p+1/\rho}{2s+2\nu+1-2/p}} \quad \text{in the critical and sparse cases.}$$

When the filter satisfies C_{low} and C_{up} the rates of Theorems 1 and 2 match except in the critical case when $\rho > \frac{p}{q}$, where the upper bound contains an extra logarithmic factor. This is also observed in density estimation or regression problems (see Donoho et al. [36] and Donoho et al. [34]), and that factor is probably part of the actual rate of R_n: the lower bound is maybe too optimistic.

Analyzing the effect of ν, we remark that the rates are similar to the ones established in the white noise model or other classical non-parametric estimation problems (examples can be found in Tsybakov [89]), except that here an additional effect reflected by ν slows the minimax speed. Indeed the convolution blurs the observations, making the estimation all the more difficult as ν is large. This parameter is called ill-posedness coefficient, explanations about this notion can be found in Nussbaum and Pereverzev [75] for example.

Concerning Theorem 3, we remark that estimator $\hat{f}_n^D$ is not optimal first by a log factor in the regular case, which is a common phenomenon for adaptive estimators as was highlighted in Tsybakov [88], and secondly by log factors with exponents proportional to $\frac{1}{\alpha}$. This is due to the difficulty to control the deviation probability of the estimated wavelet coefficients when the probability of having small eigenvalues Y_l of the convolution operator is high (ie when α is small).

The main interest of these results is that bounds of the minimax risk are established in a random operator setting, for a wide scale of L^ρ losses, and over general functional spaces which include unsmooth functions. As far as we know, the lower bound has not been established in deconvolution problems for such settings even in the case of deterministic filters.

Let us also note that condition C_{up} imposed on the filter Y is similar to the conditions generally used in other inverse problems where the singular values of the operator are required to decrease polynomially fast. Moreover condition C_{up} concerns means of eigenvalues
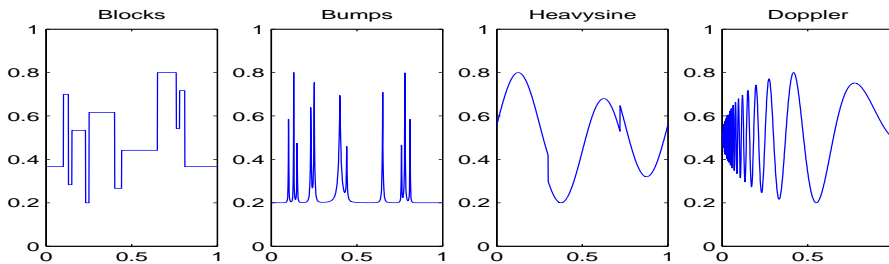
Figure 6.2: Target functions

over diadic blocs, which enables to include filters for which Fourier coefficients vary erratically individually, but not in mean, such as some boxcar filters (see Kerkyacharian et al. [58]). The case of severely ill-posed inverse problems, where the singular values decrease exponentially fast, has also been studied in Cavalier et al. [18] for example.

6.5 Simulations

To illustrate the rates obtained for the upper bound, the behaviors of estimators $\hat{f}_n^D$ and $\hat{f}_n^R$ are examined in practice for the following settings. We consider the four target functions (Blocks, Bumps, Heavisine, Doppler) represented on figure 6.2, which were used by Donoho and Johnstone in a series of papers (Donoho and Johnstone [31] for example). These functions are blurred by convolution with realizations of a random filter Y and by adding gaussian noise with root signal to noise ratio ($rsnr$) of three levels: $rsnr \in \{3, 5, 7\}$. Then the two estimators are computed in each case and their performances are examined, judging by the mean square error (MSE). For the simulation of the data and the implementation of the estimators, parts of the WaveD software package written by Donoho and Raimondo for Johnstone et al. [53] were used.

6.5.1 Distribution of the filter

A simple way to represent the blurring effect is the convolution with a boxcar filter, ie at time t one observes the mean of the unknown function on an interval $[t-a, t]$ with a random width a. However these kinds of filters have various degrees of ill posedness depending on a. For some numbers called "badly approximable" numbers, this degree is constant and equal to $3/2$. For other numbers the situation is more complicated, and the set of the badly approximable numbers has a Lebesgue measure equal to zero (more explanations can be found in Johnstone and Raimondo [52] or Johnstone et al. [53]). However new results have been found recently for almost all boxcar widths in Kerkyacharian et al. [58] where the near optimal properties of several thresholding estimators are established.

So as to keep a fixed ill posedness coefficient boxcar filters are excluded, and one considers convolutions with periodized gamma functions with parameters ν and λ:

$$Y(t) = \frac{1}{\int_0^{+\infty} s^{\nu-1}e^{-\lambda s}ds} \sum_{l \in \mathbb{N}} (t+l)^{\nu-1}e^{-\lambda(t+l)},$$
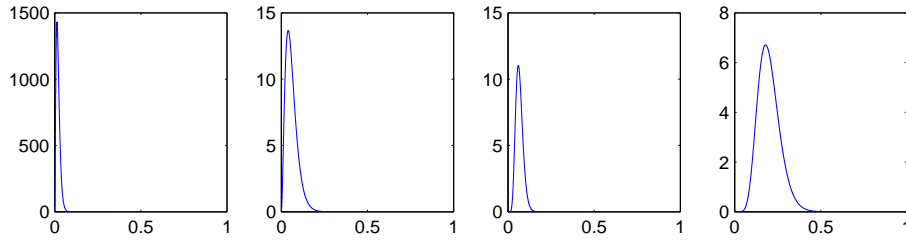
Figure 6.3: Examples of filters, from left to right: $(\nu, \lambda) \in \{(3, 150), (3, 50), (10, 150), (10, 50)\}$

where ν is a fixed shape parameter and λ is a *random* scale parameter with a probability distribution function F_α parametrized by some $\alpha > 0$:

$$F_\alpha(t) = \min\big(1, 2e^{-\frac{C_\alpha}{t^{2\alpha}}}\mathbb{I}(t \geq 0)\big),$$

where the constant C_α is set such that $E(\lambda) = 150$ for all α.

Such a filter Y satisfies conditions C_{up} and C_{low}. Some examples of its shapes are given in figure 6.3: ν and λ can be interpreted respectively as a delay and a spreading parameter. According to the minimax rates, f should be (asymptotically) more difficult to estimate for large ν and for small α. This is checked in practice in the next section.

6.5.2 Results

First we focus on the effect of ν conditionally to the filter Y. An example in medium noise for the Blocks target is given in figure 6.4, where the filter is kept constant with $\lambda = 150$: as expected, both estimators get less and less efficient when ν increases. Moreover in practice the thresholds of estimator $\hat{f}_n^D$ need to be rescaled for each ν, contrarily to those of estimator $\hat{f}_n^R$ which is thus more convenient. The same results were obtained for the other target functions and by examining the MSE of the estimators, the figures were not included for the sake of conciseness.

Next we set $\nu = 1$ and we investigate the effect of the distribution of the filter Y. Both estimators perform well for mean and high realizations of λ, but difficulties appear for small realizations which are all the more frequent as α is small: the worst case among 10 simulations is represented in figure 6.5 when $\alpha = 2$ and in figure 6.6 when $\alpha = 0.5$, and the two estimators perform more poorly in the last case. However they remain better in that case than a fixed threshold estimator (ie with thresholds completely independent of the filter) also represented in the figures.

More generally the MSE were computed for several values of α and for the three noise levels. The results are given in figure 6.7: the shape of the distribution of Y clearly affects estimator $\hat{f}_n^D$, and also $\hat{f}_n^R$ to a much lesser extent. The smaller α, the poorer they behave. Especially the Doppler and Bumps targets are not well estimated by $\hat{f}_n^D$ for small α, mainly because the high thresholds make it ignore many of the numerous details of these targets. Finally estimator $\hat{f}_n^R$ proves more convenient than estimator $\hat{f}_n^D$ when the ill-posedness varies, and also less sensitive to the weight of the probability of small eigenvalues.
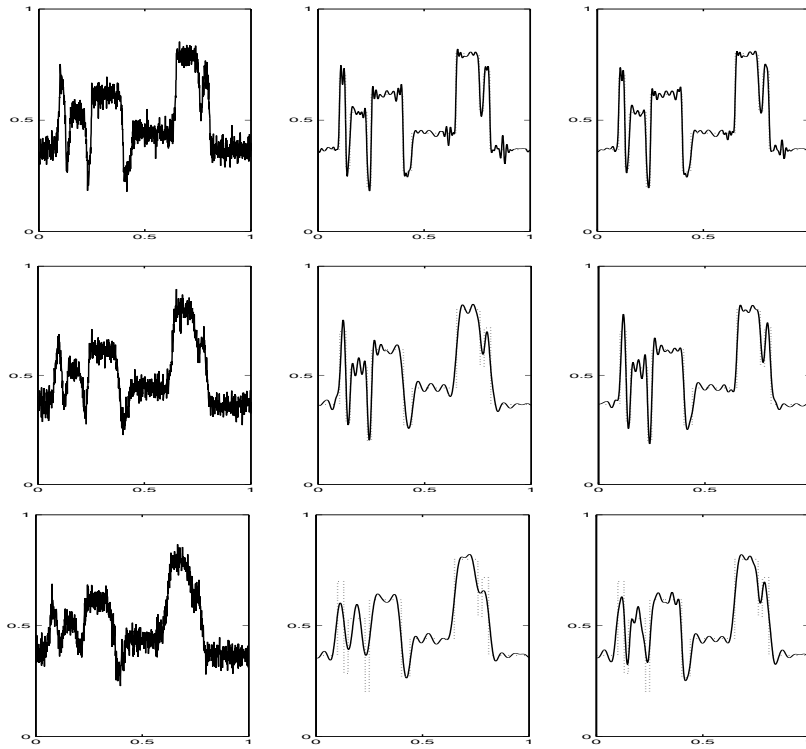
Figure 6.4: Data, estimator $\hat{f}_n^R$ and estimator $\hat{f}_n^D$ (left to right) for fixed $\lambda = 150$ and $\nu = 1$ (top), $\nu = 3$ (middle) and $\nu = 5$ (bottom)
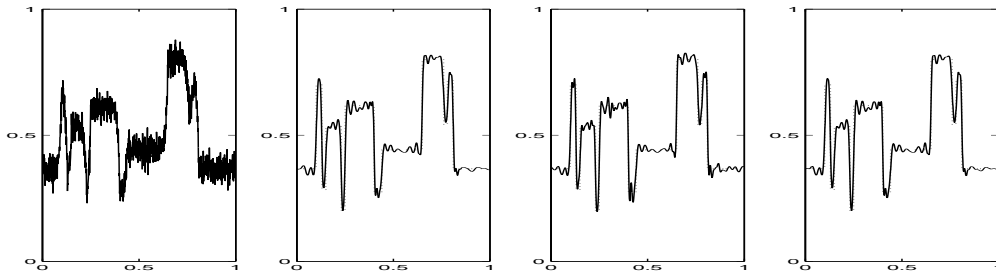

Figure 6.5: Data, estimator $\hat{f}_n^R$, estimator $\hat{f}_n^D$ and a fixed-threshold estimator (left to right) for $\alpha = 2$
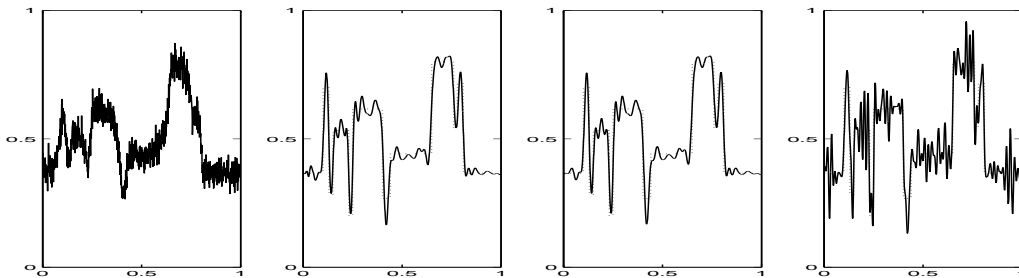

Figure 6.6: Data, estimator $\hat{f}_n^R$, estimator $\hat{f}_n^D$ and a fixed-threshold estimator (left to right) for $\alpha = 0.5$
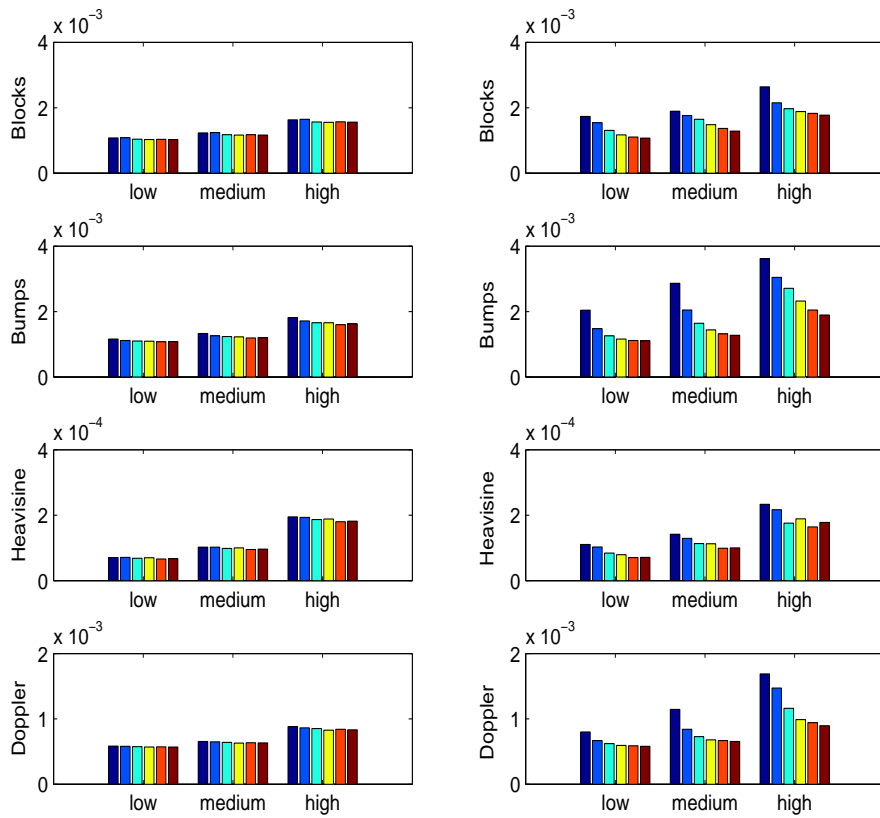
Figure 6.7: Effect of α on the MSE of estimator $\hat{f}_n^R$ (left) and estimator $\hat{f}_n^D$ (right) for each target, each level of noise and $\alpha \in \{0.5, 0.6, 0.7, 0.8, 0.9, 1\}$ (left to right in each group)

6.6 Application to real data

Deconvolution is a common problem in seismology. After travelling across Earth's mantle, source waves are observed at the surface in a smoothed form because of various propagation effects. We assume that these effects take the form of a convolution filter Y as in model (6.2), and we apply the estimators developed above to the dataset described in Stefan et al. [85] and available at: *http://mathpost.la.asu.edu/ stefan*. In that paper a gaussian filter is considered with some fixed width parameter fitted subjectively. We adopt the same approach with the following filter: $Y(t) = \frac{1}{2 \int_0^{+\infty} e^{-\lambda s} ds} \sum_{l \in \mathbb{N}} e^{-\lambda |t+l|}$. We set $\lambda = 110$, which leads to satisfactory results in practice.

The seismograms present very low gaussian noise, so the main concern here is not denoising but merely deconvolution and estimators $\hat{f}^D$ and $\hat{f}^R$ yield similar results. Figure 6.8 shows some examples of $\hat{f}^R$ for three horizontal displacement records in stations at around 90 deg epicentral distance range: the deconvolved signal is sharper and presents local variations of higher amplitude than the original signal. Furthermore the estimator enables to detect two peaks at the beginning of the earthquake for waves between around 90 and 100 deg (see the middle graph), which is invisible in the original seismogram. This is consistent with the presence of two nearly overlapping phases for such waves, as discussed in Stefan et al. [85].
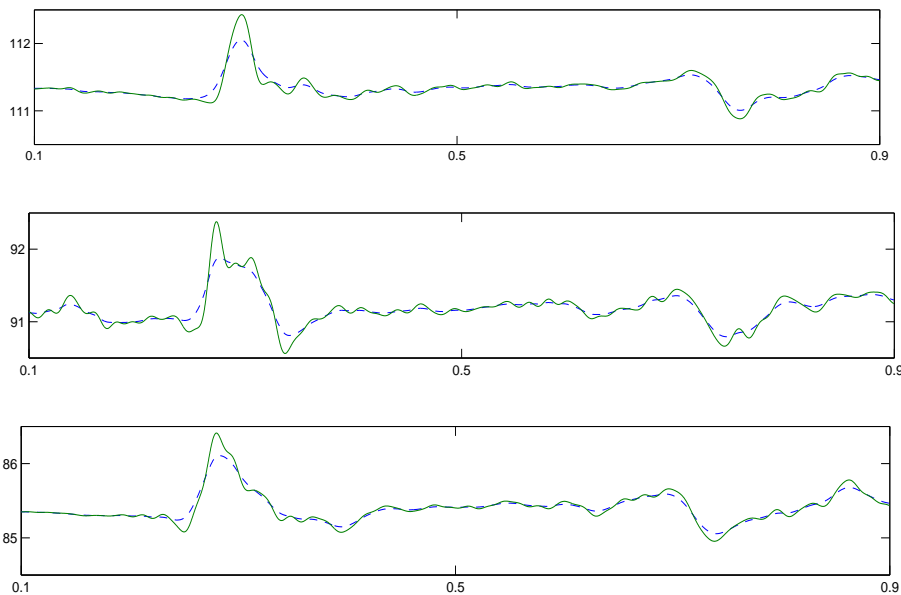

Figure 6.8: Observed seismograms (dashed line) and deconvolved seismograms (solid line), the y-axis represents displacement in degrees and the x-axis represents time for a normalized observation duration

6.7   Proofs of the lower and upper bounds

6.7.1   Lower bound

Sparse case

We use a classical lemma on lower bounds (Korostelev and Tsybakov [61]):

Lemma 4. *Let V a functional space, $d(.,.)$ a distance on V,*
for f, g belonging to V denote by $\Lambda_n(f,g)$ the likelihood ratio : $\Lambda_n(f,g) = \frac{dP_{X_n^{(f)}}}{dP_{X_n^{(g)}}}$ where
$dP_{X_n^{(h)}}$ is the probability distribution of the process X_n if h is true.
If V contains functions $f_0, f_1, \ldots, f_K$ such that :

- *$d(f_{k'}, f_k) \geq \delta > 0$ for $k \neq k'$,*

- *$K \geq \exp(\lambda_n)$ for some $\lambda_n > 0$,*

- *$\Lambda_n(f_0, f_k) = \exp(z_n^k - v_n^k)$, where z_n^k is a random variable such that there exists $\pi_0 > 0$ with $P(z_n^k > 0) \geq \pi_0$, and v_n^k are constants,*

- *$\sup_k v_n^k \leq \lambda_n$.*

Then

$$\sup_{f \in V} P_{X_n^{(f)}}\big(d(\hat{f}_n, f) \geq \delta/2\big) \geq \pi_0/2,$$

for an arbitrary estimator $\hat{f}_n$.

To use this result, we build a finite set of functions belonging to $M(s, p, q, R)$ as follows. Let $(\psi_{j,k})_{j \geq -1, k \in \mathbb{Z}}$ be an $s-$regular Meyer wavelet basis, which we periodize according to:

$$\Psi_{j,k}(x) = \sum_{l \in \mathbb{Z}} \psi_{j,k}(x + l).$$

In the sequel we denote by $(\Psi_{j,k})_{(j,k) \in \Lambda}$ the periodized Meyer wavelet basis obtained this way, where $\Lambda = \{(j, k) \mid j \geq -1; \ k \in R_j\}$ and $R_j = \{0, \ldots, 2^j - 1\}$.

Now for a fixed level of resolution j set for any $k \in R_j$:

$$f_{j,k} = \gamma \Psi_{j,k},$$

with $\gamma \lesssim 2^{-j(s+1/2-1/p)}$ such that $\|f_{j,k}\|_{s,p,q} \leq R$. Set also $f_0 = 0$.

Let us choose for d the distance $d(f, g) = \|f - g\|_\rho$. Because of the relation between the L^ρ norm of a linear combination of wavelets of fixed resolution j and the l^ρ norm of the corresponding coefficients (see Meyer [68]), we have for any $k, k' \in R_j$, $k \neq k'$:

$$d(f_{j,k'}, f_{j,k}) = \|\gamma \Psi_{j,k'} - \gamma \Psi_{j,k}\|_{L^\rho} \asymp \gamma 2^{j(1/2-1/\rho)}.$$

In this framework we have : $K = 2^j$ and $\delta \asymp \gamma 2^{j(1/2-1/\rho)}$. So as to apply the lemma, we have to find parameters $\gamma(n)$ and $j(n)$ such that the other hypotheses of the lemma are satisfied, which will be true if :

$$P_{f_{j,k}}\Big(\ln(\Lambda_n(f_0, f_{j,k})) \geq -j(n)\ln(2)\Big) \geq \pi_0 > 0,$$

uniformly for all $f_{j,k}$. Moreover we have :

$$P_{f_{j,k}}\Big(\ln(\Lambda_n(f_0, f_{j,k})) \geq -j(n)\ln(2)\Big) \geq 1 - P_{f_{j,k}}\Big(|\ln(\Lambda_n(f_0, f_{j,k}))| > j(n)\ln(2)\Big)$$
$$\geq 1 - E_{f_{j,k}}\Big(|ln(\Lambda_n(f_0, f_{j,k}))|\Big)/(j(n)\ln(2)).$$

So the previous condition is satisfied when $\gamma(n)$ and $j(n)$ are chosen such that, with a constant $0 < c < 1$:

$$E_{f_{j,k}}\Big(|ln(\Lambda_n(f_0, f_{j,k}))|\Big) \leq cj(n)\ln(2). \tag{6.4}$$

Consider two hypotheses f_0 and $f_{j,k}$, and let us determine the likelihood ratio of the corresponding distributions of the observations $(X_n(t), Y(t))_{t\in[0,1]}$. Let F be a bounded measurable function. Since Y is assumed to be independent of W and free with respect to f in (6.2), we have:

$$E_{f_{j,k}}\big[F(X^n, Y)\big] = E\Big[E\{F\big((\int_0^t f_{j,k} \star Y(s)ds + \sigma n^{-1/2}W(t), Y(t))_{t\in[0,1]}\big) \mid Y\}\Big]$$
$$= \int E\{F\big(\sigma n^{-1/2}\widetilde{W}, y\big)\}dP_Y(y),$$

where P_Y denotes the distribution of Y and $\widetilde{W}(t) = W(t) + \int_0^t \sigma^{-1}n^{1/2}f_{j,k} \star y(s)ds$.

For a given function y let $h^y_{j,k}$ be defined by: $h^y_{j,k}(t) = \sigma^{-1}n^{1/2}f_{j,k} \star y(t)$. We assumed that Y takes its values in $L^2([0, 1])$ so for each of its realization there exists a constant C_y such that for all $t \in [0, 1]$, $\int_0^t (h^y_{j,k})^2(s)ds < C_y$ and we can apply the formula of Girsanov: the process $\widetilde{W}$ is a Wiener process under the probability Q defined by

$$dQ = \exp\Big[-\int_0^1 h^y_{j,k}(t)dW(t) - \frac{1}{2}\int_0^1 (h^y_{j,k}(t))^2 dt\Big]dP.$$

Thus for any function y:

$$E_P\big[F(\sigma n^{-1/2}\widetilde{W}, y)\big] = E_Q\big[F(\sigma n^{-1/2}\widetilde{W}, y)\exp\big[\int_0^1 h^y_{j,k}(t)dW(t) + \frac{1}{2}\int_0^1 (h^y_{j,k}(t))^2 dt\big]\big]$$
$$= E_Q\big[F(\sigma n^{-1/2}\widetilde{W}, y)\exp\big[\int_0^1 h^y_{j,k}(t)d\widetilde{W}(t) - \frac{1}{2}\int_0^1 (h^y_{j,k}(t))^2 dt\big]\big]$$
$$= E_P\big[F(\sigma n^{-1/2}W, y)\exp\big[\int_0^1 h^y_{j,k}(t)dW(t) - \frac{1}{2}\int_0^1 (h^y_{j,k}(t))^2 dt\big]\big].$$

So finally:

$$\Lambda_n(f_0, f_{j,k}) = \exp\Big[-\int_0^1 \frac{f_{j,k} \star Y(t)}{\sigma n^{-1/2}}dW(t) + \frac{1}{2}\int_0^1 \big(\frac{f_{j,k} \star Y(t)}{\sigma n^{-1/2}}\big)^2 dt\Big].$$

We can now examine under which conditions (6.4) is true. We have:

$$E|\ln(\Lambda_n(f_0, f_{j,k}))| = E|\frac{\gamma n^{1/2}}{\sigma} \int_0^1 \Psi_{j,k} \star Y(t) dW(t) - \frac{\gamma^2 n}{2\sigma^2} \int_0^1 (\Psi_{j,k} \star Y(t))^2 dt| \leq A_n + B_n, \text{ with:}$$

$$B_n = \frac{\gamma^2 n}{2\sigma^2} E\left(\int_0^1 (\Psi_{j,k} \star Y(t))^2 dt\right),$$

$$A_n = \frac{\gamma n^{1/2}}{\sigma} E|\int_0^1 \Psi_{j,k} \star Y(t) dW(t)| \leq \frac{\gamma n^{1/2}}{\sigma} \left(E(\int_0^1 \Psi_{j,k} \star Y(t) dW(t))^2\right)^{1/2} \leq (2B_n)^{1/2},$$

where we used Jensen's inequality for A_n.

Let us find a bound for B_n. We introduce the Fourier coefficients of Y and $\Psi_{j,k}$ denoted by Y_l and $\Psi_{j,k,l}$ for all $l \in \mathbb{Z}$. Since the Fourier Transform of $\Psi_{j,k}$ is bounded by $2^{-j/2}$ we have:

$$B_n = \frac{\gamma^2 n}{2\sigma^2} E_{f_{j,k}}\left(\frac{1}{2\pi} \sum_{l \in \mathbb{Z}} |Y_l \Psi_{j,k,l}|^2\right) \lesssim \gamma^2 n 2^{-j} E_{f_{j,k}}\left(\sum_{l \in C_j} |Y_l|^2\right),$$

where C_j is the set of integers where the coefficients $\Psi_{j,k,l}$ are not equal to zero (it can easily be shown that this set does not depend on k).

The support of the Fourier transform of the Meyer wavelet is included in $[-\frac{2\pi}{3}, -\frac{8\pi}{3}] \cup [\frac{2\pi}{3}, \frac{8\pi}{3}]$. So $\Psi_{j,k,l} = 0$ as soon as $|2\pi 2^{-j} l| \in [\frac{2\pi}{3}, \frac{8\pi}{3}]^c$, and $C_j \subset [-2^{j+1}, -2^{j-2}] \cup [2^{j-2}, 2^{j+1}]$ for all j. Then under condition C_{low} and noticing that $Y_{-l} = Y_l$ we obtain:

$$B_n \lesssim \gamma^2 n 2^{-2\nu j}.$$

Finally, condition (6.4) holds if we choose γ and j such that:

$$\gamma^2 n 2^{-2\nu j} \lesssim j, \quad \text{and} \quad \gamma \lesssim 2^{-j(s+1/2-1/p)}.$$

We choose the following values that satisfy those two conditions:

$$\gamma \asymp 2^{-j(s+1/2-1/p)}, \quad \text{and} \quad 2^j \asymp (n/log(n))^{1/(2s+2\nu+1-2/p)}.$$

Finally, using the lemma and the inequality of Markov, for $\sigma((X_n(t), Y(t)), t \in [0,1])$−measurable estimators $\hat{f}_n$ the following bound holds:

$$\inf_{\hat{f}_n} \sup_{f \in M(s,p,q,S)} E_f(\|\hat{f}_n - f\|_\rho) \gtrsim \gamma 2^{j(1/2-1/\rho)} \asymp \left(\frac{\log(n)}{n}\right)^{\frac{s-1/p+1/\rho}{2s+2\nu+1-2/p}}.$$

Regular case

Here we consider another set of functions belonging to $M(s,p,q,R)$. We use the periodized Meyer wavelet basis $(\Psi_{j,k})$ like before. But now we set for any $\varepsilon \in \{-1,+1\}^{R_j}$:

$$f_{j,\varepsilon} = \gamma \sum_{k \in R_j} \varepsilon_k \Psi_{j,k},$$

with $\gamma \lesssim 2^{-j(s+1/2)}$ such that $\|f_{j,\varepsilon}\|_{s,p,q} \leq S$. We also set $I_{j,k} = [\frac{k}{2^j}, \frac{k+1}{2^j}]$.

We use an adaptation of lemma 10.2 in Härdle et al. [49] to the case of Meyer wavelets (that do not have compact supports) and of the norm $\|.\|_\rho$:

Lemma 5. *Suppose the likelihood ratio satisfies for some constant λ:*

$$P_{f_{j,\varepsilon}}\left(\Lambda_n(f_{j,\varepsilon^k}, f_{j,\varepsilon}) \geq e^{-\lambda}\right) \geq p_* > 0,$$

uniformly for all $f_{j,\varepsilon}$ and all $k \in R_j$, where ε^k is equal to ε except for the kth element which is multiplied by -1. Then the following bound holds:

$$\max_{\varepsilon \in \{-1,+1\}^{R_j}} E_{f_{j,\varepsilon}}(\|\hat{f}_n - f_{j,\varepsilon}\|_\rho) \geq C 2^{j/2} \gamma e^{-\lambda} p_*,$$

where C is positive and depends only on ρ.

Similarly to the sparse case, the hypothesis of this lemma is satisfied if, for a small enough constant c:

$$E_{f_{j,\varepsilon}} |\ln\left(\Lambda_n(f_{j,\varepsilon^k}, f_{j,\varepsilon})\right)| \leq c.$$

Now the log-likelihood is equal to:

$$\ln\left(\Lambda_n(f_{j,\varepsilon^k}, f_{j,\varepsilon})\right) = \frac{2\gamma n^{1/2}}{\sigma} \int_0^1 \Psi_{j,k} \star Y(t) dW(t) - \frac{2\gamma^2 n}{\sigma^2} \int_0^1 [\Psi_{j,k} \star Y(t)]^2 dt.$$

Like before, we only need to dominate the following quantity:

$$B_n = \gamma^2 n E_{f_{j,\varepsilon}}\left(\int_0^1 (\Psi_{j,k} \star Y(t))^2 dt\right).$$

We use the same bound as in the sparse case, under assumption C_{low}. The parameters have to be chosen such that:

$$\gamma^2 n 2^{-2\nu j} \lesssim 1 \quad \text{and} \quad \gamma \lesssim 2^{-j(s+1/2)}.$$

Finally the regular rate is obtained for the following choices:

$$\gamma \asymp 2^{-j(s+1/2)}, \quad \text{and} \quad 2^j \asymp n^{1/(2s+2\nu+1)}.$$

Proof. of the lemma

The Meyer wavelet satisfies $\exists A > 0$ such that $|\psi(x)| \leq \frac{A}{1+|x|^2}$. Consequently:

$$\left(\int_{I_{j,k}} |\Psi_{j,k}(x)dx|^\rho\right)^{1/\rho} = 2^{j(\frac{1}{2}-\frac{1}{\rho})}\left(\int_0^1 |\sum_{l\in\mathbb{Z}} \psi(x+2^j l)|^\rho dx\right)^{1/\rho}$$

$$\geq 2^{j(\frac{1}{2}-\frac{1}{\rho})}\left(\int_0^1 |\psi(x)|^\rho dx - \sum_{l\in\mathbb{Z}^*}\int_0^1 |\psi(x+2^j l)|^\rho dx\right)^{1/\rho}$$

$$\geq 2^{j(\frac{1}{2}-\frac{1}{\rho})}\left(\int_0^1 |\psi(x)|^\rho dx - \frac{A^\rho}{2^{2\rho j}}\sum_{l\in\mathbb{N}^*}\frac{1}{(l/2)^{2\rho}}\right)^{1/\rho}$$

$$\geq c 2^{j(\frac{1}{2}-\frac{1}{\rho})},$$

for j large enough and $c > 0$ depends only on ρ.

Then using a concavity inequality and similar arguments as in the compact support case, we have:

$$\max_{\varepsilon} E_{f_{j,\varepsilon}}(\|\hat{f}_n - f_{j,\varepsilon}\|_\rho) \geq 2^{-2^j} \sum_{\varepsilon} E_{f_{j,\varepsilon}}[\sum_{k=0}^{2^j-1} \int_{I_{j,k}} |\hat{f}_n - f_{j,\varepsilon}|^\rho]^{\frac{1}{\rho}}$$

$$\geq 2^{-2^j+j(\frac{1}{\rho}-1)} \sum_{\varepsilon} \sum_{k=0}^{2^j-1} E_{f_{j,\varepsilon}}[\int_{I_{j,k}} |\hat{f}_n - f_{j,\varepsilon}|^\rho]^{\frac{1}{\rho}}$$

$$\geq 2^{-2^j+j(\frac{1}{\rho}-1)} \sum_{k=0}^{2^j-1} \sum_{\varepsilon|\varepsilon_k=1} E_{f_{j,\varepsilon}}[(\int_{I_{j,k}} |\hat{f}_n - f_{j,\varepsilon}|^\rho)^{\frac{1}{\rho}} + \Lambda_n(f_{j,\varepsilon^k}, f_{j,\varepsilon})(\int_{I_{j,k}} |\hat{f}_n - f_{j,\varepsilon^k}|^\rho)^{\frac{1}{\rho}}]$$

$$\geq 2^{-2^j+j(\frac{1}{\rho}-1)} \sum_{k=0}^{2^j-1} \sum_{\varepsilon|\varepsilon_k=1} E_{f_{j,\varepsilon}}[\delta I\{\int_{I_{j,k}} |\hat{f}_n - f_{j,\varepsilon}|^\rho \geq \delta^\rho\} + \Lambda_n(f_{j,\varepsilon^k}, f_{j,\varepsilon})\delta I\{\int_{I_{j,k}} |\hat{f}_n - f_{j,\varepsilon^k}|^\rho \geq \delta^\rho\}]$$

with $\delta = c\gamma 2^{j(\frac{1}{2}-\frac{1}{\rho})}$.

Noticing that

$$(\int_{I_{j,k}} |\hat{f}_n - f_{j,\varepsilon}|^\rho)^{1/\rho} + (\int_{I_{j,k}} |\hat{f}_n - f_{j,\varepsilon^k}|^\rho)^{1/\rho} \geq 2\gamma(\int_{I_{j,k}} |\Psi_{j,k}(x)|^\rho)^{1/\rho} \geq 2\gamma c 2^{j(\frac{1}{2}-\frac{1}{\rho})}$$

for j large enough, the end of the proof follows as in Härdle et al. [49]. $\square$

6.7.2   Upper bounds

Properties of the estimated wavelet coefficients

The performances of the thresholding estimators rest on the properties of the estimated wavelet coefficients $\hat{\beta}_{j,k}$. In the sequel we will also need properties for the estimators $\hat{\alpha}_{j,k}$ defined the same way as $\hat{\beta}_{j,k}$ in estimator (6.3) except with Φ instead of Ψ. We have the following results:

Proposition 6. *Under condition C_{up} we have for all $j \geq -1$, $k \in R_j$ and $r > 0$,*

$$E(|\hat{\beta}_{j,k} - \beta_{j,k}|^r) \lesssim (\frac{2^{\nu j}}{\sqrt{n}})^r \quad and \quad E(|\hat{\alpha}_{j,k} - \alpha_{j,k}|^r) \lesssim (\frac{2^{\nu j}}{\sqrt{n}})^r,$$

and there exist positive constants κ, and κ' such that for all $\lambda \geq 1$,

$$P(|\hat{\beta}_{j,k} - \beta_{j,k}| \geq \frac{2^{\nu j}}{\sqrt{n}}\lambda) \lesssim 2^{-\kappa\lambda^{\frac{2\alpha}{\alpha+1}}} \quad and \quad P(|\hat{\beta}_{j,k} - \beta_{j,k}| \geq \sqrt{\frac{U_j^Y}{n}}\lambda) \lesssim 2^{-\kappa'\lambda^2},$$

where the constants in the inequalities do not depend on j, k and λ.

Proof. of Proposition 1

Remark that conditionally to the process Y, $(\hat{\beta}_{j,k} - \beta_{j,k})$ is a centered gaussian variable with variance:

$$Var(|\hat{\beta}_{j,k} - \beta_{j,k}| \quad |Y) = E[\frac{\sigma^2}{n}\sum_{l\in\mathbb{Z}}|\frac{W_l}{Y_l}\Psi_{j,k,l}|^2 \quad |Y].$$

Since the Fourier transform of the Meyer wavelet is bounded by $2^{-j/2}$ and only $l \in [-(2^{j+1} - 1), -2^{j-2}] \cup [2^{j-2}, 2^{j+1} - 1]$ has to be considered, we have for some constant $C > 0$:

$$Var(|\hat{\beta}_{j,k} - \beta_{j,k}| \quad |Y) \leq CU_j^Y/n.$$

Thus the moment of order r of $(\hat{\beta}_{j,k} - \beta_{j,k})$ is bounded by

$$E(|\hat{\beta}_{j,k} - \beta_{j,k}|^r) \lesssim E[(Var(|\hat{\beta}_{j,k} - \beta_{j,k}| \quad |Y))^{r/2}] \lesssim E[(U_j^Y/n)^{r/2}],$$

and by similar arguments the same bound holds for $(\hat{\alpha}_{j,k} - \alpha_{j,k})$ because the support of the Fourier Transform of $\varphi_{j,k}$ is $\frac{4\pi}{3}[-2^j, 2^j]$.

For the deviation probability we use a probabilistic inequality for a centered standard gaussian variable Z. Conditionally to Y we have:

$$P(|\hat{\beta}_{j,k} - \beta_{j,k}| > \frac{2^{\nu j}}{\sqrt{n}}\lambda \quad |Y) \leq P(|Z| \geq \lambda\sqrt{2^{2\nu j}/(CU_j^Y)} \quad |Y)$$

$$\lesssim \frac{1}{\lambda\sqrt{2^{2\nu j}/(CU_j^Y)}}\exp(-\frac{\lambda^2 2^{2\nu j}}{2CU_j^Y}).$$

Then we take the expectation over Y, by Cauchy Schwartz we obtain for $\lambda \geq 1$:

$$P(|\hat{\beta}_{j,k} - \beta_{j,k}| > \frac{2^{\nu j}}{\sqrt{n}}\lambda) \lesssim \sqrt{E(\frac{U_j^Y}{2^{2\nu j}})E(\exp(-\frac{\lambda^2 2^{2\nu j}}{CU_j^Y}))}.$$

The end of the proof is directly deducible from the lemma below, and the last part of Proposition 1 is easily proved by replacing $2^{\nu j}$ by $\sqrt{U_j^Y}$ in the three inequalities above.

Lemma 6. *Let X_j be the following random variable: $X_j = \frac{U_j^Y}{2^{2\nu j}}$. For all $j \geq 0$ there exists positive constants C', C'', $C(.)$ such that for all $r > 0$:*

$$E(e^{-\frac{r}{X_j}}) \leq C'e^{-C''r^{\frac{\alpha}{\alpha+1}}}, \quad and \quad E(X_j^r) \leq C(r).$$

Proof. of the lemma

For all $r > 0$ we have:

$$\begin{aligned}
E(e^{-\frac{r}{X_j}}) &= \int_0^1 P(e^{-\frac{r}{X_j}} \geq u)du \\
&= r \int_0^{+\infty} P(X_j \geq 1/u)e^{-ru}du \\
&\leq r \int_0^1 P(X_j \geq 1/u)e^{-ru}du + e^{-r} \\
&\lesssim r \int_0^1 e^{-ru-c/u^\alpha}du + e^{-r},
\end{aligned}$$

and one can check that there exists $C'' > 0$ such that $\int_0^1 e^{-ru-c/u^\alpha}du \lesssim e^{-C''r^{\frac{\alpha}{\alpha+1}}}$.

The second part of the lemma is easily proved by using similar arguments.

$\square$

$\square$

Proof of the sharp rates

In the regular and critical zones, estimator (6.3) is not optimal up to a logarithmic factor. In order to show that the rates of Theorem 1 are sharp, we exhibit estimators achieving the rates of Theorem 2. Those are not as interesting in practice as (6.3), since they depend on characteristics of f, ie they are not adaptive.

We will use the following bound to estimate the risks, which holds for any $-1 \leq j_m \leq j_M \leq \infty$ and any set of random or deterministic coefficients $\widetilde{\beta}_{j,k}$ such that the quantities below are finite:

$$E\| \sum_{j_m \leq j \leq j_M} \sum_{k \in R_j} \widetilde{\beta}_{j,k}\Psi_{j,k}\|_\rho \lesssim \sum_{j_m \leq j \leq j_M} 2^{j(\frac{1}{2}-\frac{1}{\rho})}\big(\sum_{k \in R_j} E|\widetilde{\beta}_{j,k}|^\rho\big)^{\frac{1}{\rho}}. \tag{6.5}$$

The proof is immediate by Minkowski inequality, the fact that

$$\| \sum_{k \in R_j} \widetilde{\beta}_{j,k}\Psi_{j,k}\|_\rho \asymp 2^{j(\frac{1}{2}-\frac{1}{\rho})}\|\widetilde{\beta}_{j,.}\|_{l_\rho},$$

as established in Meyer [68], and a concavity argument.

Let us denote: $\nu' = \nu + 1/2$ and $\varepsilon = ps - \nu'(\rho - p)$. We distinguish two cases: $\rho \leq p$ and $p < \rho$. In the first case $M(s,p,q,R)$ is included in the regular zone. By concavity we have:

$$\inf_{\hat{f}_n} \sup_{f \in M(s,p,q,R)} E_f\|\hat{f}_n - f\|_\rho \leq \inf_{\hat{f}_n} \sup_{f \in M(s,p,q,R)} E_f\|\hat{f}_n - f\|_p.$$

So seeing the expected rate only the case $\rho = p$ needs to be considered. We take the following linear estimator:

$$\hat{f}_n = \sum_{k \in R_{j_1}} \hat{\alpha}_{j_1,k}\Phi_{j_1,k}.$$

For any $f \in M(s, p, q, R)$ the risk is composed of a bias error and a stochastic error:

$$E_f \|\hat{f}_n - f\|_p \leq A_s + A_s,$$

with:

$$A_s = E\| \sum_{k \in R_{j_1}} (\hat{\alpha}_{j_1,k} - \alpha_{j_1,k}) \Phi_{j_1,k} \|_p \lesssim 2^{j_1(\frac{1}{2} - \frac{1}{p})} [\sum_{k \in R_{j_1}} E|\hat{\alpha}_{j_1,k} - \alpha_{j_1,k}|^p]^{\frac{1}{p}} \lesssim (\frac{2^{\nu j_1}}{\sqrt{n}}) 2^{\frac{j_1}{2}} = \frac{2^{\nu' j_1}}{\sqrt{n}},$$

$$A_b = \| \sum_{j > j_1} \sum_{k \in R_j} \beta_{j,k} \Psi_{j,k} \|_p \lesssim \sum_{j > j_1} 2^{j(\frac{1}{2} - \frac{1}{p})} (\sum_{k \in R_j} |\beta_{j,k}|^p)^{\frac{1}{p}} \lesssim \sum_{j > j_1} 2^{j(\frac{1}{2} - \frac{1}{p})} 2^{-j(s + \frac{1}{2} - \frac{1}{p})} \lesssim 2^{-j_1 s},$$

and we obtain the rate by choosing $j_1 = [\frac{log_2(n)}{2s + 2\nu'}]$.

In the second case $(p < \rho)$ we consider the following estimator:

$$\hat{f}_n = \sum_{k \in R_{j_1+1}} \hat{\alpha}_{j_1+1,k} \Phi_{j_1+1,k} + \sum_{j_1 < j < j_2} \sum_{k \in R_j} \hat{\beta}_{j,k} I_{\{|\hat{\beta}_{j,k}| \geq \lambda_j\}} \Psi_{j,k},$$

where:

$$2^{j_1} \approx n^{\frac{1}{2s+2\nu'}}, \quad 2^{j_2} \approx (\frac{n}{\log n})^{\frac{1}{2(s+\nu'-\frac{1}{p})}}, \quad \lambda_j = \eta \sqrt{U_j^Y (j - j_1)/n},$$

and $\eta > 2(\frac{2\rho\nu'}{\kappa'})^{\frac{1}{2}}$, so that we have by Proposition 1: $P(|\hat{\beta}_{j,k} - \beta_{j,k}| \geq \lambda_j) \lesssim 2^{-\kappa'\eta^2(j-j_1)}$.

We proceed as in Donoho et al. [36] by distinguishing six terms:

$$\hat{f}_n - f = \sum_{k \in R_j} (\hat{\alpha}_{j_1,k} - \alpha_{j_1,k}) \Phi_{j,k} + \sum_{j \geq j_2} \sum_{k \in R_j} \beta_{j,k} \Psi_{j,k}$$

$$+ \sum_{j_1 < j < j_2} \sum_{k \in R_j} (\hat{\beta}_{j,k} - \beta_{j,k}) \Psi_{j,k} [I_{\{|\hat{\beta}_{j,k}| \geq \lambda_j, |\beta_{j,k}| < \lambda_j/2\}} + I_{\{|\hat{\beta}_{j,k}| \geq \lambda_j, |\beta_{j,k}| \geq \lambda_j/2\}}]$$

$$+ \sum_{j_1 < j < j_2} \sum_{k \in R_j} \beta_{j,k} \Psi_{j,k} [I_{\{|\hat{\beta}_{j,k}| < \lambda_j, |\beta_{j,k}| \geq 2\lambda_j\}} + I_{\{|\hat{\beta}_{j,k}| < \lambda_j, |\beta_{j,k}| < 2\lambda_j\}}]$$

$$= e_s + e_b + e_{bs} + e_{bb} + e_{sb} + e_{ss}.$$

Like before the stochastic error is bounded by:

$$E(\|e_s\|_\rho) \lesssim \frac{2^{\nu' j_1}}{\sqrt{n}},$$

and by using Sobolev embeddings it is easy to see that:

$$E(\|e_b\|_\rho) \lesssim 2^{-j_2(s - \frac{1}{p} + \frac{1}{\rho})}.$$

The terms e_{bs} and e_{sb} can be grouped together because of the two following assertions: $\{|\hat{\beta}_{j,k}| < \lambda_j, |\beta_{j,k}| \geq 2\lambda_j\} \cup \{|\hat{\beta}_{j,k}| \geq \lambda_j, |\beta_{j,k}| < \lambda_j/2\} \subset \{|\hat{\beta}_{j,k} - \beta_{j,k}| > \lambda_j/2\}$, and $[|\hat{\beta}_{j,k}| < \lambda_j, |\beta_{j,k}| \geq 2\lambda_j] \Rightarrow [|\beta_{j,k}| \leq 2|\hat{\beta}_{j,k} - \beta_{j,k}|]$. Consequently:

$$E(\|e_{bs}\|_\rho + \|e_{sb}\|_\rho) \lesssim \sum_{j_1 < j < j_2} 2^{j(\frac{1}{2}-\frac{1}{\rho})}(E\sum_{k \in R_j} |\hat{\beta}_{j,k} - \beta_{j,k}|^\rho I_{\{|\hat{\beta}_{j,k} - \beta_{j,k}| > \lambda_j/2\}})^{\frac{1}{\rho}}$$

$$\leq \sum_{j_1 < j < j_2} 2^{j(\frac{1}{2}-\frac{1}{\rho})}(\sum_{k \in R_j} (E|\hat{\beta}_{j,k} - \beta_{j,k}|^{2\rho})^{\frac{1}{2}}(P\{|\hat{\beta}_{j,k} - \beta_{j,k}| > \lambda_j/2\})^{\frac{1}{2}})^{\frac{1}{\rho}}$$

$$\lesssim \sum_{j_1 < j < j_2} 2^{j(\frac{1}{2}-\frac{1}{\rho})}(\sum_{k \in R_j} \frac{2^{\rho\nu j}}{n^{\frac{\rho}{2}}} 2^{-\frac{\kappa'(\eta/2)^2(j-j_1)}{2}})^{\frac{1}{\rho}}$$

$$\leq \frac{2^{\nu' j_1}}{n^{\frac{1}{2}}} \sum_{0 < j < j_2 - j_1} 2^{(\nu' - \frac{\kappa'(\eta/2)^2}{2\rho})j}$$

$$\lesssim \frac{2^{\nu' j_1}}{n^{\frac{1}{2}}},$$

where we used Cauchy Schwartz inequality and Proposition 1.

For e_{bb} we use the characterization of Besov spaces:

$$E(\|e_{bb}\|_\rho) \lesssim \sum_{j_1 < j < j_2} 2^{j(\frac{1}{2}-\frac{1}{\rho})}(\sum_{k \in R_j} E|\hat{\beta}_{j,k} - \beta_{j,k}|^\rho I_{\{|\beta_{j,k}| \geq \lambda_j/2\}})^{\frac{1}{\rho}}$$

$$\lesssim \sum_{j_1 < j < j_2} 2^{j(\frac{1}{2}-\frac{1}{\rho})}(\sum_{k \in R_j} \frac{2^{\rho\nu j}}{n^{\frac{\rho}{2}}} (\frac{|\beta_{j,k}|}{\lambda_j/2})^p)^{\frac{1}{\rho}}$$

$$\lesssim \sum_{j_1 < j < j_2} (\frac{2^{j(\frac{\rho}{2}-1+(\rho-p)\nu)}}{n^{\frac{\rho-p}{2}}(j-j_1)^{\frac{p}{2}}} 2^{-pj(s+\frac{1}{2}-\frac{1}{p})}(\|f\|_{p,\infty}^s)^p)^{\frac{1}{\rho}}$$

$$\lesssim \frac{1}{n^{\frac{\rho-p}{2\rho}}} \sum_{j_1 < j < j_2} (\frac{2^{-\varepsilon j}}{(j-j_1)^{\frac{p}{2}}})^{\frac{1}{\rho}}.$$

Lastly for e_{ss} we remark that $|\beta_{j,k}|^\rho \leq (2\lambda_j)^{\rho-p}|\beta_{j,k}|^p$ and we use again the characterization of Besov spaces:

$$E(\|e_{ss}\|_\rho) \lesssim \sum_{j_1 < j < j_2} 2^{j(\frac{1}{2}-\frac{1}{\rho})}((2\lambda_j)^{\rho-p} \sum_{k \in R_j} |\beta_{j,k}|^p)^{\frac{1}{\rho}}$$

$$\lesssim \sum_{j_1 < j < j_2} (\frac{2^{j(-ps+\nu'(\rho-p))}}{n^{\frac{\rho-p}{2}}}(j-j_1)^{\frac{\rho-p}{2}}(\|f\|_{p,\infty}^s)^p)^{\frac{1}{\rho}}$$

$$\lesssim \frac{1}{n^{\frac{\rho-p}{2\rho}}} \sum_{j_1 < j < j_2} (2^{-\varepsilon j}(j-j_1)^{\frac{\rho-p}{2}})^{\frac{1}{\rho}}$$

According to these bounds e_{bs}, e_{sb} and e_s are of the same order and e_{ss} dominates e_{bb}, so we choose j_1 and j_2 so as to balance the bounds of e_b, e_s and e_{ss}.
In the regular zone we have:

$$E(\|e_{ss}\|_\rho) \lesssim (\frac{2^{-\varepsilon j_1}}{n^{\frac{\rho-p}{2}}})^{\frac{1}{\rho}},$$

and in the sparse zone:

$$E(\|e_{ss}\|_\rho) \lesssim \Big(\frac{j_2^{\frac{\rho-p}{2}} 2^{-\varepsilon j_2}}{n^{\frac{\rho-p}{2}}}\Big)^{\frac{1}{\rho}}.$$

Thus with the announced choices of j_1 and j_2 we get the prescribed rates in both zones.

Lastly in the critical zone we change the upper bound of $(\beta_{j,k})$ in e_{bb} and e_{ss} by using:

$$\sum_{j_1 < j < j_2} \Big(2^{pj(s+\frac{1}{2}-\frac{1}{p})} \sum_{k \in R_j} |\beta_{j,k}|^p\Big)^{\frac{1}{\rho}} \lesssim (j_2 - j_1)^{1-\frac{p}{\rho q}} (\|f\|_{p,q}^s)^{\frac{p}{\rho}} \quad \text{if} \quad \frac{p}{\rho} < q,$$

$$\lesssim (\|f\|_{p,q}^s)^q \quad \text{if} \quad \frac{p}{\rho} \geq q.$$

Here again e_{ss} is dominant and of the order: $E(\|e_{ss}\|_\rho) \lesssim \big(\frac{j_2}{n}\big)^{\frac{\rho-p}{2\rho}} j_2^{(1-\frac{p}{\rho q})+}$, hence the extra logarithmic factor.

Proof of the rates of the adaptive estimator

To prove Theorem 3 we use a theorem for thresholding algorithms established by Kerkyacharian and Picard (Theorem 3.1 in Kerkyacharian and Picard [59]) which holds in a very general setting where one wants to estimate an unknown function f thanks to observations in a sequence of statistical models $(E_n)_{n \in \mathbb{N}}$. It uses the Temlyakov inequalities, let us first recall this notion.

Definition 6. *Let e_n be a basis in L^ρ. It satisfies the Temlyakov property if there are absolute constants c and C such that for all $\Lambda \in \mathbb{N}$:*

$$c \sum_{n \in \Lambda} \int |e_n(x)|^\rho dx \leq \int \{\sum_{n \in \Lambda} \int |e_n(x)|^2\}^{\rho/2} dx \leq C \sum_{n \in \Lambda} \int |e_n(x)|^\rho dx.$$

Now let $(\psi_{j,k})_{j,k}$ denote a periodized wavelet basis and let $\rho > 1$ and $0 < r < \rho$. Assume that there exist a positive value $\delta > 0$, a positive sequence $(\sigma_j)_{j \geq -1}$, a positive sequence c_n tending to 0, and a subset Λ_n of $\mathbb{N}^2$ such that :

$$|\Lambda_n| \sim c_n^{-\delta} \text{ where } |S| \text{ denotes the cardinal of the set } S, \tag{6.6}$$

$$(\sigma_j \psi_{j,k})_{j,k} \text{ satisfies the Temlyakov property,} \tag{6.7}$$

$$\sup_n [\mu\{\Lambda_n\} c_n^\rho] < \infty, \tag{6.8}$$

where μ is the following measure on $\mathbb{N}^2$:

$$\mu(j,k) = \|\sigma_j \psi_{j,k}\|_\rho^\rho = 2^{j(\rho/2-1)} \sigma_j^\rho \|\psi\|_\rho^\rho.$$

Assume also that we have a statistical procedure yielding estimators $\hat{\beta}_{j,k}$ of the wavelet coefficients $\beta_{j,k}$ of f in the basis $(\psi_{j,k})_{j,k}$ and a positive value $\eta > 0$ such that for all $(j,k) \in \Lambda_n$:

$$E(|\hat{\beta}_{j,k} - \beta_{j,k}|^{2\rho}) \leq C(c_n \sigma_j)^{2\rho}, \tag{6.9}$$

$$P(|\hat{\beta}_{j,k} - \beta_{j,k}| \geq \eta \sigma_j c_n / 2) \leq C \min(c_n^{2\rho}, c_n^4). \tag{6.10}$$

Finally let $l_{r,\infty}(\mu)$ and $A(c_n^{\rho-r})$ be the following spaces and let $\hat{f}_n$ be the following estimator:

$$l_{r,\infty}(\mu) = \{f, \quad \sup_{\lambda > 0} [\lambda^q \mu\{(j,k)/|\beta_{j,k}| > \sigma_j \lambda\}] < \infty\},$$

$$A(c_n^{\rho-r}) = \{f, \quad c_n^{-(\rho-r)} \|f - \sum_{\kappa \in \Lambda_n} \beta_\kappa \psi_\kappa\|_\rho^\rho < \infty\},$$

$$\hat{f}_n = \sum_{j,k \in \Lambda_n} \hat{\beta}_{j,k} I_{\{|\hat{\beta}_{j,k}| \geq \eta \sigma_j c_n\}} \psi_{j,k}.$$

Theorem 18. *Using the objects defined above and under the hypotheses* (6.6) *to* (6.10), *we have the following equivalence:*

$$E\|\hat{f}_n - f\|_\rho^\rho \lesssim c_n^{\rho-r} \quad \Longleftrightarrow \quad f \in l_{r,\infty}(\mu) \cap A(c_n^{\rho-r}).$$

We adapt this to estimator $\hat{f}_n^D$ by setting, for given $\rho > 1$, $p > 1$, $s > 1/p$ and $q > 1$:

$$c_n = \sqrt{\frac{\log(n)^{\frac{\alpha+1}{\alpha}}}{n}}, \quad \sigma_j = 2^{\nu j}, \quad 2^{j_1} \approx \{\frac{n}{\log(n)^{\frac{\alpha+1}{\alpha}}}\}^{\frac{1}{1+2\nu}}, \quad \Lambda_n = \{(j,k)| -1 \leq j \leq j_1, k \in R_j\}.$$

With these choices we have:

$$|\Lambda_n| \asymp 2^{j_1} \asymp c_n^{-2/(1+2\nu)},$$

$$\mu(\Lambda_n) = \sum_{j=0}^{j_1-1} 2^j 2^{j(\rho/2-1)} 2^{\rho \nu j} \asymp 2^{j_1 \rho(\nu+1/2)}.$$

Consequently (6.8) and (6.6) hold with $\delta = 2/(1+2\nu)$. Condition (6.7) is also satisfied, the proof can be found in Johnstone et al. [53]. Moreover thanks to Proposition 1, it is easy to establish that the estimators $\hat{\beta}_{j,k}$ used by (6.3) satisfy (6.9) and (6.10) as soon as $\eta > 2(\frac{max(2,\rho)}{\kappa})^{\frac{\alpha+1}{2\alpha}}$.

Then we prove Theorem 3 by setting r such that the right hand side of the inequality in the first point of the theorem corresponds to the rates in the sparse and in the regular case, ie:

$$r = \rho - 2\rho \frac{s - 1/p + 1/\rho}{2s + 2\nu + 1 - 2/p},$$

or

$$r = \rho - 2\rho \frac{s}{2s + 2\nu + 1},$$

and by showing that the space over which the risk is maximized is included in the maxiset, if we add the condition $q \leq p$ in the critical case $\frac{2s+2\nu+1}{\rho} = \frac{2\nu+1}{p}$:

$$M(s,p,q,R) \subset l_{r,\infty}(\mu) \cap A(c_n^{\rho-r}).$$

The inclusion $M(s,p,q,R) \subset A(c_n^{\rho-r})$ is established in Johnstone et al. [53], and the following proof of $M(s,p,q,R) \subset l_{r,\infty}(\mu)$ uses the same arguments as Kerkyacharian et al. [58] for the boxcar blur. We have:

$$\mu\{(j,k): |\beta_{j,k}| > 2^{\nu j}\lambda\} = \sum_{j\geq 0,\, k\in R_j} 2^{j(\rho(\nu+1/2)-1)} I\{|\beta_{j,k}| > 2^{\nu j}\lambda\}$$

$$\leq \sum_j (2^{j\rho(\nu+1/2)}) \wedge (2^{j(\rho(\nu+1/2)-1)} \sum_k (|\beta_{j,k}|/(2^{\nu j}\lambda))^p$$

$$\leq \sum_j (2^{j\rho(\nu+1/2)}) \wedge (\frac{2^{-j(sp+\nu'p-\nu'\rho)}}{\lambda^p}\varepsilon_j^p),$$

where $\nu' = \nu + 1/2$ and $\varepsilon_j \in l_q$. We cut the sum at J such that $2^J \asymp \lambda^{-r/(\nu'\rho)}$.

In the regular case we have:

$$\mu\{(j,k): |\beta_{j,k}| > 2^{\nu j}\lambda\} \leq \lambda^{-r} + \frac{\lambda^{(sp-\nu'(\rho-p))\frac{r}{\nu'\rho}}}{\lambda^p},$$

and the power of λ in the second term is also exactly $-r$.

In the critical case we obtain, since $q \leq p$:

$$\mu\{(j,k): |\beta_{j,k}| > 2^{\nu j}\lambda\} \leq \lambda^{-r} + \frac{\sum_j \varepsilon_j^p}{\lambda^p} \lesssim \lambda^{-r} + \frac{\sum_j \varepsilon_j^q}{\lambda^p} \lesssim \lambda^{-r} + \lambda^{-p},$$

and $r = p$ in this case.

Lastly in the sparse case (where $r \geq p$ is satisfied) we use the Sobolev embedding $B_{p,q}^s \subset B_{r,q}^{s'}$ with $s' = s - 1/p + 1/r$. We proceed as before by cutting the sum at J such that $2^J \asymp \lambda^{-r/(\nu'\rho)}$ and noticing that $s'r + \nu'r - \nu'\rho = 0$. There exists $\widetilde{\varepsilon}_j \in l_r$ such that:

$$\mu\{(j,k): |\beta_{j,k}| > 2^{\nu j}\lambda\} \leq \sum_j (2^{j\rho\nu'}) \wedge (2^{j(\rho\nu'-1)} \sum_k (|\beta_{j,k}|/(2^{\nu j}\lambda))^r$$

$$\leq \sum_j (2^{j\rho\nu'}) \wedge (\frac{\widetilde{\varepsilon}_j^r}{\lambda^r})$$

$$\lesssim \lambda^{-r}.$$

Thus $\mu\{(j,k): 2^{\nu j}\lambda\} \lesssim 1/\lambda^r$ for both values of r, and finally using the equivalence in Theorem 4 and Jensen inequality we obtain the prescribed rates for $E\|\hat{f}_n^D - f\|_\rho$.

Chapter 7

Numerical performances of a warped wavelet estimation procedure for regression in random design

Ce chapitre est une version légèrement différente d'un article écrit en collaboration avec Christophe Chesneau, et soumis à une revue.

Abstract: The purpose of this chapter is to investigate the numerical performances of the hard thresholding procedure introduced by Kerkyacharian and Picard [57] for the non-parametric regression model with random design. That construction adopts a new approach by using a wavelet basis warped with a function depending on the design, which enables to estimate regression functions under mild assumptions on the design. We compare our numerical properties to those obtained for other constructions based on hard wavelet thresholding. The performances are evaluated on numerous simulated data sets covering a broad variety of settings including known and unknown design density models, and also on real data sets.

7.1   Motivation

Suppose we observe data $(Y_1, X_1), \ldots, (Y_n, X_n)$ where $(Y_i)_{i=1,\ldots,n}$ is characterized by the following equation:

$$Y_i = f(X_i) + s\varepsilon_i, \quad i = 1, \ldots, n, \tag{7.1}$$

the ε_i's are i.i.d centered standard normal variables, s is a fixed noise level, and the X_i's are i.i.d random variables representing the design points with density g. The aim is to recover the unknown function f from the observations. To reach this aim, we propose to focus our attention on reconstruction methods using wavelet analysis.

Wavelet thresholding algorithms are popular methods in curve estimation, as well as in nonparametric estimation problems in general. Their advantages with respect to linear procedures are well known: they provide adaptive estimators enjoying near minimax properties in a wide variety of settings, whereas linear estimators can be far from optimal in many situations as established in a series of paper by Donoho and Johnstone [31, 30], and Donoho et al. [32, 33], Donoho [28]).

We will concentrate here on the regression problem with non equispaced samples defined above. There exist numerous methods in this setting. Among them let us cite Hall and Turlach [47], Antoniadis et al. [5], Cai and Brown [14], and Maxim [66]. Compared to standard algorithms, the thresholding is notably more complicated because it has to incorporate the variations of the density of the design. As for general minimax results, a study over various function spaces and for different risks can be found in the books of Korostelev and Tsybakov [61] and Tsybakov [89] for non-parametric estimation problems, including regression with random design.

Recently a quite different algorithm was developed in Kerkyacharian and Picard [57]. The procedure stays very close to the equispaced Donoho and Johnstone's Visushrink procedure, and thus is very simple in its form (preliminary estimators are no longer needed) and in its implementation (the standard uniform threshold suffices). On the other side, the projection is done on an unusual non-orthonormal basis, called warped wavelet basis, so their analytic properties need to be studied to derive the performances of the estimator. Such a basis can be defined as a usual wavelet basis composed with the repartition function $G(y) = \int_0^y g(t)dt$. Some theoretical results, including maxiset properties (see Cohen et al. [22] and Kerkyacharian and Picard [56]) were established in their paper. Another important advantage of the warped basis estimator is that it is near optimal in the minimax sense over a large class of function spaces for a wide variety of design densities, not necessarily bounded above and below as generally required by other wavelet estimators. Basically, the condition on the design refers to the Muckenhoupt weights theory introduced in Muckenhoupt [70].

The purpose of this paper is to provide numerical performances for the warped basis procedure and to compare these results to those obtained for other wavelet procedures based on the hard thresholding rules. In many constructions, the first step consists in determining a function $Y(x)$ of the form:

$$Y(x) = \sum_m w_m(x) Y_m$$

where $w_m(x)$ is a sequence of functions suitably chosen. For instance, in Hall and Turlach [47] the w_m's correspond to a polynomial which depends to the variable $(X_i)_{i=1,...,n}$. In Cai and Brown [14] (and in Maxim [66]), the w_m's corresponds to scale wavelets warped with G. In Antoniadis et al. [5], the random design is transformed into equispaced data via a binning method and the w_m's are defined by scale wavelets. In a second step, the function Y is expanded on a standard wavelet basis and a hard thresholding algorithm is performed. In all the techniques described above, the thresholds have similar forms and depend on the quantity $\sup_t \frac{1}{g(t)}$, which corresponds to an upper bound for the variance of the estimated wavelet coefficients. For the sake of conciseness, only the construction developed by Cai and Brown [14] will be considered for the simulations since it appears to be relatively representative of these kinds of methods.

In all the estimation procedures, the nature of the density g plays an important role. First we consider the usual context of known and bounded design density g and we investigate which characteristics of the design mainly affect the behavior of each estimator. Second we consider the context of unbalanced designs, and we propose an adaptation of Cai and Brown's procedure to allow vanishing densities (the minimax properties of such a procedure are not established then, here we only provide a numerical comparison). Third, we examine the case of unknown densities.

The chapter is organized as follows. Section 2 introduces basics on wavelets and the main procedures. Section 3 gives a qualitative comparison of the estimators described below, and section 4 presents the results of the simulation study. Lastly in Section 5 the two procedures are applied to real data sets.

7.2 Estimation procedures

Let us briefly summarize the basics on wavelets that will be needed in the later sections. Let φ and ψ be respectively a scaling function and a wavelet associated to a multiresolution analysis on $\mathbb{R}$. With an appropriate treatment at the boundaries of these functions, any f of $\mathbb{L}^2([0,1])$ can be expanded into a wavelet series as:

$$f(x) = \sum_{j,k \in \Lambda} \beta_{j,k} \psi_{j,k}(x), \qquad \beta_{j,k} = \int_0^1 f(t)\psi_{j,k}(t)dt, \quad x \in [0,1],$$

where $\Lambda = \{(j,k)| -1 \leq j \leq \infty, 0 \leq k \leq 2^j - 1\}$, $\psi_{j,k}(.) = 2^{\frac{j}{2}}\psi(2^j. - k)$, $\varphi_{j,k}(.) = 2^{\frac{j}{2}}\varphi(2^j. - k)$, and for convenience we have set $\psi_{-1,k}(.) = \varphi_{0,k}(.)$. See Cohen et al. [21] and Meyer [67] for further details on wavelet bases on the unit interval $[0,1]$. For wavelets on the line we refer the reader to Daubechies [26], and the books Meyer [68] and Mallat [64].

7.2.1 Procedure based on warped wavelets

Let us consider the regression problem described in (7.1). Let us recall that the function G is defined by:

$$G(x) = \mathbb{P}(X_1 \leq x) = \int_0^x g(t)dt, \quad x \in [0,1].$$

In Kerkyacharian and Picard [57] one proposes a construction where the unknown function is expanded on a warped basis instead of a regular wavelet basis. Proceeding in such a way, the estimates of the coefficients become more natural. Let us briefly describe the construction of this procedure.

In the case of known g, we consider the following estimator:

$$\hat{\beta}_{j,k}^{\dagger} = \frac{1}{n} \sum_{i=1}^{n} Y_i \psi_{j,k}(G(X_i)),$$

for (j,k) in the set:

$$\Lambda_n = \{(j,k)| -1 \le j \le j_1(n),\ 0 \le k \le 2^j - 1\},$$

where $j_1(n)$ is an integer such that $2^{j_1(n)}$ is of the order $\sqrt{\frac{n}{\ln(n)}}$, and we perform a hard thresholding algorithm:

$$\hat{f}^{\dagger}(t) = \sum_{j,k\in\Lambda_n} \hat{\beta}_{j,k}^{\dagger} 1_{\left\{|\hat{\beta}_{j,k}^{\dagger}| \ge \kappa s \sqrt{\frac{2\ln(n)}{n}}\right\}} \psi_{j,k}(G(t)), \quad t \in [0,1],$$

where κ is a large enough constant.

In the sequel, we will refer to this estimator as **estimator** 1.

7.2.2   Procedure based on usual wavelets

Estimator 1 will be compared to a wavelet thresholding procedure based on the construction of Cai and Brown [14] in the case where the density of the design g is known and bounded from below. The construction consists in the following three steps:

1. Compute a preliminary estimator $\hat{f}$ as if the data were equispaced by using the scaling function at high resolution level $j_2(n) = \log_2(n)$:

$$\hat{f}(t) = \frac{1}{\sqrt{n}} \sum_{i=1}^{n} Y_i \varphi_{j_2,i}(t).$$

2. Warp $\hat{f}$ by the function G and compute the wavelet coefficients of the resulting function:

$$\hat{\beta}_{j,k}^{*} = \int_0^1 \hat{f}(G(t))\psi_{j,k}(t)dt,$$

for (j,k) in the set:

$$\Omega_n = \{(j,k)| -1 \le j \le j_2,\ 0 \le k \le 2^j - 1\}.$$

3. Perform a hard thresholding algorithm:

$$\hat{f}^{*}(t) = \sum_{j,k\in\Omega_n} \hat{\beta}_{j,k}^{*} 1_{\left\{|\hat{\beta}_{j,k}^{*}| \ge \kappa s \lambda_{j,k}^{*} \sqrt{\frac{2\ln(n)}{n}}\right\}} \psi_{j,k}(t), \quad t \in [0,1], \tag{7.2}$$

where

$$\lambda_{j,k}^* = \sqrt{\max_{t \in S_{j,k}} \frac{1}{g(t)}},$$

κ is a positive constant, $S_{j,k} = [2^{-j}k, 2^{-j}(k+N)]$ and N is the length of the filter associated to the wavelet.

In the sequel, we will refer to this estimator as **estimator** 2.

Comments. The choice of the threshold is linked to the variance of the $\hat{\beta}_{j,k}^*$. Following the Subsection 3.3 of Cai and Brown [14], we have:

$$nVar(\hat{\beta}_{j,k}^*) = \sum_{i=1}^{n} \left(\int_0^1 \varphi_{j_2,k}(G(x))\psi_{j,k}(x)dx \right)^2 \leq \int_{S_{j,k}} \psi_{j,k}^2(t)\frac{1}{g(t)}dt = u_{j,k}^2$$

and the threshold $\lambda_{j,k}^*$ is chosen in such a way that:

$$u_{j,k}^2 \leq (\lambda_{j,k}^*)^2.$$

In practice $u_{j,k}$ is difficult to compute, that is why $\lambda_{j,k}^*$ is used instead. In a second part of the study we propose a slight modification of estimator 2, by adapting the thresholds so as to allow constructions for vanishing densities too. Let us suppose that $\frac{1}{g}$ belongs to $\mathbb{L}^1([0,1])$ and consider the thresholding procedure (7.2) in which we replace $\lambda_{j,k}^*$ by another bound of $u_{j,k}$ defined as:

$$\widetilde{\lambda}_{j,k} = \sqrt{2^j \left(\int_{S_{j,k}} \frac{1}{g(t)}dt \right)}.$$

In the sequel, we will refer to this estimator as **estimator** $2'$.

Remark 7.2.1. *In the simulation study we will consider the case of unknown noise level s. The thresholds are thus modified by replacing s by an estimator:*

$$\hat{s} = \sqrt{\frac{1}{2(n-2)} \sum_{i=2}^{n} (Y_{(i)} - Y_{(i-1)})^2},$$

where each $Y_{(i)}$ refers to the value Y_k such that X_k is the i-th higher coordinate of the vector $(X_j)_{1 \leq j \leq n}$.

7.3 Preliminary comparison of the two estimators

7.3.1 Implementation

Thresholding algorithms

Obviously, estimator 2 (and $2'$) is more difficult to implement than estimator 1. It requires each coefficient to be compared to a specific value recalculated for each scale and shift parameter. On the contrary, the thresholds of estimator 1 are simple, and approximations
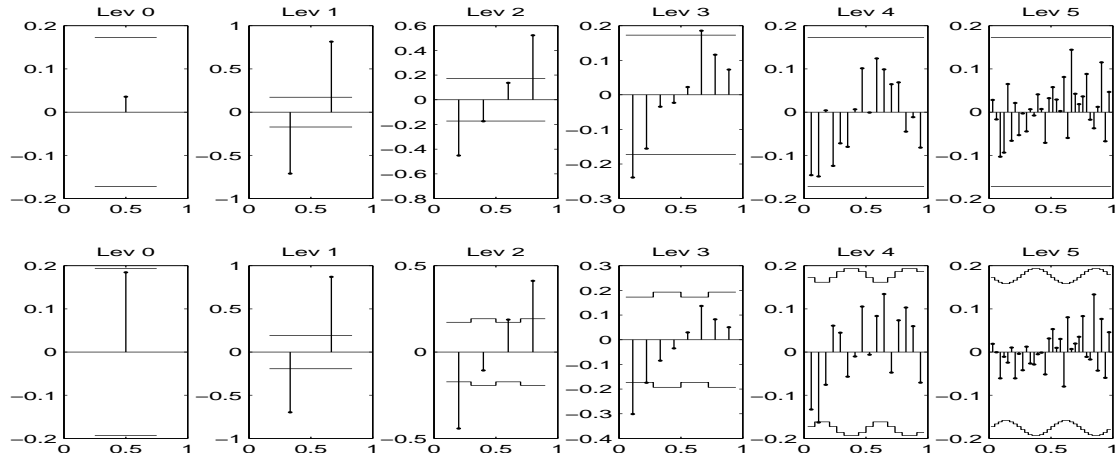
Figure 7.1: Coefficients (stems) and their corresponding thresholds (stairs) for estimator 1 (top), estimator 2 (bottom) and each level of resolution (from left to right)

of the coefficients can be computed very easily. Indeed if G is replaced by the empirical distribution function $\hat{G}_n$ in the expression of $\hat{\beta}_{j,k}^{\dagger}$ one obtains the following coefficients:

$$\hat{\beta}_{j,k} = \frac{1}{n} \sum_{i=1}^{n} Y_i \psi_{j,k}(\frac{i}{n}),$$

which can be obtained directly by performing a wavelet decomposition of the vector Y. These coefficients were used in the sequel for estimator 1 instead of coefficients $\hat{\beta}_{\lambda}^{\dagger}$.

The differences are illustrated on figure 7.1: as a toy example, the wavelet coefficients and the thresholds for a 'Sine' regression function and a 'Sine' design density (see their representations further in this paper) were computed with 2^6 observations and using the Haar basis. The figure represents the estimated detail coefficients and their thresholds from the coarsest ($j = 0$) to the highest ($j = 5$) resolution level, for estimator 1 (top) and estimator 2 (bottom). Estimator 1 needs constant thresholds, whatever the scale and the shift parameter, whereas for estimator 2 the thresholds vary with respect to the density g: the lower g on the interval $[\frac{k}{2^j}, \frac{k+1}{2^j}]$, the higher the threshold.

The case of unknown densities

In the case where g is unknown, we replace G wherever it appears in the construction of estimators 1 and 2 or 2' by the empirical distribution function of the X_i's:

$$\hat{G}_n(x) = \frac{1}{n} \sum_{i=1}^{n} 1_{\{X_i \leq x\}}.$$

Then adapting estimator 1 is quite easy: we only need to replace G in the warped basis. In the Cai and Brown procedure: first we have to warp $\hat{f}_{j_2}$ with G_n instead of G in step 1 and secondly we have to replace the thresholds in step 3 by estimators, thus a density
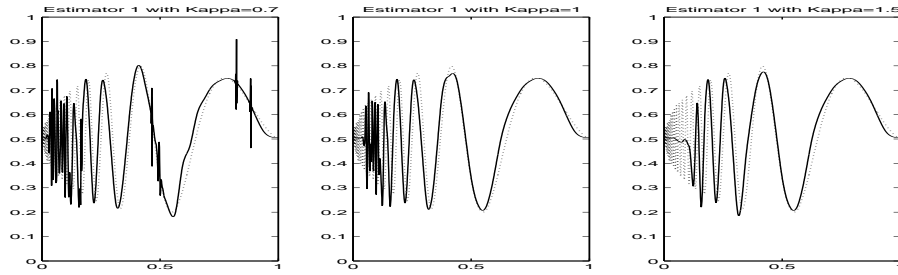
Figure 7.2: Estimator 1 for the 'Doppler' target (in dots) for three different values of κ (0.7, 1, 1.5)

estimator of g is also needed. Theoretically many techniques are available, including log spline (see Maxim [66]), Kernel or wavelet methods (see the book of Härdle et al. [49]). In the simulation study we used a method based on binning and wavelet thresholding which will be detailed further.

7.3.2 Some examples of settings

Before a thorough study in a wide variety of settings, we investigate the behaviors of the estimators in several particular models to highlight their main differences. In this subsection we take:

- number of observations: $n = 1024$,

- root signal noise ratio: $rsnr = 3$,

- wavelet basis: Symlet of order 8.

First we investigate the choice of the constant κ for the thresholds of estimator 1. There is no optimal constant suited to any setting, however choosing $\kappa = 1$ proves efficient in general as can be seen on figure 7.2: for smaller κ there remains unfiltered noise and for larger κ the first oscillations of the Doppler function are not recovered.

Let us now compare the two estimators. Predictably in most settings close to optimal conditions, i.e for smooth densities close to the uniform, the two estimators behave similarly. For example when the density is a sine function with relatively small amplitude, both estimators behave well as can be seen on figure 7.3. Secondly, estimator 1 presents some defaults when the target function is much smoother than the density of the design. Indeed in this case the warping deteriorates the regularity of the estimator which is visually less pleasant than estimator 2, see for instance figure 7.4.

Beside that smoothness effect, interesting differences appear when the design is far from uniform, i.e. when the distribution of the design points in $[0, 1]$ is very unbalanced. Two deteriorations can then be noticed for estimator 2. First it does not capture as many details of the target function as estimator 1 in the zones where the observations are sparse (figure 7.5). Secondly it presents artifacts in the high density zones (figure 7.6). These two problems have the same origin: the wide variations of g provoke disproportionate thresholds, leaving
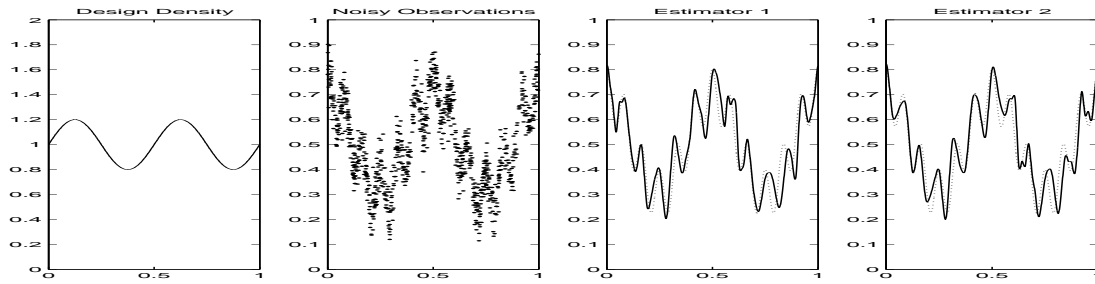
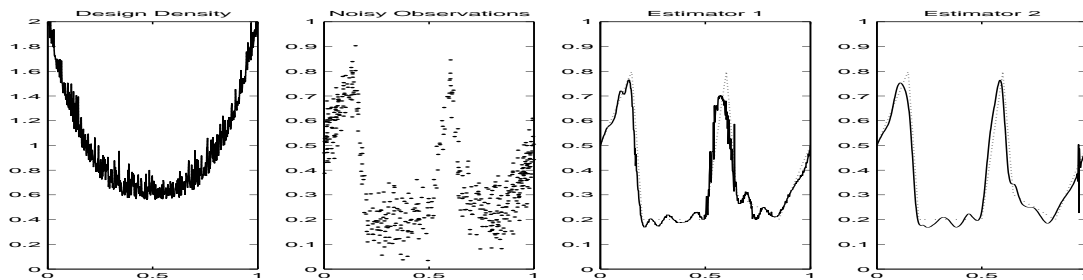Figure 7.3: The two estimators of the 'Wave' target (in dots)

Figure 7.4: The two estimators of the 'Angles' target (in dots)

some noise unfiltered when g is too high and on the contrary erasing useful details when g is too low. This can be seen respectively at level 5 in figure 7.7 and at level 9 in figure 7.8, where the thresholds associated to the two previous settings are represented.

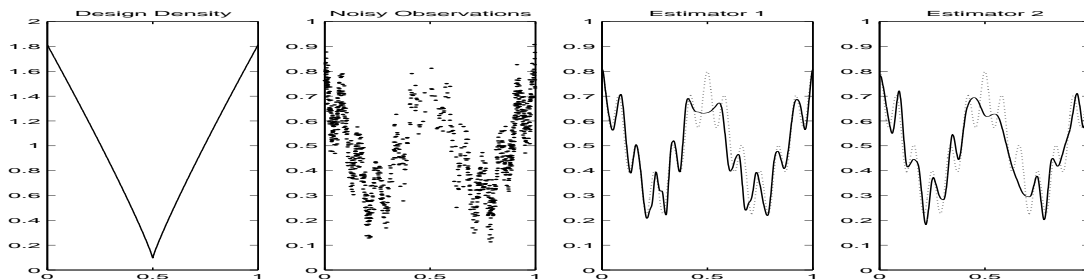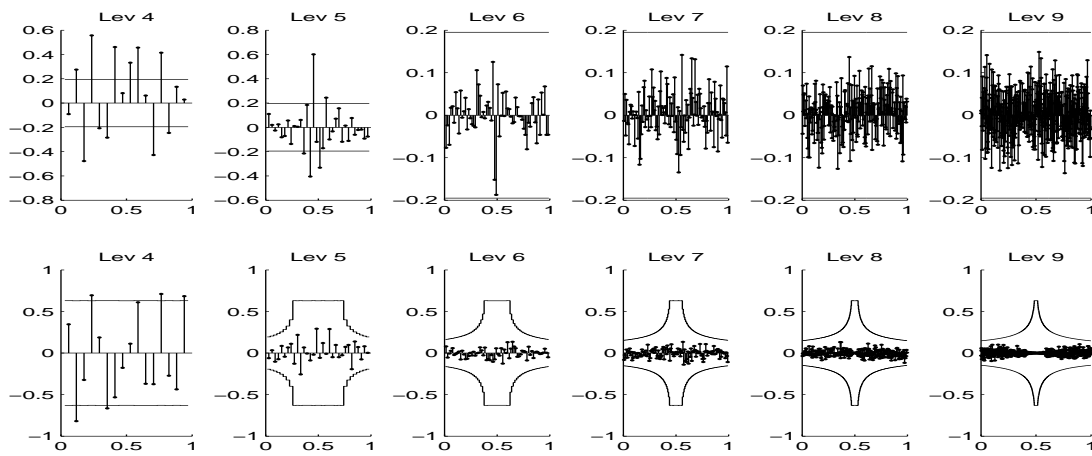The simulation study presented in the next section enables to analyze these differences more thoroughly.

Figure 7.5:   The two estimators of the 'Wave' target (in dots)
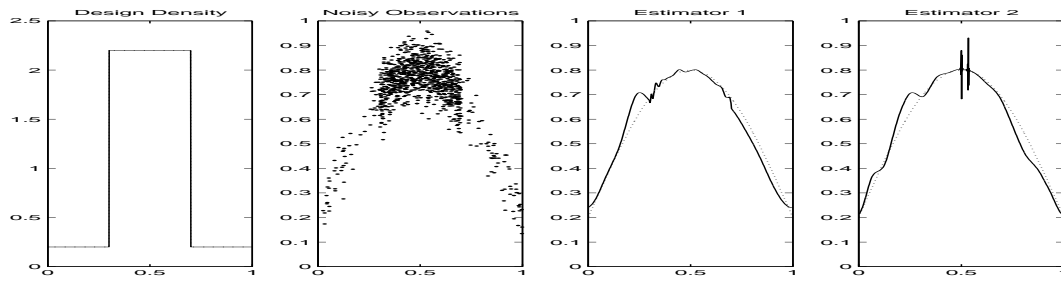
Figure 7.6:   The two estimators of the 'Sine' target (in dots)

Figure 7.7:   Coefficients (stems) and their corresponding thresholds (stairs) associated to figure 5 for estimator 1 (top), estimator 2 (bottom) and each level of resolution (from left to right)
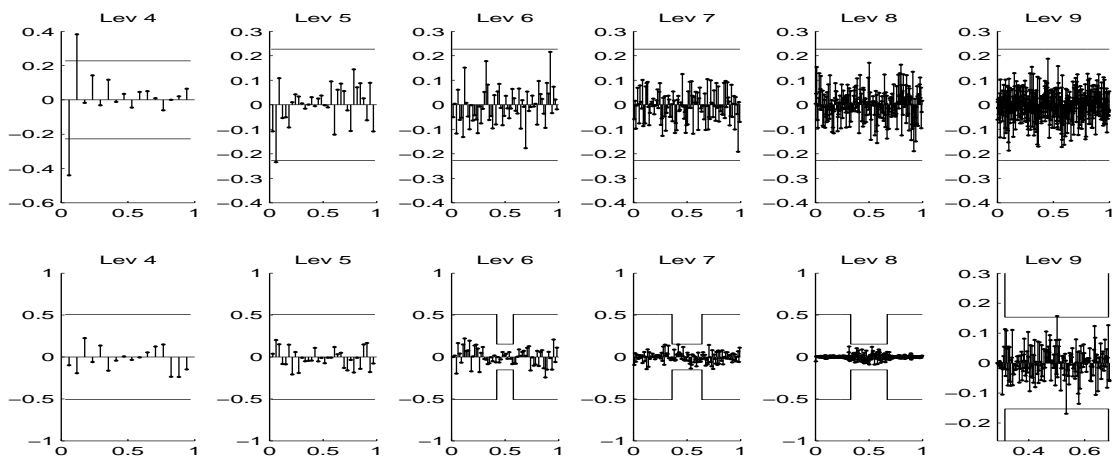

Figure 7.8:   Coefficients (stems) and their corresponding thresholds (stairs) associated to figure 6 for estimator 1 (top), estimator 2 (bottom) and each level of resolution (from left to right)
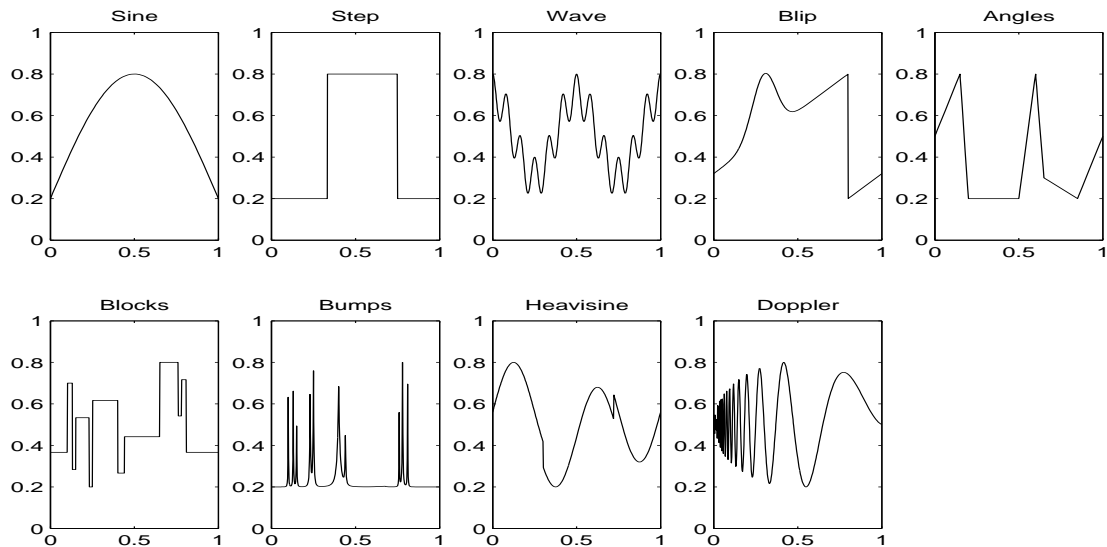
Figure 7.9:   Target functions

7.4   Simulation study

7.4.1   Description of the simulation

We compare the behavior of the two estimators for different regression functions and different densities of the design. For each one of these two factors, we used the functions represented on figures 7.9 and 7.10. Most of the target functions are borrowed from Antoniadis and Bigot [3], where they are used to highlight differences between linear and non linear estimators. We refer to their paper for the mathematical expressions. As for the densities, there are two groups: the first and second ones are uniform or slightly varying, whereas the next four ones are used to test if the estimators behave well in case of one or numerous holes in the density, i.e of zones where one has hardly any observation of the unknown function. The mathematical expressions are given in the appendix. Notice that all these functions are bounded from below.

In addition the effects of n, of the root signal to noise ratio (denoted by $rsnr$) and of the choice of the wavelet basis are examined. A series of results are given in the appendix for samples with $n \in \{2^9, 2^{10}, 2^{11}, 2^{12}\}$, $rsnr = 1$ (high noise) or $rsnr = 7$ (small noise), and the wavelet basis is the Symlet of order 8 or the Coiflet of order 3 (as in Antoniadis and Bigot [3]).

The quality of each estimator was evaluated by computing approximations of the mean integrated error (L1), the root mean integrated square error (RMSE) and the maximum deviation (MXDV). The criterium $MXDV$ reflects the amplitude of localized errors in the estimation, whereas $L1$ reflects the mean quality of the estimation along the whole domain of definition of the target function. These quantities were estimated in the following way:

- L1 is computed as the average over 100 runs of $\frac{1}{n} \sum_{i=1}^{n} |f(\frac{i}{n}) - \hat{f}(\frac{i}{n})|$.
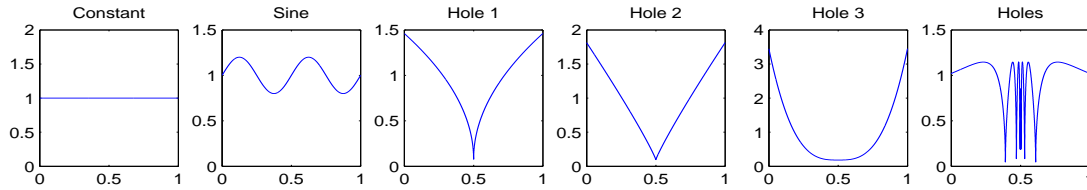
Figure 7.10: Densities of the design

- RMSE is computed as the average over 100 runs of $\sqrt{\frac{1}{n}\sum_{i=1}^{n}(f(\frac{i}{n}) - \hat{f}(\frac{i}{n}))^2}$.

- MXDV is computed as the average over 100 runs of $\max_{1 \le i \le n} |f(\frac{i}{n}) - \hat{f}(\frac{i}{n})|$.

In each run, the random variables X and ε were simulated independently of their values in the other runs.

7.4.2   Results for known and bounded densities

Let us first focus on a setting with small sample $n = 512$, high noise $rsnr = 1$ and a Symlet basis (figure 7.15). The performance of estimator 1 relatively to estimator 2 for the three criteria is given in the first column of the figure. For densities close to the uniform, the two estimators have similar performances, except that estimator 2 has a better MXDV for the Sine and Heavisine target function and the Sine density design.

On the contrary differences appear for other densities. Especially considering the L_1 loss, estimator 1 is better for moderately complicated targets, such as Wave or Blip, because it recovers details that estimator 2 ignores. This advantage is all the more significant as the the hole is wide ('Hole2' and 'Hole3' densities). For more complicated targets (Doppler or Blocks) neither estimator captures the details very well in high noise, so their performances are equivalent.

For larger samples (figure 7.17) the advantage of estimator 1 in case of holes in the design density grows more and more obvious. When $n = 4096$ estimator 2 is outperformed whatever the rsnr, the design and the target (except Heavisine). This is particularly true for 'Hole1' and 'Holes' densities, where the thresholding rule of estimator 2 is probably inadapted.

In the small noise settings, the previous comparison remains valid but the advantage of estimator 1 is generally less significant. Similarly replacing the Symlet by the Coiflet basis does not change the advantage of estimator 1 over estimator 2, but this one tends to be reduced in most settings. That may come from the fact that the Coiflet scaling functions have better approximation properties than the Symlets, and thus the detail coefficients and the thresholds play a minor role in both methods.
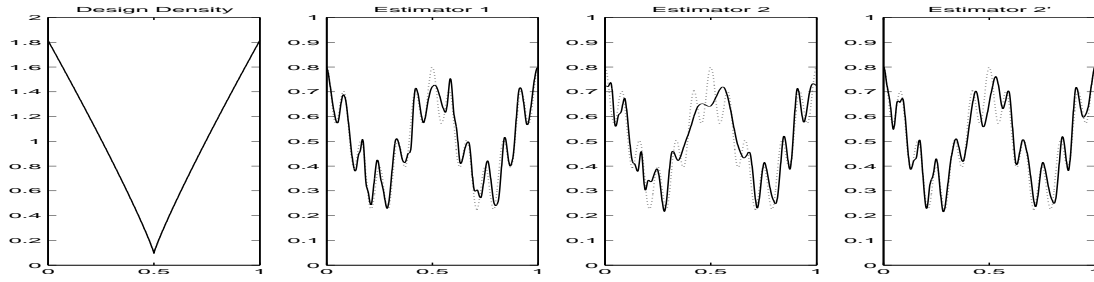
Figure 7.11:   Estimators 1, 2 and 2′ for the Wave target (in dots), $n = 1024$ and $rsnr = 3$

7.4.3   Results for known and vanishing densities

In this part the simulation study is performed with the same model parameters as before, except for three densities, namely 'Hole1' 'Hole2' and 'Holes', which are allowed to vanish (the new expressions are given in the appendix). The constant κ of estimator 2′ was fitted in practice such that the estimator behaves well whenever the design density is uniform, as it was done for estimator 1.

The results are the following. For the first two densities of figure 7.10, estimator 2′ behaves in a similar way as estimator 1 and estimator 2. However for vanishing densities, estimator 2′ corrects the main oversmoothing default of estimator 2. Indeed the thresholding method is less rough than the one used in the previous section, so the estimator behaves better now in some of the settings investigated earlier as can be seen in figure 7.11.

Nevertheless the values of the quality criteria (see figures 7.18) show that estimator 1 generally remains better than estimator 2′, even if its advantage is much smaller for densities with narrow holes such as 'Hole1' and 'Holes' in the case of high noise (first column of figures 7.18 versus first column of figure 7.17). So even with thresholds sharper than before, estimator 2′ does not manage to recover the details of the target functions as well as estimator 1, especially when the observations are sparse in a wide range of abscissa (for 'Hole2' and 'Hole3' densities).

7.4.4   Results for unknown densities

In this context, a density estimator is necessary to implement estimator 2′. In Wavelab a procedure is available, which consists first in computing an histogram H_n of the data:

$$H_n(x) = \frac{1}{n} \sum_{i=1}^{n} \sum_{j=1}^{m} (t_{j+1} - t_j)^{-1} 1_{T_j}(x) 1_{T_j}(X_i),$$

where $t_1, \ldots, t_m$ is an equispaced sample of $[0,1]$, $T_i = [t_i, t_{i+1}[$ and m is a large integer. Then a wavelet thresholding algorithm is performed on H_n.

A common choice for m is $m = [n/l]$, where the width l of the steps can be seen as a bandwidth parameter chosen according to the smoothness of the underlying density. However a fixed $l = 16$ leads to reasonable estimators so this choice was adopted in the sequel.
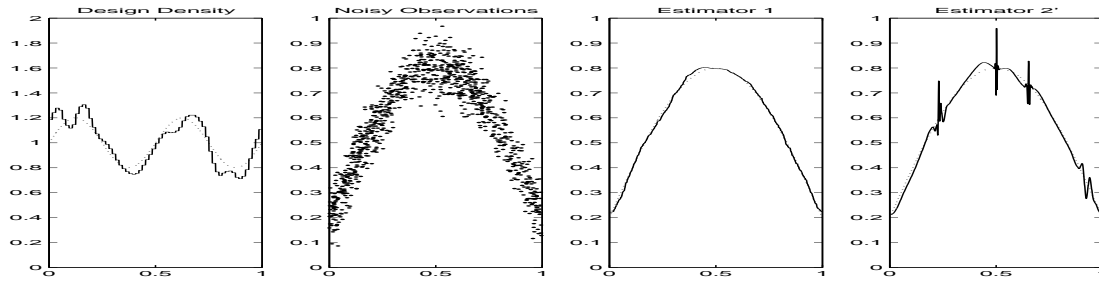
Figure 7.12: Density estimator, noisy data and the two estimators for the Sine target (in dots)

Predictably, the estimation errors in the density cause both estimators to deteriorate. The warping makes estimator 1 unsmooth in domains where the observations are sparse, and the thresholding generally leaves some noise unfiltered for estimator 2. For example in figure 7.12 artifacts appear even though the density is relatively well estimated. Some of them could have been erased, had the true thresholds been taken into account.

Analysing the three quality criteria for high noise (first column of figure 7.16), estimator 1 is now clearly stronger than estimator 2 whatever the density, especially for the maximum deviation. However for small noise the performances are close. Estimator 1 is more robust with respect to the lack of knowledge of the design density.

Conclusion. The two procedures have similar performances for smooth and homogenous design densities. For vanishing densities, estimator $2'$ is better than estimator 2 but both are generally outperformed by estimator 1, and this ranking is even clearer if unknown densities are taken into account.

7.5 Applications to real data sets

7.5.1 Ethanol data

We investigate the performance of the two wavelet thresholding procedures when applied to the ethanol data introduced by Brinkman [12]. The data consists of 88 measurements from an experiment where ethanol was burned in a one-cylinder automobile engine. The concentration of the total amount of nitric oxide and nitrogen dionide (y-axis) is related to the "equivalence ratio" (x-axis), a measure of the richness of the air ethanol mixture. To fit the data to our model, the range of the x-axis variable is linearly shifted to $[0, 1]$.

The two procedures considered here yield satisfactory results, compared to the numerous other estimators applied to this dataset (eg Antoniadis et al. [5]). As can be seen on figure 7.13, estimator 1 seems slightly better than estimator 2 for $x \in [0.7, 1]$, but globally both capture the variations in the data quite precisely. We can remark that estimator 1 is a bit unsmooth because of the warping with $\hat{G}_n$. If we wish to obtain a visually more pleasant result, an alternative is to use a smoother estimator of G.
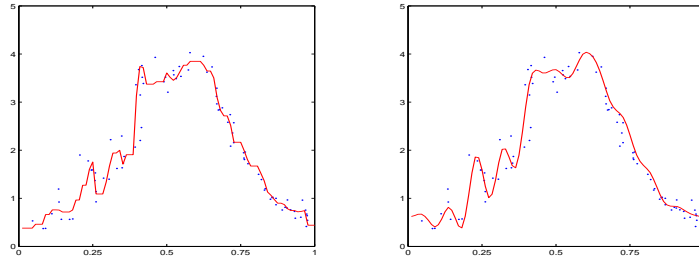
Figure 7.13:   Ethanol data (dots) with estimator 1 (left) and estimator 2 (right)

So as to quantify the performances of the the two procedures, we use a criterium developed by Nason [73] adapted to the regression model with random design. This approach consists in evaluating the following estimator of the mean square error:

$$\hat{M} = n^{-1} \sum_{i=1}^{n} (\hat{f}^{-i}(X_i) - Y_i)^2$$

where $\hat{f}^{-i}$ is each of our procedures constructed from all the data except the i-th observation (Y_i, X_i). As in Nason [73], we compute the values of $\hat{M}$ for various choices of the wavelet basis and of the coarsest level j_0. The results are similar to the ones obtained in his paper. For example the performances of estimator 1 are given in table 7.1, the best result being 103.9 versus 98 in Nason [73].

	Sym7	Sym8	Sym9	Sym10
$j_0 = 4$	156.8	145.1	119.0	127.8
$j_0 = 5$	167.5	151.4	125.6	136.8
$j_0 = 6$	140.8	139.0	103.9	126.8

Table 7.1:   Values of $\hat{M}$ ($\times 1000$) of estimator 1 for various choices of the wavelet basis and of the coarsest level j_0

7.5.2   Motorcycle acceleration data

Lastly we apply our procedures to the motorcycle acceleration data considered in Silverman [84]. These 133 observations are taken from a crash test and show the acceleration of a motorcyclist's head. The explanatory variable is time (rescaled to the unit interval) and the dependent variable is the head acceleration (in g).

As can be seen on figure 7.14, the data are heteroscedastic with an increasing variance with respect to the time. If we apply blindly the two procedures, estimator 1 exhibits a high frequency feature due to a large variance. This can be corrected by slightly increasing the level of the threshold (i.e by setting $\kappa = 1.06$ instead of $\kappa = 1$). We can notice that estimator 2 seems to be less precise than estimator 1.
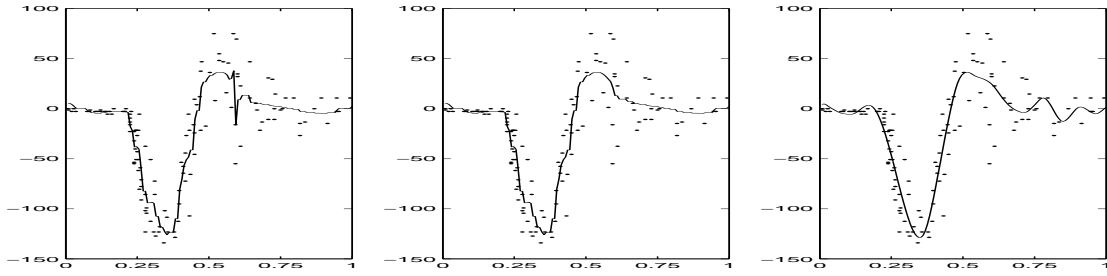
Figure 7.14: Motorcycle data (dots) with estimator 1 with $\kappa = 1$ (left), $\kappa = 1.06$ (middle) and estimator 2 (right)

7.6 Appendix

Target functions and densities

Target functions. The target functions in figure 7.9 have the following expressions:

- Sine: $f(x) = 0.2 + 0.6\sin(\pi x)$,

- Step: $f(x) = 0.2 + 0.6I\{1/3 < x < 3/4\}$,

- Wave: $f(x) = 0.5 + 0.2\cos(4\pi x) + 0.1\cos(24\pi x)$,

- Blip: $f(x) = (0.32 + 0.6x + 0.3\exp(-100(x-0.3)^2))I\{0 \le x \le 0.8\} + (-0.28 + 0.6x + 0.3\exp(-100(x-1.3)^2))I\{0.8 < x \le 1\}$,

- Angles: $f(x) = (2x+0.5)I\{0 \le x \le 0.15\} + (-12(x-0.15)+0.8)I\{0.15 < x \le 0.2\} + 0.2I\{0.2 < x \le 0.5\} + (6(x-0.5)+0.2)I\{0.5 < x \le 0.6\} + (-10(x-0.6)+0.8)I\{0.6 < x \le 0.65\} + (-0.5(x-0.65)+0.3)I\{0.65 < x \le 0.85\} + (2(x-0.85)+0.2)I\{0.85 < x \le 1\}$,

- Blocks, Bumps, Heavisine and Doppler are Donoho and Johnstone's functions (used for example in Donoho and Johnstone [31]) vertically rescaled to $[0.2, 0.8]$.

Densities. The design densities in figure 7.10 have the following expressions, up to a normalisation constant:

- Constant: $g(x) = 1$,

- Sine: $g(x) = 1 + 0.2\sin(4\pi x)$,

- Hole 1: $g(x) \asymp |x-0.5|^{0.5} + 0.04$ in section 3 and $g(x) \asymp |x-0.5|^{0.5}$ in section 4,

- Hole 2: $g(x) \asymp |x-0.5|^{0.9} + 0.03$ in section 3 and $g(x) \asymp |x-0.5|^{0.9}$ in section 4,

- Hole 3: $g(x) \asymp |x-0.5|^3 + 0.007$,

- Holes: $g(x) \asymp |\sin(\frac{1}{2|x-0.5|+0.1})|^{0.5} + 0.02$ in section 3 and $g(x) \asymp |\sin(\frac{1}{2|x-0.5|+0.1})|^{0.5}$ in section 4.

Simulation results

Some of the simulation results are summarized here graphically. Each graph provides, for a given quality criterium, the ratio of the value of the criterium for estimator 1 and the sum of the two values of the criterium for estimator 1 and estimator 2 (or 2′). Thus estimator 1 is better than estimator 2 whenever the ratio is below the value 0.5.

Each one of the six groups of nine successive columns refers to the nine target functions and to one of the six densities in the following order: 'Constant', 'Sine', 'Hole1', 'Hole2', 'Hole3' and 'Holes'.
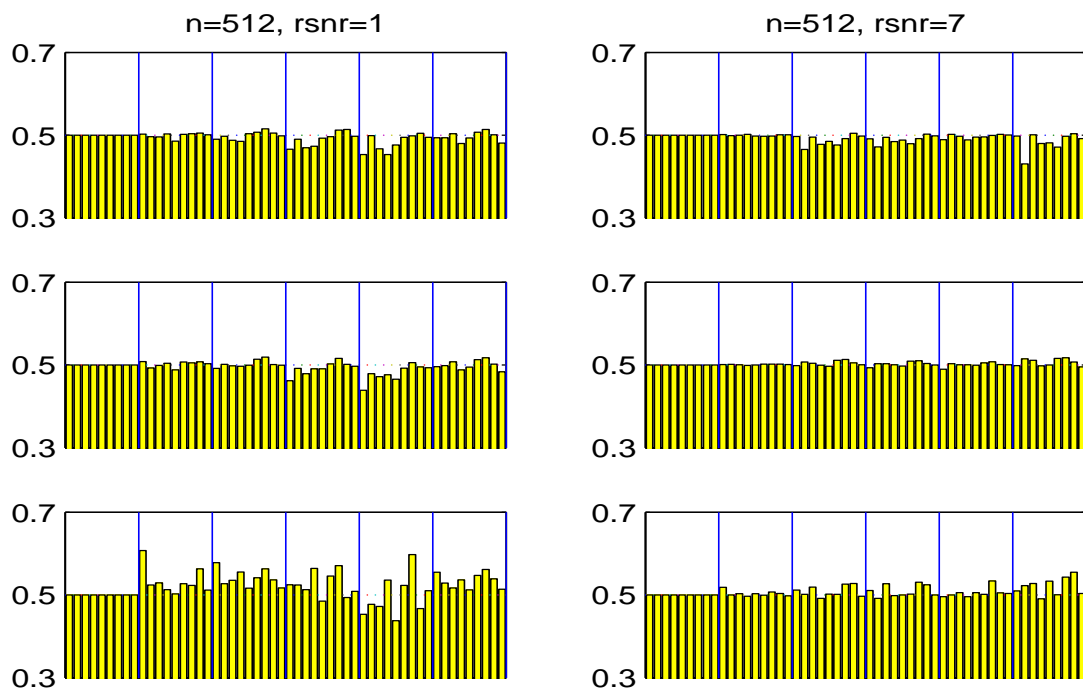

Figure 7.15:   Estimator 1 versus estimator 2: ratios of L1 (top), RMSE (middle) and MXDV (bottom) in the classical setting
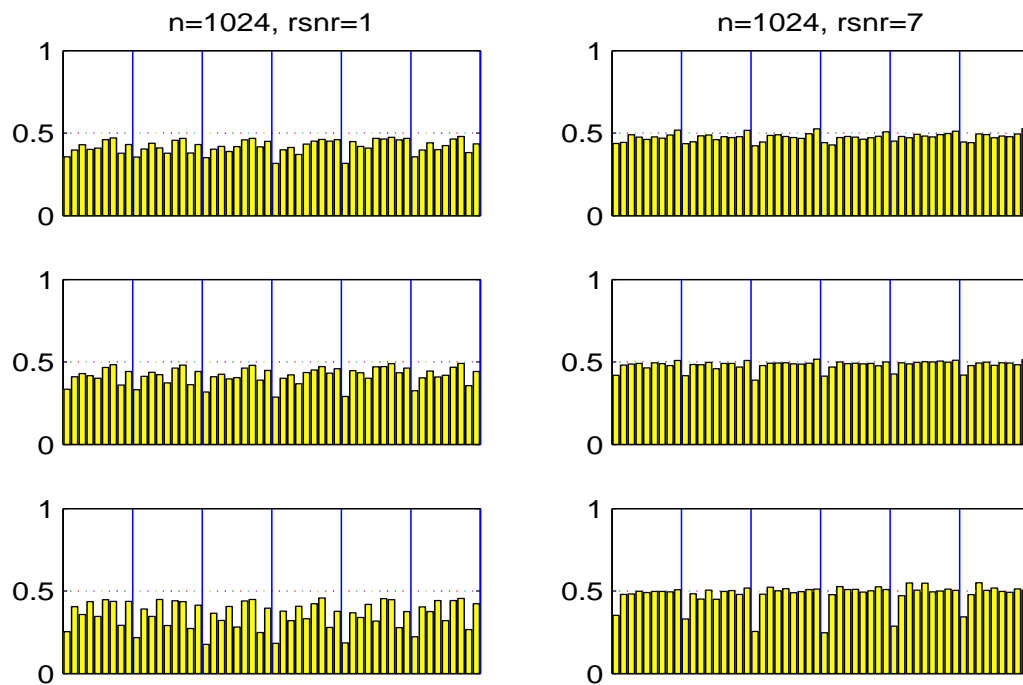
Figure 7.16:   Estimator 1 versus estimator 2: ratios of L1 for unknown densities
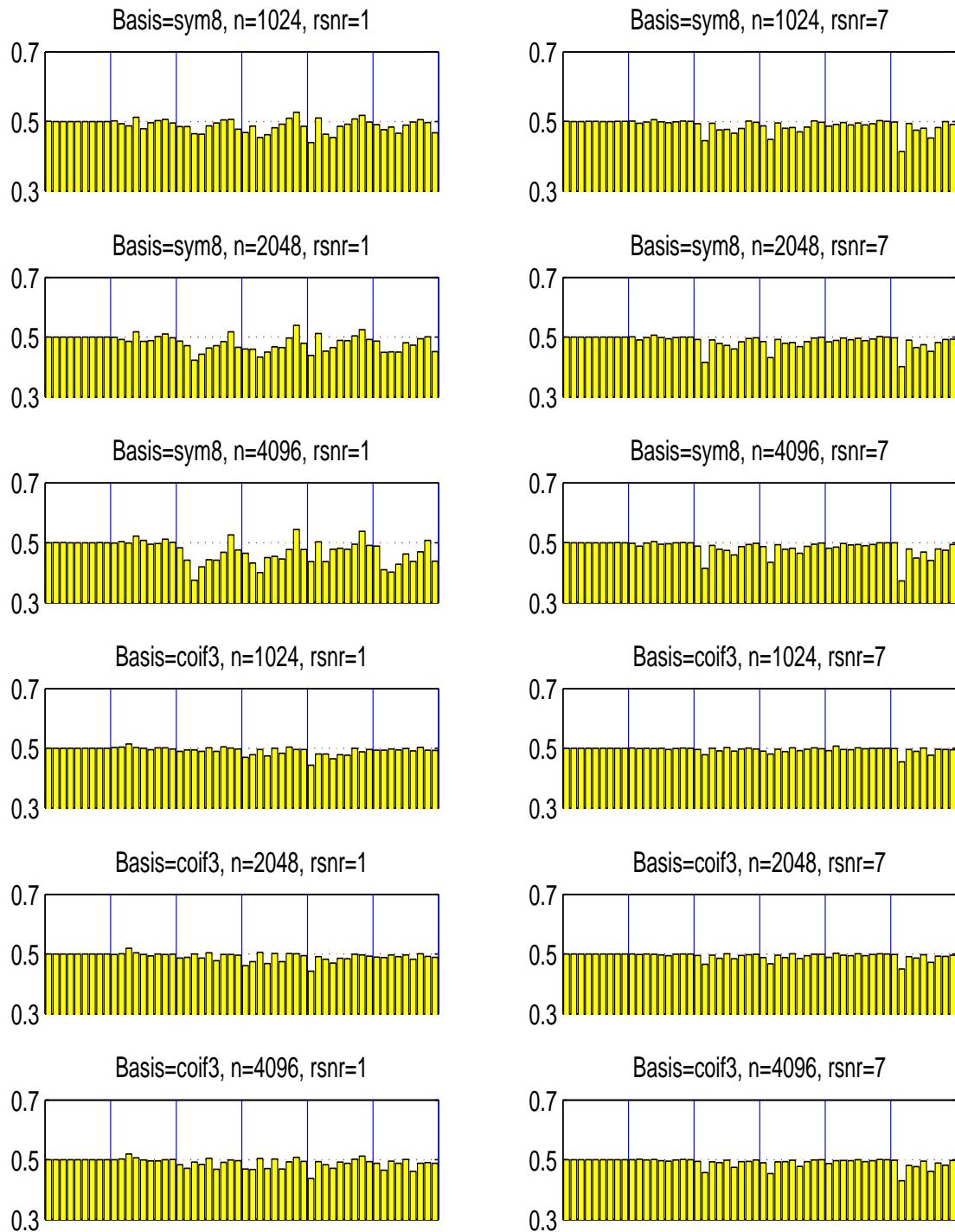
Figure 7.17:   Estimator 1 versus estimator 2: ratios of L1 in the classical setting
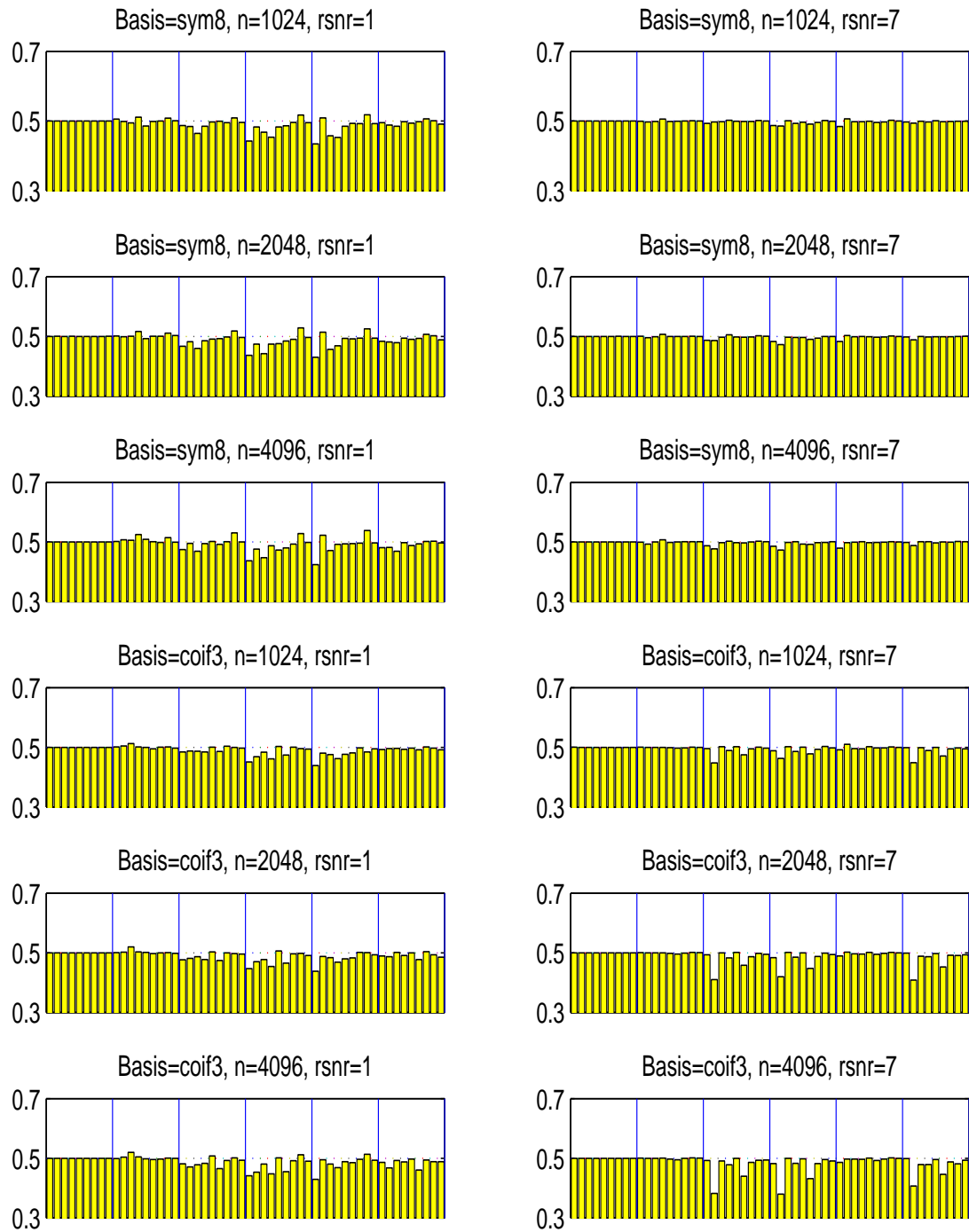
Figure 7.18:   Estimator 1 versus estimator 2′: ratios of L1 for known vanishing densities

Bibliography

[1] F. Abramovich and B. W. Silverman. Wavelet decomposition approaches to statistical inverse problems. *Biometrika*, 85(1):115–129, 1998. ISSN 0006-3444.

[2] Kenneth F. Andersen and Russel T. John. Weighted inequalities for vector-valued maximal functions and singular integrals. *Studia Math.*, 69(1):19–31, 1980/81. ISSN 0039-3223.

[3] A. Antoniadis and J. Bigot. Wavelet estimators in nonparametric regression : A comparative simulation study. *Journal of Statistical Software*, 6, 2001.

[4] A. Antoniadis and J. Bigot. Poisson inverse models. 2004. Preprint Grenoble.

[5] A. Antoniadis, G. Grégoire, and P. Vial. Random design wavelet curve smoothing. *Statistics and Probability Letters*, 35, 1997.

[6] A. Antoniadis, J. Fan, and I. Gijbels. A wavelet method for unfolding sphere size distributions. *The Canadian Journal of Statistics*, 29:265–290, 2001.

[7] F. Autin. Maxisets for density estimation on r. *Mathematical Methods of Statistics. (to appear)*, 2006.

[8] F. Autin. Maxisets for mu thresholding rules. *Test. (to appear)*, 2006.

[9] P. Baldi, G. Kerkyacharian, D. Marinucci, and D. Picard. High frequency asymptotics for wavelet-based tests for gaussianity and isotropy on the torus. *Preprint PMA*, 2006.

[10] M. Bertero and P. Boccacci. Introduction to inverse problems in imaging. *Institute of Physics, Bristol and Philadelphia*, 1998.

[11] L. Birge. A new look at an old result: Fano's lemma. *technical report. University Paris VI*, 2001.

[12] N.D. Brinkman. Ethanol- a single-cylinder engine study of efficiency and exhaust emissions. *SAE Transactions*, 90:1410–1424, 1981.

[13] C. Butucea. Deconvolution of supersmooth densities with smooth noise. *Canad. J. Statist.*, 32(2):181–192, 2004.

[14] T. Cai and L.D. Brown. Wavelet shrinkage for nonequispaced samples. *The Annals of Statistics*, 26:1783–1799, 1998.

[15] L. Cavalier. Inverse problems with non-compact operators. *J. Statist. Plann. Inference*, 136(2):390–400, 2006. ISSN 0378-3758.

[16] L. Cavalier and A. Tsybakov. Sharp adaptation for inverse problems with random noise. *Probab. Theory Related Fields*, 123(3):323–354, 2002. ISSN 0178-8051.

[17] L. Cavalier, G. K. Golubev, D. Picard, and A. B. Tsybakov. Oracle inequalities for inverse problems. *Ann. Statist.*, 30(3):843–874, 2002. ISSN 0090-5364.

[18] L. Cavalier, Y. Golubev, O. Lepski, and A. Tsybakov. Block thresholding and sharp adaptive estimation in severely ill-posed inverse problems. *Teor. Veroyatnost. i Primenen.*, 48(3):534–556, 2003. ISSN 0040-361X.

[19] Laurent Cavalier and Nicolas W. Hengartner. Adaptive estimation for inverse problems with noisy operators. *Inverse Problems*, 21(4):1345–1361, 2005. ISSN 0266-5611.

[20] Sylvie Champier and Laurence Grammont. A wavelet-vaguelet method for unfolding sphere size distributions. *Inverse Problems*, 18(1):79–94, 2002. ISSN 0266-5611.

[21] A. Cohen, I. Daubechies, and P. Vial. Wavelets on the interval and fast wavelet transforms. *Applied and Comp. Harmonic Analysis*, 1(1):54–81, 1993.

[22] A. Cohen, R. De Vore, G. Kerkyacharian, and D. Picard. Maximal q-paces with given rate of convergence for thresholding algorithms. *Appl. Comput. Harmon. Anal.*, 11: 167–191, 2000.

[23] A. Cohen, M. Hoffmann, and M. Reiss. Non linear estimation for linear inverse problems with error in the operator. *Submitted*, 2004.

[24] Albert Cohen, Marc Hoffmann, and Markus Reiss. Adaptive wavelet Galerkin methods for linear inverse problems. *SIAM J. Numer. Anal.*, 42(4):1479–1501 (electronic), 2004. ISSN 0036-1429.

[25] L.M. Cruz-Orive. Distribution-free estimation of sphere size distributions from slabs showing overprojections and truncations, with a review of previous methods. *J. Microscopy*, 131:265–290, 1983.

[26] I. Daubechies. *Ten Lectures on Wavelets*. SIAM, Philadelphia., 1992.

[27] V. Dicken and P. Maass. Wavelet-Galerkin methods for ill-posed problems. *J. Inverse Ill-Posed Probl.*, 4(3):203–221, 1996. ISSN 0928-0219.

[28] D. Donoho. Denoising by soft-thresholding. *IEEE Trans. Inform. Theory*, 41, 1995.

[29] D. Donoho. Nonlinear solution of linear inverse problems by wavelet-vaguelette decomposition. *Applied Computational and Harmonic Analysis*, 2:101–126, 1995.

[30] D. Donoho and I. Johnstone. Adaptating to unknown smoothness via wavelet shrinkage. *J . Am Stat. Assoc*, 90(432):1200–1224, 1995.

[31] D. Donoho and I. Johnstone. Ideal spatial adaptation by wavelet shrinkage. *Biometrika*, 81:425–455, 1994.

[32] D. Donoho, I. Johnstone, G. Kerkyacharian, and D. Picard. Wavelet shrinkage by optimal recovery. *Lucien LeCam Festschrift D. Pollard and G.Yang (eds)*, 1994.

[33] D. Donoho, I. Johnstone, G. Kerkyacharian, and D. Picard. Wavelet shrinkage: Asymptotia. *J. Roy. Statist. Soc. Ser.*, B(57):301–369, 1995.

[34] D. Donoho, I. Johnstone, G. Kerkyacharian, and D. Picard. Universal near minimaxity of wavelet shrinkage. *Festschrift for Lucien Le Cam*, pages 183–218, 1997.

[35] David L. Donoho. Nonlinear solution of linear inverse problems by wavelet-vaguelette decomposition. *Appl. Comput. Harmon. Anal.*, 2(2):101–126, 1995. ISSN 1063-5203.

[36] David L. Donoho, Iain M. Johnstone, Gérard Kerkyacharian, and Dominique Picard. Density estimation by wavelet thresholding. *Ann. Statist.*, 24(2):508–539, 1996. ISSN 0090-5364.

[37] R. J. Duffin and A. C. Schaeffer. A class of nonharmonic Fourier series. *Trans. Amer. Math. Soc.*, 72:341–366, 1952. ISSN 0002-9947.

[38] Sam Efromovich and Vladimir Koltchinskii. On inverse problems with unknown operators. *IEEE Trans. Inform. Theory*, 47(7):2876–2894, 2001. ISSN 0018-9448.

[39] G.P. Fan and Marron J.S. Fast implementation of nonparametric curve estimators. *J.Comp.Graphical Statist.*, 3:35–56, 1994.

[40] Jianqing Fan and Ja-Yong Koo. Wavelet deconvolution. *IEEE Trans. Inform. Theory*, 48(3):734–747, 2002. ISSN 0018-9448.

[41] C. Fefferman and E. M. Stein. Some maximal inequalities. *Amer. J. Math.*, 93:107–115, 1971. ISSN 0002-9327.

[42] M. Frazier, B. Jawerth, and G. Weiss. Littlewood paley theory and the study of functions spaces. *CMBS*, 79, 1991. AMS.

[43] Alexander Goldenshluger and Sergei V. Pereverzev. On adaptive inverse estimation of linear functionals in Hilbert scales. *Bernoulli*, 9(5):783–807, 2003. ISSN 1350-7265.

[44] G. K. Golubev. The principle of penalized empirical risk in severely ill-posed problems. *Probab. Theory Related Fields*, 130(1):18–38, 2004. ISSN 0178-8051.

[45] G. K. Golubev and F. N. Enikeeva. On minimax estimation of a fractional derivative. *Theory Probab. Appl.*, 46(4), 2001.

[46] G. K. Golubev and B. Y. Levit. Asymptotically efficient estimation in the Wicksell problem. *Ann. Statist.*, 26(6):2407–2419, 1998. ISSN 0090-5364.

[47] P. Hall and B.A. Turlach. Interpolation methods for nonlinear wavelet regression with irregularly spaced design. *The Annals of Statistics*, 25, 1997.

[48] Peter Hall and Richard L. Smith. The kernel method for unfolding sphere size distributions. *J. Comput. Phys.*, 74(2):409–421, 1988. ISSN 0021-9991.

[49] W. Härdle, G. Kerkyacharian, D. Picard, and A. Tsybakov. *Wavelets, Approximation and Statistical Applications*. Springer-Verlag, 1998.

[50] S. Harsdorf and R. Reuter. Stable deconvolution of noisy lidar signals. *Submitted to Earsel meeting*, 2000.

[51] D. R. M. Herrick, G. P. Nason, and B. W. Silverman. Some new methods for wavelet density estimation. *Sankhyā Ser. A*, 63(3):394–411, 2001. ISSN 0581-572X. Special issue on wavelets.

[52] I. M. Johnstone and M. Raimondo. Periodic boxcar deconvolution and diophantine approximation. *Annals of Statistics*, 32(5):1781–1804, 2004.

[53] I. M. Johnstone, G. Kerkyacharian, D Picard, and M. Raimondo. Wavelet deconvolution in a periodic setting. *Journal of the Royal Statistical Society*, 66(3):1–27, 2004.

[54] Iain M. Johnstone and Bernard W. Silverman. Discretization effects in statistical inverse problems. *J. Complexity*, 7(1):1–34, 1991. ISSN 0885-064X.

[55] Jérôme Kalifa and Stéphane Mallat. Thresholding estimators for linear inverse problems and deconvolutions. *Ann. Statist.*, 31(1):58–109, 2003. ISSN 0090-5364.

[56] G. Kerkyacharian and D. Picard. Minimax or maxisets? *Bernoulli*, 8(2):219–253, 2002.

[57] G. Kerkyacharian and D. Picard. Regression in random design and warped wavelets. *Bernoulli*, 10(6):1053–1105, 2004.

[58] G. Kerkyacharian, D. Picard, and M. Raimondo. Adaptive boxcar deconvolution on full lebesgue measure sets. 2005. Preprint LPMA.

[59] Gérard Kerkyacharian and Dominique Picard. Thresholding algorithms, maxisets and well-concentrated bases. *Test*, 9(2):283–344, 2000. ISSN 1133-0686.

[60] E.D. Kolaczyk. *Wavelet Methods for the Inversion of Certain Homogeneous Linear Operators in the Presence of Noisy Data*. PhD thesis, Ph.D. Thesis, Department of Statistics, Stanford University., 1994.

[61] V. Korostelev and A. Tsybakov. *Minimax theory of image reconstruction*. Springer-Verlag, 1993.

[62] R. Lipster and A. N. Shiryaev. *Statistics of random processes*, volume I. 1st edition, 1977.

[63] J. M. Loubes and V. Rivoirard. Review of rates of convergence and regularity conditions for inverse problems. *http://www.math.u-psud.fr/rivoirar/*, 2006.

[64] Stéphane Mallat. *A wavelet tour of signal processing*. Academic Press Inc., San Diego, CA, 1998. ISBN 0-12-466605-1.

[65] Peter Mathé and Sergei V. Pereverzev. Geometry of linear ill-posed problems in variable Hilbert scales. *Inverse Problems*, 19(3):789–803, 2003. ISSN 0266-5611.

[66] V. Maxim. Restauration de signaux bruités observés sur des plans d'expérience aléatoires. *Thèse de l'Université Joseph Fourier, Grenoble 1*, 2003.

[67] Y. Meyer. Ondelettes sur l'intervalle. *Rev. Mat. Iberoamericana*, 7:115–133, 1990.

[68] Yves Meyer. *Ondelettes et opérateurs. II.* Actualités Mathématiques. [Current Mathematical Topics]. Hermann, Paris, 1990. ISBN 2-7056-6126-7.

[69] Yves Meyer. *Ondelettes et opérateurs. I.* Actualités Mathématiques. [Current Mathematical Topics]. Hermann, Paris, 1990. ISBN 2-7056-6125-0.

[70] B. Muckenhoupt. Weighted norm inequalities for the hardy maximal function. *Trans. Amer. Math. Hencec*, 165, 1972.

[71] F. Narcowich, P. Petrushev, and J. Ward. Local tight frames on spheres. *SIAM J. Math. Anal.*, 2006.

[72] F. J. Narcowich, P. Petrushev, and J.M. Ward. Decomposition of besov and triebel-lizorkin spaces on the sphere. *J. Funct. Anal.*, 2006.

[73] G.P. Nason. Choice of wavelet smoothness, primary resolution and threshold in wavelet shrinkage. *Statistics and Computing*, 12:219–227, 2002.

[74] R. Neelamani, H. Choi, and R. Baranuik. Wavelet-based deconvolution for ill-conditioned systems. 2000. http://www-dsp.rice.edu/publications/pub/neelsh98icassp.pdf.

[75] M. Nussbaum and S. Pereverzev. The degree of ill-posedness in stochastic and deterministic noise models. *Preprint WIAS*, 1999.

[76] D. Nychka, G. Wahba, S. Goldfarb, and T. Pugh. Cross validated spline methods for the estimation of three-dimensional tumor size distributions from observations on two-dimensional cross sections. *J. Amer. Statist. Assoc.*, 79:832–846, 1984.

[77] OFTA. *Problèmes inverses : de l'expérimentation à la modélisation.* Observatoire Francais des Techniques Avancées, 1999.

[78] M. Pensky and B. Vidakovic. Adaptive wavelet estimator for nonparametric density deconvolution. *Annals of Statistics*, 27:2033–2053, 1999.

[79] Sergei Pereverzev and Eberhard Schock. Error estimates for band-limited spherical regularization wavelets in an inverse problem of satellite geodesy. *Inverse Problems*, 15 (4):881–890, 1999. ISSN 0266-5611.

[80] P. Petrushev and Y. Xu. Localized polynomials kernels and frames (needlets) on the ball. 2005. IMI 2005.

[81] Pencho Petrushev and Yuan Xu. Localized polynomial frames on the interval with Jacobi weights. *J. Fourier Anal. Appl.*, 11(5):557–575, 2005. ISSN 1069-5869.

[82] M. Reiss. Adaptive estimation for affine stochastic delay differential equations. *Submitted to Bernoulli*, 2004.

[83] M. Reiss. Nonparametric estimation for stochastic delay differential equations. *Ph.D. thesis, Humboldt Universität zu Berlin*, 2001.

[84] B.W. Silverman. Some aspects of the spline smoothing approach to nonparametric regression curve fitting. *J. Roy. Statist. Soc.*, 47:1–52, 1985.

[85] W. Stefan, E. Garnero, and R. A. Renaut. Signal restoration through deconvolution applied to deep mantle seismic probes. *Geophys. J. Int. Preprint*, 2005.

[86] Gábor Szegő. *Orthogonal polynomials*. American Mathematical Society, Providence, R.I., 1975.

[87] A. Tsybakov. Sharp adaptive estimation of linear functionals. *Ann. Statist.*, 29(6): 1567–1600, 2001.

[88] Alexandre Tsybakov. On the best rate of adaptive estimation in some inverse problems. *C. R. Acad. Sci. Paris Sér. I Math.*, 330(9):835–840, 2000. ISSN 0764-4442.

[89] Alexandre B. Tsybakov. *Introduction à l'estimation non-paramétrique*, volume 41 of *Mathématiques & Applications (Berlin) [Mathematics & Applications]*. Springer-Verlag, Berlin, 2004. ISBN 3-540-40592-5.

[90] G. Walter and X. Shen. Deconvolution using the meyer wavelet. *Journal of Integral Equations and Applications*, 11:515–534, 1999.

[91] S. D. Wicksell. The corpuscle problem: a mathematical study of a biometric problem. *Biometrika*, 17:84–99, 1925.

RÉSUMÉ: On se place dans le cadre de l'estimation non paramétrique pour les problèmes inverses, où une fonction inconnue subit une transformation par un opérateur linéaire mal posé, et où l'on en observe une version bruitée par une erreur aléatoire additive. Dans ce type de problèmes, les méthodes d'ondelettes sont très utiles, et ont été largement étudiées. Les méthodes développées dans cette thèse s'en inspirent, mais consistent à s'écarter des bases d'ondelettes "classiques", ce qui permet d'ouvrir de nouvelles perspectives théoriques et pratiques. Dans l'essentiel de la thèse, on utilise un modèle de type bruit blanc. On construit des estimateurs utilisant des bases qui d'une part sont adaptées à l'opérateur, et d'autre part possèdent des propriétés analogues à celles des ondelettes. On en étudie les propriétés minimax dans un cadre large, et l'on implémente ces méthodes afin d'en étudier leurs performances pratiques. Puis on s'intéresse également au cas où l'opérateur lui même est aléatoire. Dans une dernière partie, on utilise un modèle de regression en design aléatoire, et on étudie les performances numériques d'un estimateur reposant sur la déformation des bases d'ondelettes.

MOTS-CLÉS: Estimation adaptative, Estimation non paramétrique, Ondelettes, Théorie minimax, Vitesses de convergence, Déconvolution, Problèmes inverses, Ondelettes de seconde génération, Espaces de Besov, Polynômes de Jacobi, Régression en design aléatoire, Ondelettes déformées.

DISCIPLINE: MATHÉMATIQUES

ABSTRACT: Nonparametric estimation problems for inverse models consist in recovering an unknown function from the observation of a linear ill posed transformation of the function, blurred by an additive random error. In this context, wavelet methods are very useful and have been widely studied. The estimators developed in this thesis are significantly influenced by them, but also stray from decompositions in "classical" wavelet bases, which allows new theoretical and practical developments. In a main part of the thesis, one focuses on a white noise type model. One develops estimators using bases which, on the one hand are adapted to the operator of the problem, and on the other hand possess wavelet type properties. One investigates the theoretical properties of such methods in a wide minimax framework, as well as their numerical performances, by a simulation study. Then we also pay interest to the case where the operator itself is random. In the last part of the thesis, one focuses on the model of regression in random design, and one investigates the numerical performances of an estimator based on the "warping" of wavelet bases.

KEY WORDS: Adaptive estimation, Nonparametric estimation, Wavelets, Minimax theory, Rates of convergence, Deconvolution, Inverse problems, Second-generation wavelets, Besov spaces, Jacobi polynomials, Regression in random design, Warped wavelets.

Laboratoire de Probabilités et Modèles Aléatoires,
CNRS-UMR 7599, UFR de Mathématiques, case 7012
Université Paris 7, Denis Diderot
2, place Jussieu, 75251 Paris Cedex 05.